Breeding strategies for improving pest and disease resistance in wheat

by

Paula Silva

B.S., Universidad de La República, Uruguay, 2011
M.S., Universidad de La República, Uruguay, 2014

AN ABSTRACT OF A DISSERTATION

submitted in partial fulfillment of the requirements for the degree

DOCTOR OF PHILOSOPHY

Interdepartmental Genetics
College of Agriculture

KANSAS STATE UNIVERSITY
Manhattan, Kansas

2021

Abstract

Wheat is a vital cereal, providing 20% of the daily human nutritional requirements worldwide. Though there has been sizable yield gains and production increase, with the projected rise in food demand over the next 40 years, wheat yields must continue to increase at an accelerated pace to match the projected demand. However, yield production is constrained by biotic stresses and many breeding objectives remain for 'yield maintenance'. Overcoming yield constraints and losses due to plant pathogens requires developing wheat varieties resilient against pathogens through genetic resistance genes. However, genetic diversity for resistance to several biotic stresses in the primary pool of wheat is limited, such as in the case of barley yellow dwarf (BYD), wheat blast (WB), and wheat curl mite (WCM). To date, only a few resistance genes have been named against these diseases and diseases. Interestingly, most of these resistances have been introgressed from wild relative species. Wheat wild relatives offer a potential trove of untapped resistance genes against the many pathogens that threaten our wheat crop. In this study, we applied breeding strategies for improving BYD, WB, and WCM resistance in wheat with the final goal of contributing disease-resistant wheat germplasm to broaden genetic resources available for wheat breeders to sustain wheat production.

BYD is one of the most important viral diseases affecting wheat worldwide. Breeding for BYD resistance is very challenging due to the unpredictability and variability of its occurrence and difficulty of characterizing the symptoms. Four resistance genes have been named, with three of them donated by a wild relative of wheat *Thinopyrum intermedium*. In this study, we applied phenomics and genomics tools to better understand the resistance and tolerance to this disease and to facilitate the art of wheat improvement against BYD. Our results are promising but suggest that further research is needed to implement these strategies into the breeding pipeline.

WB is an emerging disease with the potential to devastate wheat production. One strategy that is still effective to control WB is genetic resistance provided by the alien segment $2N^{V}S$ introduced from *Aegilops ventricosa* into wheat. The genetic architecture behind $2N^{V}S$ is still unknown, thus, our first objective was focused on identifying the resistant gene located in this segment to better understand this destructive disease. However, $2N^{V}S$ resistance is slowly eroding and very limited resistance is available in wheat and more diverse sources should be

searched out. In this study, we thus evaluated a panel of the wild diploid wheat, *Aegilops tauschii*, and identified and mapped new resistance sources against WB. This has laid the foundation for further experiments to clone these genes.

WCM is a threatening pest for wheat, mainly by vectoring several viral diseases. To date, only five resistance genes have been identified and three of them were donated by *Ae. tauschii*. Since genetic resistance in the wheat germplasm is lacking, our study investigated the genetic basis of WCM resistance in *Ae. tauschii.* We mapped the resistance to chromosome 6D and found a single resistant haplotype across both *Ae. tauschii* lineages. We further showed that three previously named resistance genes all share the same haplotype, and we delimited the length of the introgressions into wheat. Moreover, we designed molecular markers, that once validated, will facilitate better use of this resistance in wheat.

Overall, our results contribute to better understand the genetic basis of BYD, WB, and WCM resistance and highlight both the necessity and the promise to search for novel sources of resistance in wild wheat species to broaden the genetic diversity of resistance available for wheat improvement.

Breeding strategies for improving pest and disease resistance in wheat

by

Paula Silva

B.S., Universidad de La República, Uruguay, 2011
M.S., Universidad de La República, Uruguay, 2014

A DISSERTATION

submitted in partial fulfillment of the requirements for the degree

DOCTOR OF PHILOSOPHY

Interdepartmental Genetics
College of Agriculture

KANSAS STATE UNIVERSITY
Manhattan, Kansas

2021

Approved by:

Major Professor
Jesse Poland

Copyright

Abstract

Wheat is a vital cereal, providing 20% of the daily human nutritional requirements worldwide. Though there has been sizable yield gains and production increase, with the projected rise in food demand over the next 40 years, wheat yields must continue to increase at an accelerated pace to match the projected demand. However, yield production is constrained by biotic stresses and many breeding objectives remain for 'yield maintenance'. Overcoming yield constraints and losses due to plant pathogens requires developing wheat varieties resilient against pathogens through genetic resistance genes. However, genetic diversity for resistance to several biotic stresses in the primary pool of wheat is limited, such as in the case of barley yellow dwarf (BYD), wheat blast (WB), and wheat curl mite (WCM). To date, only a few resistance genes have been named against these diseases and diseases. Interestingly, most of these resistances have been introgressed from wild relative species. Wheat wild relatives offer a potential trove of untapped resistance genes against the many pathogens that threaten our wheat crop. In this study, we applied breeding strategies for improving BYD, WB, and WCM resistance in wheat with the final goal of contributing disease-resistant wheat germplasm to broaden genetic resources available for wheat breeders to sustain wheat production.

BYD is one of the most important viral diseases affecting wheat worldwide. Breeding for BYD resistance is very challenging due to the unpredictability and variability of its occurrence and difficulty of characterizing the symptoms. Four resistance genes have been named, with three of them donated by a wild relative of wheat *Thinopyrum intermedium*. In this study, we applied phenomics and genomics tools to better understand the resistance and tolerance to this disease and to facilitate the art of wheat improvement against BYD. Our results are promising but suggest that further research is needed to implement these strategies into the breeding pipeline.

WB is an emerging disease with the potential to devastate wheat production. One strategy that is still effective to control WB is genetic resistance provided by the alien segment $2N^{V}S$ introduced from *Aegilops ventricosa* into wheat. The genetic architecture behind $2N^{V}S$ is still unknown, thus, our first objective was focused on identifying the resistant gene located in this segment to better understand this destructive disease. However, $2N^{V}S$ resistance is slowly eroding and very limited resistance is available in wheat and more diverse sources should be

searched out. In this study, we thus evaluated a panel of the wild diploid wheat, *Aegilops tauschii*, and identified and mapped new resistance sources against WB. This has laid the foundation for further experiments to clone these genes.

WCM is a threatening pest for wheat, mainly by vectoring several viral diseases. To date, only five resistance genes have been identified and three of them were donated by *Ae. tauschii*. Since genetic resistance in the wheat germplasm is lacking, our study investigated the genetic basis of WCM resistance in *Ae. tauschii.* We mapped the resistance to chromosome 6D and found a single resistant haplotype across both *Ae. tauschii* lineages. We further showed that three previously named resistance genes all share the same haplotype, and we delimited the length of the introgressions into wheat. Moreover, we designed molecular markers, that once validated, will facilitate better use of this resistance in wheat.

Overall, our results contribute to better understand the genetic basis of BYD, WB, and WCM resistance and highlight both the necessity and the promise to search for novel sources of resistance in wild wheat species to broaden the genetic diversity of resistance available for wheat improvement.

Table of Contents

List of Figures

List of Tables

Acknowledgements

I have no words to describe my gratitude for my advisor Dr. Jesse Poland. He is an inspiration to me, not only as a scientist but as a person. The truth is that I was not sure about having a male advisor since my former mentors were all female, but Jesse was more than an excellent advisor. He instilled in me how to be a better scientist, how to do quality research, and taught me the importance of collaborative work in research. I would also like to thank my committee members Drs. Allan Fritz, Bob Bowden, and Barbara Valent. Their contributions, guidance, and teaching during my doctorate have helped me to become a better researcher. I am extremely grateful to former and current Poland Lab members for their help, support, and fruitful discussions. A special thanks to all the undergrad students that helped me with greenhouse and fieldwork during these years.

For the BYD chapter, I cannot thank enough Byron Evers and Shuangye Wu, for their support with the field, greenhouse, and genotyping work. I greatly appreciate Xu Wang, Rich Brown, and Grant Williams for data collection with the drone. I appreciate very valuable input from the Fritz Lab members for fruitful discussions about BYD and wheat breeding. I would like to thank Dr. Liangliang Gao for providing the *Bdv2* prediction bioinformatics pipeline, and Dr. Jared Crain for supporting with data analyses. A big thanks to all the undergraduate students that helped with field data collection and seed cleaning and preparation.

For the WHB chapter, I would like to thank John Raupp for providing me with *Ae. tauschii* seed and all the knowledge and passion he shared about the wild relatives of wheat. I greatly appreciate Dr. Barbara Valent for the resources made available for research in Bolivia, including the structure which was already in place from previous efforts and especially the relationships with key institutions and personnel. We thank Dr. Giovana Cruppe for planning, overseeing, and coordinating personnel so that these experiments were successfully conducted. We are also grateful to Javier Kiyuna, Lidia Calderon, Diego Baldelomar, Jorge Cuellar, and Darwin Coimbra from ANAPO for their support in implementing day-to-day operations and managing field and greenhouse activities, including planting, managing, evaluating diseases, harvesting, and processing samples. A big thanks to Richard García, Fernando Pereira, and Noelia Pérez for taking care of field experiments to advance seed generations at INIA Uruguay.

For the WCM chapter, I greatly appreciate Dr. Mike Smith and his lab for providing us with mite colonies and their guidance on phenotyping and greenhouse space to conduct the phenotyping. Also, thanks to Drs. Shuyu Lui and Jackie Rudd from Texas A&M for sharing information about WCM resistance in wheat and the Lui Lab for leading the work to validate the molecular markers. Thanks to Dr. Rob Graf from AAFC/AAC Canada for providing us with seed from wheat lines carrying the *Cmc1* resistant gene.

Finally, I am very thankful to my friends and family, from here and in Uruguay, for their support and for cheering me up during this journey. I have no words to describe the support and encouragement that my husband, Pedro, has given. So many names to mention and so many good memories. K-State and The Little Apple have a place in my heart now and forever.

Dedication

To my Dad, ‘Carlitos’ Silva.

‘Be humble, be kind, be generous, and life will reward you’

Chapter 1 - Breeding Disease-Resistant Wheat

Wheat Importance and Evolution

The continuous world population growth, expected to be at 9.7 billion by 2050 (FAO, 2017), combined with more extreme weather events, are threatening food supply and food security, demanding an increase in food production. However, the grain yield of the primary staple crops has been steadily increasing, but not at the rate needed to meet these projections (Ray et al., 2012). Wheat is the most widely grown cereal, responsible for around 20% of the daily human nutrition requirements (Hawkesford et al., 2013). Wheat yield production needs to increase by 38% in order to match the projected food demand over the next 40 years. (Ray et al., 2013). Even though wheat yields are increasing, the growth rate is not enough to double its production to reach the demand (Fig. 1.1) (Ray et al., 2013). Moreover, the more extreme weather events also impact the dynamics of pathogens that have a remarkable impact on yield losses (Savary et al., 2019). One of the many complimentary strategies needed to achieve higher yields is to unlock and introduce genetic diversity from wild relatives to increase resistance against pathogens (Keller et al., 2018; Mondal et al., 2016). This will increase the genetic base of resistance in wheat and enable more robust and sustainable production in the face of less favorable and highly variable climates and increased pathogen pressure.

Wheat Origin

Cultivated bread wheat (*Triticum aestivum* L.) is an allohexaploid species with three complete sets of homoeologous chromosomes (2n = 6x = 42, AABBDD), which originated from two independent hybridization events involving three different but closely related diploid species, each contributing with one of the three subgenomes (Fig. 1.2) (Dvořák, 1976; Feldman & Levy, 2012; Pont et al., 2019). It is well documented that during polyploidization, domestication, and breeding, wheat diversity experienced a genetic bottleneck (Akhunov et al., 2010; Bevan et al., 2017; Haudry et al., 2007; Singla & Krattinger, 2016). Therefore, genetic diversity for some traits could be narrow and rarely present in the bread wheat germplasm pool (Skoracka et al., 2018; Tatineni & Hein, 2018). Notwithstanding, genetic diversity is the foundation for crop improvement. When genetic diversity is scarce, we can turn to crop wild relatives as donors of

new diversity to introduce into the breeding pipeline (Gill & Raupp, 1987; Jia et al., 2013; Singh et al., 2019; Singla & Krattinger, 2016).

The Donor of the D subgenome of Wheat

Aegilops tauschii is the diploid donor of the D genome of cultivated bread wheat (Fig. 1.2). It originates from the Caspian Sea region and is distributed from eastern Turkey to China and Pakistan. Two morphologically and genetically different lineages can be distinguished within *Ae. tauschii*, lineage 1 (L1) which has been known as subspecies *tauschii*, and L2 known as subsp. *strangulata*, the latter being the donor of the bread wheat D subgenome (Dvorak et al., 1998; Gill, 2013; Singh et al., 2019; Wang et al., 2013). Furthermore, it has been suggested the occurrence of a third lineage (L3) represented by few accessions (Singh et al., 2019). Given that *Ae. tauschii* can hybridize with wheat, it has been used as a genetic resource to improve wheat for economically important traits. Many resistance genes were originally discovered from *Ae. tauschii* have been introgressed into bread wheat and deployed into wheat varieties, confirming that is a valuable source of genetic diversity where to search for new disease resistance genes (Gill & Raupp, 1987; Kishii, 2019; Mondal et al., 2016; Singh et al., 2019).

Breeding for Disease Resistance

Diseases of wheat cause substantial economic losses and reduce yield production in all growing environments (Singh et al., 2016; Singh & Rajaram, 2002). Globally, wheat yield loss due to pathogens and pests was estimated to be 21.5%, ranging between 10.1% and 28.1% depending on the disease and the geographic region (Fig. 1.3) (Savary et al., 2019). Several strategies are offered for disease control (E.g. chemicals, cultural practices, and biological control, among others), however, genetic resistance is the best strategy as it does not have an additional cost for farmers, having huge environmental benefit by reducing the use of fungicides (Singh et al., 2016). Still, breeding for disease resistance is a long-term process, where its success depends mainly on the nature and diversity of the pathogen population, type, and availability of genetic resistance, and factors related to disease screening and selection (Singh & Rajaram, 2002).

Resistance Types

Traditionally, the different types of resistance have been described as vertical (controlled mainly by major genes) and horizontal (controlled by minor genes). The former is also named qualitative resistance and typically shows a complete or near-complete resistance response, explained primarily by canonical resistance gene types, including the nucleotide-binding domain leucine-rich repeat (NLR) family. On the other hand, horizontal resistance is also known as quantitative, explained by multiple genes of small effect usually of additive nature, providing an incomplete or partial phenotype that translates into a continuum of phenotypic variation (Poland et al., 2009; Nelson et al., 2018). Even though qualitative resistance is associated with high resistance, it is typically race-specific meaning that is effective against certain but not all pathogen races/isolates/biotypes and it is also rapidly overcome by pathogen selection and evolution. On the other hand, quantitative resistance is associated with durable resistance and in some cases is also broad-spectrum, features that are highly valuable to have in released varieties (Nelson et al., 2018). Nonetheless, authors are now avoiding the use of the terminology 'vertical' and 'horizontal', and often describing the types of resistances as PAMP-triggered immunity (PTI) and effector-triggered immunity (ETI). The immune response PTI is activated when highly conserved molecules, known as pathogen-associated molecular patterns (PAMPs), are detected by pattern recognition receptors (PRRs). PTI is the first layer of plant defense that is extracellular. However, pathogens can overcome the PTI response by secreting a different type of pathogen molecules called effectors, activating the ETI immune response. As a reaction, plants can recognize these effector molecules through the development of R proteins, with the majority of them belonging to the NLR family. The ETI response is responsible for a co-evolution between the plant and the pathogen (Dodds & Rathjen, 2010; Thomma et al., 2011). These resistance mechanisms were described in a four-phased zigzag model by Jones & Dangl (2006). Even though these two mechanisms have their characteristics and can be differentiated, there has been growing evidence indicating that a continuum exists between PTI and ETI (Thomma et al., 2011).

Disease Resistance Strategies

The ultimate goal of plant breeders working towards disease-resistance crops is to discover novel resistances and develop strategies to introduce and deploy the resistance, to ultimately prevent disease and enhance global productivity. For this reason, breeding programs are continually evaluating, selecting, and introducing germplasm to search for new sources of resistance (Nelson et al., 2018). Resistance based on a single gene, even though simple and fast to identify and incorporate, is often only effective in the short-term, rapidly 'eroding' this resistance through pathogen selection and evolution giving rise to virulent new races on the resistance gene (McDonald & Linde, 2002). However, other strategies can be implemented to achieve durable disease resistance. One strategy is to combine several resistance genes into a single background through pyramiding (McDonald & Linde, 2002). This process can be further accelerated by applying marker-assisted selection. Yet, the success depends on having identified enough genes with different recognition ranges and also the corresponding molecular marker. Another strategy is to create cassettes of genes, containing multiple genes stacked together that could be inserted as a single locus (Wulff & Moscou, 2014). This strategy was recently achieved for wheat rusts by stacking five genes conferring broad-spectrum resistance (Luo et al., 2020). However, this strategy necessitates having a deep understanding of the gene structure, a feature that is not very common for many genes since only a few have been cloned so far (Keller et al., 2018). Nonetheless, both these strategies could be achieved by combining only major genes, some major genes coupled with minor genes, or only minor genes, with the two latter approaches being more desirable to achieve durable resistance (Luo et al., 2020; Nelson et al., 2018). Moreover, cassettes stacking more than five genes, or incorporating two different cassettes could increase durability (Luo et al., 2020). Ultimately, which is the optimal strategy to achieve durable disease resistance will depend on the genotype diversity, type of reproduction system, and level of genotype flow of the pathogen population

Exploiting Resistance from Diverse Germplasm

In order to keep up with the speed of pathogen evolution, breeders are constantly searching for novel sources of resistance as pathogens erode deployed resistances and new diseases appear causing severe epidemics and yield losses (Wulff & Dhugga, 2018). Moreover, variation and

resistance for some diseases have become limited or is absent in the primary genetic pool of wheat. New resistances could be found from different sources such as landraces, germplasm collections, or wild relative species. While these non-adapted germplasm resources are often rich in diverse and novel resistance, they have many undesirable alleles, making the identification, introgression, and deployment of these resistances very challenging (Nelson et al., 2018; Wulff and Moscou, 2014). Additional variation can be achieved by directly crossing wild species with wheat, by recreating wheat-producing synthetics, by creating new diversity through mutagenesis, by genetic transformation, and by genome editing (Bevan et al., 2017; Gill & Raupp, 1987; Hawkesford et al., 2013; Nelson et al., 2018; Wulff & Dhugga, 2018).

Modern Breeding Tools

Genomic and phenomics tools are allowing us to better understand the relation between genotype and phenotype, accelerating the identification of novel resistance and cloning of resistance genes (Nelson et al., 2018; Wulff & Dhugga, 2018). The first round of application of modern tools started with the decrease in the sequencing cost by applying genome-wide association studies and genomic selection to identify quantitative trait loci and genomic regions associated with disease resistance. More recently, the second round of technological advances in sequencing strategies such as RenSeq, MutRenSeq, MutChromSeq, and AgRenSeq are facilitating and accelerating the identification of new resistance genes (Bettgenhaeuser & Krattinger, 2019) and making them available to introgress into wheat. However, all these genomic tools should be complemented by accurate, reproducible, and high-throughput phenotyping tools (Sánchez-Martín & Keller, 2019).

General Objective

The general objective of this dissertation was to contribute disease-resistant wheat germplasm to broaden genetic resources available for wheat breeders to sustain wheat production and increase our understanding of the genetic architecture and the genetic basis of disease resistance. The combination of improved germplasm with an increased understanding of the genetic basic can direct breeding efforts to more efficient breeding strategies. We studied three different diseases of wheat by applying different approaches such as genome-wide association mapping, genomic

selection, and high-throughput phenotyping. In the second chapter, we applied phenomics and genomics tools to understand the genetic architecture of the viral disease barley yellow dwarf. In the third chapter, we utilized mutagenesis and characterization of a wild relative of wheat to study the genetic basis of resistance to wheat head blast. Lastly, in the fourth chapter, we investigated the genetic basis of wheat curl mite resistance in the wheat wild relative *Aegilops tauschii.* Overall, our results contribute to better understand the genetic basis of three economically important wheat diseases and highlight both the necessity and the promise to search for novel sources of resistance in wild wheat species to broaden the genetic diversity of resistance available for wheat improvement.

References

Akhunov, E.D., Akhunova, A.R., Anderson, O.D. et al. (2010). Nucleotide diversity maps reveal variation in diversity among wheat genomes and chromosomes. *BMC genomics*, *11*(1), 702. https://doi.org/10.1186/1471-2164-11-702

Bevan, M., Uauy, C., Wulff, B. et al. (2017). Genomic innovation for crop improvement. Nature 543, 346–354 https://doi.org/10.1038/nature22011

Dodds, P. N., & Rathjen, J. P. (2010). Plant immunity: towards an integrated view of plant–pathogen interactions. Nature Reviews Genetics, 11(8), 539-548. https://doi.org/10.1038/nrg2812

Dvořák, J. (1976). The relationship between the genome of *Triticum urartu* and the A and B genomes of *Triticum aestivum*. Canadian Journal of Genetics and Cytology, 18(2), 371-377. https://doi.org/10.1139/g76-045

Dvorak, J., Luo, M. C., Yang, Z. L., & Zhang, H. B. (1998). The structure of the *Aegilops tauschii* genepool and the evolution of hexaploid wheat. Theoretical and Applied Genetics, 97(4), 657-670. https://doi.org/10.1007/s001220050942

Feldman, M., & Levy, A. A. (2012). Genome evolution due to allopolyploidization in wheat. Genetics, 192(3), 763-774. https://doi.org/10.1534/genetics.112.146316

Gill, B. S. (2013). SNPing *Aegilops tauschii* genetic diversity and the birthplace of bread wheat. New Phytologist, 198(3), 641-642. https://doi.org/10.1111/nph.12259

Gill, B. S., & Raupp, W. J. (1987). Direct Genetic Transfers from *Aegilops squarrosa* L. to Hexaploid Wheat 1. Crop Science, 27(3), 445-450. https://doi.org/10.2135/cropsci1987.0011183X002700030004x

Haudry, A., Cenci, A., Ravel, C., *et al*. (2007). Grinding up wheat: a massive loss of nucleotide diversity since domestication. Molecular biology and evolution, 24(7), 1506-1517. https://doi.org/10.1093/molbev/msm077

Hawkesford, M. J., Araus, J. L., Park, R., et al. (2013). Prospects of doubling global wheat yields. Food and Energy Security, 2(1), 34-48. https://doi.org/10.1002/fes3.15

Jia, J., Zhao, S., Kong, X., et al. (2013). *Aegilops tauschii* draft genome sequence reveals a gene repertoire for wheat adaptation. Nature, 496(7443), 91-95. https://doi.org/10.1038/nature12028

Jones, J., & Dangl, J. (2006). The plant immune system. Nature 444, 323–329. https://doi.org/10.1038/nature05286
Keller, B., Wicker, T., & Krattinger, S. G. (2018). Advances in wheat and pathogen genomics: implications for disease control. Annual Review of Phytopathology, 56, 67-87. https://doi.org/10.1146/annurev-phyto-080516-035419
Kishii, M. (2019). An update of recent use of *Aegilops* species in wheat breeding. Frontiers in Plant Science, 10, 585. https://doi.org/10.3389/fpls.2019.00585
McDonald, B. A., & Linde, C. (2002). Pathogen population genetics, evolutionary potential, and durable resistance. Annual review of phytopathology, 40(1), 349-379. https://doi.org/10.1146/annurev.phyto.40.120501.101443
Mondal, S., Rutkoski, J. E., Velu, G., et al. (2016). Harnessing diversity in wheat to enhance grain yield, climate resilience, disease and insect pest resistance and nutrition through conventional and modern breeding approaches. Frontiers in plant science, 7, 991. https://doi.org/10.3389/fpls.2016.00991
Nelson, R., Wiesner-Hanks, T., Wisser, R., & Balint-Kurti, P. (2018). Navigating complexity to breed disease-resistant crops. Nature Reviews Genetics, 19(1), 21. https://doi:10.1038/nrg.2017.82
Luo, M., Xie, L., Chakraborty, S. et al. (2020). A five-transgene cassette confers broad-spectrum resistance to a fungal rust pathogen in wheat. Nature Biotechnology, 1-6. https://doi.org/10.1038/s41587-020-00770-x
Poland, J. A., Balint-Kurti, P. J., Wisser, et al. (2009). Shades of gray: the world of quantitative disease resistance. Trends in plant science, 14(1), 21-29. https://doi.org/10.1016/j.tplants.2008.10.006
Pont, C., Leroy, T., Seidel, M., et al. (2019). Tracing the ancestry of modern bread wheats. Nature genetics, 51(5), 905-911. https://doi.org/10.1038/s41588-019-0393-z
Rasheed, A., Ogbonnaya, F. C., Lagudah, E., et al. (2018). The goat grass genome's role in wheat improvement. Nature plants, 4(2), 56-58. https://doi.org/10.1038/s41477-018-0105-1
Ray, D. K., Mueller, N. D., West, P. C., & Foley, J. A. (2013). Yield trends are insufficient to double global crop production by 2050. PloS one, 8(6), e66428. https://doi.org/10.1371/journal.pone.0066428
Ray, D. K., Ramankutty, N., Mueller, N. D., et al. (2012). Recent patterns of crop yield growth and stagnation. Nature communications, 3(1), 1-7. https://doi.org/10.1038/ncomms2296
Sánchez-Martín, J., & Keller, B. (2019). Contribution of recent technological advances to future resistance breeding. Theoretical and Applied Genetics, 132(3), 713-732. 2 https://doi.org/10.1007/s00122-019-03297-1
Savary, S., Willocquet, L., Pethybridge, S. J., et al. (2019). The global burden of pathogens and pests on major food crops. Nature ecology & evolution, 3(3), 430-439. https://doi.org/10.1038/s41559-018-0793-y
Skoracka, A., Rector, B. G., & Hein, G. L. (2018). The interface between wheat and the wheat curl mite, Aceria tosichella, the primary vector of globally important viral diseases. Frontiers in plant science, 9, 1098. https://doi.org/10.3389/fpls.2018.01098
Singh, R. P., & Rajaram, S. (2002). Breeding for disease resistance in wheat. FAO plant production and protection series, 30.

Singh, R. P., Singh, P. K., Rutkoski, J., et al. (2016). Disease impact on wheat yield potential and prospects of genetic control. Annual review of phytopathology, 54, 303-322. https://doi.org/10.1146/annurev-phyto-080615-095835

Singh, N., Wu, S., Tiwari, V., et al. (2019). Genomic analysis confirms population structure and identifies inter-lineage hybrids in *Aegilops tauschii*. Frontiers in plant science, 10, 9. https://doi.org/10.3389/fpls.2019.00009

Singla, J; Krattinger, S G. (2016). Biotic stress resistance genes in wheat. In: Wrigley, C W; Faubion, J; Corke, H; Seetharaman, K. Encyclopedia of Food Grains. Oxford: Elsevier, 388-392. https://doi.org/10.1016/B978-0-12-394437-5.00229-1

Tatineni, S., & Hein, G. L. (2018). Genetics and mechanisms underlying transmission of Wheat streak mosaic virus by the wheat curl mite. Current opinion in virology, 33, 47-54. https://doi.org/10.1016/j.coviro.2018.07.012

Thomma, B. P., Nürnberger, T., & Joosten, M. H. (2011). Of PAMPs and effectors: the blurred PTI-ETI dichotomy. The plant cell, 23(1), 4-15. https://doi.org/10.1105/tpc.110.082602

United Nations, Department of Economic and Social Affairs, Population Division. (2015). World population prospects: The 2015 revision. key findings and advance tables. New York, USA.

Wang, J., Luo, M. C., Chen, Z., et al. (2013). *Aegilops tauschii* single nucleotide polymorphisms shed light on the origins of wheat D-genome genetic diversity and pinpoint the geographic origin of hexaploid wheat. New phytologist, 198(3), 925-937. https://doi.org/10.1111/nph.12164

Wulff, B. B., & Dhugga, K. S. (2018). Wheat—the cereal abandoned by GM. Science, 361(6401), 451-452. https://doi.org/10.1126/science.aat5119

Wulff, B. B., & Moscou, M. J. (2014). Strategies for transferring resistance into wheat: from wide crosses to GM cassettes. Frontiers in Plant Science, 5, 692. https://doi.org/10.3389/fpls.2014.00692

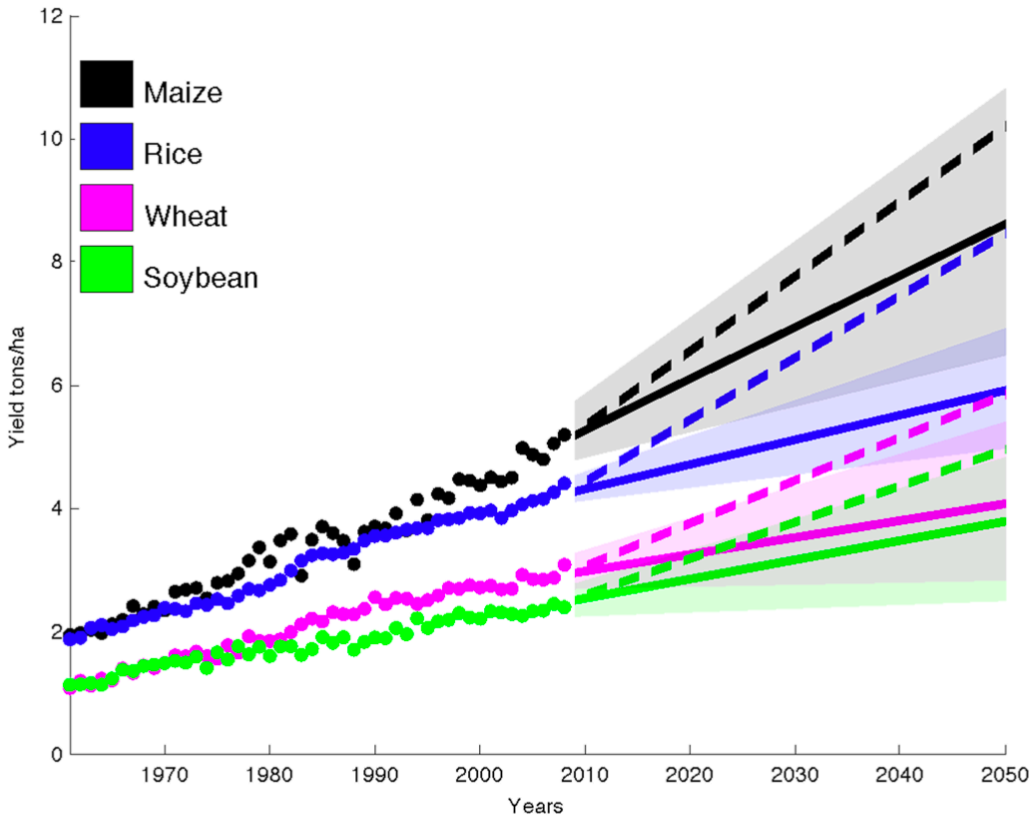

Figure 1.1 – Global projections on yield trends for the main cultivated crops.

Global projections on yield trends for maize, rice, wheat, and soybean, as described in Ray et al. (2013). Closed circles represent observed global yield data from 1961–2008. Solid lines represent the projected yield for each crop from 2009 up to 2050. Dashed lines represent the needed yield increase of 2.4% to double food production by 2050. Shading represents the 90% confidence region from 99 bootstrapped samples. Image obtained from Ray et al., 2013.

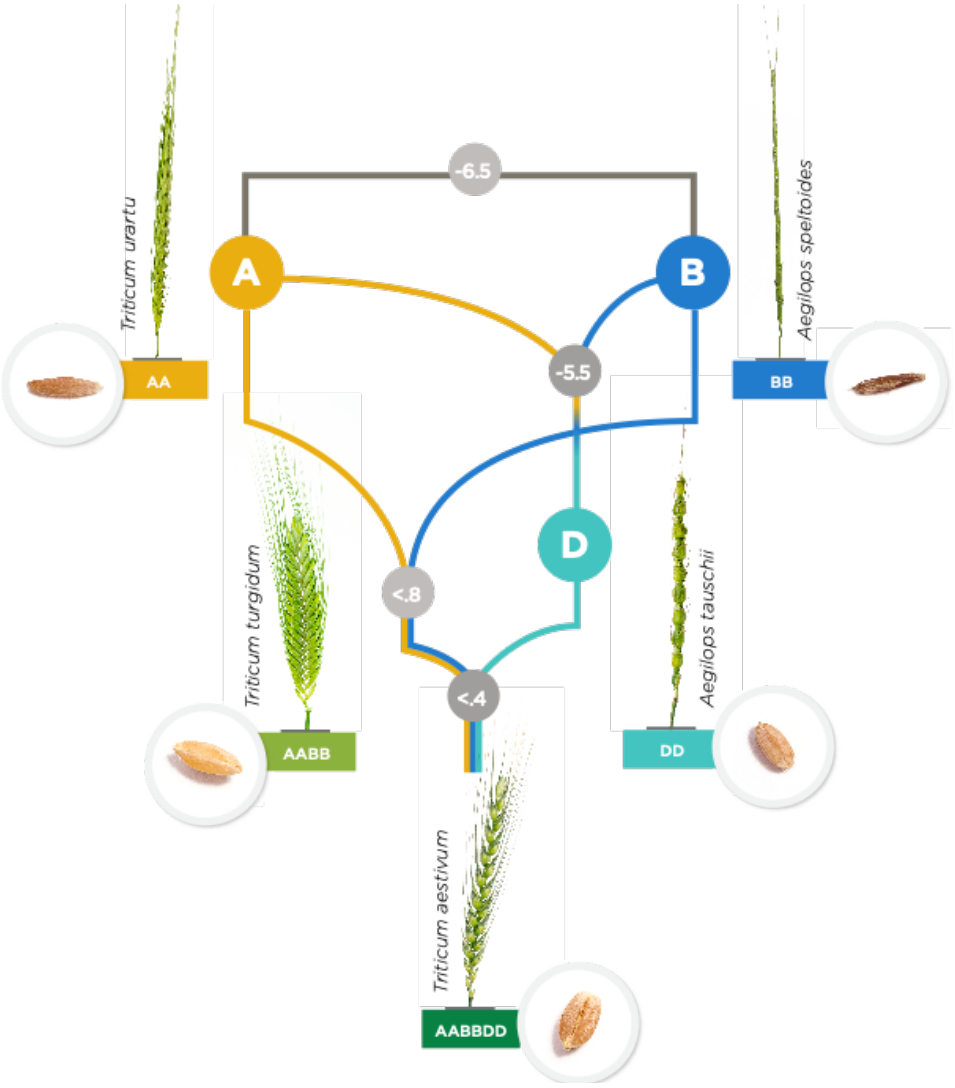

Figure 1.2 – Evolution of bread wheat.

About 6.5 million years ago (Ma) a common ancestor differentiated into the AA and BB diploid genome lineages. These formed the diploid precursor DD genome with a first hybridization approximately 5.5 Ma. Around 0.8 Ma the allotetraploid AABB genome of durum wheat (*Triticum turgidum)* evolved by hybridization between a close relative of *Aegilops speltoides* (BB) presumably extinct and *T. urartu* (AA) followed by polyploidization. Almost 4,000 years ago (ka), bread wheat originated by allopolyploidization from hybridization between domesticated emmer wheat (AABB) and *Ae. tauschii* (DD).

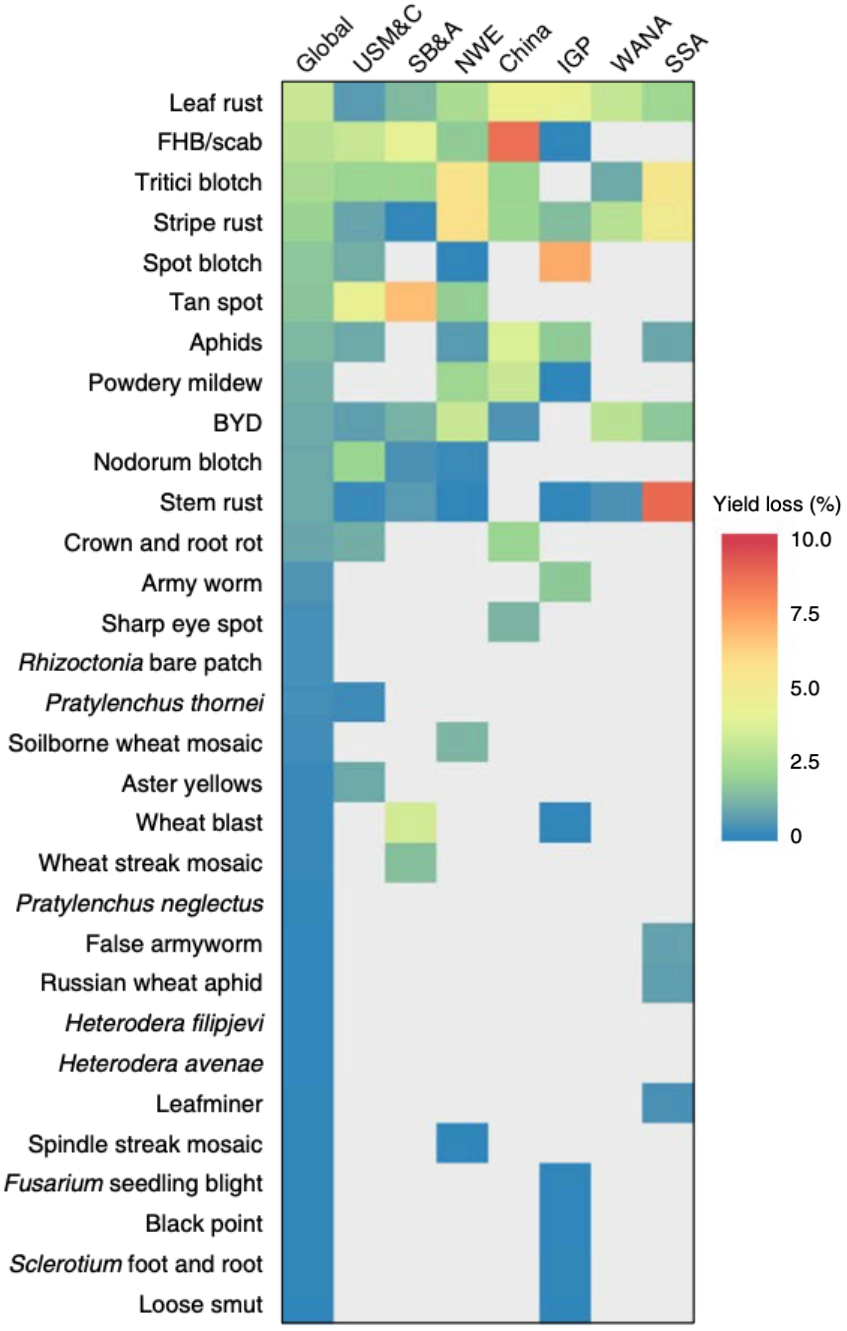

Figure 1.3 – Wheat diseases and pests.

Wheat yield losses globally and main food hotspots, per pathogen or pests as described in Savary et al., 2019. Heat map shows yield losses per pathogen or pest in percentage. Main food security hotspots: United States Midwest and Canada (USM&C); South Brazil, Paraguay, Uruguay and Argentina (SB&A); Northwest Europe (NWE); main-land China (China); the Indo-Gangetic Plain (IGP); West Asia and North Africa (WANA); Sub-Saharan Africa (SSA). Image obtained from Savary et al., 2019.

Chapter 2 - Applied phenomics and genomics tools for improving barley yellow dwarf resistance in winter wheat

General introduction about Barley Yellow Dwarf

Barley yellow dwarf (BYD) is a worldwide disease caused by aphid transmitted viruses (Shah et al., 2012). This viral disease affects all small grain cereals such as wheat, barley, and oat, and at least a hundred other grass species in the *Poaceae* family (D'arcy & Burnett, 1995). The disease was first identified in California in 1951 appearing in barley (Oswald and Houston, 1953). It is now the most widely distributed and the most economically important viral disease of wheat (Ayala et al., 2001; Ayala-Navarrete & Larkin, 2011; Choudhury et al., 2017). In Kansas, BYD is the fourth most significant wheat disease in terms of average estimated yield losses with an average yield loss of approximately 1% estimated over the past 20 years (Hollandbeck et al, 2019), equivalent to a $10 million losses per year. However, yield losses are highly variable depending on the environment, management practices, the host, and the genetic background, ranging from 5% to 80% yield losses in a single field (Miller et al., 1997; Perry et al., 2000; Gaunce and Bockus, 2015). Moreover, the wide host range and the complex lifestyle of its vectors make BYD extremely difficult to manage, and different management strategies are more optimal depending on climate and location. Thus, in many production environments, particularly the Central and Eastern regions of Kansas, BYD is often the most economically impactful disease facing growers.

Five different viral strains of barley yellow dwarf viruses, all belonging to the *Luteoviridae* family and classified into two species from different genera, Barley yellow dwarf virus (BYDV, genus *Luteovirus*) and Cereal yellow dwarf virus (CYDV, genus *Polerovirus*) can cause BYD disease (Choudhury et al. 2017). The viruses are small with icosahedral shape (~ 25 nm diameter), all composed of a single-stranded positive RNA molecule, with a genome size of 5.5-6kb (Shah et al., 2012; Krueger et al. 2003). There are more than 25 aphid species that can transmit the disease, but only four species are the primary vectors (Choudhury et al., 2017; D'arcy, 1995). The different viral strains were named to reflect the most common aphid species transmitting each strain. These are, RPV (*Rhopalosiphum padi* virus) mainly transmitted by

Rhopalosiphum padi and commonly known as bird cherry oat aphid, RMV (*Rhopalosiphum maidis* virus) mainly transmitted by *R. maidis* or corn leaf aphid, MAV (*Macrosiphum avenae* virus) specifically spread by *Sitobion avenae* or English grain aphid, SGV (*Schizaphis graminum* virus) most efficiently transmitted by *Schizaphis graminum* or greenbug, and PAV transmitted most efficiently by *R. padi* and *S. avenae* (Walls et al., 2019; Choudhury et al. 2017). In Kansas, the most common virus is PAV transmitted by the bird cherry oat aphid and the green bug (Rotenberg et al., 2015).

Virus transmission occurs only by aphid, being initiated when virus-free aphids feed on infected plants. Similarly, healthy plants become infected only after being fed by aphids carrying the viruses. Virus is not transmitted through seed and they cannot be spread mechanically. Wingless aphids survive the winter in grasses and volunteer plants from where they can directly transfer to different plants, alternatively, they can develop wings that accelerate aphid spread. The wings are formed when the quality of the host plant declines, such as at maturity, or under unfavorable environmental conditions (Chapin et al. 2001). Thus, the rate of infection, the spread of BYD and the uniformity of disease severity across a field and production zones is highly impacted by the environment and can be quite variable. Environmental factors such as light intensity and temperature, play an important role in the disease cycle of BYD. It has been shown that high light intensity, moist, and cool temperatures (below 20ºC) usually favor the expression of BYD symptoms, which may attract aphids to feed on virus-infected plants, promoting the transmission and spreading of the virus (Shah et al., 2012).

Barley yellow dwarf disease symptoms are highly variable depending on the crop, the variety, the time and developmental stage when the infection occurs, the aphid pressure, and the environmental conditions (Shah et al., 2012). More importantly, the symptoms can easily be confused with other viral disease symptoms such as wheat streak mosaic virus symptoms, and also with nutrient deficiency or environmental stresses like waterlogging, all of which makes BYD characterization in the field extremely challenging (Shah et al., 2012). BYD typical symptoms include leaf discoloration in shades of yellow, red, or purple, specifically starting at the tip of the leaf and spreading from the margins toward the base, plant stunting or dwarf appearance, biomass reduction by reducing the number of tillers, kernels per spike, kernel weight and root growth (Choudhury et al., 2019; Riedell et al., 2003), delay of heading date (D'arcy,

1995), reduction of chlorophyll content (Jensen, 1972), effects on grain quality traits such as reduction on starch content and average kernel weight (Peiris et al., 2019), and grain yield decrease.

Currently, there is no simple solution to control BYD, however, an accurate diagnosis of the presence of the viruses using immunoassays or RNA amplification methods is necessary to confirm the presence of BYDV or CYDV. Cultural methods that have been proven to impact BYD management are control of weeds and volunteer cereals, use of non-cereal cover crop rotations to minimize virus and vector reservoirs, and altering planting date by delaying sowing specifically to avoid aphid vectors and reduce aphid pressure. Another approach for BYD management is through chemical control by using systemic insecticidal seed treatment to help to reduce early aphid presence and primary spread, and foliar sprays to help with secondary spread. A very detailed study investigating the effect of planting date, genotype, and insecticidal seed treatment on BYD symptoms concluded that adopting wheat varieties with high levels of BYD resistance/tolerance was the most effective single strategy to reduce BYD. Moreover, the most desirable response was obtained when the three different management practices were combined (Bockus et al., 2016). Nevertheless, the unpredictability of the disease makes it very challenging to identify when to apply control measures, and thus making the use of genetic resistance/tolerance the most appealing and cost-effective option to control BYD.

Breeding strategies involving genetic resistance/tolerance can target either the aphids or the virus. Moreover, resistance/tolerance to the aphid can be achieved by three different strategies, antixenosis, antibiosis, or tolerance (Girvin et al., 2017). However, most of the efforts have been directed to the identification of viral tolerance, also known as 'field resistance', which has been reported to be polygenic (Qualset et al., 1973, Cisar et al., 1982; Ayala et al., 2002). It is important to make the distinction between tolerance and resistance mechanisms. Tolerant plants express fewer symptoms despite allowing multiplication of the viruses and the buildup of the viral population in the field which has huge implications for the spreading of the disease. In other words, a tolerant plant does not stop the virus but has the ability to maintain yield under BYD infection. On the other hand, resistance is based on the restriction of virus multiplication and spread, ensuring a decrease in disease symptoms. Resistance is a more desirable strategy

because allows the reduction and elimination of viral inoculum and subsequent epidemics (Comeau and Haber, 2002).

To date, no major gene conferring a large resistance effect has been identified in bread wheat, and only four resistance/tolerance genes have been described for BYD. *Bdv1*, a partially effective gene located on chromosome 7DS, is the only gene described and present in the primary pool of wheat, originally identified in the wheat cultivar 'Anza' (Singh et al., 1993; Qualset et al., 1984), providing resistance to some but not all the viruses that cause BYD (Ayala-Navarrete & Larkin, 2011). The other three named genes were all contributed by the wild relative *Thinopyrum intermedium* or wheatgrass (Zhang et al., 2009). *Bdv2* and *Bdv3* are both located on a translocation segment on wheat chromosome 7DL (Brettel et al., 1988; Sharma et al., 1995) and *Bdv4* is located on a translocation segment on chromosome 2D (Larkin et al., 1995; Lin et al., 2007). *Bdv2* was the first gene successfully introgressed in wheat breeding programs (Banks et al., 1995) and deployed into varieties. There have been various molecular markers developed for the BYD resistance genes for genotyping and to apply maker-assisted selection (Choudhury et al., 2017; Jarošová et al., 2016). Other genomic regions associated with BYD resistance have been described from wheat in almost all chromosomes (Choudhury et al., 2019; Ayala et al. 2002). Recently, the wheat streak mosaic virus resistance gene *Wsm3* has been associated with some levels of resistance against BYD, and it is likely an allele of *Bdv2* and *Bdv3* (Bernd Friebe personal communication). Furthermore, resistance to BYD has been found in other *Triticeae* species (Li and Wang, 2009; Zhang et al., 2009).

Resistance and tolerance genes to BYD in wheat are rare, and the limited genetic resistance/tolerance present in the wheat germplasm pool is very complicated to characterize, probably due to the polygenic nature of many genes of small effect. This coupled with the absence of wheat varieties with good levels of resistance/tolerance, and the difficulty of phenotype BYD symptoms makes breeding for BYD extremely challenging. Nevertheless, breeding programs have large efforts for targeting BYD resistance/tolerance due to the economic importance of this disease.

The development goal of this chapter is to release wheat lines to breeders with resistance/tolerance to BYD. The research goal is to characterize and identify promising wheat

lines for BYD resistance/tolerance by utilizing existing state-of-the-art breeding tools developed for Kansas. This chapter is focused on: Applying modern tools to improve wheat against barley yellow dwarf by evaluating KSU Wheat Breeding Program advanced breeding lines for BYD resistance/tolerance in field-screening nurseries. The objective of the study was to implement high-throughput phenotyping for BYD field characterization in order to improve the phenotyping of BYD symptoms and to characterize advance breeding lines against BYD and implement genomic predictions.

Applying modern tools to improve wheat against barley yellow dwarf

Abstract

Barley yellow dwarf (BYD) is one of the major viral diseases of cereals. In the Great Plains of the United States, BYD is one of the most significant diseases impacting wheat production. To breed resistance to BYD, selection of resistance and tolerant germplasm is needed. Phenotyping BYD symptoms, however, is extremely challenging due to a complex pathosystem with variable infection rates and disease severity, and similarities with other biotic and abiotic stresses. Moreover, breeding for resistance is additionally challenging as the wheat primary pool germplasm lacks genetic resistance with most of the few resistance genes named to date originating from a wild relative species. The objectives of this study were to, i) evaluate the use of high-throughput phenotyping tools to improve wheat BYD field phenotyping in advanced breeding lines, and ii) develop and test genomic predictions for BYD. Visual characterization, unmanned aerial systems (UAS), and genotyping-by-sequencing were used to phenotype and genotype wheat varieties and advanced breeding lines during five field seasons (2015-16 to 2019-20) under two insecticide treatments (insecticide treated versus untreated). Across all seasons, BYD severity was lower with the insecticide treatment, meanwhile, plant height ($PTHT_M$) and grain yield (GY) showed increased values. Moreover, BYD was negatively correlated or showed no correlation with $PTHT_M$ and GY. Broad-sense heritability was moderate to high for all the traits. Only 9.2% of the lines were positive for the presence of the translocated segment carrying *Bdv2* resistance gene located on chromosome 7DL. Despite the low frequency, we were able to map this region using a GWAS and demonstrated that is explained by *Bdv2*. In addition to 7DL, we mapped a potentially novel genomic region on 5AS.

Even though some of the traits collected with UAS showed to be correlated with BYD, we were not able to genetically map regions, which suggests that none of these traits has a common genetic base with BYD severity. In addition, we obtained relatively good predictive ability for BYD severity ranging between 0.06 – 0.26. Including *Bdv2* on the predictive model had a large effect for predicting BYD but almost no effect for predicting $PTHT_M$ and GY. This study was the first attempt to characterize and improve BYD field-phenotyping using HTP and apply GS to predict the disease. Further research on methods to improve BYD characterization and searching for new sources of resistance will be crucial for delivering BYD resistant germplasm.

Introduction

Wheat (*Triticum aestivum* L.) is one of the most essential food crops in the world that is constantly threatened by several biotic stresses. Among the most important viral stresses is barley yellow dwarf (BYD). This disease is widespread across the world and can cause significant reductions in yield in susceptible cultivars. The main symptoms of BYD include yellowing of leaves, stunting, and yield reduction. However, BYD incidence is very unpredictable and symptoms can be easily confused with abiotic stresses or other viral agents, making BYD phenotyping a difficult task and genetic resistance the preferred management strategy.

Resistance to BYD falls under the quantitative resistance class, where several genes with very small effects control the resistance response (Ayala et al., 2020). In addition, resistance to BYD in the wheat primary pool is very rare, making breeding for BYD resistance another challenging task. Thus, breeding for BYD resistance can be favored by applying strategies for more effective evaluation and exploitation of the resistance. In order to get a better understanding of quantitative traits, like BYD, consistent and high-throughput methods are needed for the identification of resistant/tolerant wheat lines for large-scale selection in breeding programs.

Novel genotyping and phenotyping approaches are now available to accelerate plant breeding (Mondal et al., 2016; Poland, 2015). On the one hand, we have now access to high-density genetic markers at a very low-cost owing to the rapid developments in sequencing, enabling us to apply molecular breeding for quantitative traits. Genomic selection (GS) has been proven useful

to breed for quantitative traits with complex genetic architecture and low heritability (E.g. yield, quality, and diseases such as Fusarium head blight), because it has greater power to capture loci with small effect compared with other marker-assisted selection strategies (Poland & Rutkoski, 2016; Meuwissen et al.,2001). On the other hand, high-throughput phenotyping (HTP) using unmanned aerial systems (UAS) or ground-based sensors, is proving to be useful to incorporate into breeding programs to increase genetic gain (Crain et al., 2018; Haghighattalab et al., 2016). Using the UAS for disease scoring can improve the capacity for rapid and non-biased evaluation of large field-scale numbers of entries.

Here we hypothesize that HTP using UAS and GS are effective approaches to assess field-based BYD characterization of wheat lines and have the power to boost genetic studies for BYD. The objective of this study was to assess the applicability of HTP and GS for improving BYD tolerance in wheat.

Materials and Methods

Plant Material

A total of 381 different wheat genotypes were characterized for BYD tolerance, including 30 wheat cultivars and 351 advanced breeding lines in nurseries over five years (Supplementary Table B.1). In each nursery, an unbalanced set of between 50 – 100 wheat entries were evaluated including both cultivars and breeding lines (Table 2.1). Cultivars ‘Art’ and ‘Everest’ were included in all the nurseries (seasons) as checks.

Field Experiments

Nurseries for BYD field-screening were conducted during five consecutive wheat seasons (2015-2016 to 2019-2020) (Table 2.1). Seasons 2015-16 and 2016-17 were conducted at Kansas State University (KSU) Rocky Ford experimental station (39˚13'45.60" N, 96˚34'41.21" W), whereas seasons 2017-18, 2018-19, and 2019-20 were planted at KSU Ashland Bottoms experimental station (39˚07'53.76" N, 96˚37'05.20" W). The nurseries were established for natural infections by early planting about three weeks ahead of the normal planting window in mid-September and planting spreader plots with BYD-susceptible variety ‘Art’ in borders. The nurseries included

advanced breeding lines from the KSU wheat breeding program (n = 50 – 100) and control checks plots with 'Art' (highly susceptible) and 'Everest' (tolerant), where the experimental unit was an individual six-row plot with 20 cm row spacing with plot dimensions of 1.5 m × 2.4 m. A split-plot field design with two or three replications was used where the main factor was insecticide treatment and the split factor was the wheat genotype. For the treated replications the seed was treated with insecticide at planting and 10-14 days rotation of foliar insecticide to kill the aphid vector. The control insecticide treatment received neither seed treatment nor foliar applications. Foliar fungicide was applied to the whole experiment as needed.

Phenotypic Data

Individual plots were assessed for i) BYD severity (BYD) characterized as the typical visual symptoms of yellowing and/or purpling on leaves using a 0 – 100% visual scale, determined directly after all plots were headed by recording the proportion of the plot exhibiting the symptoms (Table 2.1), ii) manual plant height/stunting (meters) ($PTHT_M$), iii) and grain yield (tons/ha) (GY, combination of test weight and moisture). The phenotypic data were recorded using the Field Book phenoapp (Rife and Poland, 2014).

High-Throughput Phenotyping (HTP)

In order to compliment the phenotypic data, we applied HTP using ground-based sensors or UAS (Table 2.2). Seasons 2015-16 and 2016-17 were characterized by a ground-based sensor system as described in Wang et al. (2018). For the other three seasons, we used a quadcopter DJI Matrice 100 (DJI, Shenzhen, China) carrying a MicaSense RedEdge-M multispectral camera (MicaSense Inc., United States). The HTP data was collected on multiple dates throughout the growth cycle from stem elongation to ripening (GS 30–90; Zadoks et al., 1974) (Table 2.2) following standard operating procedures developed within the Poland Lab at KSU (Wang et al., 2020; Wang et al., 2018). An automated pipeline was used to generate the orthomosaics and extract single plot-level phenotypic values (Wang et al., 2020; Wang et al., 2019) for digital plant height in meters ($PTHT_D$) and the normalized difference vegetation index (Rouse, 1973) (NDVI), calculated as,

$$NDVI = \frac{NIR-Red}{NIR+Red}$$ [Eq. 1]

where NIR and Red are the near-infrared and red band of the multispectral images and NDVI is the output raster layer. Both traits were selected based on their rationale for BYD characterization where PTHT is stunted with BYD and BYD most typical symptoms include chlorosis thus, influencing NDVI.

Statistical Data Analyses

First, the best linear unbiased estimator (BLUE) or adjusted mean was calculated for each entry for all the different traits (BYD, $PTHT_M$, GY, NDVI, $PTHT_D$, θ_{1NDVI}, θ_{2NDVI}, θ_{3NDVI}, θ_{1PTHT_D}, θ_{2PTHT_D}, and θ_{3PTHT_D}) individually for each season (Supplementary Table B.1), using the following model,

$$y_{ijklm} = \mu + G_i + T_j + GT_{ij} + R_{k(j)} + B_{l(k)} + C_{m(k)} + e_{ijklm}$$ [Eq. 2]

where y_{ijklm} is the phenotype for the trait of interest, μ is the overall mean, G_i is the fixed effect of the i^{th} entry (genotype), T_j is the fixed effect of the j^{th} insecticide treatment, GT_{ij} is the fixed effect of the interaction between the i^{th} entry and the j^{th} insecticide treatment (genotype by treatment effect), R_k is the random effect of the k^{th} replication nested within a treatment and distributed as iid $R_k \sim N(0, \sigma_R^2)$, $B_{l(k)}$ is the random effect of the l^{th} row nested within a replication and distributed as iid $B_{l(k)} \sim N(0, \sigma_B^2)$, $C_{m(k)}$ is the random effect of the m^{th} column nested within a replication and assumed distributed as iid $C_{m(k)} \sim N(0, \sigma_C^2)$, and e_{ijklm} is the residual for the $ijklm^{th}$ plot and distributed as iid $e_{ijklm} \sim N(0, \sigma_e^2)$. The models 'lme4' R package (Bates et al., 2014) was used for fitting the models.

The BLUE values obtained were used to inspect trait distributions and to calculate Pearson correlations between all traits. In addition, BLUE values were used to calculate the reduction in GY for each entry as the difference of GY under the different insecticide treatments. This variable reflects the level of BYD tolerance of each entry, and it was used to perform GWAS and GS analyses.

In addition, for NDVI and $PTHT_D$, and using the plot-level values extracted for the different collecting dates, we fitted a logistic non-linear regression model (Fox and Weisberg, 2011) as,

$$y = \frac{\theta_1}{1+ e^{-(\theta_2+\theta_3 x)}} + \epsilon \quad \text{[Eq. 3]}$$

where is y the phenotype for the trait of interest at the time-point x, θ_1 is the final value (upper asymptote) represented by the final NDVI or PTHT, θ_2 is the inflection point that represents the rate of senescence or time of maximum growth, θ_3 is the lag phase or onset of senescence or growth rate from planting, x is the calendar day or days of the year, and ϵ is the error (Supplementary Fig. B.3). The "nlme" R package was used for model fitting (Pinheiro et al., 2015). The model parameters obtained for each trait (θ_{1NDVI}, θ_{2NDVI}, θ_{3NDVI}, θ_{1PTHT_D}, θ_{2PTHT_D}, and θ_{3PTHT_D}) were used in addition to the other phenotypic traits to calculate BLUEs, distributions, correlations, and BLUPs.

Secondly, we used a mixed linear model to calculate the best linear unbiased predictors (BLUPs) for each entry in each nursery (season) (Supplementary Table B.1), using the same model as described in equation 2 but defining G_i, T_j, and GT_{ij} as random effects. BLUPs were used because of the unbalanced nature of the data (not all lines were evaluated in all the seasons). The BLUPs calculated for each season were then combined for GWAS and GS. Furthermore, we calculated broad-sense heritability on a line-mean basis by splitting the data for the different insecticide treatments as,

$$H^2 = \frac{\sigma_G^2}{\sigma_G^2 + \frac{\sigma_e^2}{r}} \quad \text{[Eq. 4]}$$

where σ_G^2 is the genotypic variance, σ_e^2 is the residual error variance, and r is the number of replications.

Genotypic Data

A total of 346 wheat entries were genotyped using genotyping-by-sequencing (GBS) (Poland et al., 2012) and sequenced on an Illumina Hi Seq2000. Single nucleotide polymorphisms (SNPs)

were called using Tassel GBSv2 pipeline (Glaubitz et al., 2014) and anchored to the Chinese Spring genome assembly v1.0 (International Wheat Genome Sequencing Consortium, 2014). SNP markers with minor allele frequency (MAF) < 0.01, missing data > 85%, or heterozygosity > 15% were removed from the analysis. After applying the filtering criteria, we retained 29,480 SNPs markers that were used to investigate the population structure through principal component analysis (PCA), genome-wide association analysis (GWAS), and genomic selection (GS). In addition, GBS data was used to run a bioinformatics pipeline to predict the presence or absence of the translocation on chromomere 7DL carrying the *Bdv2* gene for each entry (Supplementary Table B.1). Briefly, wheat and alien specific tags were identified using a training set of cultivars or lines that are known to be *Bdv2* positive and negative. The presence/absence of the segment was predicted based on relative counts of wheat or alien specific tags (Liangliang Gao & Kevin Dorn, under preparation).

Genome-Wide Association Analysis (GWAS)

For GWAS, the analysis was performed with a mixed linear model (Zhang et al., 2010) implemented in the 'GAPIT' R package (Lipka et al., 2012),

$$y = W_v + X\beta + Zu + e \qquad \text{[Eq. 5]}$$

where y is the vector of phenotypic BLUPs, v and β are unknown fixed effects representing marker effects and non-marker effects, respectively; and u is a vector of size n (number of individuals) for unknown random polygenic effects having a distribution with mean of zero and covariance matrix of $G = 2K\sigma_a^2$, where K is the kinship matrix calculated from the genetic markers and σ_a^2 is an unknown genetic variance. W, X and Z are the incidence matrices for v, β, and u, respectively, and e is the vector of random residual effects, normally distributed with zero mean and covariance $R = I\sigma_e^2$, where I is the identity matrix and σ_e^2 is the unknown residual variance. The threshold level for calling significant marker-trait associations and to avoid false positives was calculated using the false discovery rate correction with an experimental significance level value of 0.01. Manhattan plots were generated with 'CMplot' package in R software (https://cran.r-project.org/web/packages/CMplot/CMplot.pdf). The PCA analysis using

GBS-SNPs was performed with R software using the 'A.mat' function and the 'mean' imputation method from the 'rrBLUP' package (Endelman, 2011).

Genomic Selection (GS)

Using data from the five seasons, GS models using the genomic best linear unbiased predictor (G-BLUP) were developed to assess predictive ability. Within each season, a five-fold cross-validation method or leave-one-out strategy was implemented. For each prediction, we excluded all of the entries that were in a given season as a training population and used the entries from that excluded season as the prediction or testing population. Along with predicting all other seasons from each season, a model was evaluated with a leave-two-out cross-validation strategy, where the training population consisted of three seasons, and the remaining two seasons were predicted from the combined training population.

The GS model was fit with the training population using 'rrBLUP' *kin.blup* function (Endelman, 2011), with predictions then being made on the prediction population. The GS model equation used was,

$$y = \mu + Zu + e \qquad \text{[Eq. 6]}$$

where y is a vector of phenotypic BLUPs, μ is the overall mean, Z is an $(n \times m)$ matrix assigning markers to genotypes, u is a $(1 \times n)$ array of random effects of markers, and e is the vector of residual errors (Endelman, 2011). Predictive ability was assessed using Pearson's correlation (r) between the predicted value (G-BLUP) and the BLUP for the respective phenotype. In addition, for both GS strategies we also tested the effect of adding the presence/absence of *Bdv2* as a fixed effect cofactor, using the model,

$$y = \mu + X\beta + Zu + e \qquad \text{[Eq. 7]}$$

which combines parameters described in equation 6 and X is the matrix $(n \times 1)$ of individual observation for presence or absence of *Bdv2* and β is the fixed effect for the *Bdv2* measurements.

Results

Phenotypic data

We analyzed five years of BYD field-screening nurseries (seasons 2015-16 to 2019-20) characterizing a total of 381 wheat lines. The disease pressure and the expression of BYD associated symptoms varied each season, however, we were able to observe a significant effect of the insecticide treatment in all the seasons (Fig. 2.1). Across all seasons, BYD was lower on the insecticide-treated reps, while both $PTHT_M$ and GY increased. Season 2016-17 had the most conducive conditions for BYD screening, resulting in high average severity and a larger difference between mean values for the treated vs untreated blocks for all the manually collected traits (Fig. 2.1). There was general consistency in rank order across all seasons with the susceptible check 'Art' ranked among the highest in BYD severity (Supplementary Fig. B.1). Phenotypic correlations between the traits showed a negative correlation between BYD and GY for all the seasons and a negative or no correlation between BYD and $PTHT_M$ (Supplementary Fig. B.2). The same correlation trends were observed under both insecticide treatments. Broad-sense heritability was moderate to high for all the traits, ranging between 0.21 and 0.79 for the insecticide treated reps and between 0.41 and 0.84 for the untreated reps. Overall, across all traits, the insecticide-untreated reps showed higher H^2values, with season 2016-17 showing the higher values (Fig. 2.2).

For the HTP data collected with UAS (Table 2.2) (i.e. NDVI and $PTHT_D$), we obtained three different parameters (θ_1, θ_2, and θ_3) for each trait after fitting a logistic regression model using the data collected during the experiments (2015-16 season data was not included due to lack of quality) (Supplementary Fig. B.3). Correlations between these parameters and the phenotypic traits collected manually were different for all the traits (Supplementary Fig. B.2). For the insecticide-untreated reps, BYD resulted in a negative correlation with $\theta_2 NDVI$ and a positive correlation with θ_{3NDVI}, in most of the field seasons. We did not find a clear correlation pattern between BYD and θ_{PTHT_D}. For $PTHT_M$ we detected a positive correlation with θ_{1PTHT_D}across all seasons, and for GY we observed a positive correlation with $\theta_1 NDVI$ and $\theta_2 NDVI$, and a negative with $\theta_3 NDVI$ (Supplementary Fig. B.2).

Prediction of *Bdv2* resistance gene

We used GBS data to predict the presence/absence of the *Bdv2* resistance gene located on a translocation segment from intermediate wheatgrass on chromosome 7DL of bead wheat. We found that 33 out of the 346 wheat lines carry the *Th. intermedium* chromosomal translocation with *Bdv2* (Supplementary Table B.1). Interestingly, 28 of these *Bdv2* lines belong to the same breeding cycle, entering the advanced yield nursery stage of the KSU breeding program in the 2017-18 season. Furthermore, only 7 pedigrees are represented within the 28 *Bdv2* entries, meaning that some of these lines share exactly the same pedigree. The remaining 5 *Bdv2* lines were distributed in 2015-16 (n=3), 2018-19 (n=1), and 2019-20 (n=1). None of the lines from the season 2016-17 had the presence of *Bdv2* (Table B.1).

Population structure

We studied the population structure of 346 wheat lines using 29,480 GBS-derived SNP markers. The principal component analysis did not reveal a strong pattern of population structure (Fig. 2.3). Moreover, the variation explained by the first two principal components (7%) also supports the minimal population structure within a single breeding program. In addition, we explored if population structure had an association with the breeding status of the lines, the presence/absence of *Bdv2*, and the adjusted BYD severity score. We observed that the majority of the wheat cultivars released by KSU breeding program were located outside the cluster grouping all the breeding lines (Fig. 2.3A) and that all the lines with the presence of *Bdv2* cluster together (Fig. 2.3B). We did not identify any pattern for BYD severity associated with the population structure (Fig. 2.3C).

Genome-wide association analysis (GWAS)

To investigate the genetic architecture of BYD we performed GWAS analyses for all collected traits using the BLUP values for 346 lines and 29,480 SNP markers collected with GBS looking for any loci with singularly large effect. The first two principal components from PCA and the kinship matrix were included in the mixed model to account for population structure and genetic relatedness. We found significant marker-trait associations for BYD severity on chromosomes 5AS, 7AL, and 7DL (Fig. 2.4A). The highest peak was observed on the proximal end of

chromosome 7DL, located at 571 Mbp – 637 Mbp. To test the hypothesis that this association was explained by the resistance gene *Bdv2* (located on chromosome 7DL), we investigated the haplotypes defined by the 16 SNP markers associated with BYD severity and we were able to identify two haplotypes that exactly matched the presence or absence of *Bdv2* (Fig 2.4A). Besides, we also performed GWAS using the presence/absence of *Bdv2* as a binary phenotype. We mapped the same genomic region using both BYD severity and *Bdv2* presence/absence (Fig. 2.4B). This analysis (Fig. 2.4B) also detected the peak on chromosome 7AL, suggesting that the SNP markers on the 7AL peak are miss-anchored markers that should have mapped to 7DL. Lastly, we explored the effect of *Bdv2* on the adjusted mean of BYD and BYD BLUPs and we observed that the presence of *Bdv2* has a positive effect on both traits, reducing the disease severity c.a 10% (Fig. 2.5A). The significant peak on chromosome 5AS, located at 46 Mbp – 103 Mbp, was explained by 10 SNP markers, comprising two main haplotypes, one of them associated with reduced BYD severity (Fig 2.5B). When we combined the different 5AS haplotypes with the presence or absence of *Bdv2*, we observed that the presence of *Bdv2* had a positive effect, reducing the levels of BYD when combined with both 5AS haplotypes (Fig. 2.5C), and suggesting an additive effect. Unfortunately, we did not find any evident peak with significantly associated markers rather a few associations explained by single SNP marker, for the other evaluated traits (Supplementary Fig. B.4).

Genomic selection (GS)

To evaluate the potential of GS to predict BYD disease severity, we fit several GS models to the phenotypic BLUPs of BYD, PTH_M, and reduction in GY. To determine the predictive ability of GS, we used a five-fold cross-validation model or leave-one-out model to each trait individually by excluding one season as the testing population and using the remaining four seasons as the training population. Across all traits, prediction ability, calculated as the correlation between predicted value (GBLUP) and the phenotypic BLUP, ranged from -0.08 to 0.26. Nonetheless, there were differences between traits (Fig. 2.6). There was relatively good predictive ability for BYD severity ranging between 0.06 – 0.26, in comparison with $PTHT_M$ and reduction in GY resulting in a lower range from 0.02 – 017 and -0.08 – 0.2, respectively (Fig. 2.6). Evaluating the conformation of the training population, we observed that when including 2016-17 season,

prediction abilities were the highest for BYD but the lowest for the other two traits, implying that season 2016-17 is either a good season to train the models and / or a difficult season to predict.

To further investigate the power of GS, we developed models using a leave-two-out strategy, where two seasons were excluded from the training population and used as the testing population. We fitted GS models for all possible two-season combinations. This strategy resulted in slightly smaller training populations which decreased overall predictive ability (Fig. 2.6). This result was evident for BYD predictions where excluding two seasons had a larger negative impact. Lastly, we inquire into the effect of adding information about the presence/absence of the *Bdv2* resistance gene as a phenotypic fixed covariate into the GS models. Across the three traits there were differences in the effect of *Bdv2* on the predictive ability, showing a large effect for predicting BYD but almost no effect for $PTHT_M$ and reduction in GY (Fig. 2.6). The improved predictive ability for BYD was clearly reflected with the decrease of prediction ability obtained when season 2017-18 was excluded from the training population since most of the lines with the presence of *Bdv2* were evaluated in that season.

Discussion

Phenotypic data

The success of breeding for BYD resistance/tolerance is highly impacted by the ability to extensively characterize breeding material but also in how precise the disease characterization could be achieved. Even though BYD is spread worldwide, its incidence in a given year depends on several factors such as aphid pressure, planting date, and environmental conditions (E.g. temperature, rainfall, frost, etc.). In this study, we evaluated winter wheat advanced breeding lines during five seasons implementing a rigorous field approach, that ultimately allowed us to consistently have plots with BYD infection and contrasting uninfected or low incident plots. Moreover, by using large yield-size plots we were able to calculate the reduction in GY and use this parameter as an estimate of tolerance. However, the expression of BYD symptoms was highly inconsistent during the different seasons. Seasons 2015-16 and 2016-17 showed the best expression of the disease symptoms, supported by the wide range of BYD severity between treated and untreated replications (Fig. 2.1). Interestingly, both these seasons were conducted in the same experimental field (Table 2.1), suggesting that this location could favor the expression

of BYD. Moreover, weather conditions were variable for all the seasons, suggesting that these had a huge impact on the disease occurrence. While temperature records were similar for all the seasons, precipitation records did show some differences. Season 2017-18 was dryer than normal, with 34% less precipitation than the 30 years historical average (1981 – 2010). On the other hand, season 2018-19 was rainier than normal, with 58% more precipitation than the 30 years historical average (Supplementary Table B.2).

High-throughput phenotyping

Evaluating BYD resistance/tolerance using visual phenotypic selection can be challenging due to the complex nature of the disease and open to error (Poland and Nelson 2011). The use of HTP with UAS is gaining popularity within breeding programs because it further improves selection based on classical phenotyping. Accurate phenotyping is crucial for understanding the genetic basis of quantitative and complex traits like BYD. In this study, we used the UAS to complement the traditional BYD scoring. This tool improved our capacity for rapid and non-biased evaluation of large field-scale numbers of entries for BYD resistance/tolerance. We were able to determine strong correlation patterns between visual BYD severity and HTP derived parameters (Supplementary Fig. B.2), however, none of the traits collected with UAS had a common genetic base with BYD severity (Fig. 2.4 and Supplementary Fig. B.4). Disease scoring using HTP is scaling fast among breeding programs, however, how effectively use this data remains challenging. Some studies have shown that data collected with sensor-based tools can substitute and/or improve classical disease visual evaluation (Kumar et al., 2016; Sankaran et al., 2010; Zheng et al., 2018), however, from the best of our knowledge, our study is the first attempt to characterize BYD in wheat using HTP.

Genome-wide association analysis

Using GWAS we detected three quantitative trait loci (QTLs) on chromosomes 5AS, 7AL, and 7DL for BYD severity BLUPs values. To declare a QTL we considered only the regions having several SNP markers in linkage disequilibrium, clearly showing a peak, and not regions explained by single SNPs. We confirmed that the 7DL QTL was explained by the presence of the *Bdv2* resistance gene. Even though only 33 wheat lines resulted positive for the presence of

Bdv2, we still had enough power to detect its effect, suggesting that *Bdv2* has a strong effect on BYD under Kansas field conditions (Fig. 2.5). The relatively high heritability values obtained for the untreated replications (Fig. 2.2) allowed to detect a minor QTL on 5AS. A different study reported a QTL at 38cM on the short arm of chromosome 5A associated with yellowing symptoms caused by BYD (Marza et al., 2005). However, more information is needed to investigate if these QTLs are the same. Although the GWAS result found other significant markers (Fig. 2.4), these were ignored since they were individual SNPs which we assumed to be spurious associations. The only other study reporting GWAS for BYD in wheat was able to identify several markers associated with BYD resistance on chromosomes 2A, 2B, 6A, and 7A (Choudhury et al., 2019). However, in the study, the significance was defined by setting a very flexible significant threshold (significant level of $P < 0.001$ ($-\log10 (P) > 3$), and most of the association were explained by individual SNP markers, therefore probably detecting false-positive associations. GWAS results for the other traits used in this study did not discover genomic regions associated with the traits (Supplementary Fig. B.4). With our results we have confirmed the quantitative nature and complex genetic architecture of BYD resistance/tolerance, thus, moving forward with testing GS as a plausible strategy to study the genetic architecture of BYD.

Genomic selection

We evaluated several different GS models to identify the best approach for predicting BYD (Fig. 2.6). Overall, we observed some trends including i) incorporating years with consistent BYD disease data in the training population increased the model predictive ability, ii) predicting years with high disease pressure is equally difficult, iii) using major effect QTL, such as *Bdv2*, had increased prediction performance, suggesting that it is responsible for much of the predictive power. These results suggest that GS based on G-BLUP with *Bdv2* as fixed effects would lead to the greatest genetic gain for BYD breeding. Using selected major QTL as a fixed effect to improve GS models was suggested in a simulation study (Bernardo, 2014) and also demonstrated with empirical studies (Rutkoski et al., 2014). Nonetheless, using *Bdv2* as a fixed effect in our GS strategies did not consistently improve the predictive ability for PTH_M or reduction in GY. However, there was not a consistent distribution of *Bdv2* allele across the cohorts. Our GS models resulted in low predictive ability values for BYD if compared with other GS studies for

disease resistance (reviewed by Poland & Rutkoski, 2016). However, since this is the first report of GS for BYD resistance/tolerance in wheat, we do not have similar results to make better comparisons and this remains a challenging pathosystem with low heritability of the resistance in wheat. Moreover, the correlation between HTP parameters and BYD phenotypes was interesting, but not sufficient to be useful in combination with GS in the germplasm tested.

Conclusions

We were able to show that *Bdv2* has a major effect controlling BYD resistance/tolerance in the KSU breeding germplasm. Our study was unable to discover new genomic regions associated with resistance or tolerance to BYD other than the potentially novel QTL on chromosome 5AS, supporting the limited resistance available in the current wheat gene pool and the highly polygenic nature of the trait. Moreover, our study was the first attempt to characterize and improve BYD field-phenotyping using HTP and apply GS to predict the disease. HTP traits showed strong correlation patterns with BYD severity, however, none of these parameters shared a common genetic architecture with BYD severity. The GS predictive ability results that we found in this study open the door for further improvement and testing GS implementation for breeding for BYD resistance/tolerance. Continuing on the improvement of BYD characterization and on the search of new sources of resistance using other species related to wheat, will be crucial to broadening the resistant genes available to introgress into wheat germplasm.

Acknowledgements

This material is based upon work supported by Kansas Wheat Commission Award No: B65336 "Integrative and Innovative Approaches to Diminish Barley Yellow Dwarf Epidemics Kansas Wheat". PS was supported through a U.S. Fulbright-ANII Uruguay Scholarship. Any opinions, findings, and conclusions or recommendations expressed in this material are those of the author(s) and do not necessarily reflect the views of the industry partners.

References

Ayala-Navarrete, L., & Larkin, P. (2011). Wheat virus diseases: breeding for resistance and tolerance. World wheat book: a history of wheat breeding, Lavoisier, Paris, 2, 1073-107.

Ayala, L., Henry, M., Van Ginkel, M., et al. (2002). Identification of QTLs for BYDV tolerance in bread wheat. Euphytica, 128(2), 249–259. https://doi.org/10.1023/A:1020883414410

Ayala, L., Van Ginkel, M., Khairallah, M., et al. (2001). Expression of *Thinopyrum intermedium*-derived Barley yellow dwarf virus resistance in elite bread wheat backgrounds. Phytopathology, 91(1), 55–62. https://doi.org/10.1094/PHYTO.2001.91.1.55

Banks, P. M., Davidson, J. L., Bariana, H., & Larkin, P. J. (1995). Effects of barley yellow dwarf virus on the yield of winter wheat. Australian Journal of Agricultural Research, 46(5), 935-946.

Bernardo, R. (2014). Genomewide selection when major genes are known. Crop Science, 54(1), 68-75. https://doi.org/10.2135/cropsci2013.05.0315

Bockus, W. W., De Wolf, E. D., & Todd, T. C. (2016). Management strategies for barley yellow dwarf on winter wheat in Kansas. Plant Health Progress, 17(2), 122–127. https://doi.org/10.1094/PHP-RS-15-0050

Brettell, R. I. S., Banks, P. M., Cauderon, Y., Chen, X., et al. (1988). A single wheatgrass chromosome reduces the concentration of barley yellow dwarf virus in wheat. Annals of Applied Biology, 113(3), 599–603. https://doi.org/10.1111/j.1744-7348.1988.tb03337.x

Chapin, J. W., Thomas, J. S., Gray, S. M., et al. (2001). Seasonal Abundance of Aphids (Homoptera: *Aphididae*) in Wheat and Their Role as Barley Yellow Dwarf Virus Vectors in the South Carolina Coastal Plain. Journal of Economic Entomology, 94(2), 410–421. https://doi.org/10.1603/0022-0493-94.2.410

Choudhury, S., Hu, H., Fan, Y., et al. (2019). Identification of new QTL contributing to barley yellow dwarf virus-PAV (BYDV-PAV) resistance in wheat. Plant Disease, 103(11), 2798–2803. https://doi.org/10.1094/PDIS-02-19-0271-RE

Choudhury, Shormin, Hu, H., Meinke, H., et al. (2017). Barley yellow dwarf viruses: infection mechanisms and breeding strategies. Euphytica, Vol. 213, pp. 1–22. https://doi.org/10.1007/s10681-017-1955-8

Cisar, G., Brown, C. M., & Jedlinski, H. (1982). Diallel analyses for tolerance in winter wheat to the barley yellow dwarf virus 1. Crop Science, 22(2), 328-333.

Comeau, A., & Haber, S. (2002). Breeding for BYDV tolerance in wheat as a basis for a multiple stress tolerance strategy. Barley Yellow Dwarf Disease: Recent Advances and Future Strategies, 82.

Crain, J., Mondal, S., Rutkoski, J., et al. (2018). Combining High-Throughput Phenotyping and Genomic Information to Increase Prediction and Selection Accuracy in Wheat Breeding. The Plant Genome, 11(1), 170043. https://doi.org/10.3835/plantgenome2017.05.0043

D'arcy, C. J. (1995). Symptomatology and host range of barley yellow dwarf. Barley yellow dwarf, 40, 9-28.

D'Arcy, C. J., & Burnett, P. A. (1995). Barley yellow dwarf: 40 years of progress. Retrieved from https://agris.fao.org/agris-search/search.do?recordID=US19960029148

Endelman, J. B. (2011). Ridge Regression and Other Kernels for Genomic Selection with R Package rrBLUP. The Plant Genome, 4(3), 250–255. https://doi.org/10.3835/plantgenome2011.08.0024

Gaunce, G. M., & Bockus, W. W. (2015). Estimating Yield Losses Due to Barley Yellow Dwarf on Winter Wheat in Kansas Using Disease Phenotypic Data. Plant Health Progress, 16(1), 1–6. https://doi.org/10.1094/php-rs-14-0039

Girvin, J., Whitworth, R. J., Rojas, L. M. A., & Smith, C. M. (2017). Resistance of select winter wheat (*Triticum aestivum*) cultivars to *Rhopalosiphum padi* (Hemiptera: *Aphididae*). Journal of Economic Entomology, 110(4), 1886–1889. https://doi.org/10.1093/jee/tox164

Glaubitz, J. C., Casstevens, T. M., Lu, F., Harriman, J., et al. (2014). TASSEL-GBS: A High-Capacity Genotyping by Sequencing Analysis Pipeline. PLoS ONE, 9(2), e90346. https://doi.org/10.1371/journal.pone.0090346

Haghighattalab, A., González Pérez, L., Mondal, S., et al. (2016). Application of unmanned aerial systems for high throughput phenotyping of large wheat breeding nurseries. Plant Methods, 12(1), 1–15. https://doi.org/10.1186/s13007-016-0134-6

Hollandbeck, GF., DeWolf, E., and Todd, T. (2019). Kansas cooperative plant disease survey report. Preliminary 2019 Kansas wheat disease loss estimates. October 2, 2019 https://agriculture.ks.gov/divisionsprograms/plant-protect-weed-control/reports-and-publications

IWGSC, A. R., Eversole, K., Feuillet, C., Keller, B., Rogers, J., & Stein, N. (2018). Shifting the limits in wheat research and breeding using a fully annotated reference genome. Science, 361(6403), eaar7191-eaar7191.

Jarošová, J., Beoni, E., & Kundu, J. K. (2016). Barley yellow dwarf virus resistance in cereals: Approaches, strategies and prospects. Field Crops Research, 198, 200–214. https://doi.org/10.1016/j.fcr.2016.08.030

Jensen, S. G., & Van Sambeek, J. W. (1972). Differential Effects of Barley Yellow Dwarf Virus on the Physiology of Tissues of Hard Red Spring Wheat. Phytopathology, 62(2), 290. https://doi.org/10.1094/phyto-62-290

Krueger, E. N., Beckett, R. J., Gray, S. M., & Allen Miller, W. (2013). The complete nucleotide sequence of the genome of Barley yellow dwarf virus-RMV reveals it to be a new *Polerovirus* distantly related to other yellow dwarf viruses. Frontiers in Microbiology, 4(JUL), 1–11. https://doi.org/10.3389/fmicb.2013.00205

Kumar, S., Röder, M. S., Singh, R. P., et al. (2016). Mapping of spot blotch disease resistance using NDVI as a substitute to visual observation in wheat (*Triticum aestivum* L.). Molecular Breeding, 36(7), 1–11. https://doi.org/10.1007/s11032-016-0515-6

Larkin, P. J., Banks, P. M., Lagudah, E. S., et al. (1995). Disomic *Thinopyrum intermedium* addition lines in wheat with barley yellow dwarf virus resistance and with rust resistances. Genome, 38(2), 385–394. https://doi.org/10.1139/g95-050

Li, H., & Wang, X. (2009). *Thinopyrum ponticum* and *Th. intermedium*: the promising source of resistance to fungal and viral diseases of wheat. Journal of Genetics and Genomics, 36(9), 557–565. https://doi.org/10.1016/S1673-8527(08)60147-2

Lin, Z. S., Cui, Z. F., Zeng, X. Y., et al. (2007). Analysis of wheat-*Thinopyrum intermedium* derivatives with BYDV-resistance: Analysis of wheat-*Th.intermedium* derivatives. Euphytica, 158(1–2), 109–118. https://doi.org/10.1007/s10681-007-9435-1

Lipka, A. E., Tian, F., Wang, Q., et al. (2012). GAPIT: genome association and prediction integrated tool. Bioinformatics, 28(18), 2397–2399. https://doi.org/10.1093/bioinformatics/bts444

Marza, F., Bai, G. H., Carver, B. F., & Zhou, W. C. (2005). Quantitative trait loci for yield and related traits in the wheat population Ning7840× Clark. Theoretical and Applied Genetics, 112(4), 688-698. https://doi.org/10.1007/s00122-005-0172-3

Meuwissen, T. H., Hayes, B. J., & Goddard, M. E. (2001). Prediction of total genetic value using genome-wide dense marker maps. Genetics, 157(4), 1819-1829. https://doi.org/10.1093/genetics/157.4.1819

Miller, W. A., & Rasochová, L. (1997). Barley yellow dwarf viruses. Annual Review of Phytopathology, Vol. 35, pp. 167–190. https://doi.org/10.1146/annurev.phyto.35.1.167

Mondal, S., Rutkoski, J. E., Velu, G., et al. (2016). Harnessing diversity in wheat to enhance grain yield, climate resilience, disease and insect pest resistance and nutrition through conventional and modern breeding approaches. Frontiers in plant science, 7, 991. https://doi.org/10.3389/fpls.2016.00991

Oswald, J. W.; Houston, B. E. (1953). The Yellow-dwarf Virus Disease of Cereal Crops. Phytopathology, 43(3), 128-136. https://www.cabdirect.org/cabdirect/abstract/19550500462

Perry, K. L., Kolb, F. L., Sammons, B., et al. (2000). Yield effects of Barley yellow dwarf virus in soft red winter wheat. Phytopathology, 90(9), 1043–1048. https://doi.org/10.1094/PHYTO.2000.90.9.1043

Peiris, K. H., Bowden, R. L., Todd, T. C., Bockus, W. W., Davis, M. A., & Dowell, F. E. (2019). Effects of barley yellow dwarf disease on wheat grain quality traits. Cereal Chemistry, 96(4), 754-764. https://doi.org/10.1002/cche.10177

Pinheiro, J., Bates, D., DebRoy, S., & Sarkar, D. (2015). R Core Team. 2015. *nlme*: linear and nonlinear mixed effects models. R package version 3.1-120. R package version, 3-1.

Poland, J. (2015). Breeding-assisted genomics. Current Opinion in Plant Biology, Vol. 24, pp. 119–124. https://doi.org/10.1016/j.pbi.2015.02.009

Poland, J. A., & Nelson, R. J. (2011). In the eye of the beholder: The effect of rater variability and different rating scales on QTL mapping. Phytopathology, 101(2), 290–298. https://doi.org/10.1094/PHYTO-03-10-0087

Poland, J. a., & Rife, T. W. (2012). Genotyping-by-Sequencing for Plant Breeding and Genetics. The Plant Genome Journal, 5(3), 92. https://doi.org/10.3835/plantgenome2012.05.0005

Poland, J., & Rutkoski, J. (2016). Advances and Challenges in Genomic Selection for Disease Resistance. Annual Review of Phytopathology, 54(1), 79–98. https://doi.org/10.1146/annurev-phyto-080615-100056

Qualset, C. O., Williams, J. C., Topcu, M. A., & Vogt, H. E. (1973). The barley yellow-dwarf virus in wheat: importance, sources of resistance, and heritability. In Proceedings, Fourth International Wheat Genetics Symposium, Columbia, Missouri (pp. 465-470).

Riedell, W. E., Kieckhefer, R. W., Langham, M. A. C., & Hesler, L. S. (2003). Root and Shoot Responses to Bird Cherry-Oat Aphids and Barley yellow dwarf virus in Spring Wheat. Crop Science, 43(4), 1380–1386. https://doi.org/10.2135/cropsci2003.1380

Rife, T. W., & Poland, J. A. (2014). Field Book: An Open-Source Application for Field Data Collection on Android. Crop Science, 54(4), 1624–1627. https://doi.org/10.2135/cropsci2013.08.0579

Rotenberg, D., Bockus, W. W., Whitfield, A. E., et al. (2016). Occurrence of viruses and associated grain yields of paired symptomatic and non-symptomatic tillers in Kansas winter wheat fields. Phytopathology, 106(2), 202-210. https://doi.org/10.1094/PHYTO-04-15-0089-R

Rouse Jr, J. W. (1973). Monitoring the vernal advancement and retrogradation (green wave effect) of natural vegetation.

Rutkoski, J. E., Poland, J. A., Singh, R. P., et al. (2014). Genomic Selection for Quantitative Adult Plant Stem Rust Resistance in Wheat. The Plant Genome, 7(3). https://doi.org/10.3835/plantgenome2014.02.0006

Sankaran, S., Mishra, A., Ehsani, R., & Davis, C. (2010). A review of advanced techniques for detecting plant diseases. Computers and Electronics in Agriculture, 72(1), 1–13. https://doi.org/10.1016/j.compag.2010.02.007

Shah, S. J. A., Bashir, M., & Manzoor, N. (2012). A review on barley yellow dwarf virus. In Crop Production for Agricultural Improvement (Vol. 9789400741164, pp. 747–782). https://doi.org/10.1007/978-94-007-4116-4_29

Sharma, H., Ohm, H., Goulart, L., et al. (1995). Introgression and characterization of barley yellow dwarf virus resistance from *Thinopyrum intermedium* into wheat. Genome, 38(2), 406–413. https://doi.org/10.1139/g95-052

Singh, Peter A. Burnett, M. Albarrfin, and S. R. (1993). *Bdv1*: A Gene for Tolerance to Barley Yellow Dwarf Virus in Bread Wheats Ravi. Crop Science, 33(April), 231–234.

Walls, J., Rajotte, E., & Rosa, C. (2019). The past, present, and future of barley yellow dwarf management. Agriculture (Switzerland), 9(1), 1–16. https://doi.org/10.3390/agriculture9010023

Wang, X., Silva, P., Bello, N. M., et al. (2020). Improved Accuracy of High-Throughput Phenotyping From Unmanned Aerial Systems by Extracting Traits Directly From Orthorectified Images. Frontiers in Plant Science, 11. https://doi.org/10.3389/fpls.2020.587093

Wang, X., Singh, D., Marla, S., Morris, G., & Poland, J. (2018). Field-based high-throughput phenotyping of plant height in sorghum using different sensing technologies. Plant Methods, 14(1), 53. https://doi.org/10.1186/s13007-018-0324-5

Yu, J., Pressoir, G., Briggs, W. H., et al. (2006). A unified mixed-model method for association mapping that accounts for multiple levels of relatedness. Nature Genetics, 38(2), 203–208. https://doi.org/10.1038/ng1702

Zhang, Z., Lin, Z., & Xin, Z. (2009). Research progress in BYDV resistance genes derived from wheat and its wild relatives. Journal of Genetics and Genomics, 36(9), 567–573. https://doi.org/10.1016/S1673-8527(08)60148-4

Zheng, Q., Huang, W., Cui, X., et al. (2018). Identification of Wheat Yellow Rust Using Optimal Three-Band Spectral Indices in Different Growth Stages. Sensors, 19(1), 35. https://doi.org/10.3390/s19010035

Table 2.1 - Field experimental details for the five wheat nurseries

Season	2015-2016	2016-2017	2017-2018	2018-2019	2019-2020
Location	Rocky Ford farm		Ashland Bottoms farm		
	39˚13'45.60" N, 96˚34'41.21" W		39˚07'53.76" N, 96˚37'05.20" W		
Planting Date	Sep. 17, 2015	Sep. 12, 2016	Sep. 19, 2017	Sep. 17, 2018	Sep. 17, 2019
Number of Entries	68	52	81	81	107
Number of Plots	504	360	400	392	684
Field Design	split-plot with insecticide treatment as major factor effect and wheat genotype as secondary factor				
Replications	3	3	2	2	2
Plot Size	6 rows plots - 1.5 m × 2.4 m				
BYD Evaluation	April 28, 2016	May 12, 2017	May 19, 2018	May 13, 2019	May 19, 2020
Harvesting Date	June 20, 2016	June 19, 2017	June 23, 2018	June 28, 2019	June 25, 2020

Table 2.2 - High-throughput phenotypic data details of the image acquisition in the five wheat nurseries.

Season	2015-2016	2016-2017	2017-2018	2018-2019	2019-2020
UAS Platform	PheMU		DJI Matrice 100		
Imaging Sensor	multiple digital single-lens reflex (DSLR) cameras		MicaSense RedEdge-M		
Flight/Pass speed	0.3–0.5 m/s		2 m/s		
Flight Dates	2016-03-31 2016-04-07 2016-04-14 2016-05-06	2017-03-28 2017-04-13 2017-05-01 2017-05-09 2017-05-21 2017-05-23 2017-05-30 2017-06-05 2017-06-13	2018-03-30 2018-04-04 2018-04-12 2018-04-19 2018-04-23 2018-05-16 2018-06-13	2019-04-01 2019-04-09 2019-04-19 2019-04-26 2019-05-02 2019-05-10 2019-05-15 2019-05-23 2019-05-31 2019-06-05 2019-06-12 2019-06-17	2020-03-20 2020-04-11 2020-04-23 2020-05-03 2020-05-19 2020-06-05 2020-06-11
Flight/Pass altitude	0.5 m above the canopy		20 m AGL		
In-Air Flight Duration	NA		~ 11–14 min		

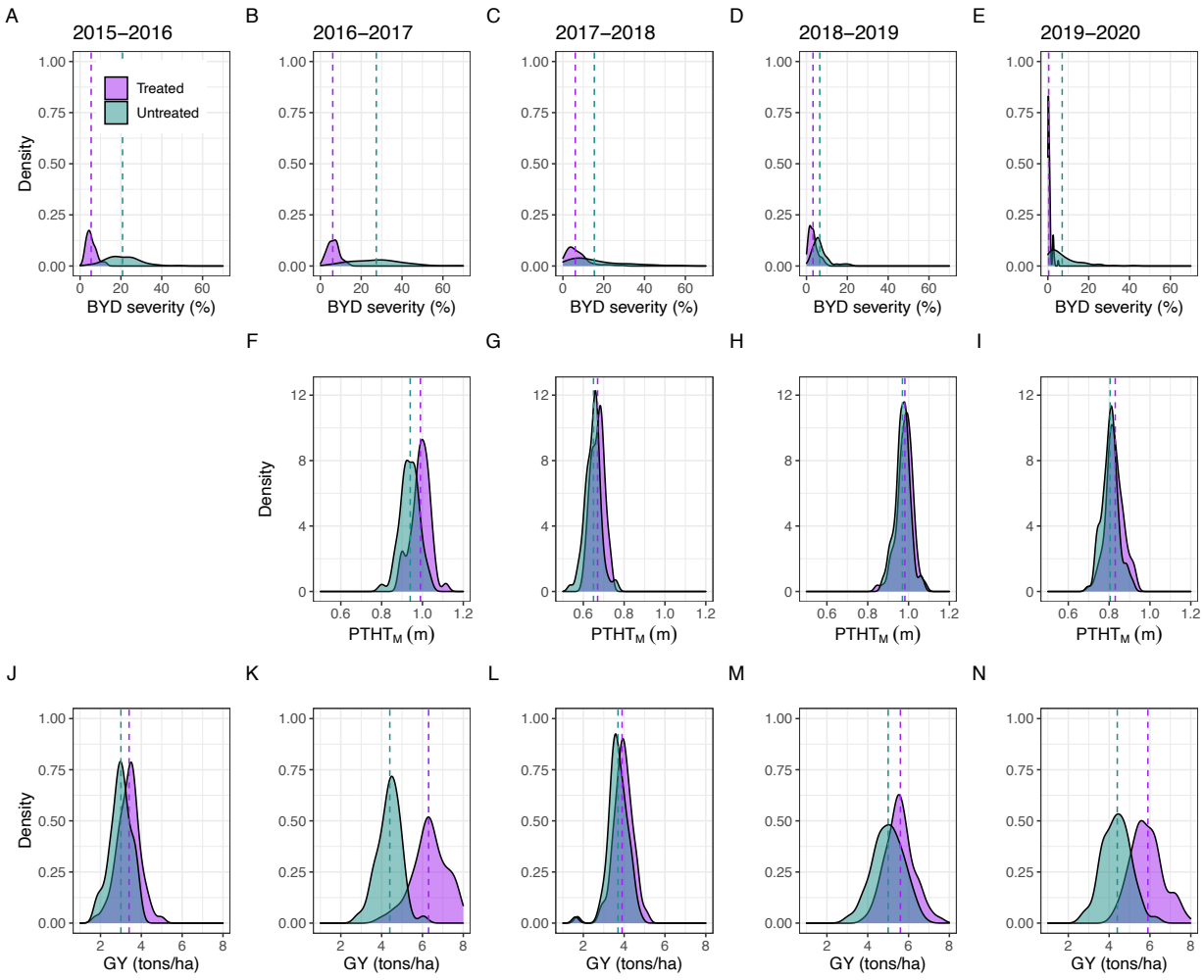

Figure 2.1 – Phenotypic data description.

Adjusted phenotypic values for the traits collected manually for five different field seasons (2015-2016 to 2019-2020). A-E): BYD severity (BYD) characterized as the typical visual symptoms of yellowing/purpling on leaves using a 0 – 100% visual scale, F-I) manual plant height/stunting (meters) (PTHTM), note that the trait was not recorded for the 2015-2016 season, and J-N) grain yield (tons/ha) (GY, combination of test weight and moisture). Insecticide-treated and untreated replications are represented by purple and green, respectively. The dashed line represents the mean value for the trait in each treatment.

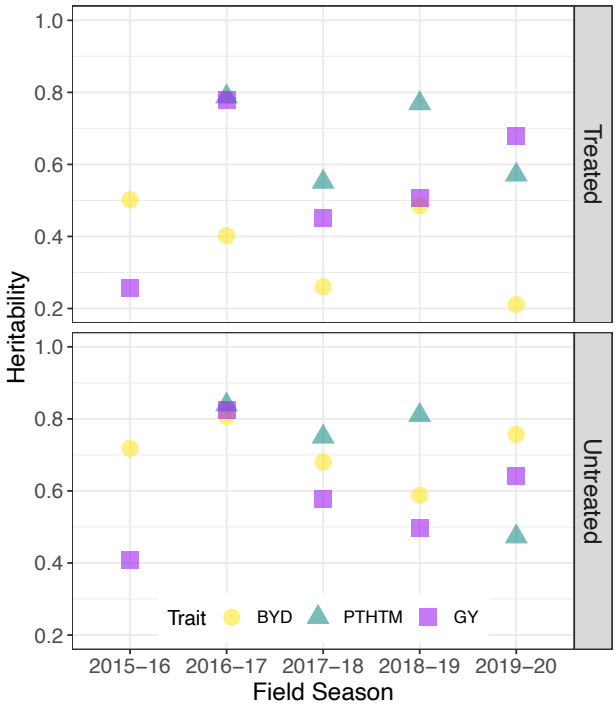

Figure 2.2 – Broad-sense heritability.

Broad-sense Heritability for the traits collected manually during five different field seasons under two insecticide treatments. Data points for the different traits are represented with different colors and shapes.

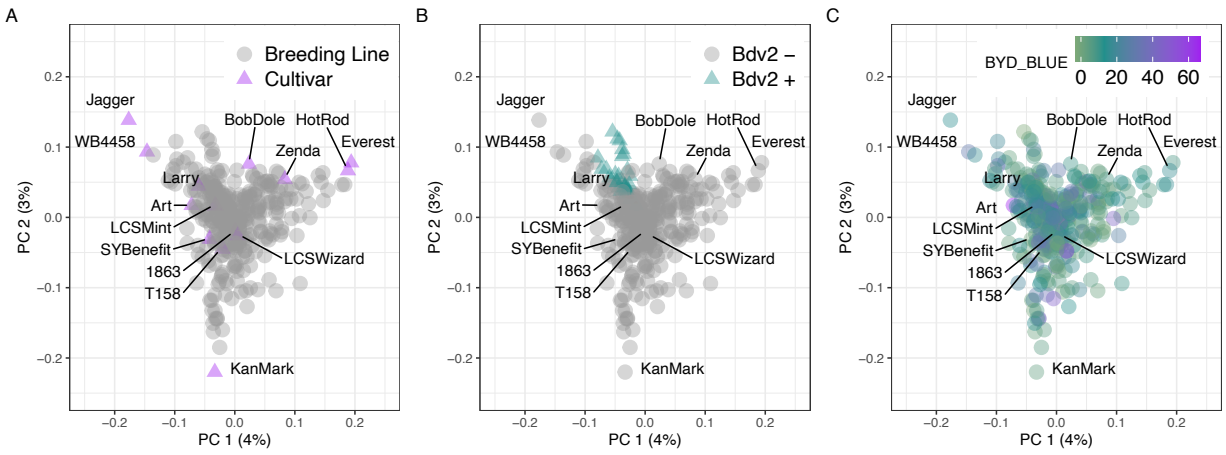

Figure 2.3 – Population structure.

Scatterplot of the first two principal component axis, made from principal component analysis on the marker matrix, n = 357 wheat lines, markers = 29,480. Each data point represents an individual wheat line that is color-coded by A) breeding status, B) prediction of *Bdv2* presence/absence, and C) adjusted mean for BYD severity (BYD BLUE) scored visually. Total variance explained by each principal component (PC) is listed on the axis.

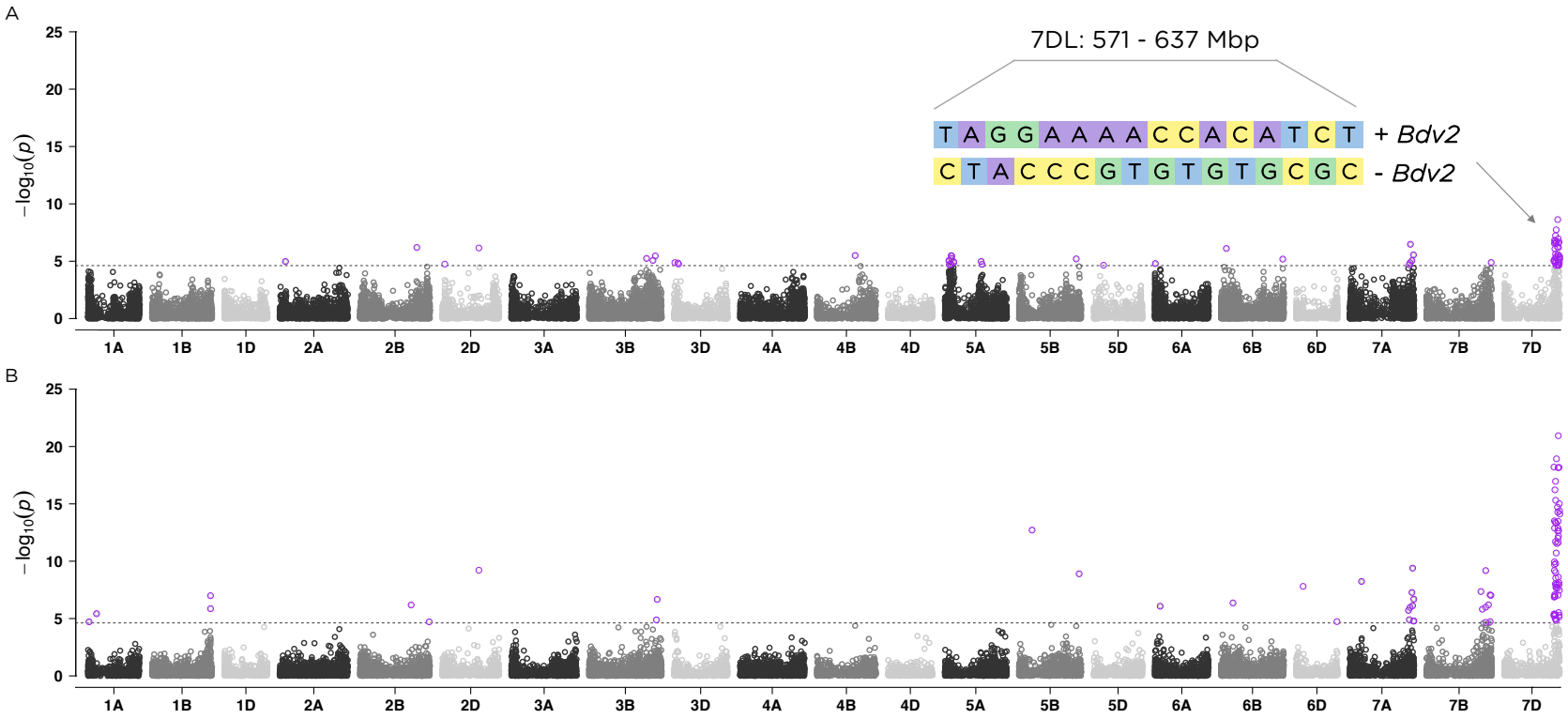

Figure 2.4 – Genome-wide association analyses.

Manhattan plots showing the marker-trait associations using 346 accessions and 29,480 SNP markers obtained with genotyping-by-sequencing (GBS) for A) BYD severity BLUPs and B) presence/absence of *Bdv2* resistance gene. The 21 wheat chromosomes with physical positions are on the x-axis and y-axis is the –log10 of the p-value for each SNP marker. Horizontal dashed lines represent the false discovery rate threshold at 0.01 level and data points highlighted in purple and above the threshold represent SNPs significantly associated with the trait. Chromosome labels are placed in the middle of the chromosome. For BYD severity we detail the length of the region and the haplotypes defined by the significant SNP markers.

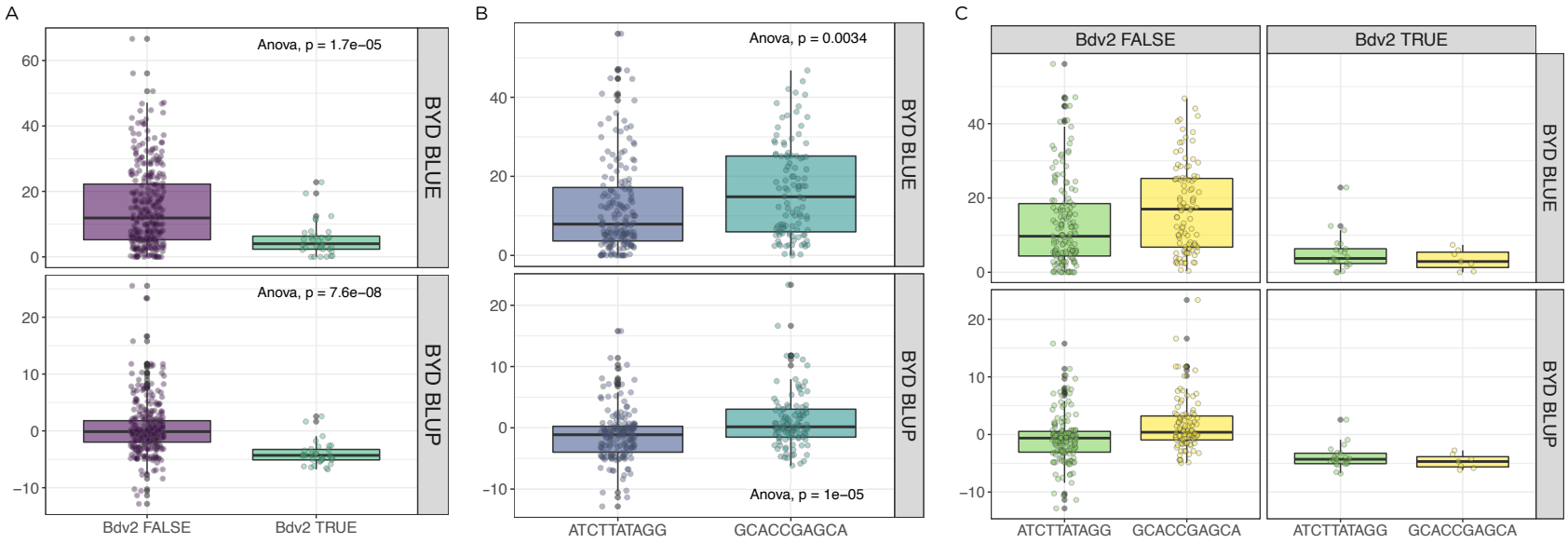

Figure 2.5 – Effect of *Bdv2* resistance gene and 5A QTL on BYD.

Effect of A) the translocation segment carrying the resistance gene *Bdv2*, B) the two haplotypes for the significant region on chromosome 5AS, and C) the combination of *Bdv2* resistance gene and 5A haplotype, on Barley yellow dwarf (BYD) disease severity. Boxplots showing the significant reduction of BYD disease severity by averaging the phenotypic best linear unbiased estimated (BLUE) or best linear unbiased predicted (BLUP) values for the lines.

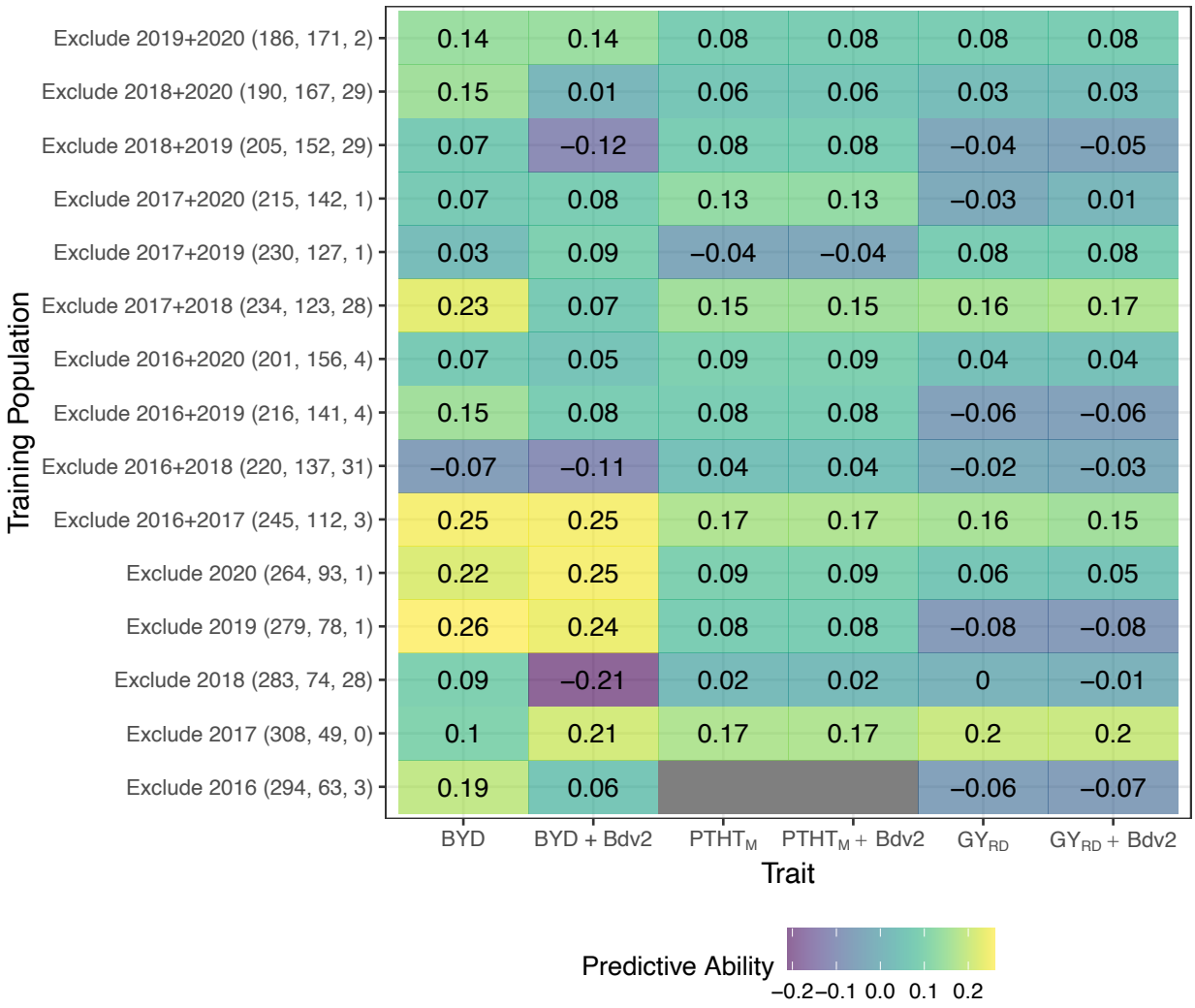

Figure 2.6 – Genomic selection (GS) models predictive ability.

Each column represents one trait, and each row shows the conformation of the training population, showing within the parenthesis the size of the training population, the size of the testing population, and the number of lines with presence of *Bdv2* resistance gene. The value in each cell represents the predictive ability which is the correlation between the GS predicted value (GBLUP) and the phenotypic best linear unbiased predictor (BLUP).

Chapter 3 - Understanding the Genetic Basis of Resistance to Wheat Head Bast

Abstract

Wheat blast (WB), caused by *Magnaporthe oryzae Triticum* (MoT) pathotype, is an emerging disease in South Asia, with the potential to devastate wheat production worldwide. WB was first reported in Brazil in 1985, however, it was not until its emergence in Bangladesh in 2016 that international attention began to focus on this disease. To date, only two major resistance genes, Rmg8 and RmgGR119, still hold potential for effectiveness under field conditions. Besides, the $2N^{V}S$ segment from the wild relative *Aegilops ventricosa* was reported to confer wheat head blast (WHB) resistance. However, there is unclear information regarding the level of resistance conferred by $2N^{V}S$ in different genetic backgrounds and against different MoT isolates. Moreover, there is no information regarding which genes(s) on $2N^{V}S$ are responsible for conferring WHB resistance. The objectives of this study were to i) characterize the WHB resistance conferred by the alien segment $2N^{V}S$ and ii) search for new genomic regions associated with resistance to WHB in the wild relative *Aegilops tauschii*. To characterize the genetic resistance on $2N^{V}S$, we developed EMS populations derived from five $2N^{V}S$ spring bread wheat varieties showing different levels of WHB resistance. In total, we obtained around 8800 M1 mutant plants. Derived M2 lines are being tested under field conditions in Bolivia to select for susceptible mutant lines. So far, we have identified 60 susceptible mutant candidate lines, all from one population, that will be sequenced to identify the causal mutation. For the exploration of new resistance genes, we evaluated a panel of 226 *Ae. tauschii* accessions under controlled conditions and used genome-wide association mapping to identify novel genomic regions. We were able to identify resistant accessions from both lineages, and we mapped WHB resistance on chromosome 7D for lineage 1 and 1D and 2D for lineage 2. Overall, these breeding strategies will help researchers and breeders to better understand the disease and breed germplasm resistant to WB.

General introduction about Wheat Blast

The pathogen *Magnaporthe oryzae* (Mo, synonym of *Pyricularia oryzae*) is a single species with the ability to infect more than 50 species of grasses (Valent et al., 2020; 2019). This pathogenic fungus is well known as the causal agent of rice blast and has recently received increased international attention for causing disease outbreaks in wheat. Mo is divided into lineages or pathotypes, which specialize in causing disease on different hosts, including the pathotype *Oryza* (MoO), pathotype *Lolium* (MoL), and pathotype *Triticum* (MoT), which cause disease in rice, ryegrass, and wheat, respectively (Tosa et al., 2004). Certain pathotypes are also capable of infecting other species, such as MoO infecting barley (Gladieux et al., 2018).

Wheat blast (WB) is endemic to South America, first described in Brazil in 1985 (Igarashi et al., 1986), and rapidly spreading to neighboring countries such as Bolivia (Barea & Toledo, 1996), Paraguay (Viedma, 2005), and Argentina (Cabrera & Gutierrez, 2007; Perelló et al., 2015). The disease remained restricted in South America until 2016 when it was reported in Bangladesh (Malaker et al., 2016). Moreover, alarming but not surprising, only one year later was reported to appear in India (Bhattacharya & Pal 2017), a major wheat-producing country. WB has further spread to the African continent with recently being found in Zambia in 2017 (Tembo et al., 2020).

WB symptomatology can occur on all above-ground organs, including bleaching of heads (called wheat head blast – WHB) as the most characteristic symptom in the field and small (Cruz & Valent, 2017). A detailed description on WB symptoms and signs is described in Valent et al. (2021). WB can affect seed quality and has the potential to produce yield losses up to 100% in wheat production fields (Duveiller et al., 2016; Goulart et al., 2007; Kohli et al., 2010). Wheat producers have difficulty controlling the disease based on the rapid development of the disease in susceptible wheat varieties, coupled with very limited genetic resistance and limited fungicide efficacy to control WB when the climate favors the disease (Cruz et al., 2019; Cruz & Valent, 2017). For this reason, farmers stop growing wheat in regions where the disease is established.

At the time of the appearance of MoT in Asia, two explanations were possible to understand the emergence of the disease in another continent; either the fungus entered as an exotic disease in

infected seeds or that it was a host jump from a local pathogen adapting to a new host. It was soon determined based on several independent studies that MoT isolates collected from wheat regions in Bangladesh were similar to MoT isolates from South America, indicating that the emergence in Bangladesh was due to the spread from South America, presumably in infested seed (Islam et al., 2016; Malaker et al., 2016). These results alert us to the ability for the large-scale spreading of MoT, indicating that WB has the potential to emerge in new countries and become pandemic, threatening wheat production around the world.

Another possible source of emergence of WB in new geographical regions is the occurrence of recombination between Mo isolates from different pathotypes that share common hosts, which translates into greater pathotype diversity and a high ability to evolve and adapt to new hosts (Gladieux et al., 2018; Langner et al., 2018). Of particular note is that a recent evolutionary analysis revealed that MoT originated from a host jump from an MoL isolate along with a high selection pressure for mutation and loss of function of a single avirulence gene (Inoue et al., 2017). Furthermore, it was shown that the only report of the occurrence of WB in wheat in U.S. was most likely explained by a host jump of a native MoL (Farman et al., 2017). Additional evidence of the high evolutionary risk for MoT changing virulence spectrum is the potential that isolates of Mo affecting other related crops, such as barley and oat, have huge pathogen populations and mutants can undergo a host jump, which will further complicate the situation of WB pathology (Inoue et al., 2017). MoT high evolutionary potential explained in part by having a mixed reproductive system (sexual and asexual recombination), also explains the large diversity levels found for the MoT pathotype (Gladieux et al., 2018; Maciel et al., 2014), which ultimately makes WB hard to control.

Genetic resistance is the one strategy for disease control that does not have an additional cost for farmers, having huge environmental benefits by reducing the use of fungicides. To date, nine resistance genes have been described (*Rmg1-Rmg8* and *RmgGR119*), which only five of them are host resistance genes, preventing MoT isolates from infecting wheat (*Rmg2*, *Rmg3*, *Rmg7*, *Rmg8*, and *RmgGR119*) (Anh et al., 2015; Tagle et al., 2015; Wang et al., 2018; Zhan et al., 2008). From these five, only two (*Rmg8* and *RmgGR119*) still hold effectiveness against current MoT, however, their effect has not yet been proven under field conditions (Cruppe et al., 2019). The other four genes (*Rmg1*, *Rmg4*, *Rmg5*, and *Rmg6*) are non-host resistance genes, playing a role in

preventing isolates from other Mo pathotypes (i.e. isolates from pathotypes *Avenae*, *Digitaria*, and *Lolium*) from infecting wheat (Anh et al., 2015; Vy et al., 2014). Moreover, it was recently shown that the alien translocation from *Aegilops ventricosa*, $2N^VS$, confers resistance to WHB, although, the resistance is partial since not all materials that possess the fragment are resistant (Cruppe et al., 2019, 2020; Cruz et al., 2016). However, new data suggest that the resistance conferred by $2N^VS$ is being overcome by recent isolates that show greater aggressiveness (Cruppe et al., 2019, 2020). Thus, it is essential to continue with the characterization of germplasm to search for new sources of resistance.

This chapter is divided into two parts. In the first subchapter, we focused on the known source of WHB resistance, the $2N^VS$ translocation on wheat chromosome 2A. We hypothesize that the $2N^VS$ translocated fragment carries a single, dominant resistance gene controlling WHB disease resistance and the objective was to understand the genetics of resistance conferred by the $2N^VS$/2A translocation by developing mutant populations. For the second subchapter, we focused on wild wheat germplasm characterization against WHB. The hypothesis is that *Ae. tauschii* is a source of genes for host-plant resistance to WHB and the objective was to characterize a collection of the wheat wild relative *Ae. tauschii* to identify novel sources of resistance against WHB.

Subchapter 3A) Understanding the genetics of resistance conferred by the $2N^VS$/2A translocation

Introduction

Genetic resistance to wheat blast (WB) was first proposed to follow the gene-for-gene model where an avirulence (*Avr*) gene in the pathogen is recognized by a complementary resistance (*R*) gene in the host, leading to resistance or no infection response (Anh et al., 2015, 2018; Flor, 1971). Several independent studies have shown that resistance to WHB is mainly explained by the presence of the $2N^VS$/2A translocation (Cruppe et al., 2019, 2020; Cruz et al., 2016). However, recent studies support the hypothesis that both, qualitative (following the gene-for-gene model) and quantitative resistance mechanisms are present in the interaction between MoT and wheat (Cruz & Valent, 2017; Goddard et al., 2020). Moreover, it has been proposed that different resistance mechanisms predominate in leaves or heads based on a low correlation of

symptoms (Maciel et al., 2014) and also between seedling and adult plant stages based on lack of colocalization of quantitative trait loci (QTL) (Goddard et al., 2020). In this sense, resistance to wheat head blast (WHB), the most common and severe symptom of WB, is thought to be mostly quantitative due to its continuous range of disease severity response (Cruppe et al., 2019; Cruz et al., 2016; Maciel et al., 2014). However, when the wheat line displays a highly resistant phenotype, a qualitative-type response is commonly observed showing necrotic lesions that resemble a hypersensitive response (Cruppe et al., 2019), suggesting that the trait could be controlled by typical nucleotide-binding site leucine-rich repeat (NLR) type resistance gene and associated defense pathways.

The $2N^{V}S$ segment was first introgressed into wheat from the wild relative *Aegilops ventricosa* via the wheat cultivar VPM1 (Maia, 1967). It is located on the distal end of the short arm of chromosome 2A, spanning about 33 Mbp (Gao et al., 2020). The translocation has been well studied and it is widely used in breeding programs since it harbors additional resistance genes against other diseases such as leaf rust (*Lr37*), stripe rust (*Yr17*), and stem rust (*Sr38*) (Bariana & McIntosh, 1993, 1994), root-knot nematode (*Rkn3*) (Williamson et al., 2013), and cereal cyst nematode (*Cre5*) (Jahier et al., 2001). In addition to disease resistance, this segment has been associated with increased lodging tolerance (Singh et al., 2019) and higher yield (Gao et al., 2020), with no associated yield penalty (Williamson et al., 2013). Moreover, the segment has recently been shown to carry many NLR genes (Gao et al., 2020). However, there is no information regarding which gene(s) are responsible to control WHB resistance with unknown the resistance mechanism behind the $2N^{V}S$/2A translocation.

This study hypothesizes that the $2N^{V}S$ translocated segment carries a single, dominant resistance gene controlling WHB disease resistance. The objective was to understand the genetics of resistance conferred by the $2N^{V}S$/2A translocation by developing mutant populations and identifying the gene responsible for resistance to WHB.

Materials and Methods

Plant Material

Five spring wheat lines all carrying the $2N^{V}S$ segment and with good levels of resistance against MoT and agronomic adaptation to locations in South America with endemic MoT populations were selected to create mutant populations. This included: two wheat varieties from Brazil, 'TBIO Sossego' and 'TBIO Sintonia', both with < 40% WHB severity under field disease evaluations; two Bolivian varieties, 'Yoyau' previously known as 'AN/TR-120', and 'Urubo', both with < 20% WHB severity; and one line developed by CIMMYT, 'Milan-2', with a WHB severity response < 20%. The presence of the $2N^{V}S$ segment in these five varieties was confirmed by a PCR assay (Cruppe et al., 2019).

'TBIO Sossego' is a medium cycle spring wheat released in 2015 by the Brazilian breeding company Biotrigo (https://biotrigo.com.br/cultivares/portfolio/tbio_sossego/41), with pedigree 'BIO08400´S/4/Quartzo5/Quartzo'. 'TBIO Sintonia' is a short cycle spring wheat released in 2013 by Biotrigo (https://biotrigo.com.br/cultivares/portfolio/tbio_sintonia/31) with pedigree 'Marfim/Quartzo//Marfim'. 'Yoyau' is a short spring variety developed by CIMMYT and released by ANAPO specifically for its resistance against WB, with pedigree 'ATTILA/3*BCN//BAV92/3/TILHI/5/BAV92/3/PRL/SARA//TSI/VEE#5/4/CROC_1/AE.SQUARROSA (224)//2*OPATA'. 'Urubo' is a medium-short spring wheat line developed by CIMMYT and released by CIAT with pedigree 'Milan/Munia'. The spring line 'Milan-2' was developed by CIMMYT and its pedigree is 'Inallettabile-96/Mentana'.

Mutagenesis and populations development

For the EMS treatment, we first optimized the EMS dosage curve for each wheat genotype to obtain a 50% survival rate. To select the concentration that gave the closest to 50% survival rate, batches of 50 seeds were treated with ten different EMS concentrations, from 0% to 0.9%, with 0% used as a germination rate control. The seed was soaked in water overnight and then placed in flasks with the EMS solution on the orbital shaker at 60rpm overnight. The seed was washed with running tap water for 2-3 hours and the EMS residue was inactivated with an equal volume of 0.1 M NaOH and 20% w/v Sodium Thiosulfate for 24 hours. The seeds were planted in root

trainers and the survival rate was recorded 12-15 days after planting by comparing to 0% EMS as control. Second, we proceeded to perform the seed treatment with the selected EMS concentrations to create the mutant populations.

To obtain a target population of 2000 mutant lines, approximately 4000 seeds, designated as M0 seeds, were soaked in EMS solution using the same procedure as described above. The treated seeds, referred to as M1 seeds, were sown individually to become M1 plants and allowed to self-pollinate. Since the M1 genotype is chimeric (Comai & Henikoff, 2006), individual spikes (M2 seeds) were selected from M1 plants and five M2 seeds per line were sown in one pot and later thinned to leave a single M2 plant per line. At this point, the M2 genotype can be homozygous dominant, heterozygous, or homozygous recessive for the mutation (Comai & Henikoff, 2006). Leaf tissue from each M2 plant was collected and stored at -80°C for subsequent DNA extraction. The rest of the M2 seed was stored at 4°C. Similarly, M3 seeds were obtained from collecting individual spikes from M2 plants and the harvested seed was divided into three sets. One set was sent to Bolivia for field phenotyping, the second set was sent to Uruguay for generation advancement, and the third set was stored at 4°C (Fig. 3.1).

Field phenotyping

The evaluation of M3 and subsequent M4 lines against WB was done in Bolivia in collaboration with the Association of Producers of Oilseeds and Wheat (ANAPO) as a part of the long-studying KSU wheat blast research. Irrigated field trials were conducted during field seasons of 2018 to 2020, either in Okinawa city (17°14'33.832" S, 62°53'21.412" W) during April-August (winter season) or in Quirusillas city (18°19'45.922" S, 63°56'51.442" W) during December-March (summer season). For all the experiments, about 50 seeds from each line were planted in a 1-meter row with 20 cm spacing between rows using a randomized incomplete block design consisting of ten 1-m row plots, where the outside rows were one of two check varieties. The spring wheat variety 'Atlax' was used as a susceptible check and the resistant variety used to make the respective EMS population was used for the resistant check. The eight inside rows were mutagenized lines being evaluated. Also, spreader rows with the cultivar 'Atlax' were planted surrounding the complete nursery and every two incomplete blocks (Fig. 3.2).

A highly aggressive monosporic race 2 isolate (isolate 008) collected in Quirusillas city in 2015 (Cruppe et al., 2019) was used to artificially inoculate the spreader rows. Inoculum production and field inoculations were done following previously described protocols (Cruppe et al., 2019; Cruz et al., 2016). WB incidence and severity were scored on the heads at Feekes GS 11.1 (milky ripe stage of grain development) and Feekes GS 11.2 (soft dough stage of grain development). Incidence was measured as the average of diseased spikes and severity as the average of infected spikelets. Both traits were recorded using a visual scale from 0 to 100%. Candidate mutant lines were identified as being more susceptible than the WHB score of the resistant parent. Only the lines showing greater susceptibility than the resistant check, either by higher incidence or higher severity, were selected and harvested for further evaluation.

Seed from the selected lines increased in Uruguay was sent to Bolivia for a new round of field evaluations using the same field design and methodology as previously described. After two rounds of field evaluations, each candidate mutant line was replicated in 3 row-plots under the same field design and disease conditions, to formally test if susceptible mutant lines are significantly different from the $2N^{V}S$ resistant donor line.

Results

Mutagenesis and populations development

Five mutagenized populations in spring hexaploid wheat using EMS as a chemical mutagen were developed. The spring wheat lines carrying the $2N^{V}S$ fragment used to create the populations were previously characterized as resistant or moderately resistant to WHB (Cruppe et al., 2019).

The EMS dosages selected to mutagenize the populations were 0.5% for 'TBIO Sossego', 0.4% for 'TBIO Sintonia' and 'Milan-2', and 0.3% for 'Yoyau' and 'Urubo' (Fig. 3.3). In all cases, the % of germination of the untreated seed (EMS 0%) ranged between 72 – 95%. When the exact value of 50% survival rate was not obtained, we selected the closer EMS concentration to the accepted value. Most plants appeared no different from the parental line; however mutant phenotypes in M1 plants were observed and in some rare cases, plants with abnormal phenotypes observed in greenhouse-grown plants were removed for posterior evaluations. Some of the most common phenotypes observed on the M1 mutant plants were height mutants, both tall and dwarf,

compact heads, partial or full sterility, a few mutants displaying albinism, among others. The population sizes obtained for each resistant donor line after mutagenizing the M0 seed and sowing M1 seed were, 944 M1 plants for 'TBIO Sossego' population, 2910 M1 plants for 'TBIO Sintonia' population, 1763 M1 plants for 'Yoyau' population, 906 M1 plants for 'Urubo' population, and 2300 Mi plants for 'Milan-2' population. Only M2 lines with more than 100 seeds were sent to Bolivia for phenotyping.

Field phenotyping

To date, only the populations developed from 'TBIO Sossego' and part of 'TBIO Sintonia' were evaluated against WHB under field conditions in Bolivia. For 'TBIO Sossego', the M2 seed of 933 lines were scored against WHB under field conditions in the summer of 2018 in Quirusillas city. However, we were able to collect data for only 197 lines. For this experiment, the mean WHB scores for the susceptible check 'Atlax' were 99% incidence and 97% severity. The resistant parent 'TBIO Sossego' resulted in 9% incidence and 4% severity (Fig. 3.4A). Using the WHB scores from the resistant parent as the cutoff, 109 M2 lines showing higher values of WHB incidence and severity were selected (Fig. 3.4A) and plants showing susceptible symptoms were individually harvested. WHB disease phenotype for the selected M2 plants ranged between 9% and 100% for incidence and between 4% and 100% for severity. In total, 480 individual M2 plants were harvested from the 109 susceptible M2 lines. Since the seed harvested from Bolivian experiments was colonized by the fungus and germination was compromised, 460 plants belonging to the same 109 M2 lines but increased in Uruguay were added to the experiment, totaling 940 M3 lines to evaluate in a new field experiment.

These 940 M3 lines were planted during the 2019 winter season in Okinawa city and phenotypic data was recorded for 708 lines. For this experiment, the mean WHB scores for the susceptible check 'Atlax' were 99% incidence and 97% severity. The resistant parent 'TBIO Sossego' resulted in a 46% incidence and 22% severity (Fig. 3.4B). Based on these values, 124 M3 lines showed higher WHB levels compared to the resistant parent, and 721 individually harvested plants were selected (Fig. 3.4B). From these 721 M4 lines we obtained good quality seed for 520 M4 lines that were planted in a new field experiment in 2019 summer season. Unfortunately, this field experiment was lost due to an extreme WB pressure during the early

establishment of the plants which killed the entire nursery. However, we had remnant seed to repeat the experiment for 391 M4 lines. These were evaluated during the 2020 winter season in Okinawa city repeating each line in 3-row plots. For this experiment, phenotypic data were collected for all the 391 lines. The mean WHB scores for the susceptible check 'Atlax' were 99% incidence and 94% severity. The resistant parent 'TBIO Sossego' resulted in a 40% incidence and 30% severity (Fig. 3.4C). Based on the phenotypic response of the resistant parent we selected 102 lines that trace back to 23 pedigrees or initial M1 plants (Fig. 3.4D). From these, 60 lines that trace back to 22 pedigrees, were planted using 3 rows per line during the 2020 summer season in Quirusillas to confirm the susceptible phenotype. Seed from these 60 lines was shipped from Bolivia to the Biosecurity Research Institute at Kansas State University where plant tissue will be collected for subsequent DNA extraction and sequencing.

For 'TBIO Sintonia', M2 seed of 1433 lines (almost half the compete population) was planted during the 2019 winter season in Okinawa city. WHB incidence and severity of the susceptible check 'Atlax' were 95% and 85%, respectively. For the resistant parent 'TBIO Sintonia' the WHB scores resulted in 57% incidence and 33% severity (Fig. 3.5). A total of 284 M2 lines had higher WHB values compared with the resistant parent, which derived in 1474 M3 lines planted in the 2019 summer season. From these1474 M3 lines, seed for 1349 lines was obtained from the increase conducted in Uruguay. These 1474 M3 lines were planted in 2019 summer season. Unfortunately, this field experiment got lost due to extreme WB pressure during the early establishment of the plants which killed the entire nursery.

Discussion

Mutagenesis and populations development

Mutagenizing with EMS became popular when it was used in combination with rapid mutational screening to discover targeting induced local lesions in genomes (TILLING) as a reverse genetic strategy to determine the function of a gene by exploring individuals that possess the mutated gene (McCallum et al., 2000; Waugh et al., 2006). Moreover, EMS is easy to use, does not require sophisticated equipment, and produces high mutation frequency (Sikora et al., 2011). Even though the main objective of this study was not to develop TILLING populations, the availability of an assembly for the $2N^{v}S/2A$ translocation in the wheat cultivar 'Jagger' (Gao et

al., 2020) would benefit and assist in TILLING these EMS populations to discover mutations in genes of interest by applying reverse genetic approaches (Comai & Henikoff, 2006). Moreover, these lines could be used for further forward genetic approaches and directly by breeding programs since the introduced variation is non-transgenic. Seed at the M2 stage for the five mutant populations generated in this study is available for distribution with the research community.

An additional EMS-mutagenized population already exists in the wheat cultivar 'Jagger' carrying the $2N^{v}S/2A$ translocation (Rawat et al., 2019). However, since 'Jagger; has a winter growth habit, performing field phenotyping in South America, where spring habit is desirable, would have been possible but challenging. To our knowledge, the EMS-derived mutant populations developed in this study plus a mutant population created with the Australian cultivar 'Scepter' are the only EMS-derived populations available in a spring wheat background carrying the $2N^{v}S/2A$ chromosome-segment translocation (Urmil Bansal personal communication). In this sense, we have begun a collaboration with the research group working with the 'Scepter' mutant population to join efforts on characterizing and elucidating the function of many of the resistance genes located on the $2N^{v}S/2A$ translocation.

Ethyl Methane Sulfonate (EMS) is an alkylating base modifying agent widely used to produce novel allelic variation in genes by causing mainly transitions from G/C to A/T randomly across the genome (Comai & Henikoff, 2006; Greene et al., 2003). Therefore, beginning with a large population size is important to increase the chances to get the mutation of interest (Sikora et al., 2011). In this study, we used an initial M0 population of c.a. 4000 seeds, a size that is considered large but remaining a manageable number of mutagenized plants to screen for the phenotype of interest. Several studies have used either larger or smaller population sizes, still achieving good mutation frequencies (Chen et al., 2012; Lethin et al., 2020; Slade et al., 2005; Uauy et al., 2009). A different strategy to capture a larger number of mutations is selecting more than a single M2 plant (Chen et al., 2012). However, by starting with a larger M0 population and following single-seed descent of the M2 seed, genetic redundancy of mutations is avoided. In our study, we used five different wheat cultivars carrying the targeted translocation. By using several genetic backgrounds we increased the probability to find the mutation in a more favorable genetic background that may or may not mask the phenotype. This becomes crucial

since the known effect of the genetic background on the differential expression of $2N^{v}S$ resistance (Cruppe et al., 2019; Cruz et al., 2016).

The optimal EMS concentration selected to mutagenize the seed depends on the ploidy of the species. The polyploid nature of wheat naturally provides genetic buffering against the effect of mutations (Dubcovsky & Dvorak, 2007) which allows higher mutation rates in EMS experiments (Comai & Henikoff, 2006; Waugh et al., 2006). However, the optimal EMS dosage varies in response to the genetic background (Uauy et al., 2009). Several different EMS concentrations have been used for mutagenizing wheat to achieve an optimal survival rate (Chen et al., 2012; Lethin et al., 2020; Mishra et al., 2016; Slade et al., 2005; Uauy et al., 2009). Not surprisingly, we obtained different EMS dosages for the different genotypes (Fig. 3.3), a result that highlights the effect of the genetic background and the importance to test the target dosage rate for the genotype of interest. Taking into account the germination rate for each resistant donor, the survival rate obtained for the M1 seed treated with the selected EMS dosage calculated from the optimal survival rate ranged between 50% and 150%. This means that for some lines, the optimal EMS dosage selected failed to obtain a 50% survival rate.

The same polyploid nature of wheat that allows a species to tolerate high EMS dosages also impacts the identification of recessive mutant alleles due to the genomic redundancy between the different sub-genomes. This redundancy could complicate the identification of a phenotype by masking the effect of recessive alleles (Chen et al., 2012; Krasileva et al., 2017). In our study, the redundancy caused by homologues on the other two genomes (B and D) is not of concern since we are targeting a dominant gene, located in a non-recombining segment that is present only in the A genome of wheat.

This study has generated novel genetic resources for characterizing resistance to WHB and to explore the array of resistance genes located on the $2N^{v}S$ translocation on chromosome 2A of hexaploid wheat. These mutant lines in combination with sequencing will enable cloning the gene(s) controlling the trait. EMS mutagenesis can be coupled with several different sequencing techniques depending on the nature of the trait (Bettgenhaeuser & Krattinger, 2019). For example, MutMap+ is a fast and affordable technique suitable for any gene with a strong phenotype (Bettgenhaeuser & Krattinger, 2019; Fekih et al., 2013a). MutMap+ allows the

identification of causal mutations by bulking DNA from M3 mutants and wild-type lines without the necessity of making crosses and developing extra populations as in MutMap (Abe et al., 2012; Fekih et al., 2013b). However, in our case it is not clear how this approach would work since the non-recombining nature of the $2N^{V}S/2A$ fragment does not allow implementing fine mapping. A different strategy is MutRenSeq that combines EMS mutagenesis and NLR enrichment capture array to discover the causal gene associated with a phenotype (Steuernagel et al., 2016). In our case, it is currently not clear based on the host-pathogen interaction if we would expect the WHB resistance to be controlled by an NLR gene family, therefore MutRenSeq might not be a suitable approach. An alternative strategy that does not depends on recombination or fine mapping and also overcomes the necessity of the candidate gene belonging to the NLR family is MutChromSeq (Sánchez-Martín et al., 2016). MutChromSeq overcomes the bias of exome-capture approaches such as MutRenSeq, by combining mutagenesis, genome reduction by chromosome flow sorting, and sequencing. In this strategy, the genomic sequence of mutant lines is compared against the wild-type sequence to identify causal mutations. This strategy has been used successfully to clone genes in wheat (Sánchez-Martín et al., 2016). However, a critical limitation of MutRenSeq is the need to flow sort target chromosomes which is technically challenging and can only be done by few research groups. The final strategy which is being applied for our mutant populations is to develop a sequence capture array to enrich for genes of interest in the target region. In this case, the design of such array is made possible by having the genome assembly of multiple wheat genomes with $2N^{V}S$ which provides high confidence, high-quality gene sequence to design the bait probes. With the development of this array, we will be able to enrich and sequence all genes on $2N^{V}S$ in each of the mutant lines and then apply the principles of MutRenSeq.

Based on our original hypothesis that the $2N^{V}S$ carries a single, dominant resistance gene controlling WHB disease resistance, the identification of WHB susceptible mutant lines (i.e. isolines for the mutation) in the EMS populations supports the hypothesis of a single gene. The identification of susceptible lines was favored by characterizing large populations in a conducive environment for the disease (Bettgenhaeuser & Krattinger, 2019). However, it remains unclear if the targeted gene belongs to the NLR-family. Also in favor of our single-gene hypothesis, the excepted mutation rate that supports more than one gene is extremely low and it would

necessitate finding sufficient candidate mutant lines showing loss-of-function for all the involved genes, which is almost impossible. Cloning genes that control quantitative resistance, commonly not explained by NLR genes, using mutational cloning could be challenging. However, this could be simplified using the isolines created in this study to differentiate the trait.

Conclusions

We will continue with the characterization of the EMS populations against WHB under field conditions for a final evaluation and confirmation of the increased susceptibly of the mutant lines. We will also use the disease evaluation scores for the 'TBIO Sossego' population from the 2020 summer season in Quirusillas to confirm the phenotype of WHB susceptible candidate mutant lines that will be sequenced to discover mutations and identify candidate genes. The final goal is to find the causal mutation(s) controlling WHB resistance located in the $2N^{V}S/2A$ wheat translocation. In our study, the induced diversity is useless from the breeding point of view to improve WB, however, the germplasm developed is a valuable resource for functional genomics, providing a powerful tool to uncover variation associated with the $2N^{V}S/2A$ translocation in bread wheat.

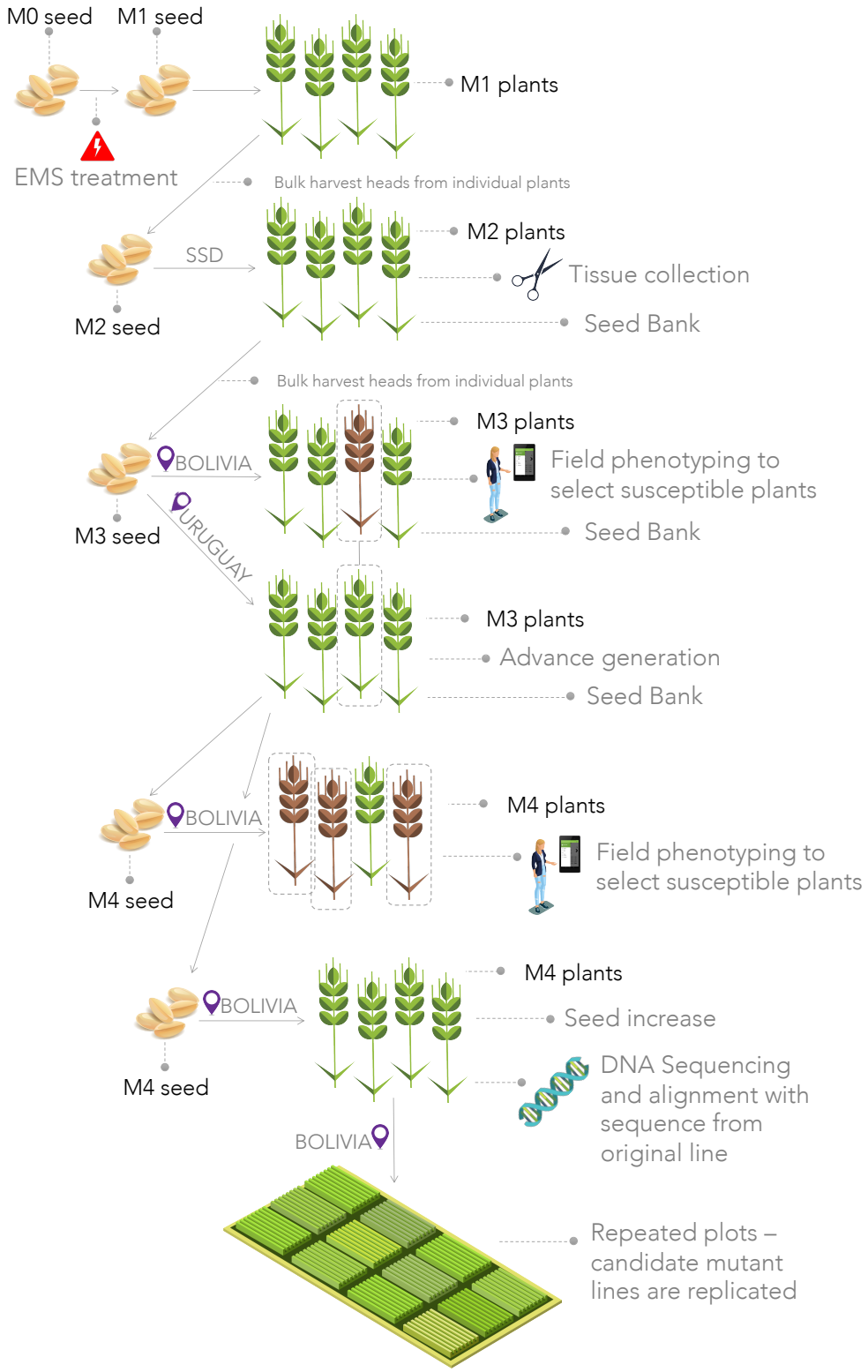

Figure 3.1 – Scheme of population development, field evaluations, and tissue collection.

Figure 3.2 – Field trial layout.

Field experiments located in Okinawa city in Bolivia in 2019. The purple dashed lines indicate border plots planted with the susceptible ‘Atlax’. Blue dashed lines delimit two rows planted with the checks ‘Atlax’ (red, susceptible) and ‘TBIO Sossego’ (green, resistant) in zigzag. Candidate mutant lines with increased severity are shown with yellow arrows.

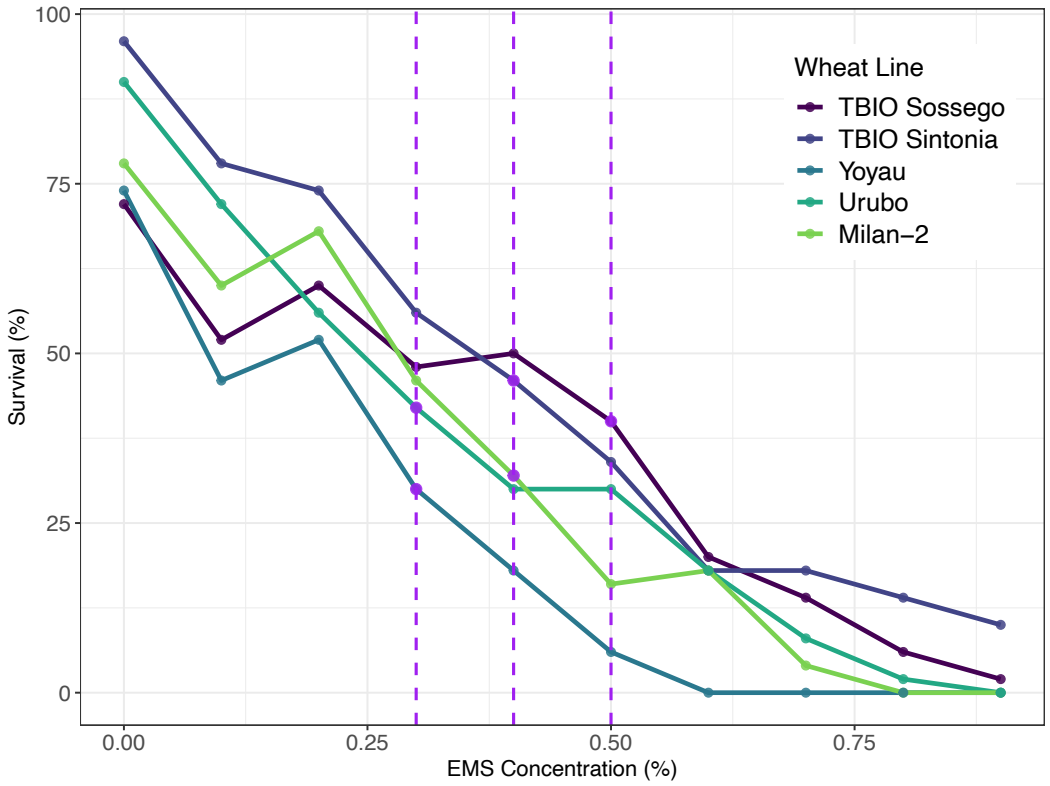

Figure 3.3 – EMS survival rate results.

Calculation of EMS dosages causing a 50% survival rate to select the EMS concentration to treat the M0 seed from the different spring wheat lines selected. Purple dots highlight the 50% survival or killing rate and the purple dashed line shows the EMS concentration selected.

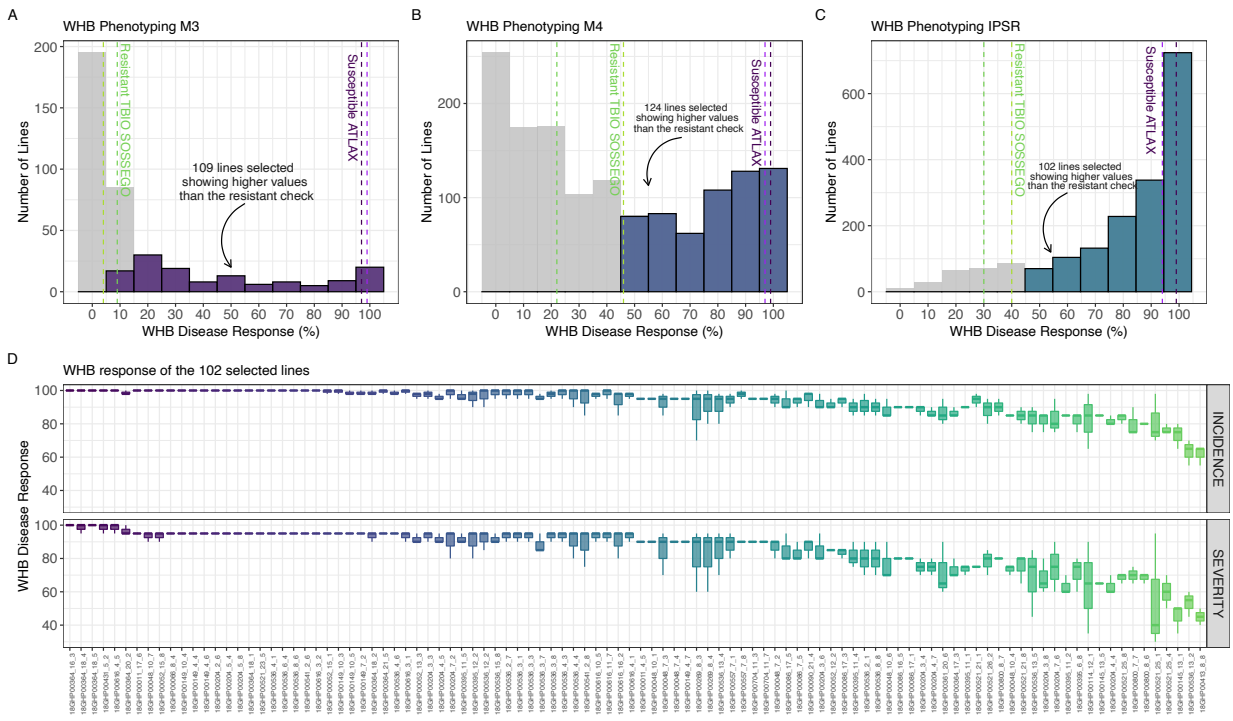

Figure 3.4 – Wheat head blast (WHB) response of 'TBIO Sossego' mutagenized lines.

Distribution of WHB phenotypes (incidence and severity) at each field experiment. A) distribution of M3 lines, B) distribution of M4 lines, and C) distribution of M5 lines. In each plot, the highlighted area shows the distribution of the selected lines showing higher levels of susceptibility compared with the resistant check 'TBIO Sossego'. D) each M5 line was planted in 3 plots to assess repeatability.

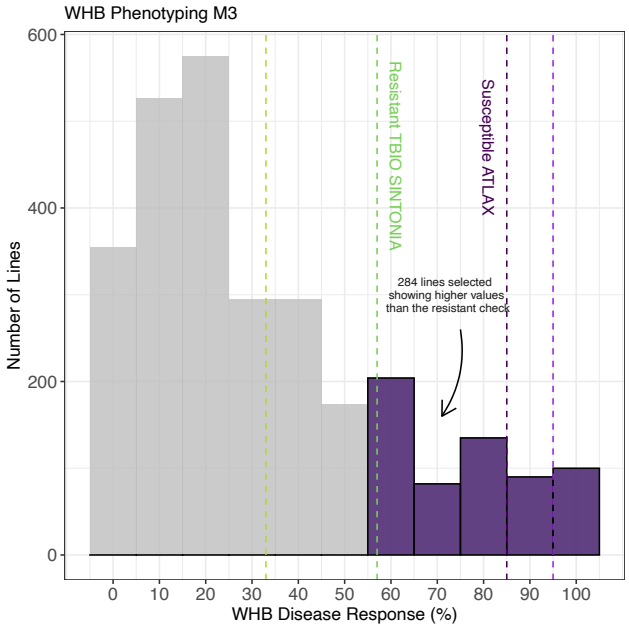

Figure 3.5 – Wheat head blast (WHB) response of 'TBIO Sintonia' mutagenized lines.

Distribution of M3 lines planted for 2019 winter season in Okinawa City in Bolivia. Selected mutant lines showing higher WHB response than the resistant check are highlighted.

Subchapter 3B) Characterizing a collection of the wild relative *Ae. tauschii* to identify novel sources of resistance against wheat head blast

Introduction

Wheat resistance to diseases and pests has been significantly improved through the identification, introgression and deployment of novel genes from different wild relatives representing the primary, secondary, and tertiary pools of the cultivated wheat (Friebe et al., 1996; Molnár-Láng et al., 2015). Among these, species belonging to the genus *Aegilops* have been one of the most useful wild species in wheat breeding for identifying and introgressing novel sources of genetic resistance (Kishii, 2019; Schneider et al., 2008; Zhang et al., 2015). A good example of this is *Ae. ventricosa* derived wheat head blast (WHB) resistance conferred by the $2N^{V}S/2A$ chromosome-segment translocation (Cruz et al., 2016). Furthermore, one of the most important species in the genus is *Ae. tauschii* because it is the D subgenome donor to bread wheat. Due to its homologous D subgenome with wheat and its greater genetic diversity, *Ae. tauschii* is an important source of genetic diversity for wheat improvement (Börner et al., 2015a). *Ae*. *tauschii* is the diploid progenitor of hexaploid wheat ($2n = 2x = 14$, DD) that evolved about 5.5 million years ago (Rasheed et al., 2018). Two morphologically and genetically different lineages can be distinguished within *Ae*. *tauschii*, lineage 1 (L1) which has been known as subspecies *tauschii* and L2 known as subsp. *strangulata* . Furthermore, the occurrence has been suggested of a third lineage (L3) represented by few accessions (Singh et al., 2019). The origin of the wheat D subgenome has been traced to L2, which was likely one or very few accessions (Lagudah et al., 1991; Wang et al., 2013). As a result, bread wheat experienced a significant genetic bottleneck and only a small fraction of the available genetic diversity from the D subgenome is represented in the cultivated bread wheat germplasm pool (Rasheed et al., 2018). An example of an economically important trait for which the cultivated bread wheat germplasm lacks diversity is wheat head blast (WHB). Several studies have reported a very limited repertoire of resistance genes against WHB in bread wheat (Cruppe et al., 2019, 2020; Cruz et al., 2016; Ferreira et al., 2020; Goddard et al., 2020; He et al., 2020; Juliana et al., 2020). Therefore, identifying new resistance genes is of top priority to broaden the available genetic resources against WHB. In this sense, wild species related to wheat have been used as resistance

sources for plant breeding showing abundant unexploited genetic diversity (Hao et al., 2020; Johansson et al., 2020; Kishii, 2019; Rakszegi et al., 2020).

Motivated by the extensive use of wild wheat relatives as treasure troves of resistance genes against several different pathogens and the fact that the only useful source of resistance against WHB was introgressed from a wild species, we hypothesized that *Ae. tauschii* is an unexploited source of genes for resistance to WHB that could be utilized for wheat resistance breeding. Supporting this, previous studies using a small number of accessions have reported the existence of resistance for WHB within the *Ae. tauschii* pool and synthetic wheats (Bockus et al., 2012; Cruppe et al., 2019; Cruz et al., 2010). The objectives of our study were to i) characterize the level of resistance to WHB across a diverse panel of *Ae. tauschii*, ii) identify genomic regions associated with WHB resistance, and iii) characterize the genetic architecture of resistance in the wild wheat relative *Ae. tauschii*.

Materials and Methods

Plant Material

A total of 226 *Ae. tauschii* accessions were obtained from the Wheat Genetics Resource Center (WGRC) at Kansas State University in Manhattan, KS, United States, including 80 from lineage 1 (L1) and 146 from lineage 2 (L2) (Supplementary Table C.1). Lineage designation, geographic origin, and passport data are available from Singh et al. (2019). The accessions were selected because most have been sequenced with whole-genome-sequencing (WGS) data through the open wild wheat consortium (OWWC - http://www.openwildwheat.org) and genotyping-by-sequencing (GBS) data, obtained from Singh et al. (2019).

Phenotypic data

The experiments under controlled conditions were carried out in ANAPO, Bolivia during 2018-2020, as a part of the long-studying KSU wheat blast research. Accessions from L1 and L2 were evaluated in independent experiments. Five seeds per accession were grown in 15-cm diameter pots, and two pots were evaluated for each accession and used as replications. After the plants were in two leaf stage, a vernalization period of eight weeks in a cold room at 4°C and 9h light :15h dark was completed prior to transplanting and inoculation. Fully emerged *Ae. tauschii*

heads were inoculated with the race 2 isolate 008 collected in Bolivia in 2015 (Cruppe et al., 2019). When it was possible, at least 10 head per pot per accession were inoculated. Inoculum preparation and inoculation method were done following previously described protocols (Cruppe et al., 2019; Cruz et al., 2016). WHB disease severity was evaluated at five-time points at 10, 12, 14, 16, and 18 days after inoculation (dai). Individual heads from the same accession were rated separately using a 0 to 100% scale to represent the percentage of diseased spikelets. Control checks were included every time, using the winter wheat varieties 'Jagalene' and 'Everest' as resistant and susceptible checks, respectively.

Genotypic data

Genotyping-by-sequencing (GBS) was used to discover polymorphic variants across the *Ae. tauschii* panel. Variants were called using the reference genome assembly Aet v4.0 (NCBI BioProject PRJNA341983). GBS data from Singh et al. (2019) was used first including accessions from both lineages and later by splitting the data into the different lineages and removing the accessions with no phenotypic data. An additional filtering step to remove marker loci with minor allele frequency (MAF) < 0.01, missing data > 80%, and/or heterozygosity > 20%, was performed to keep only high-quality SNP markers for further analysis.

Statistical analyses

Phenotypic data

Disease severity was assessed at multiple time points to characterize the disease progress. First, the best linear unbiased estimator (BLUE) or adjusted means were calculated for each time point evaluation using the model,

$$y_{ij} = \mu + R_i + G_j + e_{ij} \quad \text{[Eq. 1]}$$

where y_{ij} is the WHB severity at a unique time point j calculated by averaging multiple single head observations at that time point, μ is the overall mean, R_i is the random effect of the i^{th} replication and assumed distributed as iid $R_i \sim N(0, \sigma_R^2)$, G_j is the fixed effect of the j^{th} accession (genotype), and e_{ij} are the random left-over residual errors and assumed as iid

distributed $e_{ij} \sim N(0, \sigma_e^2)$. The BLUE values obtained for each evaluation time point were used to calculate the area under the disease progress curve (AUDPC) (Madden et al., 2007) (Supplementary Table C.1) using the R package 'agricolae' (De Mendiburu & Simon, 2015) as,

$$\text{AUDPC}_{(k)} = \sum_{i=1}^{n} \frac{(y_i - y_{i+1})}{2} (t_{i+1} - t_i) \quad \text{[Eq. 2]}$$

where, n is the number of disease evaluations, y_i is the WHB disease severity measurement at time point (t_i), y_{i+1} is the WHB disease severity measurement at a consecutive time point (t_{i+1}), and $y_i = y_0$ is the first disease severity observed at the first inoculation time point (t_0) at 10 dai.

Using the same model described in Eq. 1 but defining the genotype effect G_i as a random effect we estimated the variance components for each term and computed broad-sense heritability (H^2) using the 'lme4' package in R (Bates et al., 2014) as,

$$H^2 = \frac{\sigma_G^2}{\sigma_G^2 + \frac{\sigma_e^2}{r}} \quad \text{[Eq. 3]}$$

where, σ_G^2 is the genotypic variance, σ_e^2 is the residual error variance, and r is the number of replications.

Population structure

High-quality SNP markers were used to perform principal component analysis (PCA) to study population structure for each lineage separately. The PCA analysis was performed with the imputed marker score matrix calculated with R software using the 'A.mat' function from the 'rrBLUP' package (Endelman, 2011). PCA was performed for each lineage separately and the calculated principal components were used to control for population structure in the association analysis.

Association analysis

A mixed linear model was implemented for genome-wide association analysis (GWAS) as described by Yu et al. (2006), using the 'rrBLUP' package in R (Endelman, 2019),

$$y = X\beta + Zu + S\tau + e \quad \text{[Eq. 4]}$$

where $y_{(n\,x\,1)}$ is the vector of BLUE values or phenotypic adjusted means, $X_{(n\,x\,f)}$ is the matrix of fixed covariates, $\beta_{(f\,x\,1)}$ is the vector of fixed effects including the intercept and population structure covariates, $Z_{(n\,x\,n)}$ is the kinship matrix calculated from markers and relating of $y_{(n\,x\,1)}$ to $u_{(n\,x\,1)}$, $u_{(n\,x\,1)}$ is the vector of polygenic background, $S_{(n\,x\,1)}$ is the vector of marker scores for the single marker being evaluated with values -1, 0, or 1, τ is a scalar representing the additive marker allele effect to be estimated, and e is the residual error distributed $N(0, \sigma_e^2)$. The mixed model implemented in equation Eq. 4 test each marker independently to estimate τ.

The GWAS model was run for the five evaluation time points and AUDPC, first combining all the accession from both lineages and in a second step for each lineage individually. The threshold level for calling significant marker-trait associations and to avoid false positives was calculated using the Bonferroni correction with an experimental significance level alpha value of 0.05. Manhattan plots were generated with 'CMplot' package in R software (https://cran.r-project.org/web/packages/CMplot/CMplot.pdf).

Results

Phenotypic data

In total, we recorded more than 3300 disease measurements taking into account all accessions, checks, replication and time point evaluations. WHB severity showed a wide variation within the *Ae. tauschii* panel used in this study and the progress of the disease increased at each time point evaluation (Fig. 3.6). The susceptible check 'Everest' recorded and AUPDC value of 574.2 and 574.6, for L1 and L2 experiments, respectively. Meanwhile, the resistant check 'Jagalene' was 306.4 and 18.4 (Fig.3.6). Overall, we found more susceptible than resistant accessions, with most of the resistant accessions belonging to L2. The mean AUDPC values were 464.4 and 356.2, for L1 and L2, respectively (Supplementary Table C.1). An accession was considered resistant if the WHB severity value at 18 dai was < 20%. For L1, we observed 8 resistant accessions with WHB severity at 18 dai ranging between 3.7% and 19.9%, with a mean value of 10.9%. The corresponding AUDPC values were between 12.2 and 74.3, with a mean AUDPC of 44.5 (Fig. 3.6). For L2, we observed 27 resistant accessions with WHB severity at

18 dai ranging between 2.9% and 17.3%, with mean 10.6%. The corresponding AUDPC values were between 11.3 and 98.5, with a mean AUDPC of 46.1 (Fig. 3.6). WHB AUDPC values were plotted on a map based on passport information to investigate if resistance was associated with geographical origin. From the geographical distribution map (Fig 3.6), we did not find any evident pattern since most resistant accessions are spread across the natural habitat.

Phenotypic correlations between the five evaluation time points and AUDPC was high (> 0.75) for both lineages, slightly decreasing when comparing time points further apart (Fig. 3.7). For both lineages, AUDPC had a higher phenotypic correlation with 14 dai. H^2 values were also high for all the evaluation time points, with values for L1 marginally higher than values for L2 for 10-, 12-, and 14 dai, and the opposite situation for 16-, and 18 dai (Fig. 3.7).

Genotypic data and Population structure

From a total of 13,135 SNP markers obtained from Singh et al (2019), we removed the accessions with no phenotypic data and filtered the markers to retain 10,998 SNP markers. Filtering for the different lineages separately we obtained 5,100 SNPs and 6,491 SNPs for L1 and L2, respectively. We then used these SNPs to calculate the additive relationship matrix to perform the PCA and check the population structure within each lineage (Fig. C.1). The first three PCs explained 30% and 34% of the variation, for L1 and L2, respectively. Phenotypic response to WHB at 18 dai and the AUDPC values were used to color the accessions to assess if population structure was cofounded with resistance. We did not observe a strong pattern of resistant versus susceptible clusters. (Fig. C.1).

Association analysis

To investigate the hypothesis that WHB resistance in *Ae. tauschii* is determined by genetic components we first calculated the H^2. To further explore this hypothesis and specifically determine if WHB in *Ae. tauschii* is an oligogenic trait explained by a few loci with large effect we perform GWAS. The GWAS analysis was conducted combining both lineages and for each lineage separately (Fig. 3.8). For the combined analysis we found significant marker-trait associations above the Bonferroni threshold on the proximal end of chromosome 7D (Fig. 3.8). These associations were significant for 10-, 12 dai, and AUDPC. The interval was estimated at

627.2 Mbp, comprising three SNP markers that defined four different haplotypes (Fig. 3.9). From the four haplotypes, two were common for both lineages. Moreover, the most resistant haplotype for each lineage were different (Fig. 3.9). Performing the analysis for each lineage separately also detected this QTL on chromosome 7DL for both lineages (Fig. 3.8). For L1, this QTL was the only significant association detected, and the associations were significant for 10-, 12-, 14 dai, and AUDPC (Fig. 3.8). The associated interval was estimated at position 627.1 Mbp, comprising five SNP markers that defined two different haplotypes, one associated with reduced WHB AUDPC and WHB severity at 18 dai (Fig. C.2). For L2, we found additional significant associations on chromosomes 1DS, 2DL, and 7DL (Fig. 3.8). These associations were significant for AUDPC and at least one evaluation time point. On the distal end of chromosome 1D, we obtained one association at 6.5 Mbp defined by a single SNP marker (QTL1). For chromosome 2DL, the genomic region was estimated at position 508.3 Mbp and was defined by a single SNP marker (QTL2). For chromosome 7DL, we found two different associations both explained by a single SNP marker, one located at 570.1 Mbp (QTL3) and one located at 636.1 Mbp (QTL4) (Fig. C.2 and Fig. C.3). The combination of favorable alleles for the four QTLs lead to eight different combinations present within the L2 accessions. An additive effect was not observed since the accessions combining the four QTLs did not express lower AUDPC values (Fig. C.2).

Discussion

Phenotypic data

Resistance to WHB on both lineages was previously reported (Cruppe et al., 2019; Bockus et al., 2012). In this study, we found resistant accessions (WHB severity < 20% at 18 DAI) from both lineages, though the majority were from L2 (Fig. 3.6). Our results are in agreement with previous results finding L2 accessions TA10142, TA1616, TA1624, and TA1644 resistant to WHB (Cruppe et al., 2019; Bockus et al., 2012). However, for other accessions evaluated in these studies we observed some discrepancies, probably explained by different MoT isolates used to inoculate (T-25 – Bockus et al., 2012, B-71 – Cruppe et al., 2019 or 008 – this study). By comparing our results with those from Cruppe et al. (2019), we found 19 accessions (eight from L1 and 11 from L2) that had more than 20% WHB severity of difference at 14 dai, with values from our study being less susceptible. Moreover, we also found 3 accessions (2 from L1

and 1 form L2) displaying higher WHB severity values in our study. These differences could be explained by different experimental conditions and/or by using different isolates to evaluate the accessions, which supports a gene-for-gene genetic architecture for the MoT – *Ae. tauschii* pathosystem. Consistency on the phenotypic value for the wheat cultivar 'Everest' used as a susceptible check confirms that the inoculation method was successful (Fig. 3.6). However, for the resistant check 'Jagalene' we observed a difference between the L1 (AUDPC 306.4) and L2 (AUDPC 18.4) experiments. This difference could be explained by loss of virulence in the 008-isolate used in the L2 experiment, meaning that the phenotypic responses could be underestimated and therefore resistant accessions were probably overestimated. Isolate aggressiveness is presumably increasing as reported by Cruppe et al. (2020). In this study, we used the isolate 008 collected in Quirusillas, Bolivia in 2015. There are now more recent isolates available that could be used to further characterize the *Ae. tauschii* collection to assess resistance and confirm if the accessions we found resistant in this study still hold resistance against more aggressive isolates.

Pearson's correlations and H^2 for the phenotypic values between the different evaluation time points were high (Fig 3.7). Thus, selecting less time point evaluations for future experiments using phenotypic characterization of WHB could be sufficient to achieve consistent and repeatable evaluations. Based on our results we recommend including 14 dai as one of the more descriptive evaluation time point to assess the disease response, also highly correlated with AUDPC (Fig. 3.7).

Resistant *Ae. tauschii* accessions from both lineages displayed a highly resistant phenotype, expressing the typical necrotic flecks that resemble a hypersensitive response (HR) (Fig. C.4). The HR response is associated with qualitative resistance, following the gene-for-gene model, where an avirulence (*Avr*) gene in the pathogen is recognized by a complementary resistance (*R*) gene in the host, leading to hypersensitive resistance or no infection response (Flor, 1971). In this scenario, we hypothesize that resistance to WHB in *Ae. tauschii* is qualitative, suggesting that the trait could be controlled by typical nucleotide-binding site leucine-rich repeat (NLR) type resistance genes. In addition, it would be also expected to observe a strong isolate by genotype interaction when evaluating several different isolates. Supporting this postulate, many

resistance genes in rice to the rice blast disease caused by MoO (same fungus but different pathotype to MoT) have been identified to belong to the NLR family (Deng et al., 2020).

Association analysis

Aegilops tauschii has been widely used as a source for novel resistance genes against many biotic stresses (Börner et al., 2015; Cox, 1992; Gill & Raupp, 1987; Kishii, 2019; Rasheed et al., 2018). An example of this are the non-host resistance genes *Rmg1* and *Rmg6*, effective against *Avena* and *Lolium* pathotypes, respectively, located on chromosome 1D (Inoue et al., 2017; Takabayashi et al., 2002; Vy et al., 2014). Moreover, resistance to WHB has been reported in *Ae. tauschii* and synthetic wheat based on phenotypic characterization only (Bockus et al., 2012; Cruppe et al., 2019; Cruz et al., 2010). Our study is the first report of genetic mapping of resistance to WHB in the *Ae. tauschii* germplasm. Even though it could be argued that *Ae. tauschii* was most probably not exposed to MoT in its natural habitat, we were able to identify that chromosomes 1DS, 2DL, and 7DL harbor resistance against WHB (Fig. 3.8). However, we only evaluated one isolate from race 2 (isolate 008). Evaluating more isolates, mostly from different MoT races and collected recently, would be beneficial in order to identify additional genomic regions controlling WHB in *Ae. tauschii*. In addition, characterizing WHB in other wild species related to wheat could help to broaden the resistance sources available to battle this disease (Kishii, 2019). Though, preliminary phenotypic data evaluating alien substitution lines derived from *Ae. speltoides* and *Haynaldia villosa* did not show promising results (Cruppe & Silva, 2020, unpublished). In addition, we evaluated the hard red winter wheat germplasm line KS89WGRC04, derived from a cross using the resistant *Ae. tauschii* accession TA1695 (Gill et al., 1991) against isolate 008, which resulted in susceptibly for WHB, averaging 97.5 % severity from 10 inoculated heads at 14 dai. Several other lines generated through direct cross with resistant *Ae. tauschii* accessions have been released by the wheat genetics resource center (WRGC) at Kansas State University (KSU) (www.kstate.edu/wgrc/genetic_resources/germ_plasm_releases_from_the_wgrc.html) that could be evaluated against MoT isolates (Supplementary Table C.2). More interestingly, this germplasm was created and released for resistance to one or multiple diseases and pests.

In this study, we found resistant accessions from both lineages, and the same genomic region was identified by GWAS combining both lineages which suggests that the same gene is controlling WHB resistance. To further investigate this hypothesis, we conducted the GWAS separating the lineages. Under this scenario, resistance was also mapped on the same position on chromosome 7DL for both lineages supporting the hypothesis of a common gene. However, different lineages could have the same or different haplotypes for the gene. Based on our haplotype analysis we observed different resistant haplotypes across both lineages, however, this could be constrained by using only three SNP markers to define the haplotypes. Additional QTLs were identified on chromosomes 1DS, 2DL, and 7DL for L2 accessions. Resistance genes *Rmg1* and *Rmg6* both were mapped to chromosome 1D however, we do not expect that either of the genomic regions mapped to chromosome 1D in this study is explained by the presence of these genes since isolate 008 used to conduct the inoculations most probably lacks the *Avr* genes PWT3 and PWT4 isolated from and *Avena* isolate (Inoue et al., 2017), thus being avirulent for *Ae. tauschii*. However, Inoue et al. (2020) suggested that MoT isolates could acquire PWT4 through horizontal transfer. Furthermore, whole-genome sequence data for the isolate 008 has already been generated (Cruppe, 2020) and it could be used to investigate if 008 carries the *Avr* genes PWT3 or PWT4. Further analyses are needed to define if these are real associations or artifacts of the analysis.

Resistant accessions identified here could be utilized to introduce WHB resistance into the wheat pool either by directly crossing them with hexaploid wheat (Gill & Raupp, 1987) or through the production of synthetic wheat (Li et al., 2018). In the former scenario, using spring wheat could favor the process to facilitate further field blast characterization in South America. A good strategy to start could be searching all the synthetic wheat collections available to identify if some of the resistant *Ae. tauschii* accessions identified in this and other studies have been already utilized. Additionally, wheat cultivars with known presence of *Ae. tauschii* resistant accessions on their pedigree and lacking the main source of WHB resistance, the $2N^{v}S$ translocation, could be selected to investigate if they have the resistant haplotype at the target locus and then be phenotypically evaluated for WHB severity. This approach will allow us to easily introgress this resistance into the breeding pipeline. For example, the wheat cultivar 'TAM 112' lacks the $2N^{v}S$ fragment but is highly resistant to WHB (Cruz et al., 2016) and interestingly possess in its

pedigree the *Ae. tauschii* L2 accessions TA2460 and TA1618 (Rudd et al., 2014), which are highly resistant and intermediate to WHB, respectively. Therefore, using mapping populations already developed with 'TAM 112' could help to rapidly identify the WHB resistance, which is ready to incorporate into breeding programs.

Another strategy to further investigate the genomic regions mapped in this study is to apply the AgRenSeq pipeline for discovering and cloning NLR genes (Arora et al., 2019). Since we have hypothesized that WHB resistance in *Ae. tauschii* is qualitative, this methodology has the potential to reveal if the WHB associated genomic regions found in this study are explained by genes belonging to the NLR family. Another approach is to use the available whole-genome sequencing data generated by the Open Wild Wheat Consortium (http://www.openwildwheat.org/), that is available for most of the accessions evaluated in this study. Several recent studies have been conducted aiming to identify novel resistance in the hexaploid wheat pool (Cruppe et al., 2020; Goddard et al., 2020; Juliana et al., 2019; 2020; He et al., 2020; Ferreira et al., 2020). All these studies found the $2N^{v}S$ alien fragment as the major source of WB resistance and other additional minor effect QTL located on several chromosomes. Therefore, major resistance genes or sources in the primary pool of wheat are very limited. These minor effect QTLs would be useful if combined with a major effect gene or by pyramiding several together to achieve good levels of resistance. A recent study has shown that the presence of the $2N^{v}S/2AS$ translocation is very common in CIMMYT and KSU wheat breeding programs (Gao et al., 2020). Moreover, it has also been reported that the resistance conferred by $2N^{v}S$ is eroding (Cruppe et al., 2020) which brings a challenging situation for breeding resistance to WB. Efforts should be guided to continuing with the identification of non-$2N^{v}S$ resistance sources, the discovery of more resistance genes, and the evaluation of relatives of wheat, which will become crucial for maintaining genetic resistance for WB.

Conclusions

This is the first report of genomic regions from *Ae. tauschii* associated with resistance to WHB. We were able to show that *Ae. tauschii,* the donor of the D subgenome of hexaploid bread wheat, has resistance against WHB. However, further research is needed to reach the gene level and understand the various mechanisms of this resistance. We have also found that many of the

resistant accessions found in this study have been already utilized to introgress into bread wheat, potentially accelerating the deployment of this novel resistance. Major, qualitative-type, resistance to WHB available in the current wheat gene pool is limited, therefore, continuing on this search using other species related to wheat, and different MoT isolates will be crucial to broadening the resistance genes available to introgress into wheat germplasm. Ultimately, untapped genetic diversity to identifying new sources of resistance will facilitate to breed wheat against WHB.

Acknowledgements

This material is based upon work supported by the National Science Foundation under Award No. (1822162) "Phase II IUCRC at Kansas State University Center for Wheat Genetic Resources WGRC" and support of industry partners, through support from the Kansas Wheat Commission and Kansas State University. PS was supported through a U.S. Fulbright-ANII Uruguay Scholarship. Any opinions, findings, and conclusions or recommendations expressed in this material are those of the author(s) and do not necessarily reflect the views of the National Science Foundation or industry partners.

References

Abe, A., Kosugi, S., Yoshida, K., et al. (2012). Genome sequencing reveals agronomically important loci in rice using MutMap. Nature Biotechnology, 30(2), 174–178. https://doi.org/10.1038/nbt.2095

Anh, V. L., Anh, N. T., Tagle, et al. (2015). *Rmg8*, a New Gene for Resistance to Triticum Isolates of *Pyricularia oryzae* in Hexaploid Wheat. Phytopathology, 105(12), 1568–1572. https://doi.org/10.1094/PHYTO-02-15-0034-R

Anh, V. L., Inoue, Y., Asuke, S., et al. (2018). *Rmg8* and *Rmg7*, wheat genes for resistance to the wheat blast fungus, recognize the same avirulence gene AVR-Rmg8. Molecular Plant Pathology, 19(5), 1252–1256. https://doi.org/10.1111/mpp.12609

Arora, S., Steuernagel, B., Gaurav, K., et al. (2019). Resistance gene cloning from a wild crop relative by sequence capture and association genetics. Nature Biotechnology, 37(2), 139–143. https://doi.org/10.1038/s41587-018-0007-9

Barea, G., & Toledo, J. (1996). Identificación y zonificación de *Pyricularia* o brusone (*Pyricularia oryzae*) en el cultivo de trigo en el departamento de Santa Cruz. Centro de Investigación Agrícola Tropical. Informe Técnico. Proyecto de Investigación Trigo. Santa Cruz de la Sierra, Bolivia, 76-86.

Bariana, H. S., & McIntosh, R. A. (1993). Cytogenetic studies in wheat. XV. Location of rust resistance genes in VPM1 and their genetic linkage with other disease resistance genes in chromosome 2A. Genome, 36(3), 476–482. https://doi.org/10.1139/g93-065

Bariana, H. S., & McIntosh, R. A. (1994). Characterization and origin of rust and powdery mildew resistance genes in VPM1 wheat. Euphytica, 76(1–2), 53–61. https://doi.org/10.1007/BF00024020

Bates, D., Mächler, M., Bolker, B., & Walker, S. (2014). Fitting Linear Mixed-Effects Models Using *lme4*. Journal of Statistical Software, 67(1). https://doi.org/10.18637/jss.v067.i01

Bettgenhaeuser, J., & Krattinger, S. G. (2019). Rapid gene cloning in cereals. Theoretical and Applied Genetics, Vol. 132, pp. 699–711. https://doi.org/10.1007/s00122-018-3210-7

Bhattacharya, R., & Pal, S. (2017). Deadly wheat blast symptoms enters India through the Bangladesh border, Bengal govt burning crops on war footing. Kolkata: Hindustan Times. Available online at: http://www.hindustantimes.com/kolkata/deadly-wheat-blast-symptoms-enters-india-through-the-bangladesh-border-bengal-govt-burning-crops-on-war-footing/story-3zoWQ0H7sdMU4HxQyzWUsN.html (Accessed January 11, 2021).

Bockus, W., Cruz, C., Kalia, B., et al. (2012). Reaction of selected accessions of *Aegilops tauschii* to wheat blast, 2011. Plant Dis. Manage. Rep. 6:CF005.

Börner, A., Ogbonnaya, F. C., Röder, M. S., et al. (2015). *Aegilops tauschii* Introgressions in Wheat. In Alien Introgression in Wheat (pp. 245–271). https://doi.org/10.1007/978-3-319-23494-6_10

Brown-Guedira, G. L., Fritz, A. K., Gill, B. S., et al. (2004). Registration of KS00WGRC44 leaf rust-resistant hard red winter wheat germplasm. Crop science, 44(2), 702-703. https://doi.org/10.2135/cropsci2004.7020

Brown-Guedira, G. L., Cox, T. S., Bockus, W. W., et al. (1999). Registration of KS96WGRC38 and KS96WGRC39 Tan Spot-Resistant Hard Red Winter Wheat Germplasm. Crop science, 39(2), 596-596.

Cabrera, M. G., & Gutiérrez, S. (2007). Primer registro de *Pyricularia grisea* en cultivos de trigo del NE de Argentina. Jornada de Actualización en Enfermedades de Trigo.

Chen, L., Huang, L., Min, D., et al. (2012). Development and Characterization of a New TILLING Population of Common Bread Wheat (*Triticum aestivum* L.). PLoS ONE, 7(7), e41570. https://doi.org/10.1371/journal.pone.0041570

Comai, L., & Henikoff, S. (2006, February). TILLING: Practical single-nucleotide mutation discovery. Plant Journal, Vol. 45, pp. 684–694. https://doi.org/10.1111/j.1365-313X.2006.02670.x

Cox, T. S., Bockus, W. W., Gill, B. S., et al. (1999). Registration of KS96WGRC40 hard red winter wheat germplasm resistant to wheat curl mite, Stagnospora leaf blotch, and Septoria leaf blotch. Crop science, 39(2), 597-597. https://doi.org/10.2135/cropsci1999.0011183X003900020070x

Cox, T. S., Hussein, T., Sears, R. G., & Gill, B. S. (1997). Registration of KS92WGRC16 winter wheat germplasm resistant to leaf rust. Crop science, 37(2), 634-634. https://doi.org/10.2135/cropsci1997.0011183X003700020064x

Cox, T. C., Sears, R. G., & Gill, B. S. (1992). Registration of KS90WGRC10 leaf rust-resistant hard red winter wheat germplasm. Crop science, 32(2), 506-506. https://doi.org/10.2135/cropsci1992.0011183X003200020060x

Cox, T. S. (1992). Resistance to Foliar Diseases in a Collection of *Triticum tauschii* Germ Plasm. Plant Disease, 76(10), 1061. https://doi.org/10.1094/pd-76-1061

Cruppe, G. (2020). Wheat blast management through identification of novel sources of genetic resistance and understanding of disease dynamics. Retrieved from website: https://krex.k-state.edu/dspace/handle/2097/40317

Cruppe, G., Cruz, C. D., Peterson, G., et al. (2019). Novel sources of wheat head blast resistance in modern breeding lines and wheat wild relatives. Plant Disease, 104(1), 35–43. https://doi.org/10.1094/PDIS-05-19-0985-RE

Cruppe, G., Silva, P., Lemes da Silva, C., et al. (2020). Genome-wide association reveals limited benefits of pyramiding the 1B and 1D loci with the 2N^{v}S translocation for wheat blast control. Crop Science, csc2.20397. https://doi.org/10.1002/csc2.20397

Cruz, C.D., Peterson, G. L., Bockus, W. W., et al. (2016). The 2NS Translocation from *Aegilops ventricosa* Confers Resistance to the Triticum Pathotype of *Magnaporthe oryzae*. Crop Science, 56(3), 990–1000. https://doi.org/10.2135/cropsci2015.07.0410

Cruz, C. D., Santana, F. M., Todd, T. C., et al. (2019). Multi-environment assessment of fungicide performance for managing wheat head blast (WHB) in Brazil and Bolivia. Tropical Plant Pathology, 44(2), 183–191. https://doi.org/10.1007/s40858-018-0262-9

Cruz, C. D., & Valent, B. (2017). Wheat blast disease: danger on the move. Tropical Plant Pathology, Vol. 42, pp. 210–222. https://doi.org/10.1007/s40858-017-0159-z

Cruz, M. F. A., Prestes, A. M., Maciel, J. L. N., & Scheeren, P. L. (2010). Partial resistance to blast on common and synthetic wheat genotypes in seedling and in adult plant growth stages. Tropical Plant Pathology, 35(1), 24–31. Retrieved from https://www.cabdirect.org/cabdirect/abstract/20103353156

De Mendiburu, F., & Simon, R. (2015). Agricolae-Ten years of an open source statistical tool for experiments in breeding, agriculture and biology (No. e1748). PeerJ PrePrints.

Deng, Y., Ning, Y., Yang, D. L., et al. (2020). Molecular Basis of Disease Resistance and Perspectives on Breeding Strategies for Resistance Improvement in Crops. Molecular Plant, Vol. 13, pp. 1402–1419. https://doi.org/10.1016/j.molp.2020.09.018

Dubcovsky, J., & Dvorak, J. (2007). Genome plasticity a key factor in the success of polyploid wheat under domestication. Science, Vol. 316, pp. 1862–1866. https://doi.org/10.1126/science.1143986

Duveiller, E., He, X., & Singh, P. K. (2016). Wheat blast: An emerging disease in South America potentially threatening wheat production. World wheat book, 3, 1107-1122.

Dvořák, J. (2014). Sequencing the *Aegilops tauschii* genome. The "Sequencing the *Aegilops Tauschii* Genome" Project, 2, 1. Retrieved from http://aegilops.wheat.ucdavis.edu/ATGSP/AetPage_v5.pdf

Dvořák, J., Luo, M.-C., Yang, Z.-L., & Zhang, H.-B. (1998). The structure of the *Aegilops tauschii* gene pool and the evolution of hexaploid wheat. Theoretical and Applied Genetics, 97(4), 657–670. https://doi.org/10.1007/s001220050942

Endelman, J. B. (2011). Ridge Regression and Other Kernels for Genomic Selection with R Package *rrBLUP*. The Plant Genome Journal, 4(3), 250. https://doi.org/10.3835/plantgenome2011.08.0024

Endelman, J. (2019). Package "*rrBLUP*." Retrieved from http://mirrors.nics.utk.edu/cran/web/packages/rrBLUP/rrBLUP.pdf

Farman, M., Peterson, G., Chen, L., et al. (2017). The *Lolium* Pathotype of *Magnaporthe oryzae* Recovered from a Single Blasted Wheat Plant in the United States. Plant Disease, 101(5), 684–692. https://doi.org/10.1094/PDIS-05-16-0700-RE

Fekih, R., Takagi, H., Tamiru, M., et al. (2013). MutMap+: Genetic Mapping and Mutant Identification without Crossing in Rice. PLoS ONE, 8(7), e68529 https://doi.org/10.1371/journal.pone.0068529

Ferreira, J. R., Torres, G. A. M., Consoli, L., et al. (2020). Quantitative trait loci conferring blast resistance in hexaploid wheat at adult plant stage. Plant Pathology, 70(1), 100–109. https://doi.org/10.1111/ppa.13278

Flor, H. H. (1971). Current status of the gene-fob-gene concept. Retrieved from www.annualreviews.org

Friebe, B., Jiang, J., Raupp, W. J., et al. (1996). Characterization of wheat-alien translocations conferring resistance to diseases and pests: Current status. Euphytica, 91(1), 59–87. https://doi.org/10.1007/BF00035277

Gao, L., Koo, D. H., Juliana, P., et al. (2020). The *Aegilops ventricosa* 2N^{v}S segment in bread wheat: cytology, genomics and breeding. Theoretical and Applied Genetics, 1, 3. https://doi.org/10.1007/s00122-020-03712-y

Gill, B. S., Friebe, B., Raupp, W. J., et al. (2006). Wheat genetics resource center: the first 25 years. Advances in Agronomy, 89, 73-136. https://doi.org/10.1016/S0065-2113(05)89002-9

Gill, B. S., Wilson, D. L., Raupp, W. J., et al. (1991). Registration of KS89WGRC4 Hard Red Winter Wheat Germplasm with Resistance to Hessian Fly, Greenbug, and Soil-Borne Mosaic Virus. Crop Science, 31(1), 246–246. https://doi.org/10.2135/cropsci1991.0011183x003100010080x

Gill BS, Wilson DL, Raupp WJ, et al. (1991). Registration of KS89WGRC3 and KS89WGRC6 hessian fly resistant and hard red winter wheat germplasm. Crop Sci 31:245 https://www.k-state.edu/wgrc/publications/1991/1242.pdf

Gill, B. S., & Raupp, W. J. (1987). Direct Genetic Transfers from *Aegilops squarrosa* L. to Hexaploid Wheat. Crop Science, 27(3), 445–450. https://doi.org/10.2135/cropsci1987.0011183x002700030004x

Gill BS, Hatchett JH, Cox TS, et al. (1986). Registration of KS8SWGRCO1 hessian fly resistant hard red winter wheat germplasm. Crop Sci 26:1266-1267. https://www.k-state.edu/wgrc/publications/1986/8689.pdf

Gladieux, P., Condon, B., Ravel, S., et al. (2018). Gene flow between divergent cereal- and grass-specific lineages of the rice blast fungus *Magnaporthe oryzae*. MBio, 9(1), 2020. https://doi.org/10.1128/mBio.01219-17

Goddard, R., Steed, A., Chinoy, C., et al. (2020). Dissecting the genetic basis of wheat blast resistance in the Brazilian wheat cultivar BR 18-Terena. BMC Plant Biology, 20(1), 1–15. https://doi.org/10.1186/s12870-020-02592-0

Goulart, A. C. P., Sousa, P. G., & Urashima, A. S. (2007). Danos em trigo causados pela infecção de *Pyricularia grisea*. Summa Phytopathologica, 33(4), 358–363. https://doi.org/10.1590/s0100-54052007000400007

Greene, E. A., Codomo, C. A., Taylor, et al. (2003). Spectrum of chemically induced mutations from a large-scale reverse-genetic screen in Arabidopsis. Genetics, 164(2), 731–740. Retrieved from www.proweb.org/parsesnp

Hao, M., Zhang, L., Ning, S., et al. (2020). The Resurgence of Introgression Breeding, as Exemplified in Wheat Improvement. Frontiers in Plant Science, 11(March), 1–11. https://doi.org/10.3389/fpls.2020.00252

He, X., Muhammad, ·, Kabir, R., et al. (2020). QTL mapping for field resistance to wheat blast in the Caninde#1/ Alondra population. Springer, 133(9), 2673–2683. https://doi.org/10.1007/s00122-020-03624-x

Igarashi, S., Utiamada, C. M., Igarashi, L. C., et al. (1986). Ocorrência de *Pyricularia* sp. em trigo no estado do Paraná. Reunião Nacional de Pesquisa de Trigo, 14, 57.

Inoue, Y., Vy, T. T. P., Tani, D., & Tosa, Y. (2020). Suppression of wheat blast resistance by an effector of *Pyricularia oryzae* is counteracted by a host specificity resistance gene in wheat. New Phytologist, 229(1), 488–500. https://doi.org/10.1111/nph.16894

Inoue, Y., Vy, T. T. P., Yoshida, K., et al. (2017). Evolution of the wheat blast fungus through functional losses in a host specificity determinant. Science, 357(6346), 80–83. https://doi.org/10.1126/science.aam9654

Islam, M. T., Croll, D., Gladieux, P., et al. (2016). Emergence of wheat blast in Bangladesh was caused by a South American lineage of *Magnaporthe oryzae*. BMC Biology, 14(1), 84. https://doi.org/10.1186/s12915-016-0309-7

Jahier, J., Abelard, P., Tanguy, M., et al. (2001). The *Aegilops ventricosa* segment on chromosome 2AS of the wheat cultivar 'VPM1'carries the cereal cyst nematode resistance gene Cre5. Plant Breeding, 120(2), 125-128. https://doi.org/10.1046/j.1439-0523.2001.00585.x

Johansson, E., Henriksson, T., Prieto-Linde, M. L., et al (2020). Diverse Wheat-Alien Introgression Lines as a Basis for Durable Resistance and Quality Characteristics in Bread Wheat. Frontiers in Plant Science, 11(July), 1–15. https://doi.org/10.3389/fpls.2020.01067

Juliana, P., He, X., Kabir, M. R., et al. (2020). Genome-wide association mapping for wheat blast resistance in CIMMYT's international screening nurseries evaluated in Bolivia and Bangladesh. Scientific Reports, 10(1), 15972. https://doi.org/10.1038/s41598-020-72735-8

Kishii, M. (2019). An update of recent use of Aegilops species in wheat breeding. Frontiers in Plant Science, 10, 585. https://doi.org/10.3389/fpls.2019.00585

Kohli, M. M., Mehta, Y. R., Guzman, E., et al. (2011). *Pyricularia* blast–a threat to wheat cultivation. Czech Journal of Genetics and Plant Breeding, 47(Special Issue).

Krasileva, K. V., Vasquez-Gross, H. A., Howell, T., et al. (2017). Uncovering hidden variation in polyploid wheat. Proceedings of the National Academy of Sciences of the United States of America, 114(6), E913–E921. https://doi.org/10.1073/pnas.1619268114

Lagudah, E. S., Appels, R., Brown, A. H. D., & McNeil, D. (1991). The molecular–genetic analysis of *Triticum tauschii*, the D-genome donor to hexaploid wheat. Genome, 34(3), 375–386. https://doi.org/10.1139/g91-059

Langner, T., Białas, A., & Kamoun, S. (2018). The blast fungus decoded: Genomes in flux. MBio, Vol. 9. https://doi.org/10.1128/mBio.00571-18

Lethin, J., Shakil, S. S. M., Hassan, S., et al. (2020). Development and characterization of an EMS-mutagenized wheat population and identification of salt-tolerant wheat lines. BMC Plant Biology, 20(1), 18. https://doi.org/10.1186/s12870-019-2137-8

Li, A., Liu, D., Yang, W., et al. (2018). Synthetic Hexaploid Wheat: Yesterday, Today, and Tomorrow. Engineering, Vol. 4, pp. 552–558. https://doi.org/10.1016/j.eng.2018.07.00

Maciel, J. L. N., Ceresini, P. C., Castroagudin, V. L., et al. (2014). Population structure and pathotype diversity of the wheat blast pathogen *Magnaporthe oryzae* 25 years after its

emergence in Brazil. Phytopathology, 104(1), 95–107. https://doi.org/10.1094/PHYTO-11-12-0294-R
Madden, L. V., Hughes, G., & Van Den Bosch, F. (2007). The study of plant disease epidemics.
Maia, N. (1967). Obtention des bles tendres resistants au pietin-verse par croisements interspecifiques bles x Aegilops. CR Acad. Agric. Fr, 53, 149-154.
Malaker, P. K., Barma, N. C., Tiwary, T. P., et al. (2016). First report of wheat blast caused by *Magnaporthe oryzae* pathotype *triticum* in Bangladesh. Plant Disease. https://doi.org/10.1094/PDIS-05-16-0666-PDN
McCallum, C. M., Comai, L., Greene, E. A., & Henikoff, S. (2000). Targeted screening for induced mutations. Nature Biotechnology, 18(4), 455–457. https://doi.org/10.1038/74542
Mishra, A., Singh, A., Sharma, M., et al. (2016). Development of EMS-induced mutation population for amylose and resistant starch variation in bread wheat (*Triticum aestivum*) and identification of candidate genes responsible for amylose variation. BMC Plant Biology, 16(1), 1–15. https://doi.org/10.1186/s12870-016-0896-z
Molnár-Láng, M., Ceoloni, C., & Doležel, J. (2015). Alien introgression in wheat: Cytogenetics, molecular biology, and genomics. In Alien Introgression in Wheat: Cytogenetics, Molecular Biology, and Genomics. https://doi.org/10.1007/978-3-319-23494-6
Perelló, A., Martinez, I., & Molina, M. (2015). First report of virulence and effects of *Magnaporthe oryzae* isolates causing wheat blast in Argentina. Plant Disease, 99(8), 1177. https://doi.org/10.1094/PDIS-11-14-1182-PDN
Rakszegi, M., Molnár, I., Darkó, É., et al. (2020). Editorial: *Aegilops*: Promising Genesources to Improve Agronomical and Quality Traits of Wheat. Frontiers in Plant Science, 11(July), 2016–2019. https://doi.org/10.3389/fpls.2020.01060
Rasheed, A., Ogbonnaya, F. C., Lagudah, E., et al. (2018). The goat grass genome's role in wheat improvement. Nature Plants, 4(2), 56–58. https://doi.org/10.1038/s41477-018-0105-1
Rawat, N., Joshi, A., Pumphrey, M., et al. (2019). A TILLING Resource for Hard Red Winter Wheat Variety Jagger. Crop Science, 59(4), 1666–1671. https://doi.org/10.2135/cropsci2019.01.0011
Rudd, J. C., Devkota, R. N., Baker, J. A., et al. (2014). 'TAM 112' Wheat, Resistant to Greenbug and Wheat Curl Mite and Adapted to the Dryland Production System in the Southern High Plains. Journal of Plant Registrations, 8(3), 291–297. https://doi.org/10.3198/jpr2014.03.0016crc
Sánchez-Martín, J., Steuernagel, B., Ghosh, S., et al. (2016). Rapid gene isolation in barley and wheat by mutant chromosome sequencing. Genome Biology, 17(1), 1–7. https://doi.org/10.1186/s13059-016-1082-1
Schneider, A., Molnár, I., & Molnár-Láng, M. (2008). Utilization of *Aegilops* (goatgrass) species to widen the genetic diversity of cultivated wheat. Euphytica, Vol. 163, pp. 1–19. https://doi.org/10.1007/s10681-007-9624-y
Sikora, P., Chawade, A., Larsson, M., et al. (2011). Mutagenesis as a Tool in Plant Genetics, Functional Genomics, and Breeding. International Journal of Plant Genomics, 2011, 13. https://doi.org/10.1155/2011/314829
Singh, D., Wang, X., Kumar, U., et al. (2019). High-Throughput Phenotyping Enabled Genetic Dissection of Crop Lodging in Wheat. Frontiers in Plant Science, 10, 394. https://doi.org/10.3389/fpls.2019.00394

Singh, N., Wu, S., Tiwari, V., et al. (2019). Genomic Analysis Confirms Population Structure and Identifies Inter-Lineage Hybrids in *Aegilops tauschii*. Frontiers in Plant Science, 10(January), 1–13. https://doi.org/10.3389/fpls.2019.00009

Slade, A. J., Fuerstenberg, S. I., Loeffler, D., et al. (2005). A reverse genetic, nontransgenic approach to wheat crop improvement by TILLING. Nature Biotechnology, 23(1), 75–81. https://doi.org/10.1038/nbt1043

Steuernagel, B., Periyannan, S. K., Hernández-Pinzón, I., et al. (2016). Rapid cloning of disease-resistance genes in plants using mutagenesis and sequence capture. Nature Biotechnology, 34(6), 652–655. https://doi.org/10.1038/nbt.3543

Tagle, A. G., Chuma, I., & Tosa, Y. (2015). *Rmg7*, a New Gene for Resistance to Triticum Isolates of *Pyricularia oryzae* Identified in Tetraploid Wheat. Phytopathology, 105(4), 495–499. https://doi.org/10.1094/PHYTO-06-14-0182-R

Takabayashi, N., Tosa, Y., Oh, H. S., & Mayama, S. (2002). A gene-for-gene relationship underlying the species-specific parasitism of *Avena/Triticum* isolates of *Magnaporthe grisea* on wheat cultivars. Phytopathology, 92(11), 1182–1188. https://doi.org/10.1094/PHYTO.2002.92.11.1182

Tembo, B., Mulenga, R. M., Sichilima, S., et al. (2020). Detection and characterization of fungus (*Magnaporthe oryzae* pathotype *Triticum*) causing wheat blast disease on rain-fed grown wheat (*Triticum aestivum* L.) in Zambia. PLOS ONE, 15(9), e0238724. https://doi.org/10.1371/journal.pone.0238724

Tosa, Y., Hirata, K., Tamba, H., et al. (2004). Genetic constitution and pathogenicity of Lolium isolates of *Magnaporthe oryzae* in comparison with host species-specific pathotypes of the blast fungus. Phytopathology, 94(5), 454–462. https://doi.org/10.1094/PHYTO.2004.94.5.454

Uauy, C., Paraiso, F., Colasuonno, P., et al. (2009). A modified TILLING approach to detect induced mutations in tetraploid and hexaploid wheat. BMC Plant Biology, 9(1), 1–14. https://doi.org/10.1186/1471-2229-9-115

Valent, B., Cruppe, G., Stack,J., et al. (2021) Recovery plan for wheat blast caused by *Magnaporthe oryzae* pathotype *triticum*. Plant Health Progress, accepted.

Valent, B., Singh, P. K., He, X., et al. (2020). Chapter 13: Blast Diseases: Evolution and Challenges of a Staple Food Crop Fungal Pathogen. Pages 267-292 in: Emerging Plant Diseases and Global Food Security. J. B. Ristaino and A. Records, eds. American Phytopathological Society Press, St. Paul, MN.

Valent, B., Farman, M., Tosa, Y., et al. (2019). *Pyricularia graminis-tritici* is not the correct species name for the wheat blast fungus: response to Ceresini et al. (MPP 20:2). Mol. Plant Pathol. 20:173-179. doi: 10.1111/mpp.12778

Viedma, L. Q. (2005). Wheat blast occurrence in Paraguay. Phytopathology, 95(6).

Vy, T. T. P., Hyon, G. S., Nga, N. T. T., et al. (2014). Genetic analysis of host-pathogen incompatibility between Lolium isolates of *Pyricularia oryzae* and wheat. Journal of General Plant Pathology, 80(1), 59–65. https://doi.org/10.1007/s10327-013-0478-y

Wang, J., Luo, M.-C., Chen, Z., et al. (2013). *Aegilops tauschii* single nucleotide polymorphisms shed light on the origins of wheat D-genome genetic diversity and pinpoint the geographic origin of hexaploid wheat. New Phytologist, 198(3), 925–937. https://doi.org/10.1111/nph.12164

Wang, S., Asuke, S., Vy, T. T. P., et al. (2018). A New Resistance Gene in Combination with *Rmg8* Confers Strong Resistance Against *Triticum* Isolates of *Pyricularia oryzae* in a

Common Wheat Landrace. Phytopathology, 108(11), 1299–1306. https://doi.org/10.1094/PHYTO-12-17-0400-R

Waugh, R., Leader, D. J., McCallum, N., & Caldwell, D. (2006). Harvesting the potential of induced biological diversity. Trends in Plant Science, Vol. 11, pp. 71–79. https://doi.org/10.1016/j.tplants.2005.12.007

Williamson, V. M., Thomas, V., Ferris, H., & Dubcovsky, J. (2013). An *Aegilops ventricosa* translocation confers resistance against root-knot nematodes to common wheat. Crop Science, 53(4), 1412–1418. https://doi.org/10.2135/cropsci2012.12.0681

Yu, J., Pressoir, G., Briggs, W. H., et al. (2006). A unified mixed-model method for association mapping that accounts for multiple levels of relatedness. Nature Genetics, 38(2), 203–208. https://doi.org/10.1038/ng1702

Zhan, S. W., Mayama, S., & Tosa, Y. (2008). Identification of two genes for resistance to *Triticum* isolates of *Magnaporthe oryzae* in wheat. Genome, 51(3), 216–221. https://doi.org/10.1139/G07-094

Zhang, P., Dundas, I. S., McIntosh, R. A., et al. (2015). Wheat–*Aegilops* Introgressions. In Alien Introgression in Wheat (pp. 221–243). https://doi.org/10.1007/978-3-319-23494-6_9

Zhang, Z., Ersoz, E., Lai, CQ. et al. (2010). Mixed linear model approach adapted for genome-wide association studies. Nat Genet 42, 355–360. https://doi.org/10.1038/ng.546

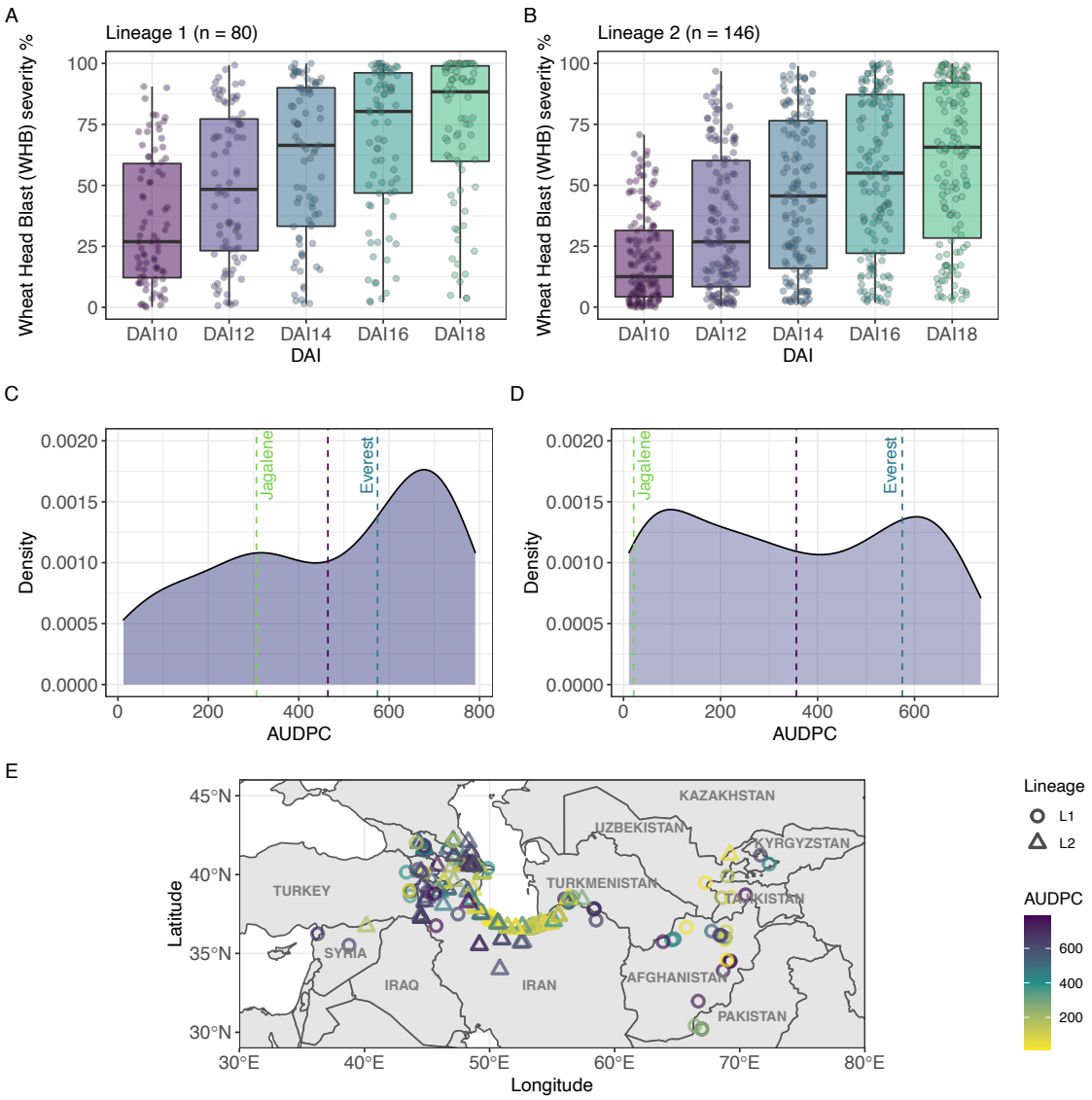

Figure 3.6 – Phenotypic data description.

Phenotypic response of *Aegilops tauschii* accessions to Wheat head blast (WHB), inoculated with isolate 008. Boxplot showing WHB severity (0 – 100 %) at 10-, 12-, 14-, 16-, and 18 days after inoculation (dai) for A) 80 lineage 1 (L1) accessions) and B) 146 lineage 2 (L2) accessions. C) Distribution of the area under the disease progress curve (AUDPC) for L1 and D) L2. The dashed lines correspond to the mean AUDPC value for all the accessions (purple), and for the resistant (green, 'Jagalene') and susceptible (blue, 'Everest') checks. E) Map showing the geographical distribution of accessions based on passport information (latitude and longitude). Two L1 accessions (TA10135: AUDPC 221.6 and TA10136: AUDPC 655.5) from Northeastern China were excluded from the map for better visualization. The color gradient corresponds to WHB AUDPC values.

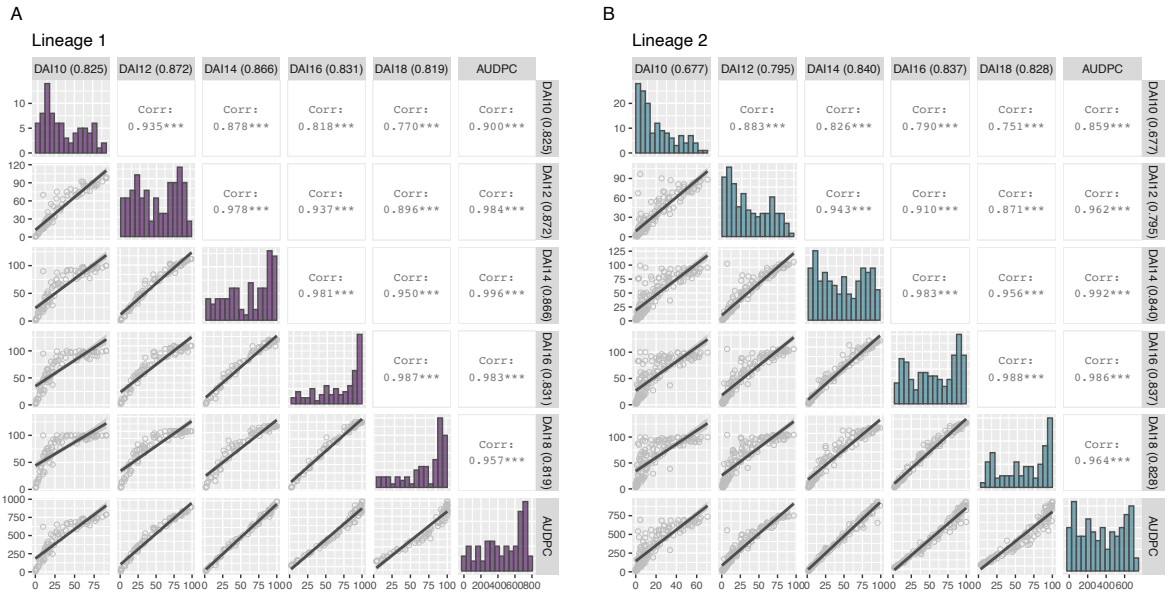

Figure 3.7 – Phenotypic correlations.

Scatterplots and histograms showing distribution and Pearson's correlation values for wheat head blast (WHB) severity at 10-, 12-, 14-, 16-, and 18 days after inoculation (DAI) and the area under the disease progress curve (AUDPC). Column headers include the broad-sense heritability value for the trait.

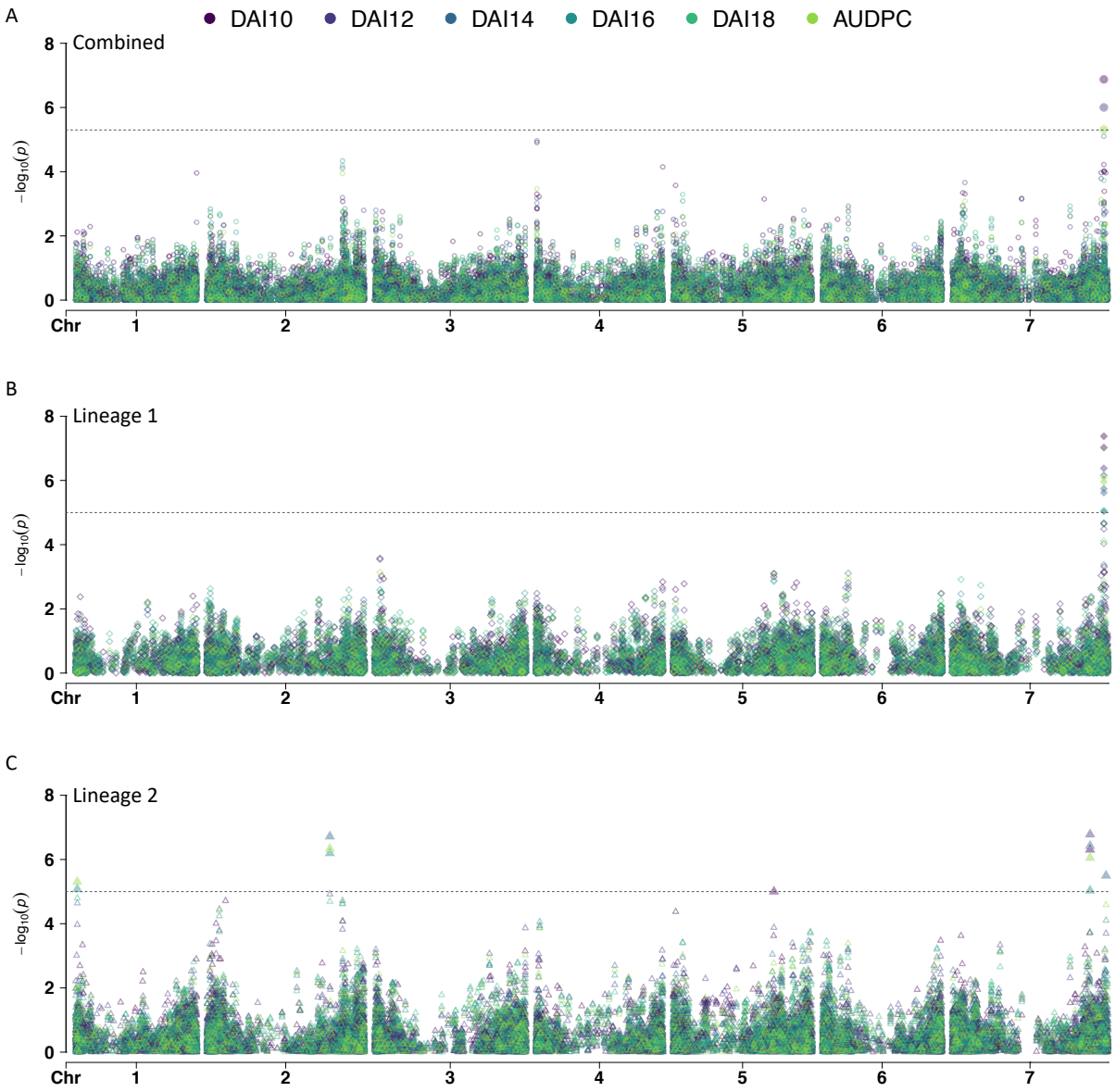

Figure 3.8 – Genome-wide association analyses.

Manhattan plots showing the marker-trait associations for wheat head blast at five evaluation time points (10, 12, 14, 16, and 18 DAI) and the area under the disease progress curve (AUDPC), using genotyping-by-sequencing data (GBS) for A) combined panel with 226 *Aegilops tauschii* accessions from both lineages and 10,998 SNP markers, B) 80 lineage 1 *Ae. tauschii* accessions and 5,100 SNP markers, and C) 146 lineage 2 *Ae. tauschii* accessions and 6,491 SNP markers. The seven *Ae. tauschii* chromosomes with physical positions are on the x-axis and y-axis is the –log10 of the p-value for each SNP marker. Chromosome labels are placed in the middle of each chromosome. Dashed horizontal lines correspond to the Bonferroni threshold at 0.05.

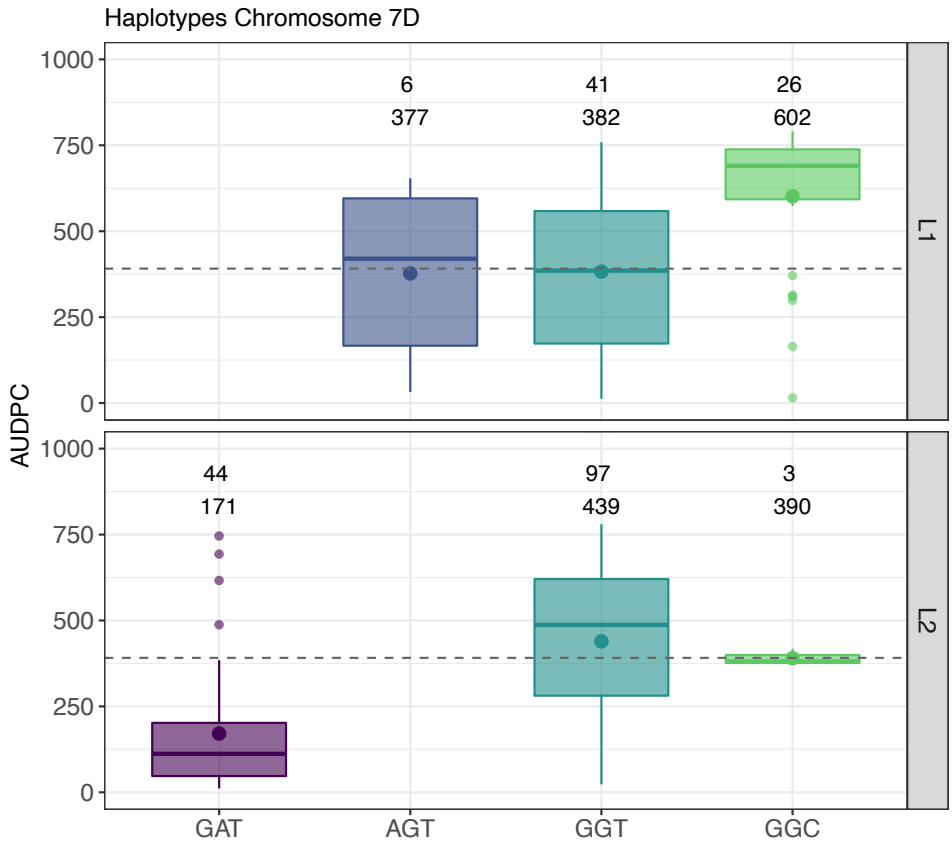

Figure 3.9 – Chromosome 7DL haplotypes.

Boxplots of wheat head blast (WHB) phenotypic response for the different haplotypes detected by GWAS combining lineage 1 and lineage 2 *Ae. tauschii* accessions. The number of accessions in each group and the mean phenotypic values is shown at the top of each boxplot.

Chapter 4 - Genetic Basis of wheat curl mite resistance in the wheat wild relative *Aegilops tauschii*

Abstract

Wheat is one of the most important cereals with the potential to mitigate the challenge of global food security. However, the lack of diversity for some agronomically important traits coupled with the danger imposed by pests and pathogens have the potential to constrain wheat production. When genetic diversity is scarce, plant breeding programs can turn to crop wild relatives as donors of novel sources of diversity. *Aegilops tauschii* is the donor of the D genome of the cultivated bread wheat and has been used as a valuable source of novel disease resistance genes. The use of wild relatives together with the advances of phenomic and genomic tools can assist in rapidly identifying, select, and introgress new diversity into adapted wheat germplasm. Wheat curl mite (WCM) is a threatening pest for wheat, mainly because of vectoring wheat streak mosaic virus. To investigate the genetic basis of WCM resistance in *Ae. tauschii* we characterized a panel of *Ae. tauschii* accessions against WCM and used genome-wide association mapping to identify genomic regions associated with resistance. We tested 388 accessions against WCM biotype 1 infestation under controlled conditions using a 0 to 4 visual scale. Whole-genome sequencing and genotyping-by-sequencing data found strong association with a locus on chromosome 6DS across both lineages, previously identified as *Cmc1* and *Cmc4*. Following this discovery, we sought to elucidate the origin and genetic relationship between resistance genes *Cmc1*, *Cmc4*, and a presumed novel allele found in the wheat cultivar 'TAM 112' (Cmc_{TAM112}), and to delimit the introgression in hexaploid wheat. Haplotype analysis for the resistance region on chromosome 6DS revealed a unique resistance haplotype within the resistant accessions across both *Ae. tauschii* lineages suggesting that WCM resistance has a single unique origin in *Ae. tauschii*, transferred via admixture across *Ae. tauschii* and later introgressed into wheat. We were also able to demonstrate that the resistance genes *Cmc1*, *Cmc4*, and Cmc_{TAM112} all share the same haplotype; therefore, they are all the same genes with different names. Finally, we delimited the *Ae. tauschii* introgression carrying WCM resistance into wheat and show that independent introgression events resulted in fragments with different lengths. The extensive haplotype analysis across *Ae. tauschii* and wheat introgressions enabled us to design diagnostic molecular markers that can be used in marker-assisted selection. Overall, these

results contribute to better understand the genetic basis of WCM resistance and highlight the necessity of screening other potential sources of resistance to broaden the available genes to breed wheat against WCM.

Introduction

Aegilops tauschii Cosson is the diploid donor of the D subgenome of hexaploid wheat (*Triticum aestivum* L.) and comprises three distinct phylogenetic lineages, lineage 1 (L1) known as ssp. *tauschii*, lineage 2 (L2) known as ssp. *strangulate*,a nd lineage 3 (L3) (Dvořák et al., 1998; Singh et al., 2019). The hybridization event between *Ae. tauschii* and tetraploid durum wheat (*Triticum turgidum*) gave rise to hexaploid bread wheat (*Triticum aestivum* L.) around 8,000 years ago in the Caspian Sea region. This original hybridization involved a limited group of *Ae. tauschii* L2 accessions, possibly as few as two (Caldwell et al., 2004; Lagudah et al., 1991; Wang et al., 2013). Therefore, the origin of hexaploid wheat led to a considerable loss of genetic diversity in the D subgenome. Further, additional bottlenecks through selection and modern breeding have resulted in cultivated bread wheat lacking diversity for some economically important traits. This is further compounded by new and emerging diseases. *Ae. tauschii* has been used successfully as a donor of many abiotic and biotic stresses and, thus, is a valuable source for wheat improvement (Rasheed et al., 2018).

The wheat curl mite (WCM, *Aceria tosichella* Keifer) is one of the most important pests affecting wheat production globally. Along with foliage injury, rolling, and trapping, the critical yield loss comes by vectoring economically significant viruses, such as wheat streak mosaic virus (WSMV) (Slykhuis, 1955), wheat mosaic virus (also known as high plains virus) (Seifers et al., 1997), brome streak mosaic virus (Gotz & Maiss, 1995), and triticum mosaic virus (Seifers et al., 2008), which cause huge epidemics and yield losses worldwide (Navia et al., 2013). In the Great Plains of the United States, these viruses are widespread, causing significant damage to wheat producers. In Kansas, WSMV is one of the most prevalent and destructive diseases of wheat, with a 20 years average yield loss of 1.26% (Hollandbeck et al, 2019). WSMV alone caused a 5.6% yield loss estimated at more than $75 million in 2017 (http://kswheat.com/growers/wheat-streak-mosaic-virus) and it also holds the state record of maximum loss for a single disease causing 13% yield loss in 1988 (Bockus et al., 2001).

Moreover, WCM also transmits WSMV to many other cereal crops, promoting the dispersion of the virus to other regions. Even though cultural practices are an important strategy to control WCM and WSMV, genetic resistance is the most environmental and economically friendly solution to reduce wheat yield losses caused by these pathogens and provide additional resources to growers for economically and environmentally sustainable production (Harvey et al., 2005; Singh et al., 2018).

Genetic resistance to WCM has been identified almost exclusively from distant wild relatives of wheat (Aguirre-Rojas et al., 2017; Chen et al., 1996; Chen et al., 2003; Dhakal et al., 2018; Li et al., 2005, 2002; Malik et al., 2003a; Malik et al., 2003b; Martin et al., 1976; Richardson et al., 2014; Thomas et al., 1998; Thomas & Conner, 1986; Whelan & Hart, 1988; Whelan & Thomas, 1989). To date, four resistance genes have been named (*Cmc1 – Cmc4*), all identified from wild relatives and transferred to wheat (Malik et al., 2003b; Thomas & Conner, 1986; Whelan & Hart, 1988; Whelan & Thomas, 1989). Resistance genes *Cmc1* and *Cmc4*, first identified in *Ae. tauschii* and assigned to the wheat chromosome 6DS, were previously designated as different genes (Malik et al., 2003b). Resistance gene *Cmc*1 was originally identified from the *Ae. tauschii* accession 'CI4' from Afghanistan, but no information regarding lineage classification exists for this accession (Thomas & Conner, 1986; Malik et al., 2003b). On the other hand, resistance gene *Cmc4* was originally mapped in the wheat line 'KS96WGRC40' that possesses resistance to WCM derived from the resistant *Ae. tauschii* L1 accession TA2397 (Cox et al., 1999; Malik et al., 2003b). Recently, a resistance gene derived from the wheat cultivar 'TAM 112' (Cmc_{TAM112}) was also mapped to 6DS (Dhakal et al., 2018) and overlapped with *Cmc*4, suggesting that they tag the same locus (Zhao et al., 2019). Resistance in 'TAM 112' derives from the L2 accession TA1618 (Rudd et al., 2014). Moreover, there is no information regarding the relationship between *Cmc1*, *Cmc4*, and Cmc_{TAM112}. The origin of resistance from different sources and particularly from different subspecies/lineages of *Ae. tauschii* supported the notion that these were unique genes, or at a minimum, different alleles of the same gene.

Here we hypothesize that *Ae. tauschii* accessions are a diverse collection with resistant (R) and susceptible (S) accessions to WCM. Furthermore, and based on the literature, we postulate that resistance genes *Cmc1*, *Cmc*4, and Cmc_{TAM112} are allelic forms of the same gene, and this can be inferred based on haplotype compositions around the resistance locus. This hypothesis would

necessitate that admixture exists between the lineages to support that the WCM resistance has a single origin and was introgressed from L1 to L2. The objectives of this study were therefore, i) to characterize a panel of *Ae. tauschii* accessions for resistance to WCM, ii) to identify genomic regions associated with WCM resistance and characterize the genetic architecture of resistance, iii) to elucidate the origin and genetic relationship between resistance genes *Cmc*1, *Cmc*4, and Cmc_{TAM112}, iv) to delimit the introgression into hexaploid wheat and, v) to design molecular markers that can be used in marker-assisted-selection (MAS).

Materials and Methods

Plant Material

A total of 388 *Ae. tauschii* accessions were obtained from the Wheat Genetics Resource Center (WGRC) at Kansas State University in Manhattan, KS, United States, including 246 from L1 and 142 from L2. Lineage designation, geographic origin, and passport data are available from Singh et al. (2019). In addition, we included 36 wheat lines representing released cultivars and elite breeding parents from the U.S. Central Plains and Canada wheat breeding programs for sequencing purposes and haplotype characterization. All these lines had previous information for their response to WCM infestation.

Mite Colonies

Aceria tosichella (Keifer) biotype 1 colonies were mass-reared grown and maintained under controlled conditions at 24 °C and 14h:10h (light:dark), using the susceptible variety 'Jagger'. Mites were obtained by previously grown colonies from the Entomology Lab at Kansas State University. The original biotype 1 colony originates from Tripp county in South Dakota and its virulence/avirulence pattern and identity were confirmed in a previous study (Chuang et al., 2017). The general virulence/avirulence pattern of WCM biotype 1 has been previously reported as avirulent for *Cmc1*, *Cmc2*, *Cmc3*, and *Cmc4* (Chuang et al., 2017; Harvey et al., 1995; Harvey et al., 1999; Hein et al., 2012). A single colony consisted of an individual pot with around 50 seeds. At the two leaf stage plants were infested with leaves colonized by adult mites. Colonies were placed inside 45 cm x 45 cm x 75 cm mite-proof cages covered with 36 μm mesh screen (ELKO Filtering Co., Zurich, Switzerland) to avoid contamination until being used to infest the

Ae. tauschii accessions. Mites development and population number were checked weekly under the magnifier. Water and fertilizer were added as needed.

Phenotypic data

Accessions from L1 and L2 were evaluated in independent experiments. Six plants per accession were individually grown in 5 cm x 5 cm x 5 cm pots under controlled conditions at 24 °C and 14h:10h (light:dark). Pots were arranged randomly in an incomplete block design where the block was the tray fitting 32 pots (8 rows and 4 columns). A single pot with the susceptible check 'Jagger' was included in each tray. Accessions were infested at two leaf stage with mites collected from infested pieces of leaves from the susceptible colonies and spread as straw over the pots. Plants were evaluated individually 10 – 14 days after infestation. WCM damage was assessed as curled or trapped leaves, using a visual scale from 0 to 4, with 0 being no symptoms and score of 1 to 4 as increasing levels of curliness or trapped leaves (Fig. 4.1).

A linear regression model was used to account for the experimental design and to calculate the best linear unbiased estimator (BLUE) for each accession. The model fitted was,

$$y_{ijkl} = \mu + G_i + T_j + R_{k(j)} + C_{l(j)} + e_{ijkl} \quad \text{[Eq. 1]}$$

where y_{ijkl} is the phenotypic value, μ is the overall mean, G_i is the fixed effect of the i^{th} accession (genotype), T_j is the random effect of the j^{th} tray assumed distributed as iid $T_j \sim N(0, \sigma_T^2)$, $R_{k(j)}$ is the random effect of the k^{th} row nested within the j^{th} tray assumed distributed as iid $R_{k(j)} \sim N(0, \sigma_R^2)$, $C_{l(j)}$ is the random effect of the l^{th} column nested within the j^{th} tray assumed distributed as iid $C_{l(j)} \sim N(0, \sigma_C^2)$, and e_{ijkl} is the residual error distributed as iid $e_{ijkl} \sim \mathrm{N}(0, \sigma_e^2)$.

Summary statistics (mean, standard deviation, frequency distribution), correlation analysis, and analysis of variance (ANOVA) for WCM resistance were calculated using R statistical software. To calculate broad-sense heritability (H^2), variance components were obtained using the same model described in Eq. 1 but defining the genotype effect (G_i) as random and assumed distributed as iid $G_i \sim N(0, \sigma_G^2)$. Variance components were calculated using the 'lme4' package

in R (Bates et al., 2014). H^2 was computed as the ratio of the genetic variance to the phenotypic variance as,

$$H^2 = \frac{\sigma_G^2}{\sigma_G^2 + \frac{\sigma_e^2}{r}} \quad \text{[Eq. 2]}$$

where, σ_G^2 is the genotypic variance, σ_e^2 is the residual error variance, and r is the number of replications.

Sequencing data

Single nucleotide polymorphisms (SNPs) markers discovered using genotyping-by-sequencing (GBS) were obtained from Singh et al. (2019). An additional filtering step was done after removing the accessions that were not characterized in this study. SNP markers with minor allele frequency (MAF) < 0.01, missing data > 80%, and heterozygosity > 20% were removed from the analysis. High-quality GBS-SNP markers were used to perform principal component analysis (PCA), genome-wide association analysis (GWAS), and haplotype analysis. To perform the haplotype analysis, we selected all the SNP markers within the genomic region detected by GWAS. Haplotypes were investigated manually by ordering each SNP next to the phenotypic response for all the accessions, and by averaging the phenotypic adjusted values over the accessions.

In addition to GBS data, we also collected whole-genome sequencing (WGS) data for 234 *Ae. tauschii* accessions, 110 from L1, and 124 from L2. WGS data were obtained through the OWWC (http://www.openwildwheat.org). Libraries were prepared with Illumina TruSeq library kit with size selection of 350bp insert following manufacture's recommendations and were sequenced to a 10x coverage using Illumina paired end sequencing of 2x150bp reads. WGS reads were aligned to the *Ae. tauschii* assembly Aet v4.0 using Bowtie2 v2.4.1 (Langmead & Salzberg, 2012). Parallel variant calling by breaking the reference into 4Mb intervals was done with Bcftools v1.6 (Li, 2011) using mpileup with parameters -q 20 -a DP, DV and with parameters call -mv -f GQ. Filtering parameters used to retain a marker were minimum read depth of 2 and 4 for homozygous and heterozygous, respectively, minimum SNP quality of 40,

and MAF > 0.01. WGS-SNP markers were used to confirm the GWAS analysis performed with GBS-SNP markers and to perform haplotype analysis.

Furthermore, we generated WGS data for 36 wheat lines. Libraries for the wheat lines were prepared for WGS with Illumina TruSeq library kit with size selection of 350bp insert following manufacture's recommendations and were sequenced to 10x coverage using Illumina paired end sequencing of 2x150bp reads. WGS reads for these wheat lines and 85 selected *Ae. tauschii* accessions were also aligned to an in-silico synthetic hexaploid reference genome created by combining the A and B genomes from the hexaploid wheat 'Jagger' and the *Ae. tauschii* genome assembly (Aet v4.0; NCBI BioProject PRJNA341983) as the D genome. The alignment was done using hisat2 default parameters (Kim et al., 2019). The alignment SAM results were converted to bam format using samtools (Li et al., 2009) with "view -f 2 -bhs" parameter. Bcftools v1.6 (Heng Li, 2011) was then used for mpileup with parameters -q 20 -a DP, DV and call variants with parameters call -mv -f GQ for, i) short arm of chromosome 6D (0 – 230 Mbp), and ii) resistance region on 6DS (1.9 – 2.7 Mbp) previously defined by mapping analysis. To obtain high-quality SNP markers, vcf files were filtered using bcftools v1.6 (Heng Li, 2011) and a customized pipeline. SNP markers with read depth (DP>= 4), quality (QUAL > 30), MAF > 0.1, missing data < 85%, and heterozygosity < 5% were retained for further analysis. High-quality WGS-SNP markers were used to perform clustering analyses (ADMIXTURE and phylogenies), haplotype analysis, and to delimit the extent of the introgression into wheat. Sequence haplotypes were determined by the exact sharing of variants and by percent identity doing multiple sequence alignment using blastn of NCBI BLAST v2.6.0 (Altschul et al., 1990).

Clustering analyses

Principal component analysis (PCA) and ADMIXTURE (Alexander et al., 2009) were used to study population structure. The PCA analysis using GBS-SNPs was performed with the imputed marker score matrix calculated with R software using the 'A.mat' function from the 'rrBLUP' package (Endelman, 2011). To detect structure with ADMIXTURE using WGS-SNP markers we used 10-fold cross-validation with fixed population number at k=3. To run the analysis, we first converted .vcf files to .bed files using plink v1.07 (Purcell et al., 2007). Results were plotted using 'ggplot2' in R software (Wickham, 2016). Phylogenetic analyses were performed

to validate the introgression from *Ae. tauschii* into hexaploid wheat and to investigate the hypothesis that admixture exists between lineages and the resistance to WCM was originated in L1 and introgressed into L2. Phylogenetic analyses were implemented with, i) variants for the short arm of chromosome 6D (0 – 230 Mbp), ii) variants for the resistance region detected with association mapping (1.9 – 2.7 Mbp), and iii) variants for the final delimited resistance region (2.3 – 2.6 Mbp). The matrices of genetic distances were calculated using 'dist' function and converted to a 'phylo' object, and the 'plot.phylo' function was used to plot the neighbor-joining unrooted trees, using the 'ape' package (Paradis & Schliep, 2019).

Genome-wide association analysis (GWAS)

For GWAS, the analysis was performed with a mixed linear model (Zhang et al., 2010) implemented in the GAPIT R package (Lipka et al., 2012),

$$y = W_v + X\beta + Zu + e \qquad \text{[Eq. 5]}$$

where *y* is the vector of phenotypic BLUPs, v and β are unknown fixed effects representing marker effects and non-marker effects, respectively; and u is a vector of size n (number of individuals) for unknown random polygenic effects having a distribution with mean of zero and covariance matrix of $G = 2K\sigma_a^2$, where K is the kinship matrix calculated from the genetic markers and σ_a^2 is an unknown genetic variance. W, X and Z are the incidence matrices for v, β, and u, respectively, and e is the vector of random residual effects, normally distributed with zero mean and covariance $R = I\sigma_e^2$, where I is the identity matrix and σ_e^2 is the unknown residual variance. The association analyses were performed for the complete set of accessions and also for each lineage separately, using both GBS-SNPs and WGS-SNPs. To run the GWAS model with both lineages combined, the first three PC were included to account for population structure based on the PCA. The first three PC and the first four PC were used for the analysis of L1 and L2, respectively. The threshold level for calling significant marker-trait associations and to avoid false positives was calculated using the Bonferroni correction with an experimental significance level alpha value of 0.01. Manhattan plots were generated with 'CMplot' package in R software (https://cran.r-project.org/web/packages/CMplot/CMplot.pdf).

Delimitation of the introgression into hexaploid wheat

To delimit the extent of the *Ae. tauschii* introgression conferring resistance to WCM into hexaploid wheat, we used WGS data for five WCM resistant wheat lines (Table 4.1) and two of the *Ae. tauschii* resistant donor accessions, TA2397 and TA1618. 'KS96WGRC40' resistance donor is the L1 accession TA2397 and the original line where *Cmc4* was mapped (Cox et al., 1999; Malik et al., 2003b). 'LS902' is a resistant breeding line from Canada that has the original germplasm 'KS96WGRC40' in its pedigree. 'TAM 112' resistance donor is the L2 accession TA1618 (PI-268210) through the cultivar 'Largo', and the line where Cmc_{TAM112} was mapped (Dhakal et al., 2018; Rudd et al., 2014). 'TAM 115'and 'TAM 204' are both resistant varieties derived from 'TAM 112'. Of particular note is that both wheat lines 'KS96WGRC40' and 'TAM 112' have in their pedigrees the *Ae. tauschii* L2 accession TA2460, which is susceptible to WCM. In addition, wheat lines 'Radiant' and 'AAC Elevate' were used as sources of *Cmc1* resistance gene. 'Radiant' resistance donor is the *Ae. tauschii Cmc1* donor accession 'CI4' via the synthetic hexaploid wheat 'PGR16635' (Thomas et al., 2012; Thomas & Conner, 1986; Whelan & Thomas, 1989). 'AAC Elevate' is a newer cultivar with resistance from 'Radiant'. WGS data alignment, variant calling, variant filtering, and phylogenetic analyses were performed as previously described. Sequences were compared manually and aligned with blastn of NCBI BLAST v2.6.0 (Altschul et al., 1990).

KASP markers primer design

Using the WGS data within the resistant region (2.3 – 2.6 Mbp) for all resistant entries including seven wheat lines and 20 *Ae. tauschii*, and all 29 susceptible wheat lines we looked for bi-allelic variants that discriminate between R and S entries. We used the *Ae. tauschii* reference genome assembly (Aet v4.0; NCBI BioProject PRJNA341983) to obtain the context sequence for each variant, extracting 200bp on each side of the selected variant and using that sequence to perform a BLAST to the wheat assembly (CS_refseqv1.0) in order to avoid sequences that hit off sites. The context sequences were uploaded to the software PolyMarker (Ramirez-Gonzalez et al., 2015) to design primers sequences following the software recommendations.

Results

Phenotypic data

Phenotypic evaluation for resistance to WCM identified both lineages having resistant and susceptible accessions. Moreover, both lineages also had accessions across the whole range of resistant to susceptible phenotypes (visual scale 0 to 4). Overall, we found more susceptible than resistant accessions, with most of the resistant accessions belonging to L1, with only a few representing L2. For L1, the majority of the susceptible accessions were assigned a score of 4, and the phenotypic mean value was 2.11 (Fig. 4.2A). On the other hand, the majority of L2 accessions were assigned to level 3, but with a higher mean value of 2.94 (Fig. 4.2A). All samples corresponding to the susceptible check 'Jagger' were classified into the susceptibility level 2. Broad-sense heritability estimates were 0.62 and 0.64 for L1 and L2, respectively. WCM phenotypic responses were plotted on a map based on passport information to investigate if resistance to WCM was associated with geographical origin and determine if resistant accessions cluster together into small groups. From the geographical distribution map, we can see that majority of the resistant accessions originate from the extremes of *Ae. tauschii* natural habit, and that the majority were collected in Afghanistan (Fig. 4.2B).

Sequencing data, clustering analyses, and GWAS

Initially, a total of 13,135 putative GBS-SNP markers were obtained from Singh et al (2019). After filtering for the 388 accessions used in this study, a total of 13,069 high-quality SNP markers were retained. Filtering for the different lineages separately resulted in 4,979 SNPs and 6,570 SNPs for L1 and L2, respectively. Similar distribution of SNP markers along the chromosomes was observed for the different lineages with high density at the chromosome end, with very few SNPs located on the centromeric regions (Fig. D.1). SNP marker distribution for chromosomes 1D – 7D was similar for all cases, where chromosome 7D was the most marker-saturated and chromosome 4D the least. For the WGS data, retained SNP markers for the 234 *Ae. tauschii* accessions were 27.7 million showing a uniform distribution along the chromosomes (Fig. D.1). In addition, for the subset of 85 accessions and 36 wheat lines we were able to discover 947,937 SNP markers for chromosome 6DS (position 0 – 230 Mbp), and 2,899 SNP markers for the resistance region on 6DS (1.9 – 2.7 Mbp).

The additive relationship matrix to perform the PCA was estimated with the complete set of 13,069 GBS-SNP markers. Lineage designation was used to differentiate the accessions that were separated in different clusters corresponding to the different lineages (Fig. 4.3). The first three PCs explained 64% of the variation. The first PC explaining 56% of the variation separated the accessions according to their lineages. The second and third components each explained 4% of the variation, separating within the lineages. Phenotypic response to WCM was used to color the accessions to assess if population structure was confounded with resistance. For L1, resistant accessions were present in all the different sub-clusters. However, for L2, resistant accessions were clustered in a smaller group, suggesting that the resistance might be explained by the same resistance gene(s) (Fig. 4.3). In addition, PCA was performed separately for each lineage, confirming that population structure exists within the lineages (data not shown). Based on PCA results, the first three PC were included as a fixed effect in the mixed model to run the GWAS analyses.

To investigate the hypothesis that *Ae. tauschii* accessions are a diverse collection with resistant and susceptible accessions to WCM and that WCM resistance in *Ae. tauschii* is determined by genetic components, specifically oligogenic large effects, we studied the genetic architecture of resistance to WCM using GWAS. The GWAS analysis was conducted combining both lineages and for each lineage separately. Moreover, the analyses were performed using GBS-SNP and WGS-SNP markers (Fig. 4.4). The first 3 PC inferred with PCA and genetic relatedness (kinship) were included in the mixed model to account for population structure and spurious associations. We found significant marker-trait associations above the Bonferroni threshold on the distal end of chromosome 6DS (Fig. 4.4). The same genomic region was mapped using both GBS and WGS data, and when the GWAS was performed combining both lineages and for each lineage separately. The associated interval was estimated at position1.9 – 2.7Mpb.

Based on GBS data, the significant region comprised 11 SNP markers defining 12 different haplotypes (Fig. 4.5A). To study the hypothesis that a unique haplotype is associated with WCM resistance we grouped all the accessions under the same haplotype and calculated the average WCM phenotypic value for the group (Fig. 4.5A). We found that the most resistant haplotype was the same for both lineages and that all the resistant accessions were grouped within that resistant haplotype. This contrasts with the expectation that the two lineages are genetically

separated. In addition, L1 resulted in more haplotype categories than L2, 10 and 5, respectively. Out of the 10 haplotypes classes in L1, seven were unique for L1 and not present within L2 accessions. In the same line, L2 presented 2 unique haplotypes. Moreover, the most common susceptible haplotype for each lineage was the less common haplotype for the other lineage (Fig. 4.5A).

Based on WGS data, the significant region included 1,335 SNP markers. To illustrate the haplotypes on the region we selected 12 SNP markers based on an FDR p-value < 0.01, which defined four haplotypes (Fig. 4.5B). Only one haplotype was found to be associated with resistance for both lineages. Furthermore, both lineages had the same most predominant susceptible haplotype (Fig. 4.5B). Moreover, nine genes were annotated within the region, with only four of them having polymorphisms for the gene sequence. BLAST output for these four genes resulted in the putative candidate genes, gene 1: AET6Gv20009000 – d RING/U-box superfamily protein (2126647 – 2137694bp), gene 2: AET6Gv20009100 – Protein disulfide-isomerase (2133893 – 2142474bp), gene 3: AET6Gv20009400 – Transmembrane protein (2221354 – 2236422bp), and gene 4: AET6Gv200010000 – E3 ubiquitin-protein ligase (2300973 – 2313934bp). An important note is that the *Ae. tauschii* reference assembly (Aet v4.0; NCBI BioProject PRJNA341983) is from a susceptible accession, therefore, any hypothesis about the gene controlling WCM resistance is preliminary.

To further examine the haplotype structure around the targeted region and to investigate the relationship between the resistance genes *Cmc1*, *Cmc4*, and Cmc_{TAM112}, we evaluated the haplotype sequence for a subset of 85 *Ae. tauschii* accessions from both lineages together with 36 hexaploid wheat lines including varieties with WCM resistance introgressed from *Ae. tauschii*. We found that all the resistant entries share a common haplotype within the genomic region of 2.3 – 2.6 Mbp on chromosome 6D, including 292 WGS-SNP markers (Fig. 4.6).

We then hypothesized that the WCM resistance found in *Ae. tauschii* across both lineages was from a single origin and that the resistance in L2 was derived from admixture between the lineages. From this hypothesis we would predict to observe i) admixture in the resistant accessions from L2, particularly for chromosome 6D and ii) a gene/haplotype level phylogeny that contrasts the established *Ae. tauschii* subspecies and instead grouped resistant accession

from both lineages together. Phylogenetic analyses for the selected *Ae. tauschii* group using variants within the resistance region (2.3 – 2.6 Mbp) showed all L2 resistant accessions clustering within a L1 resistant group (Fig. 4.7), giving gene-level phylogeny contrasting to the known species-level phylogeny (Fig. 4.7). Likewise, the ADMIXTURE analysis showed *Ae. tauschii* accessions and wheat lines were assigned with probabilities of ancestry to different groups with the resistant accessions showing admixture between lineages (Fig. 4.7). Together this supports that admixture exists between the lineages and that the WCM resistance in *Ae. tauschii* has a single origin and was introgressed from L1 to L2.

Delimitation of the introgression into hexaploid wheat

Given the observed L1 to L2 admixture, we hypothesized that these independent L1 and L2 resistance sources in hexaploid wheat are the same. Based on this hypothesis, we would again expect to have a single common haplotype across all wheat lines regardless of the donor *Ae. tauschii* accessions. Testing this hypothesis, we observed the same common resistance haplotype at the WCM resistance locus across all resistant hexaploid wheat lines (Fig. 4.6 and 4.7), further supporting that WCM resistance has a single origin and was introgressed from L1 to L2 and then with modern breeding independently introgressed from both lineages into wheat. In addition, we were able to define that the *Ae. tauschii* donors of the resistance genes *Cmc4* and Cmc_{TAM112}, and resistant wheat lines carrying either *Cmc1*, *Cmc4*, or Cmc_{TAM112} all share the same haplotype at the 2.3 – 2.6 Mbp interval despite being from different lineages and carrying introgressions from different sources. Therefore, we demonstrated that 'KS96WGRC40' and 'LS902' with WCM resistance derived from *Cmc4*, 'Radiant' and 'AAC Elevate' with *Cmc1* derived resistance, and 'TAM 112', 'TAM 115' and 'TAM 204' with resistance derived from Cmc_{TAM112}, all have the same haplotype. This result supports that *Cmc1*, *Cmc4*, and Cmc_{TAM112} are all the same genes with different names.

The length of the introgressed fragment from *Ae. tauschii* into wheat carrying WCM resistance was delimited by comparing WGS data for resistant wheat lines and the corresponding *Ae. tauschii* donors (Table 4.1). In the first case, by comparing the wheat line 'KS96WGRC40' and the L1 *Ae. tasuchii* donor TA2397 we found that the introgression fragment extends from 0 – 41.5 Mbp on chromosome 6D. Further selection in the derived line 'LS902' shortened the

introgressed fragment to 11.8 Mbp. For the second case, we compared the wheat variety 'TAM 112' and the L2 *Ae. tauschii* donor TA1618, and we were able to delimit the introgression to the first 11.9 Mbp. The same fragment was found in the variety 'TAM 204' which is the result of one generation of breeding from 'TAM 112'. In 'TAM 115', a second-generation breeding derivative from 'TAM 112', we observed that subsequent selection shortened the introgressed fragment to the first 7.9 Mbp.

KASP markers primer design

Using all the entries with the resistant haplotype versus the susceptible wheat lines we were able to identify four bi-allelic variants. This way, the designed markers will be diagnostic for WCM resistance across the Great Plains of U.S. and Canada. We extracted the context sequence around the four bi-allelic SNPs and using the software PolyMarker we design KASP markers. However, from the four candidate variants, only one has the potential to be a good diagnostic marker (chr6D_2553254). From the other three, one falls within a repetitive region hitting in 989 positions on the reference genome and we were not able to design a marker, another hits the wheat genome on 2 contigs and primers were not designed because of low GC content, and the third one hits the wheat genome on 3 contigs but primers were successfully designed. Detailed information about the primers is presented in Table 4.2.

Discussion

Phenotypic data and mite colonies

Ae. tauschii covers a wide geographic range from eastern Turkey to China. Here we used accessions collected covering the entire distribution range and we found that most of the WCM resistant accessions are located outside the area of origin but spread across the natural habitat (Fig. 4.2). Resistance to WCM on both lineages was previously reported (Carrera et al., 2012; Malik et al., 2003a). In this study, we found resistant accessions from both lineages, even though the majority were from L1 (Fig.4.2). The reduced number of L2 resistant accessions could be the reason why the wheat germplasm pool lacks resistance to WCM. The wheat cultivar 'Jagger' was used as a susceptible check. Consistency on 'Jagger' phenotypic value confirms that the infestation method was successful, and the same infestation pressure was

achieved for all the trays. Even though the infestation method used in this study was proven to be effective (Khalaf et al., 2019; Murugan et al., 2011), it could be less precise than placing mites directly into individual plants. However, our results agree with previous studies showing that *Ae. tauschii* accessions TA1695, TA2394, and TA2397 display a resistance phenotype against WCM biotype 1 (Carrera et al., 2012; Malik et al., 2003a). Interestingly, all the resistant accessions from L2 presented a similar plant type, with purple coleoptile and open leaves (Fig. D.2), suggesting that resistance is conditioned by the same resistance gene(s).

Two genetically different WCM biotypes coexist in the United States: biotype 1, mainly found in South Dakota, Montana, Kansas, and Texas, and biotype 2 mainly from Nebraska (Hein et al., 2012; A. Skoracka et al., 2014). However, some reports have shown mite colonies collected from Nebraska falling into the biotype 1 classification (Hein et al., 2012). Nevertheless, both biotypes can be found overlapping their geographic distribution (Skoracka et al., 2018). Biotype 1 is avirulent to all WCM resistance genes and biotype 2 is virulent to *Cmc2*, *Cmc3*, and *Cmc4* (Chuang et al., 2017; Harvey et al., 1999) and no information exist for *Cmc1*. However, there is no clear association between the biotype class and the virulence/avirulence pattern against the resistance genes. Even though resistance conferred by some *Cmc* resistance genes against specific mite biotypes remains durable (like the resistance provided by *Cmc4* against some biotype 1 colonies), it is critical to find new sources of resistance to broaden the available genes to fight WCM because mite populations can adapt and overcome resistance sources such as in the case of *Cmc3* (Harvey et al., 1997). In this study, we used a known source of biotype 1 mites and therefore we assume we did not have any mixed populations. Because the biotype 1 is avirulent for *Cmc1* and *Cmc4*, our mapping results were not able to differentiate between these two genes. However, we later demonstrated that both genes have the same resistant haplotype.

Most of the studies on WCM only score symptoms based on a categorical scale of resistance or susceptibility, even though it was shown that plant symptoms alone not always indicate the actual plant response to the pathogen (Matrin et al., 1976). Furthermore, it was shown that plant symptoms and number of mites present in the plant do not always correlate (Richardson et al., 2014) .The phenotyping method used in this study was selected to account for heterogeneous accessions, those which replicated plants showing different scorings. Following this method, we were able to obtain good repeatability based on the moderately high values of H^2. Also, the

visual scale 0 to 4 was selected in order to account for a range of responses with different susceptibility levels. Here we have demonstrated that the severity of leaf curling as a phenotype for WCM resistance follow a continuous phenotype (Fig. 4.2) rather than a presence/absence category classification. Therefore, where to draw a line to define whether an accession is resistant or susceptible is not straightforward. Given this ambiguity, we focused only on the accessions with conclusive phenotype at the extremes of the phenotypic spectrum, and only those were selected to perform the phylogenetic analyses and haplotype comparison (Fig. 4.6 and Fig. 4.7).

Sequencing data, clustering analyses, and GWAS

Selecting a genotyping platform is important and depends on what is the research question to investigate. Here, we used two different platforms, GBS and WGS, and both identified the same genomic region associated with WCM resistance (Fig. 4.4). However, GWAS using GBS data showed higher association scores compared to WGS data. This result could be explained by the difference in population size used between both analyses, 388 for GBS versus 234 for WGS. Moreover, the haplotypes delineated by each platform were also similar (Fig. 4.5). However, WGS was more specific, providing much more level of detail and information. By using WGS data we were able to investigate in depth the sequence haplotype for the candidate region something that probably cannot be done at that level of detail with GBS data. Furthermore, we were able to design KASP markers in order to incorporate MAS for WCM into wheat breeding pipelines.

Population structure for *Ae. tauschii* was already studied and confirmed on several reports (Dvorak et al., 1998; Nyine et al., 2020; Singh et al., 2019; Wang et al., 2013). Here we also confirmed the known strong population between lineages and also structure within lineages based on geographic origin (Fig.4.3). In addition, we observed a relationship between population structure and WCM response (Fig. 4.2). From the phylogenetic analyses, we observed the expected close relationship between L2 and wheat as the donor of the D genome of hexaploid wheat (Gill, 2013; Wang et al., 2013). Moreover, both lineages also showed some level of intra-lineage structure and this was not evident for wheat (Fig. 4.7).

Aegilops tauschii has been widely used as a source for novel resistance genes against many biotic stresses (Börner et al., 2015; Cox, 1992; Gill & Raupp, 1987; Rasheed et al., 2018). An example of this are the WCM resistance genes *Cmc1* and *Cmc4* investigated in this study and mapped to chromosome 6DS (Malik et al., 2003b; Whelan & Thomas, 1989) In this study, we confirmed that chromosome 6DS harbors resistance against WCM (Fig. 4.4). However, this chromosome region was the only region associated with resistance and, thus, we were not able to identify novel genomic regions. Several approaches could be implemented to expand the collection of WCM resistant genes available for breeding. First, other mite colonies different to the biotype 1 colony that we used in this study should be tested to evaluate if other genomic regions are contributing to WCM resistance. Malik et al. (2003a) tested five different mite colonies and suggested that *Ae. tauschii* holds at least five resistance genes for WCM. Second, search for resistance in other wild species (Friebe et al., 1996; Kishii, 2019; Mirzaghaderi & Mason, 2019) - other related species have shown resistance to WCM such as *Dassypyrum villosum* (L.) Candargy (Chen et al., 1996; Li et al., 2002) and *Thinopyrum ponticum* (Podp) Barkworth & D.R. Dewey and *T. araraticum* (Whelan et al., 1986). Furthermore, the translocation 1BL·1RS from rye into wheat also possess some WCM resistance (Aguirre-Rojas et al., 2017; Matrin et al., 1976).

Resistance genes *Cmc1* and *Cmc4* were both transferred to the short arm of chromosome 6DS in wheat, however by doing an allelism test Malik et al. (2003b) showed that they segregate independently. However, several points could be argued about the results presented by Malik et al. (2003b). First, independent segregation (genes located 50cM apart) should not be excepted for linked genes located in the same chromosome arm. For example, for two different genes located 20cM apart (approximate half of a chromosome arm), the expected F2 ratio in a population of 400 individuals is 396R:4S, which contradicts the reported ratio by Malik et al. (2003b) of 353R:22S. Second, the data presented about the virulence of mite colonies used in the study is not conclusive evidence of WCM symptoms because they are based on the number of mites rather than the severity. Furthermore, the response (number of mites) was compared between two different species (wheat and *Ae. tauschii*). Third, they concluded that the accession TA2394 had the same resistance as *Cmc1* and here we demonstrated that the accession TA2394 possess the same haplotype as TA2397 (donor of *Cmc4*), and TA1618 (donor of Cmc_{TAM112}) (Fig. 4.6). In

addition, the resistance gene *Cmc*$_{TAM112}$ was recently mapped to chromosome 6DS (Dhakal et al., 2018) and it has been suggested that corresponds to *Cmc4* because they overlap their position in the genome (Zhao et al., 2019). We know that the *Ae. tauschii* donor of *Cmc4*, the L1 accession TA2397, was originally collected from Afghanistan. But there is no information to which lineage the *Cmc1* donor accession belongs. However, we do know it was originally collected in Afghanistan, and no L2 accession comes from Afghanistan (Singh et al., 2019) suggesting that it could be classified as L1. Our study found that the three genes, *Cmc1*, *Cmc4*, and *Cmc*$_{TAM112}$ share the same resistance haplotype (Fig. 4.6) and therefore strongly supports that they are indeed the same gene. Based on this conclusion, we propose to use *Cmc1* as the common name for this gene from now on, replacing the designations of *Cmc4*, and *Cmc*$_{TAM112}$. Further, we demonstrate that identification and utilization of a resistance gene from a different genetic source (e.g. different subspecies in *Ae. tauschii*) is not sufficient to consider that the gene is truly novel. In this example with WCM resistance, though *Cmc1*, *Cmc4*, and *Cmc*$_{TAM112}$ were introgressed from completely different *Ae. tauschii* sources, they were indeed the same locus due to a previously undiscovered ancient admixture between the subspecies. Detailed genetic characterization of a resistance locus is therefore needed to truly conclude the identity and relationship of individual genes.

Delimitation of the introgression into hexaploid wheat

Developing improved varieties with introgressions from *Ae. tauschii* into hexaploid wheat can be achieved by direct crossing creating an aneuploid (ABDD, n=28), which is then restored to hexaploid (AABBDD, 2n=42) through backcrossing (Gill & Raupp, 1987). The resistance gene *Cmc4* was originally transferred from the *Ae. tauschii* L1 accession TA2397 into the hexaploid wheat germplasm 'KS96WGRC40' (Cox et al., 1999), and was genetically mapped to chromosome 6D (Malik et al., 2003b) in agreement with our association analyses results (Fig. 4.4). Recently, resistance to WCM in the wheat cultivar 'TAM 112' (*Cmc*$_{TAM112}$) was also mapped to 6D (Dhakal et al., 2018). The 'TAM 112' resistance locus has the same genetic position as *Cmc*4, suggesting that they are the same locus (Zhao et al., 2019). However, resistance in 'TAM 112' was introgressed from the L2 accession TA1618 (Rudd et al., 2014), which previously contradicted that they would be the same gene. However, we demonstrate here that all of the WCM resistant wheat germplasm and varieties carry a common haplotype at the

position of 2.3 – 2.6 Mbp on chromosome 6DS (Fig. 4.6). We also showed that with targeted breeding and selection for the WCM resistance, independent introgression events have unique donor introgression segments with different lengths. After the initial introgression event, further selection can reduce the extent of the introgressed segments, like it was shown for 'LS902' and 'TAM 115', derived lines from 'KS96WGRC40' and 'TAM 112', respectively.

KASP markers primer design

One output from genetic studies with a direct impact on breeding programs is the development of molecular markers in order to apply MAS. Even though KASP markers targeting *Cmc4* and *Cmc$_{TAM112}$* have been previously designed and reported (Dhakal et al., 2018; Zhao et al., 2019), they are not fully diagnostic or perfectly associated with the gene. In this study, two KASP markers located within the resistance region were designed that can be used for MAS of *Cmc1*, *Cmc4*, and *Cmc$_{TA112}$* derived WCM resistance. Further validation of these markers is needed in order to check their applicability.

Conclusions

We were able to show that *Cmc1*, *Cmc4*, and *Cmc$_{TAM112}$* all have an identical haplotype for 300kb at the genomic region identified for WCM resistance on the short arm of chromosome 6D, strongly supporting that they are the same gene. This is a great support for diagnostic markers for breeding WCM resistance and informs the use of these various germplasm. However, our study was not able to discover new genomic regions associated with resistance to WCM and giving realization that there is actually limited resistance available in the current wheat gene pool with the previously presumed three different resistance genes actually all being the same gene from different sources. Therefore, continuing this search using other species related to wheat, and different mite biotypes will be crucial to broadening the resistant genes available to introgress into wheat germplasm. Ultimately, untapped genetic diversity to identifying new sources of resistance will facilitate to breed wheat against WCM.

Acknowledgements

This material is based upon work supported by the National Science Foundation under Award No. (1822162) "Phase II IUCRC at Kansas State University Center for Wheat Genetic Resources WGRC" and support of industry partners, through support from the Kansas Wheat Commission and Kansas State University. PS was supported through a U.S. Fulbright-ANII Uruguay Scholarship. The whole-genome sequencing data for the *Ae. tauschii* collection is provided through the Open Wild Wheat Consortium (http://www.openwildwheat.org/). Any opinions, findings, and conclusions or recommendations expressed in this material are those of the author(s) and do not necessarily reflect the views of the National Science Foundation or industry partners.

References

Aguirre-Rojas, L., Khalaf, L., Garcés-Carrera, S., et al. (2017). Resistance to Wheat Curl Mite in Arthropod-Resistant Rye-Wheat Translocation Lines. Agronomy, 7(4), 74. https://doi.org/10.3390/agronomy7040074

Alexander, D. H., Novembre, J., & Lange, K. (2009). Fast model-based estimation of ancestry in unrelated individuals. Genome Research, 19(9), 1655–1664. https://doi.org/10.1101/gr.094052.109

Altschul, S. F., Gish, W., Miller, W., et al. (1990). Basic local alignment search tool. Journal of Molecular Biology, 215(3), 403–410. https://doi.org/10.1016/S0022-2836(05)80360-2

Bates, D., Mächler, M., Bolker, B., & Walker, S. (2014). Fitting Linear Mixed-Effects Models Using *lme4*. Journal of Statistical Software, 67(1). https://doi.org/10.18637/jss.v067.i01

Bockus, W. W., Appel, J. A., Bowden, R. L., et al. (2001). Success stories: Breeding for wheat disease resistance in Kansas. Plant Disease, 85(5), 453-461.

Börner, A., Ogbonnaya, F. C., Röder, M. S., et al. (2015). *Aegilops tauschii* Introgressions in Wheat. In Alien Introgression in Wheat (pp. 245–271). https://doi.org/10.1007/978-3-319-23494-6_10

Caldwell, K. S., Dvorak, J., Lagudah, E. S., et al. (2004). Sequence polymorphism in polyploid wheat and their D-genome diploid ancestor. Genetics, 167(2), 941–947. https://doi.org/10.1534/genetics.103.016303

Carrera, S. G., Davis, H., Aguirre-Rojas, L., et al. (2012). Multiple Categories of Resistance to Wheat Curl Mite (Acari: *Eriophyidae*) Expressed in Accessions of *Aegilops tauschii*. Journal of Economic Entomology, 105(6), 2180–2186. https://doi.org/10.1603/EC12252

Chen, Q., Conner, R. L., & Laroche, A. (1996). Molecular characterization of *Haynaldia villosa* chromatin in wheat lines carrying resistance to wheat curl mite colonization. Theoretical and Applied Genetics, 93–93(5–6), 679–684. https://doi.org/10.1007/BF00224062

Chen, Q, Conner, R. L., Li, H. J., et al. (2003). Molecular cytogenetic discrimination and reaction to wheat streak mosaic virus and the wheat curl mite in Zhong series of wheat –

Thinopyrum intermedium partial amphiploids. Genome, 46(1), 135–145. https://doi.org/10.1139/g02-109
Chuang, W.-P., Rojas, L. M. A., Khalaf, L. K., et al. (2017). Wheat Genotypes with Combined Resistance to Wheat Curl Mite, Wheat Streak Mosaic Virus, Wheat Mosaic Virus, and Triticum Mosaic Virus. Journal of Economic Entomology, 110(2), tow255. https://doi.org/10.1093/jee/tow255
Cox, T. S. (1992). Resistance to Foliar Diseases in a Collection of *Triticum tauschii* Germ Plasm. Plant Disease, 76(10), 1061. https://doi.org/10.1094/pd-76-1061
Cox, T. S., Bockus, W. W., Gill, B. S., et al. (1999). Registration of KS96WGRC40 Hard Red Winter Wheat Germplasm Resistant to Wheat Curl Mite, Stagnospora Leaf Blotch, and Septoria Leaf Blotch. Crop Science, 39(2), 597–597. https://doi.org/10.2135/cropsci1999.0011183X003900020070x
Dhakal, S., Tan, C.-T., Anderson, V., et al. (2018). Mapping and KASP marker development for wheat curl mite resistance in "TAM 112" wheat using linkage and association analysis. Molecular Breeding, 38(10), 119. https://doi.org/10.1007/s11032-018-0879-x
Dvořák, J., Luo, M.-C., Yang, Z.-L., & Zhang, H.-B. (1998). The structure of the *Aegilops tauschii* gene pool and the evolution of hexaploid wheat. Theoretical and Applied Genetics, 97(4), 657–670. https://doi.org/10.1007/s001220050942
Endelman, J. B. (2011). Ridge Regression and Other Kernels for Genomic Selection with R Package *rrBLUP*. The Plant Genome Journal, 4(3), 250. https://doi.org/10.3835/plantgenome2011.08.0024
Friebe, B., Jiang, J., Raupp, W. J., et al. (1996). Characterization of wheat-alien translocations conferring resistance to diseases and pests: Current status. Euphytica, 91(1), 59–87. https://doi.org/10.1007/BF00035277
Gill, B. S. (2013). SNPing *Aegilops tauschii* genetic diversity and the birthplace of bread wheat. New Phytologist, 198(3), 641–642. https://doi.org/10.1111/nph.12259
Gill, B. S., & Raupp, W. J. (1987). Direct Genetic Transfers from *Aegilops squarrosa* L. to Hexaploid Wheat 1. Crop Science, 27(3), 445-450. https://doi.org/10.2135/cropsci1987.0011183X002700030004x
Gotz, R., & Maiss, E. (1995). The complete nucleotide sequence and genome organization of the mite-transmitted brome streak mosaic virus in comparison with those of potyviruses. Journal of General Virology, 76(8), 2035–2042. https://doi.org/10.1099/0022-1317-76-8-203
Graf, R. J., Beres, B. L., Randhawa, H. S., et al. (2015). Le blé de force rouge d'hiver AAC Elevate. Canadian Journal of Plant Science, 95(5), 1021–1027. https://doi.org/10.4141/CJPS-2015-094
Harvey, T. L., Martin, T. J., & Seifers, D. L. (1995). Survival of five wheat curl mite, *Aceria tosichilla* Keifer (Acari:*Eriophyidae*), strains on mite resistant wheat. experimental and applied acarology, 19(8), 459–463. https://doi.org/10.1007/BF00048264
Harvey, T. L., Martin, T. J., Seifers, D. L., & Sloderbeck, P. E. (1997). Change in Virulence of Wheat Curl Mite Detected on TAM 107 Wheat. Crop Science, 37(2), 624–625. https://doi.org/10.2135/cropsci1997.0011183X003700020052x
Harvey, T. L., Seifers, D. L., Martin, T. J., et al. (1999). Survival of Wheat Curl Mites on Different Sources of Resistance in Wheat. Crop Science, 39(6), 1887–1889. https://doi.org/10.2135/cropsci1999.3961887x

Harvey, Tom L., Seifers, D. L., Martin, T. J., & Michaud, J. P. (2005). Effect of resistance to wheat streak mosaic virus on transmission efficiency of wheat curl mites. Journal of Agricultural and Urban Entomology, 22(1), 1–6.

Hein, G. L., French, R., Siriwetwiwat, B., & Amrine, J. W. (2012). Genetic Characterization of North American Populations of the Wheat Curl Mite and Dry Bulb Mite. Journal of Economic Entomology, 105(5), 1801–1808. https://doi.org/10.1603/EC11428

Hollandbeck, GF., DeWolf, E., and Todd, T. (2019). Kansas cooperative plant disease survey report. Preliminary 2019 Kansas wheat disease loss estimates. October 2, 2019 https://agriculture.ks.gov/divisionsprograms/plant-protect-weed-control/reports-and-publications

Khalaf, L., Chuang, W. P., Aguirre-Rojas, L. M., et al. (2019). Differences in *Aceria tosichella* population responses to wheat resistance genes and wheat virus transmission. Arthropod-Plant Interactions, 13(6), 807–818. https://doi.org/10.1007/s11829-019-09717-9

Kim, D., Paggi, J. M., Park, C., et al. (2019). Graph-based genome alignment and genotyping with HISAT2 and HISAT-genotype. Nature Biotechnology, 37(8), 907–915. https://doi.org/10.1038/s41587-019-0201-4

Kishii, M. (2019). An update of recent use of *Aegilops* species in wheat breeding. Frontiers in Plant Science, 10, 585. https://doi.org/10.3389/fpls.2019.00585

Lado, B., Matus, I., Rodríguez, A., et al. (2013). Increased genomic prediction accuracy in wheat breeding through spatial adjustment of field trial data. G3 (Bethesda, Md.), 3(12), 2105–2114. https://doi.org/10.1534/g3.113.007807

Lagudah, E. S., Appels, R., Brown, A. H. D., & McNeil, D. (1991). The molecular–genetic analysis of *Triticum tauschii*, the D-genome donor to hexaploid wheat. Genome, 34(3), 375–386. https://doi.org/10.1139/g91-059

Langmead, B., & Salzberg, S. L. (2012). Fast gapped-read alignment with Bowtie 2. Nature Methods, 9(4), 357–359. https://doi.org/10.1038/nmeth.1923

Li, H (2011). A statistical framework for SNP calling, mutation discovery, association mapping and population genetical parameter estimation from sequencing data. Bioinformatics, 27(21), 2987–2993. https://doi.org/10.1093/bioinformatics/btr509

Li, H, Handsaker, B., Wysoker, A., et al. (2009). The Sequence Alignment/Map format and SAMtools. Bioinformatics, 25(16), 2078–2079. https://doi.org/10.1093/bioinformatics/btp352

Li, H, Conner, R. L., Chen, Q., et al. (2005). Promising genetic resources for resistance to wheat streak mosaic virus and the wheat curl mite in wheat-*Thinopyrum* partial amphiploids and their derivatives. Genetic Resources and Crop Evolution, 51(8), 827–835. https://doi.org/10.1007/s10722-005-0001-1

Li, H, Conner, R. L., Chen, Q., et al. (2002). Different reactions to the wheat curl mite and Wheat streak mosaic virus in various wheat - *Haynaldia villosa* 6V and 6VS lines. Plant Disease, 86(4), 423–428. https://doi.org/10.1094/PDIS.2002.86.4.423

Lipka, A. E., Tian, F., Wang, Q., et al. (2012). GAPIT: genome association and prediction integrated tool. Bioinformatics, 28(18), 2397–2399. https://doi.org/10.1093/bioinformatics/bts444

Malik, R., Brown-Guedira, G. L., Smith, C. M., et al. (2003a). Genetic Mapping of Wheat Curl Mite Resistance Genes and in Common Wheat. Crop Science, 43(2), 644. https://doi.org/10.2135/cropsci2003.0644

Malik, Renu, Smith, C. M., Brown-Guedira, G. L., et al. (2003b). Assessment of *Aegilops tauschii* for Resistance to Biotypes of Wheat Curl Mite (Acari: Eriophyidae). Journal of Economic Entomology, 96(4), 1329–1333. https://doi.org/10.1603/0022-0493-96.4.1329

Matrin, T.J., Harvey, T.L., Livers, R. W. (1976). Resistance to Wheat Streak Mosaic Virus and its Vector, *Aceria tulipae*. Phytopathology, (66), 346–349. Retrieved from https://www.apsnet.org/publications/phytopathology/backissues/Documents/1976Articles/Phyto66n03_346.PDF

Mirzaghaderi, G., & Mason, A. S. (2019, May 1). Broadening the bread wheat D genome. Theoretical and Applied Genetics, Vol. 132, pp. 1295–1307. https://doi.org/10.1007/s00122-019-03299-z

Murugan, M., Cardona, P. S., Duraimurugan, P., et al. (2011). Wheat Curl Mite Resistance: Interactions of Mite Feeding with Wheat Streak Mosaic Virus Infection. Journal of Economic Entomology, 104(4), 1406–1414. https://doi.org/10.1603/ec11112

Navia, D., de Mendonça, R. S., Skoracka, A., et al. (2013). Wheat curl mite, *Aceria tosichella*, and transmitted viruses: An expanding pest complex affecting cereal crops. Experimental and Applied Acarology, 59(1–2), 95–143. https://doi.org/10.1007/s10493-012-9633-

Nyine, M., Adhikari, E., Clinesmith, M., et al. (2020). Genomic patterns of introgression in interspecific populations created by crossing wheat with its wild relative. G3: Genes, Genomes, Genetics, 10(10), 3651-3661. https://doi.org/10.1534/g3.120.401479

Paradis, E., & Schliep, K. (2019). ape 5.0: an environment for modern phylogenetics and evolutionary analyses in R. Bioinformatics, 35(3), 526–528. https://doi.org/10.1093/bioinformatics/bty633

Purcell, S., Neale, B., Todd-Brown, K., et al. (2007). PLINK: A tool set for whole-genome association and population-based linkage analyses. American Journal of Human Genetics, 81(3), 559–575. https://doi.org/10.1086/519795

Ramirez-Gonzalez, R. H., Uauy, C., & Caccamo, M. (2015). PolyMarker: A fast polyploid primer design pipeline. Bioinformatics, 31(12), 2038–2039. https://doi.org/10.1093/bioinformatics/btv069

Rasheed, A., Ogbonnaya, F. C., Lagudah, E., et al. (2018). The goat grass genome's role in wheat improvement. Nature Plants, 4(2), 56–58. https://doi.org/10.1038/s41477-018-0105-1

Richardson, K., Miller, A. D., Hoffmann, A. A., & Larkin, P. (2014). Potential new sources of wheat curl mite resistance in wheat to prevent the spread of yield-reducing pathogens. Experimental and Applied Acarology, 64(1), 1–19. https://doi.org/10.1007/s10493-014-9808-9

Rudd, J. C., Devkota, R. N., Baker, J. A., et al. (2014). 'TAM 112' Wheat, Resistant to Greenbug and Wheat Curl Mite and Adapted to the Dryland Production System in the Southern High Plains. Journal of Plant Registrations, 8(3), 291–297. https://doi.org/10.3198/jpr2014.03.0016crc

Rudd, J. C., Devkota, R. N., Ibrahim, A. M., et al (2019). 'TAM 204' Wheat, Adapted to Grazing, Grain, and Graze-out Production Systems in the Southern High Plains. Journal of Plant Registrations, 13(3), 377–382. https://doi.org/10.3198/jpr2018.12.0080crc

Seifers, D. L., Harvey, T. L., Martin, T. J., & Jensen, S. G. (1997). Identification of the Wheat Curl Mite as the Vector of the High Plains Virus of Corn and Wheat. Plant Disease, 81(10), 1161–1166. https://doi.org/10.1094/PDIS.1997.81.10.1161

Seifers, D. L., Martin, T. J., Harvey, T. L., et al. (2008). Triticum mosaic virus: A New Virus Isolated from Wheat in Kansas. https://doi.org/10.1094/PDIS-92-5-0808

Singh, K., Wegulo, S. N., Skoracka, A., & Kundu, J. K. (2018). Wheat streak mosaic virus: a century old virus with rising importance worldwide. Molecular Plant Pathology, 19(9), 2193–2206. https://doi.org/10.1111/mpp.12683

Singh, N., Wu, S., Tiwari, V., Sehgal, S., et al. (2019). Genomic Analysis Confirms Population Structure and Identifies Inter-Lineage Hybrids in *Aegilops tauschii*. Frontiers in Plant Science, 10(January), 1–13. https://doi.org/10.3389/fpls.2019.00009

Skoracka, A., Rector, B., Kuczyński, L., et al. (2014). Global spread of wheat curl mite by its most polyphagous and pestiferous lineages. Annals of Applied Biology, 165(2), 222–235. https://doi.org/10.1111/aab.12130

Skoracka, A, Rector, B. G., & Hein, G. L. (2018). The Interface Between Wheat and the Wheat Curl Mite, *Aceria tosichella*, the Primary Vector of Globally Important Viral Diseases. Frontiers in Plant S. Frontiers in Plant Science, 9(July), 1–8. https://doi.org/10.3389/fpls.2018.01098

Thomas, J. B., Conner, R. L., & Graf, R. J. (2012). Radiant hard red winter wheat. Canadian Journal of Plant Science, 92(1), 169–175. https://doi.org/10.4141/cjps2011-082

Thomas, J., Chen, Q., & Talbert, L. (1998). Genetic segregation and the detection of spontaneous wheat-alien translocations. Euphytica, 100(1–3), 261–267. https://doi.org/10.1007/978-94-011-4896-2_45

Thomas, Julian B., & Conner, R. L. (1986). Resistance to Colonization by the Wheat Curl Mite in *Aegilops squarrosa* and its Inheritance after Transfer to Common Wheat 1. Crop Science, 26(3), 527–530. https://doi.org/10.2135/cropsci1986.0011183X002600030019x

Wang, J., Luo, M.-C., Chen, Z., et al. (2013). *Aegilops tauschii* single nucleotide polymorphisms shed light on the origins of wheat D-genome genetic diversity and pinpoint the geographic origin of hexaploid wheat. New Phytologist, 198(3), 925–937. https://doi.org/10.1111/nph.12164

Whelan, E. D. P., Conner, R. L., Thomas, J. B., & Kuzyk, A. D. (1986). Transmission of a wheat alien chromosome translocation with resistance to the wheat curl mite in common wheat, *Triticum aestivum* L. Canadian Journal of Genetics and Cytology, 28(2), 294–297. https://doi.org/10.1139/g86-042

Whelan, E. D. P., & Hart, G. E. (1988). A spontaneous translocation that transfers wheat curl mite resistance from decaploid *Agropyron elongatum* to common wheat. Genome, 30(3), 289–292. https://doi.org/10.1139/g88-050

Whelan, E. D. P., & Thomas, J. B. (1989). Chromosomal location in common wheat of a gene (*Cmcl*) from *Aegilops squarrosa* that conditions resistance to colonization by the wheat curl mite. Genome, 32(6), 1033–1036. https://doi.org/10.1139/g89-548

Wickham, H. (2016). ggplot2 -Positioning Elegant Graphics for Data Analysis. In Springer. https://doi.org/10.1007/978-3-319-24277-4

Yu, J., Pressoir, G., Briggs, W. H., et al. (2006). A unified mixed-model method for association mapping that accounts for multiple levels of relatedness. Nature Genetics, 38(2), 203–208. https://doi.org/10.1038/ng1702

Zhang, Z., Ersoz, E., Lai, CQ. et al. (2010). Mixed linear model approach adapted for genome-wide association studies. Nat Genet 42, 355–360. https://doi.org/10.1038/ng.546

Zhao, J., Abdelsalam, N. R., Khalaf, L., et al. (2019). Development of Single Nucleotide Polymorphism Markers for the Wheat Curl Mite Resistance Gene Cmc4. Crop Science, 59(4), 1567–1575. https://doi.org/10.2135/cropsci2018.11.0695

Table 4.1 - Information about the wheat lines used to delimit the length of the *Aegilops tauschii* introgression into chromomere 6DS of wheat and to study the haplotype structure. All the lines are known to be resistant to wheat curl mite.

Line name	WCM gene	*Ae. tauschii* donor	Lineage	Pedigree	Breeding Program	Citation
Radiant	*Cmc1*	CI4	unknown	Norstar*6/PGR16635//Norwin/ UT125512	AAFC LRC	(Thomas et al., 2012)
AAC Elevate	*Cmc1*	CI4	unknown	Radiant//AC Bellatrix/N95L1226	AAFC LRC	(Graf et al., 2015)
KS96WGRC40	*Cmc4*	TA2397	L1	KS93U69*2/TA2397	WGRC - KSU	(Cox et al., 1999)
LS902	*Cmc4*	TA2397	L1	W286-36/3/S96-35//McClintock/KS96WGRC40	AAFC LRC	Graf, R. pers.comm.
TAM 112	Cmc_{TAM112}	TA1618	L2	U1254-7-9-2-1/TXGH10440	TAMU	(Rudd et al., 2014)
TAM 115	Cmc_{TAM112}	TA1618	L2	TAM 112/TX02U2508	TAMU	Rudd, J. pers.comm.
TAM 204	Cmc_{TAM112}	TA1618	L2	TAM 112/TX01M5009	TAMU	(Rudd et al., 2019)

AAFC LRC - Lethbridge Research Centre (LRC) of Agriculture and Agri-Food Canada (AAFC), Lethbridge, AB, Canada

WGRC - KSU - Wheat Genetics Resource Center, Kansas State University, KS, USA

TAMU - Texas A&M AgriLife Research, TX, USA

Table 4.2 - KASP markers. Primer sequences and associated information for the two designed KAP markers. The sequence underlined on both left primers corresponds to FAM and HEX sequence for left primer1 and left primer2, respectively. Melting temperatures and number and positions of contigs (from wheat reference genome ChSp v1.0) were the primers hit are also included.

primer_name	left_primer1	primer_name	left_primer2	primer_name	right_primer	contigs	contig_regions	F_FAM_Tm	F_HEX_Tm	REV_Tm
chr6D_2521030_T_FAM_F	GAAGGTGACCAAGTTCATGCTTGCATAGAGGTAACCTACTTTCTTT	chr6D_2521030_C_HEX_F	GAAGGTCGGAGTCAACGGATTTGCATAGAGGTAACCTACTTTCTTC	chr6D_2521030_REV	TGGCACCTATGTCCAGATTGTCA	3	chr6D:2444369-2444769 chr5B:428606020-428606176 chr6B:72204760-72204887	57.746	58.125	61.647
chr6D_2553254_G_FAM_F	GAAGGTGACCAAGTTCATGCTCGCCCCTCTAGCCATACACC	chr6D_2553254_A_HEX_F	GAAGGTCGGAGTCAACGGATTCGCCCCTCTAGCCATACACT	chr6D_2553254_REV	CCTTTGTCACCCTCAGCCAG	1	chr6D:2470221-2470621	62.101	61.116	60.607

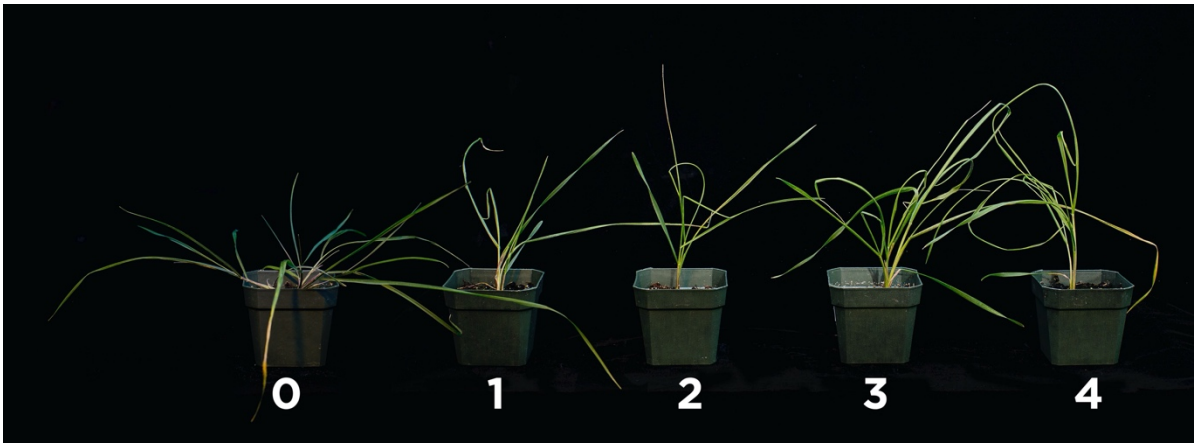

Figure 4.1 – Phenotypic scale used to evaluate wheat curl mite (WCM) symptoms. Illustration of Wheat Curl Mite symptoms and visual scale (0 – 4) used to characterize the *Aegilops tauschii* accessions. A value of 0 represents no symptoms and 1 – 4 represents increasing levels of leaf curling and stunting severity.

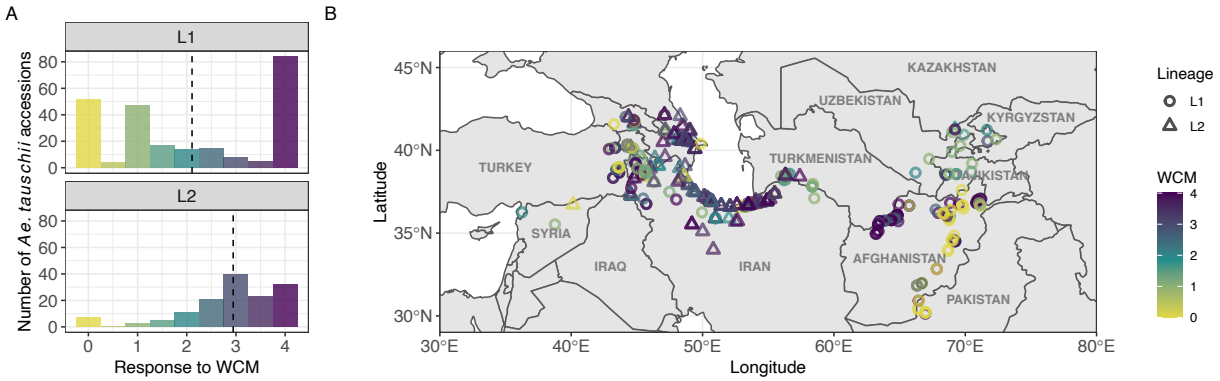

Figure 4.2 – Phenotypic data description.

Response to WCM. A) Phenotypic distribution of 388 *Aegilops tauschii* accessions infested with wheat curl mite (WCM) biotype 1. The dashed black lines correspond to the mean phenotypic value for each lineage. B) Map showing the geographical distribution of accessions based on passport information. L1: lineage 1, L2: lineage 2. Two susceptible L1 accessions from Northeastern China were excluded from the map for better visualization. The color gradient corresponds to WCM adjusted phenotypic values.

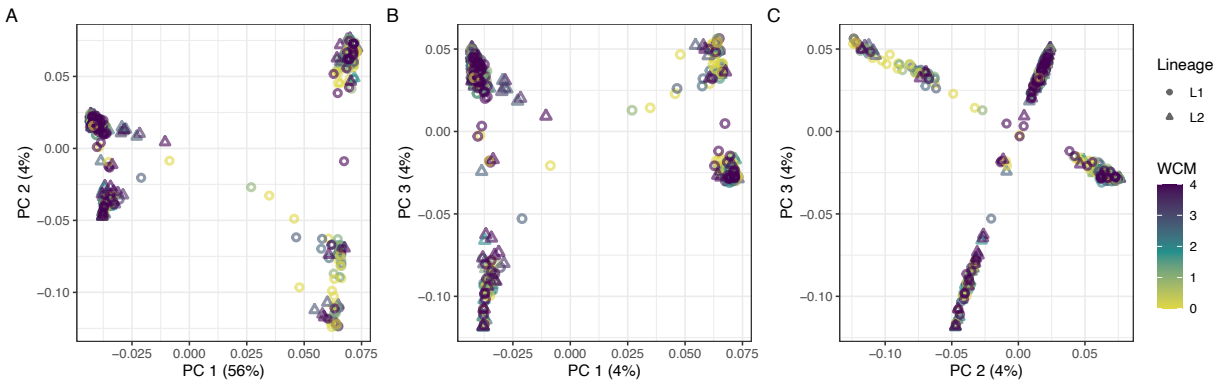

Figure 4.3 – Population structure.

Principal component analysis (PCA) plot using GBS-SNP markers for lineage1 (L1) and lineage 2 (L2) showing the first three components and the percentage of variation explained by each component. Accessions are colored based on phenotypic response to wheat curl mite (WCM) infestation. Empty circles represent L1 and empty triangles represent L2.

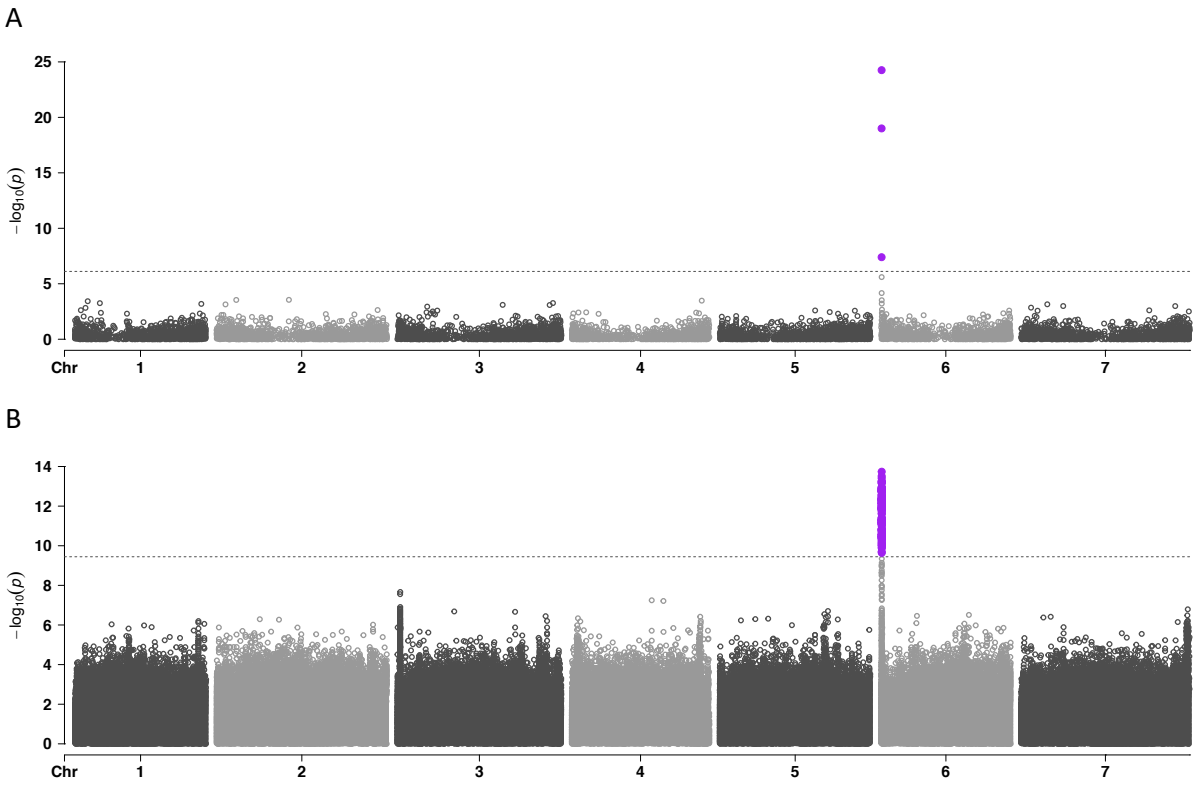

Figure 4.4 – Genome-wide association analyses.
Manhattan plots showing the marker-trait associations for wheat curl mite using A) genotyping-by-sequencing data (GBS) for 388 accessions and 13,069 SNP markers, and B) whole-genome-sequencing data (WGS) for 234 accessions and 3 million SNP markers (selected randomly out of the 27.7 million markers discovered). The seven *Aegilops tauschii* chromosomes with physical positions are on the x-axis and y-axis is the –log10 of the p-value for each SNP marker. Dashed horizontal line represents the Bonferroni threshold at 0.01 level. Chromosome labels are placed in the middle of each chromosome.

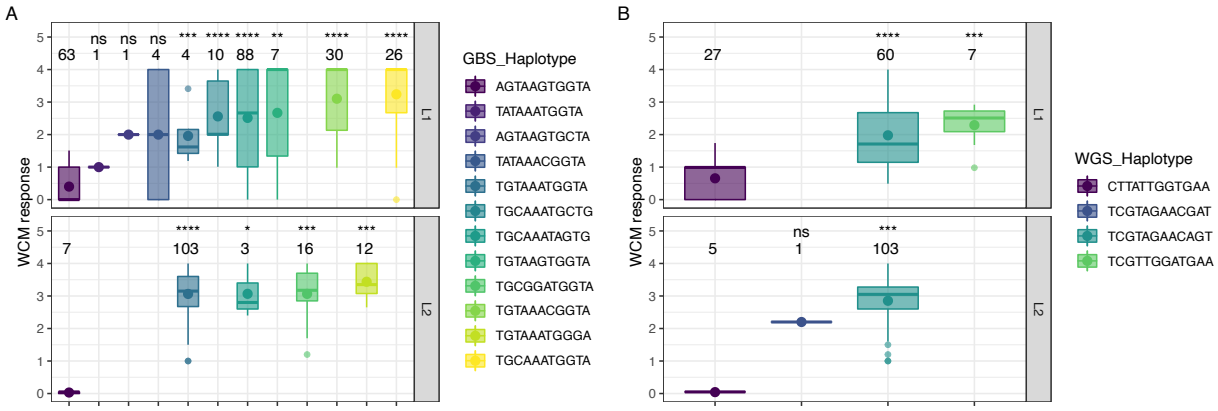

Figure 4.5 – Chromosome 6DS haplotypes.

Boxplots of wheat curl mite (WCM) phenotypic response for the different haplotypes detected by GWAS using A) GBS-SNP markers or B) WGS-SNP markers. The number of accessions grouped in each haplotype class is shown at the top of each boxplot. A significant t-test was done using the most resistant haplotype as the reference group. L1: lineage 1, L2: lineage 2, ns: non-significant.

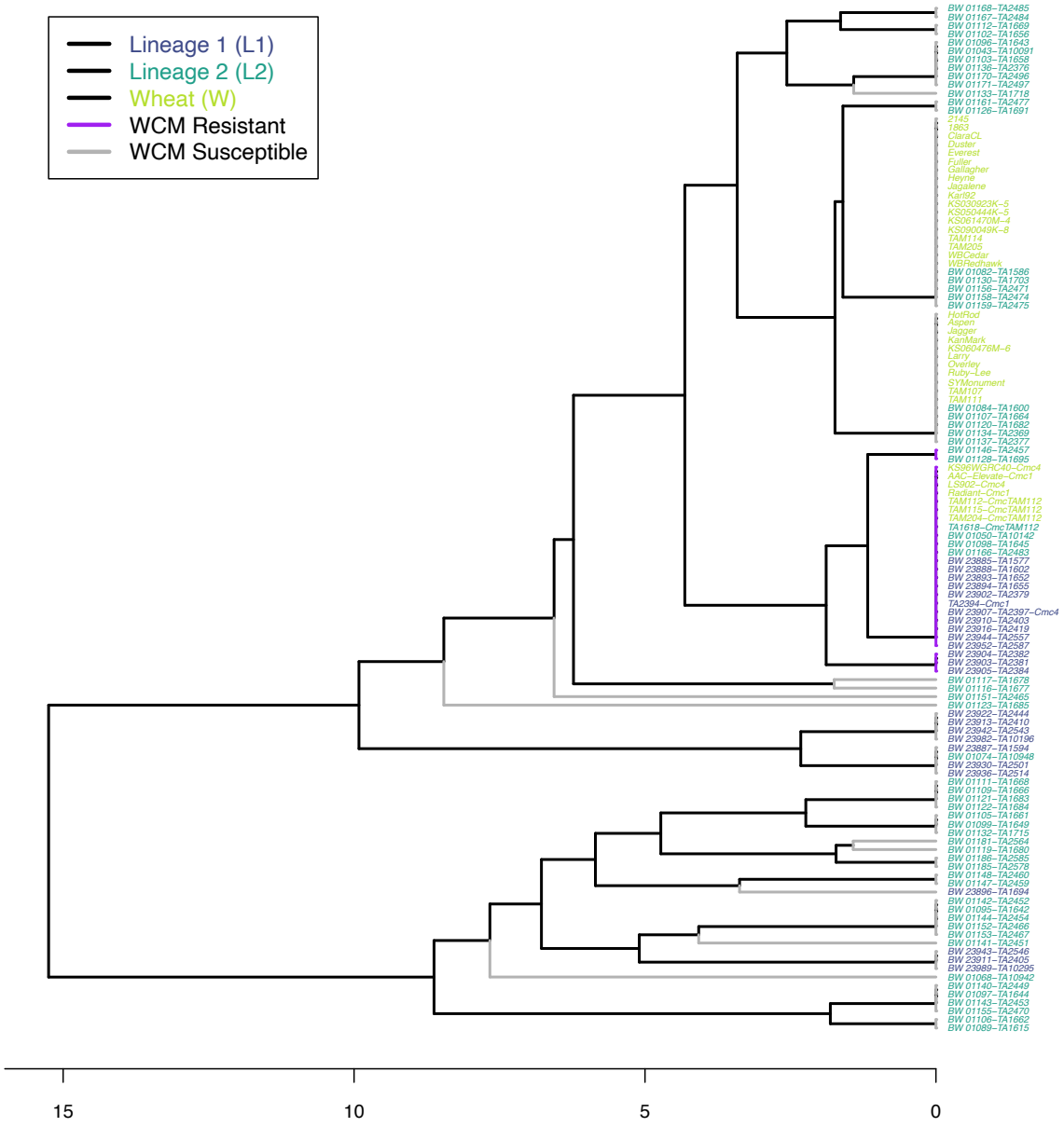

Figure 4.6 – Phylogenetic analysis for the resistance interval on chromosome 6DS at 2.3 – 2.6Mbp.

Phylogenetic analysis using Neighbor-joining clustering method for 292 SNP markers within the resistance interval on chromosome 6DS at 2.3 – 2.6Mbp, showing the relationship between 85 selected *Ae. tauschii* from L1 (blue) and L2 (red), and 36 wheat lines (green). Purple branches represent accessions that are resistant to wheat curl mite (WCM) infestation. The 292 WGS-SNP markers were obtained by removing all missing data and heterozygosity.

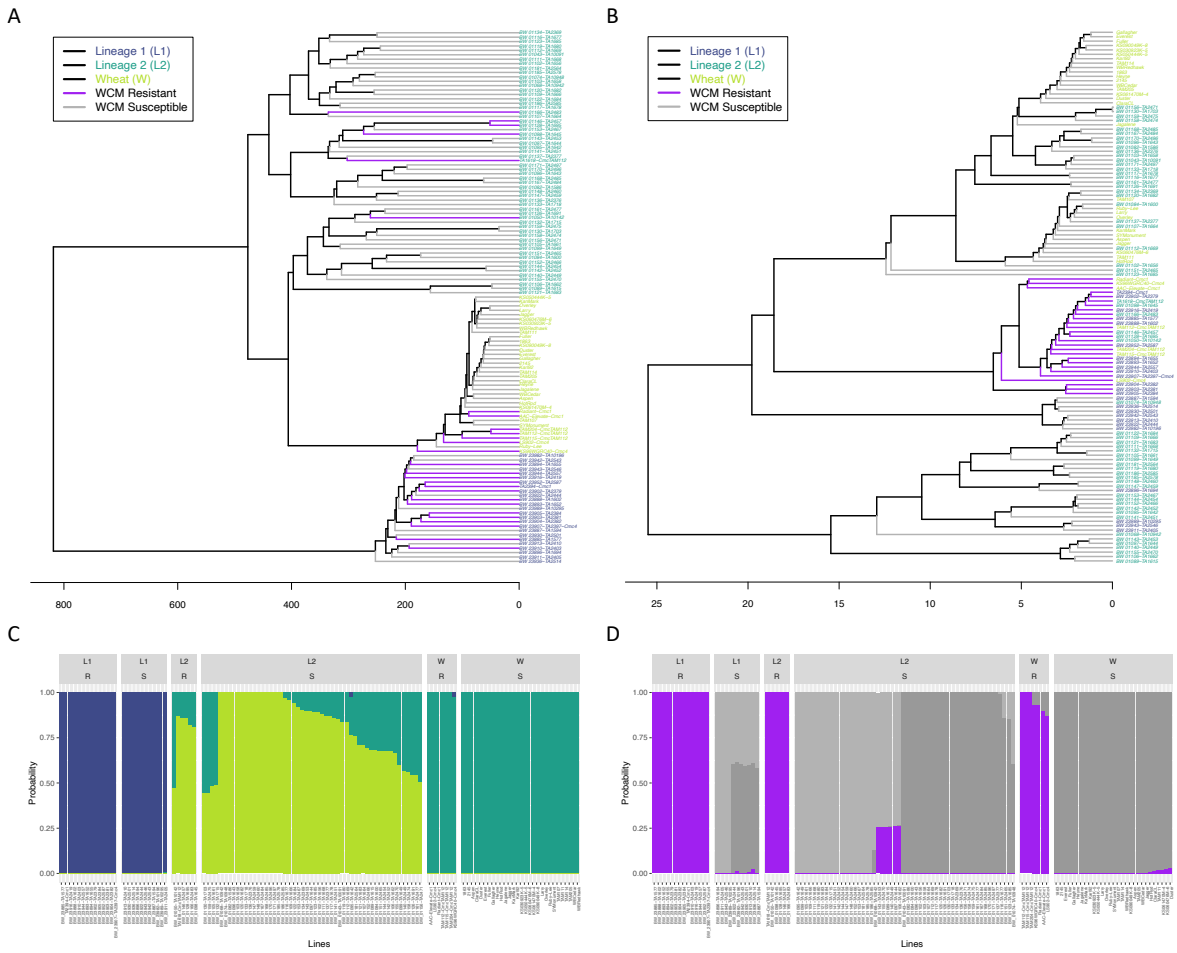

Figure 4.7 – Clustering analyses.

Phylogenetic analysis using Neighbor-joining clustering method showing the relationship between lineage 1 (L1), lineage 2 (L2), and, wheat (W) for A) 947,937 markers on the short arm of chromosome 6D (0 – 230Mbp) and B) 1,002 markers on the identified genomic region associated with resistance at 2.3 – 2.6Mbp on the distal end of chromosome 6DS. Tip labels are colored based on species as follows: blue L1, red L2 and green wheat. Purple branches represent lines that are resistant (R) and grey represents susceptible (S) lines to wheat curl mite (WCM) infestation. ADMIXTURE results for C) short arm of chromosome 6D (0 – 230Mbp) and D) resistance region on the distal end of chromosome 6D (2.3 – 2.6Mbp).

Appendix A - Copyright Information

This appendix contains copyright information for licenses required to republish the content in this dissertation.

Figure 1.1 is taken from Ray et al. (2013) as it is, and figure 1.3 is taken and modified from Savary et al. (2019), and we do not claim any rights on that image. Any requests for modifying and republishing should be directed to the original author.

Except Figure 1.1 and Figure 1.3, all the content in this dissertation is the original research material that has not been published yet, and we reserve the right to publish it first. Permission is required from the original author before using, distributing and reproducing any content from this dissertation, and provided the work is properly credited.

Appendix B - Supplementary Material Chapter 2

This appendix contains supplementary figures and tables for Chapter 2.

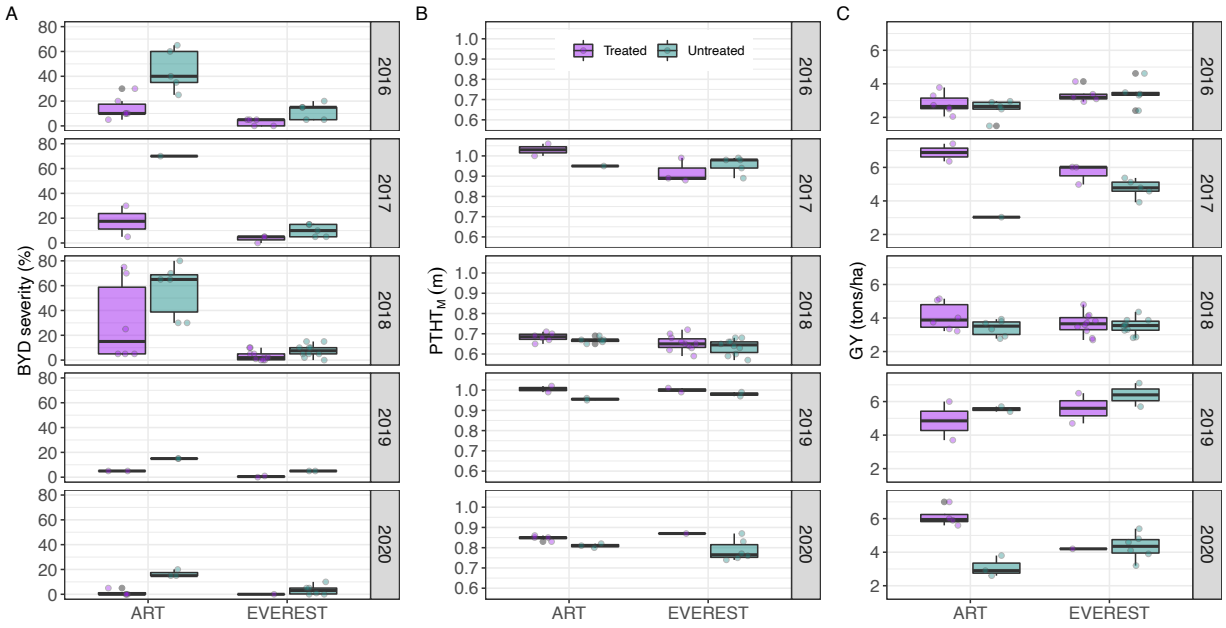

Figure B.1 - Boxplots showing the phenotypic response of the wheat checks 'Art' (susceptible) and 'Everest' (tolerant) for A) barley yellow dwarf (BYD) disease severity (%), B) manual plant height (PTHTM) (m) and C) grain yield (GY) (tons/ha). Adjusted phenotypic values are shown for both insecticide treatment replications (treated and untreated)

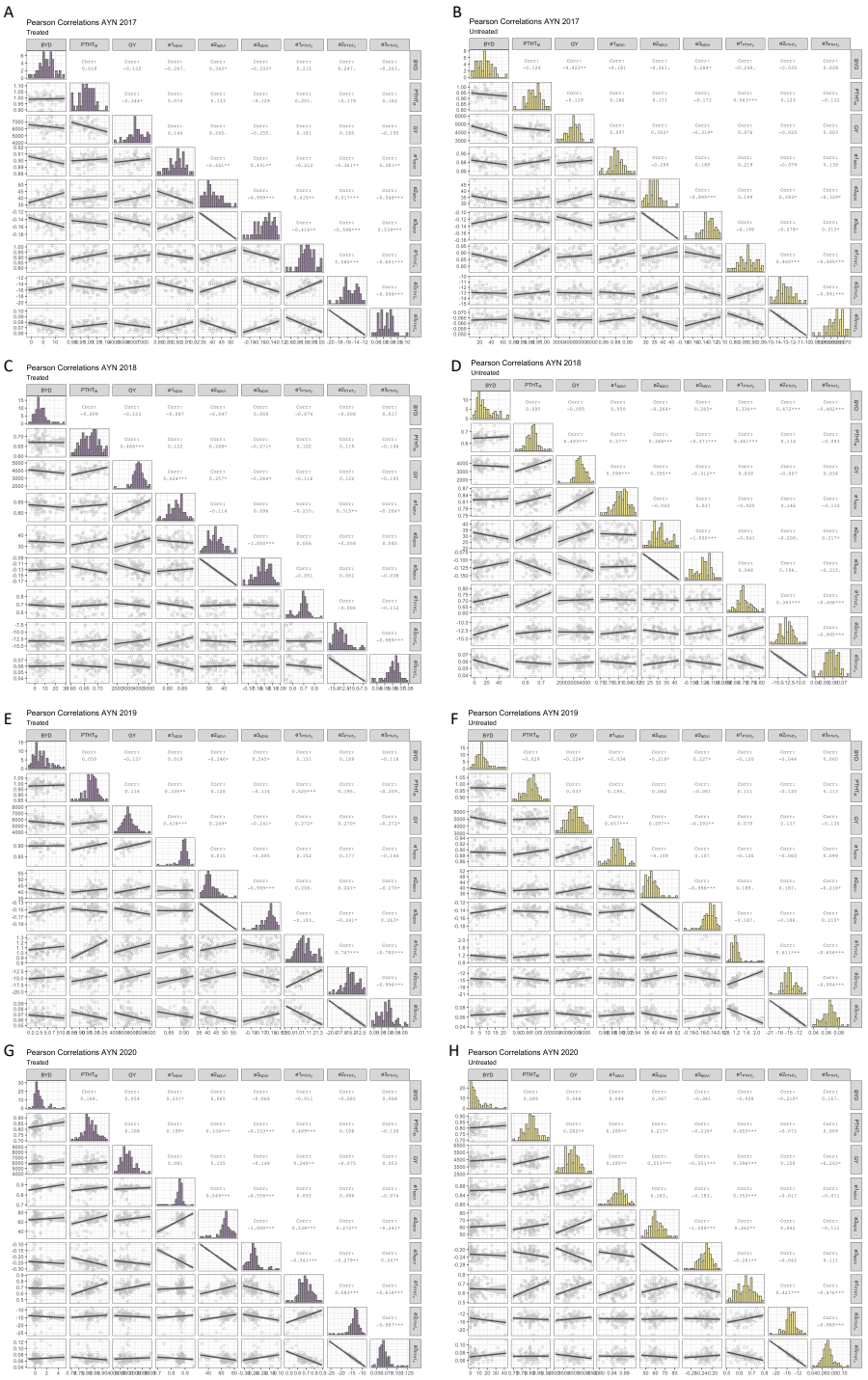

Figure B.2 - Scatterplots showing distribution and Pearson's correlation values for the phenotypic traits studied during all the field seasons under two insecticide treatments (treated and untreated). A-B) season 2016-17, C-D) season 2017-18, E-F) season 2018-19, and G-H) season 2019-20.

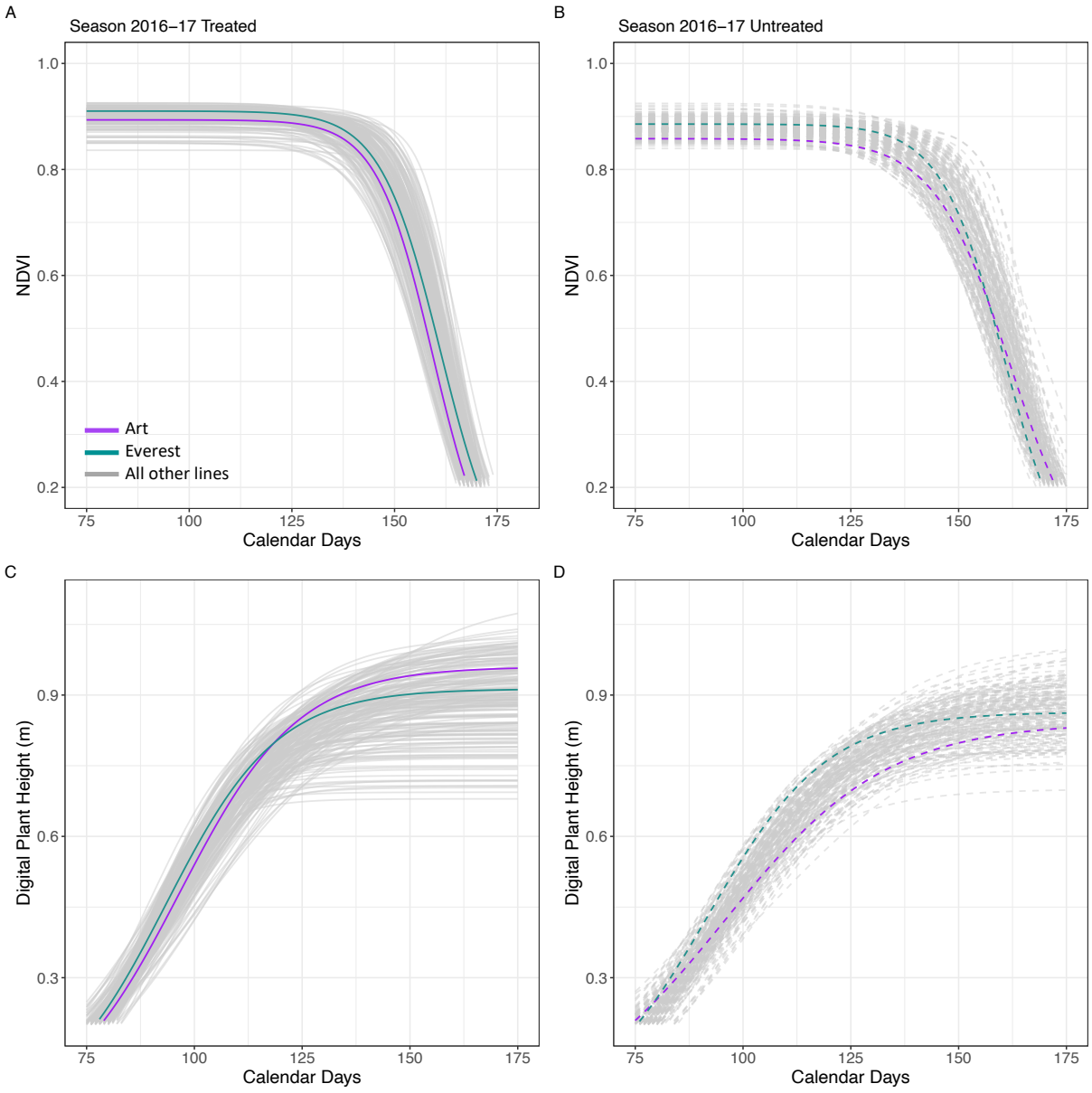

Figure B.3 – Growth trajectories and adjustment of the non-linear regression model of wheat lines for A-B) normalized difference vegetation index (NDVI) and C-D) digital plant height (meters). The data used correspond to season 2016-17 phenotypic data. Calendar days is the number of days starting at January 1, 2017.

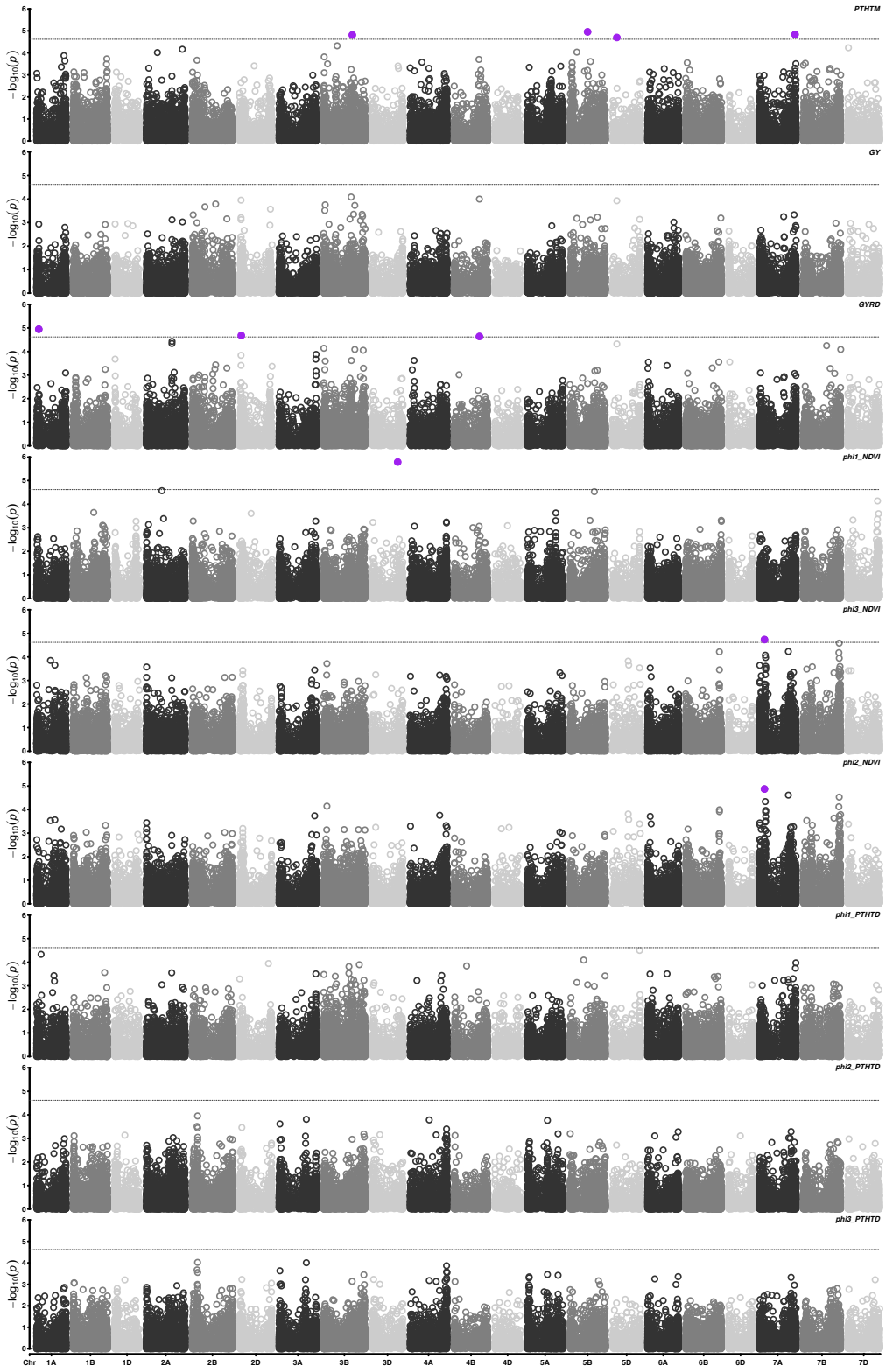

Figure B.4 - Manhattan plots showing genome-wide association analysis (GWAS) results for the phenotypic traits collected during the study.

Table B.1 – List of wheat entries phenotypically evaluated in the study. The table includes the type of entry (cultivar or breeding line), the season that the entry was evaluated, the result for the prediction of the presence/absence of the segment carrying the resistance gene *Bdv2*, and the best linear unbiased predictors (BLUPs) for all the phenotypic traits collected.

				BLUPs									
Entry	Type	Season	*Bdv2*	byd_untrt	ptht.m_untrt	yield_untrt	yield_rd	ndvi_ø1	ndvi_ø2	ndvi_ø3	ptht.d_ø1	ptht.d_ø2	ptht.d_ø3
1863	cultivar	2015-16	FALSE	-1.13	NA	-4.68	-0.98	NA	NA	NA	NA	NA	NA
KanMark	cultivar	2015-16	FALSE	-6.77	NA	-7.92	-14.82	NA	NA	NA	NA	NA	NA
KS080030-M-10	breeding line	2015-16	FALSE	0.79	NA	1.63	5.60	NA	NA	NA	NA	NA	NA
KS080045-M-1	breeding line	2015-16	NA	-1.14	NA	5.93	9.91	NA	NA	NA	NA	NA	NA
KS080051-M-1	breeding line	2015-16	FALSE	0.99	NA	1.87	0.59	NA	NA	NA	NA	NA	NA
KS080076-M-5	breeding line	2015-16	FALSE	-3.13	NA	-0.81	1.86	NA	NA	NA	NA	NA	NA
KS080080-M-14	breeding line	2015-16	FALSE	3.05	NA	0.87	-0.43	NA	NA	NA	NA	NA	NA
KS080080-M-17	breeding line	2015-16	FALSE	1.59	NA	-4.97	-7.78	NA	NA	NA	NA	NA	NA
KS080093-K-18	breeding line	2015-16	FALSE	5.58	NA	-0.52	-9.56	NA	NA	NA	NA	NA	NA

	breeding	2015-	FAL										
KS080093-M-1	line	16	SE	-0.08	NA	-0.74	-0.52	NA	NA	NA	NA	NA	NA
	breeding	2015-	FAL										
KS080093-M-18	line	16	SE	4.58	NA	6.39	6.22	NA	NA	NA	NA	NA	NA
	breeding	2015-	TRU										
KS080099-M-3	line	16	E	-6.77	NA	6.76	8.45	NA	NA	NA	NA	NA	NA
	breeding	2015-	TRU										
KS080099-M-4	line	16	E	-4.23	NA	3.66	1.45	NA	NA	NA	NA	NA	NA
	breeding	2015-	TRU										
KS080099-M-9	line	16	E	-6.25	NA	-5.06	-6.23	NA	NA	NA	NA	NA	NA
	breeding	2015-	FAL										
KS080128-K-3	line	16	SE	-1.92	NA	-0.38	3.00	NA	NA	NA	NA	NA	NA
	breeding	2015-	FAL										
KS080139-K-5	line	16	SE	-0.93	NA	-5.01	-3.87	NA	NA	NA	NA	NA	NA
	breeding	2015-	FAL										
KS080144-M-6	line	16	SE	-0.67	NA	-0.44	3.39	NA	NA	NA	NA	NA	NA
	breeding	2015-											
KS080159-M-1	line	16	NA	2.98	NA	1.75	0.54	NA	NA	NA	NA	NA	NA
	breeding	2015-	FAL										
KS080234-M-11	line	16	SE	2.44	NA	-5.41	0.77	NA	NA	NA	NA	NA	NA
	breeding	2015-	FAL										
KS080261-K-3	line	16	SE	-1.72	NA	1.00	-2.91	NA	NA	NA	NA	NA	NA
	breeding	2015-	FAL										
KS080315-K-5	line	16	SE	3.05	NA	1.04	6.86	NA	NA	NA	NA	NA	NA

	breeding	2015-	FAL										
KS080363-M-1	line	16	SE	4.24	NA	1.47	2.21	NA	NA	NA	NA	NA	NA
	breeding	2015-	FAL										
KS080382-K-8	line	16	SE	1.79	NA	3.41	-2.93	NA	NA	NA	NA	NA	NA
	breeding	2015-	FAL										
KS080382-M-17	line	16	SE	-4.11	NA	-1.00	-7.00	NA	NA	NA	NA	NA	NA
	breeding	2015-	FAL										
KS080426-M-7	line	16	SE	7.63	NA	2.44	9.90	NA	NA	NA	NA	NA	NA
	breeding	2015-	FAL										
KS080448-K-1	line	16	SE	2.86	NA	6.19	1.63	NA	NA	NA	NA	NA	NA
	breeding	2015-	FAL										
KS080554-K-2	line	16	SE	1.26	NA	-1.74	-6.39	NA	NA	NA	NA	NA	NA
	breeding	2015-	FAL										
KS080554-K-4	line	16	SE	0.79	NA	3.95	7.28	NA	NA	NA	NA	NA	NA
	breeding	2015-	FAL										
KS080581-K-1	line	16	SE	-1.92	NA	5.00	4.27	NA	NA	NA	NA	NA	NA
	breeding	2015-	FAL										
KS080597-M-4	line	16	SE	0.53	NA	-1.74	-2.72	NA	NA	NA	NA	NA	NA
	breeding	2015-	FAL										
KS080655-K-2	line	16	SE	-4.06	NA	0.34	1.90	NA	NA	NA	NA	NA	NA
	breeding	2015-	FAL										
KS080655-M-2	line	16	SE	0.52	NA	1.59	5.09	NA	NA	NA	NA	NA	NA
	breeding	2015-	FAL										
KS080655-M-4	line	16	SE	3.44	NA	0.66	-0.53	NA	NA	NA	NA	NA	NA

	breeding	2015-	FAL										
KS080669-K-2	line	16	SE	-0.94	NA	7.87	12.94	NA	NA	NA	NA	NA	NA
	breeding	2015-	FAL										
KS080679-K-3	line	16	SE	-1.72	NA	-3.16	-2.62	NA	NA	NA	NA	NA	NA
	breeding	2015-	FAL				-						
KS080698-M-10	line	16	SE	-2.25	NA	-2.33	11.12	NA	NA	NA	NA	NA	NA
	breeding	2015-	FAL				-						
KS080851-K-1	line	16	SE	2.13	NA	-5.32	10.80	NA	NA	NA	NA	NA	NA
	breeding	2015-	FAL										
KS080881-K-3	line	16	SE	1.05	NA	-0.89	-3.77	NA	NA	NA	NA	NA	NA
	breeding	2015-	FAL										
KS080906-M-3	line	16	SE	-0.99	NA	-4.64	-1.45	NA	NA	NA	NA	NA	NA
	breeding	2015-	FAL										
KS080932-M-3	line	16	SE	-1.79	NA	1.67	15.91	NA	NA	NA	NA	NA	NA
	breeding	2015-	FAL										
KS080942-K-3	line	16	SE	1.53	NA	6.34	7.67	NA	NA	NA	NA	NA	NA
	breeding	2015-	FAL										
KS080988-M-6	line	16	SE	-0.26	NA	-2.32	3.00	NA	NA	NA	NA	NA	NA
	breeding	2015-	FAL										
KS080999-M-4	line	16	SE	-4.64	NA	3.40	2.48	NA	NA	NA	NA	NA	NA
	breeding	2015-	FAL										
KS081057-K-1	line	16	SE	-1.47	NA	-4.00	-7.70	NA	NA	NA	NA	NA	NA
	breeding	2015-	FAL										
KS081067-M-15	line	16	SE	-4.43	NA	8.40	14.95	NA	NA	NA	NA	NA	NA

	breeding	2015-	FAL										
KS081067-M-4	line	16	SE	2.86	NA	0.75	4.55	NA	NA	NA	NA	NA	NA
	breeding	2015-	FAL										
KS081069-M-5	line	16	SE	-3.18	NA	4.87	2.41	NA	NA	NA	NA	NA	NA
	breeding	2015-	FAL				-						
KS081078-M-3	line	16	SE	5.96	NA	-8.03	10.74	NA	NA	NA	NA	NA	NA
	breeding	2015-	FAL										
KS081078-M-6	line	16	SE	-0.46	NA	-0.82	-2.82	NA	NA	NA	NA	NA	NA
	breeding	2015-	FAL										
KS081079-K-6	line	16	SE	-1.87	NA	-3.03	-5.94	NA	NA	NA	NA	NA	NA
	breeding	2015-	FAL										
KS081079-K-9	line	16	SE	-0.93	NA	-0.57	1.05	NA	NA	NA	NA	NA	NA
	breeding	2015-	FAL										
KS081098-K-2	line	16	SE	6.64	NA	-0.71	-2.18	NA	NA	NA	NA	NA	NA
	breeding	2015-	FAL										
KS081098-K-3	line	16	SE	2.45	NA	2.06	3.65	NA	NA	NA	NA	NA	NA
	breeding	2015-	FAL										
KS081098-M-7	line	16	SE	5.03	NA	0.13	2.89	NA	NA	NA	NA	NA	NA
KS10DH0003-	breeding	2015-	FAL										
107	line	16	SE	-3.18	NA	1.66	0.42	NA	NA	NA	NA	NA	NA
KS10DH0003-	breeding	2015-	FAL										
12	line	16	SE	-1.86	NA	1.87	1.46	NA	NA	NA	NA	NA	NA
KS10DH0003-	breeding	2015-	FAL										
89	line	16	SE	-2.65	NA	2.69	7.84	NA	NA	NA	NA	NA	NA

	breeding	2015-	FAL				-						
KS10DH0068-3	line	16	SE	1.52	NA	-11.57	16.35	NA	NA	NA	NA	NA	NA
	breeding	2015-	FAL										
KS10DH0068-9	line	16	SE	-2.52	NA	-8.35	-2.52	NA	NA	NA	NA	NA	NA
	breeding	2015-	FAL										
KS10DH0084-2	line	16	SE	1.71	NA	-2.75	-0.22	NA	NA	NA	NA	NA	NA
KS10DH0084-	breeding	2015-	FAL										
42	line	16	SE	1.91	NA	-4.74	4.10	NA	NA	NA	NA	NA	NA
	breeding	2015-					-						
KS10DH0084-7	line	16	NA	1.78	NA	-7.30	15.94	NA	NA	NA	NA	NA	NA
	breeding	2015-	FAL										
KS10DL0072-15	line	16	SE	4.70	NA	1.06	4.61	NA	NA	NA	NA	NA	NA
KSOCW07S031	breeding	2015-	FAL										
T-K-14	line	16	SE	-2.45	NA	0.62	-4.74	NA	NA	NA	NA	NA	NA
		2015-	FAL										
LCSWizard	cultivar	16	SE	-2.92	NA	8.51	7.25	NA	NA	NA	NA	NA	NA
		2015-											
SYMonument	cultivar	16	NA	1.40	NA	2.30	0.29	NA	NA	NA	NA	NA	NA
										-			-
		2016-	FAL				146.9	6.03E-	6.71E-	2.82E-	6.56E-	3.39E-	2.47E-
HotRod	cultivar	17	SE	-5.61	0.00	139.38	9	04	01	03	03	03	05
								-			-		-
	breeding	2016-	FAL					1.05E-	9.16E-	1.27E-	1.63E-	1.17E-	5.93E-
KS090024K-7	line	17	SE	-3.61	0.01	54.65	66.16	03	02	04	03	02	05

KS090028K-19	breeding line	2016-17	FALSE	-4.17	-0.01	12.69	35.66	-1.23E-04	5.67E-01	-1.98E-03	1.22E-02	1.30E-02	-7.21E-05
KS090028K-25	breeding line	2016-17	FALSE	0.32	0.01	-193.16	-290.51	2.82E-03	-6.30E-01	2.29E-03	2.30E-02	1.97E-02	-1.05E-04
KS090028K-26	breeding line	2016-17	FALSE	-1.92	0.00	105.44	75.84	-3.95E-04	5.05E-01	-2.14E-03	2.17E-02	2.43E-02	-1.33E-04
KS090028K-4	breeding line	2016-17	FALSE	7.38	0.01	103.37	343.78	2.64E-04	-2.49E-01	9.08E-04	3.07E-02	2.34E-02	-1.40E-04
KS090036K-10	breeding line	2016-17	FALSE	-2.79	-0.01	-77.89	61.94	-1.32E-03	-1.99E-01	-7.51E-04	-5.44E-03	-6.99E-03	5.04E-05
KS090041K-1	breeding line	2016-17	FALSE	-10.26	0.01	-52.84	14.78	-2.24E-03	1.49E+00	-5.67E-03	-3.65E-03	-3.76E-03	-1.90E-05
KS090049K-14	breeding line	2016-17	FALSE	-7.50	0.00	35.02	-250.19	-1.85E-03	2.78E+00	-1.02E-02	-1.84E-02	-7.14E-03	-4.82E-05
KS090049K-6	breeding line	2016-17	FALSE	-1.08	0.00	-146.18	-442.80	-1.82E-03	1.28E+00	-4.41E-03	-2.26E-02	-2.35E-02	-1.36E-04

KS090049K-8	breeding line	2016-17	FALSE	7.83	-0.01	27.74	-193.31	-3.39E-04	2.22E+00	-8.24E-03	6.73E-03	-1.61E-02	-8.68E-05
KS090373K-2	breeding line	2016-17	FALSE	-6.88	0.00	-42.94	-273.69	-7.31E-05	-6.25E-01	2.02E-03	1.22E-02	1.05E-02	-5.38E-05
KS090373K-7	breeding line	2016-17	FALSE	-10.57	0.00	-39.22	-243.80	-1.44E-03	7.86E-01	-3.16E-03	1.49E-02	-8.01E-03	-4.22E-05
KS090387K-9	breeding line	2016-17	FALSE	0.30	-0.01	-70.48	-143.27	-5.70E-05	-4.80E-01	-1.61E-03	5.92E-03	-2.55E-03	-1.26E-05
KS090391K-10	breeding line	2016-17	NA	11.55	-0.01	-243.04	-415.82	-6.00E-04	-1.24E+00	-4.59E-03	6.77E-03	-2.23E-02	-1.25E-04
KS090391K-2	breeding line	2016-17	FALSE	10.18	0.00	-109.35	-301.88	-6.70E-04	-4.72E-01	-1.73E-03	-8.34E-03	-1.99E-02	-1.03E-04
KS090391M-2	breeding line	2016-17	FALSE	-3.24	0.00	37.68	-97.84	-2.47E-03	-1.56E+00	-5.70E-03	-6.32E-03	-8.38E-03	-2.84E-05
KS090410M-3	breeding line	2016-17	FALSE	0.23	0.01	-203.05	-325.85	-3.01E-03	-1.77E+00	-6.67E-03	-1.60E-02	-9.93E-03	-4.83E-05

KS090438K-9	breeding line	2016-17	FALSE	7.94	0.00	-202.34	-333.25	1.60E-03	-1.90E+00	7.36E-03	4.88E-03	5.48E-03	1.81E-05
KS090438M-2	breeding line	2016-17	FALSE	-4.95	0.00	-17.02	-14.39	1.21E-03	-4.28E-01	1.71E-03	4.20E-03	3.69E-03	2.02E-05
KS090485K-11	breeding line	2016-17	FALSE	3.77	-0.01	-36.69	-295.95	1.42E-03	-9.46E-01	3.62E-03	2.67E-02	1.35E-02	9.16E-05
KS090501K-12	breeding line	2016-17	FALSE	0.77	0.00	-19.10	46.23	1.38E-03	-5.42E-01	2.00E-03	3.01E-03	2.99E-03	9.61E-07
KS090529K-1	breeding line	2016-17	NA	-2.35	0.00	-53.78	16.77	1.63E-03	-9.12E-01	3.14E-03	7.09E-03	9.71E-03	3.32E-05
KS090529K-18	breeding line	2016-17	FALSE	0.08	0.00	1.41	81.88	6.70E-04	-6.79E-01	2.50E-03	5.57E-03	2.46E-02	1.14E-04
KS090616K-1	breeding line	2016-17	FALSE	4.32	0.01	-62.66	-328.05	1.73E-03	-1.32E-01	2.06E-04	6.01E-03	4.11E-04	9.85E-06
KS090616K-4	breeding line	2016-17	FALSE	0.55	0.01	205.23	478.09	1.78E-03	2.86E+00	1.08E-02	1.38E-03	1.46E-03	1.16E-05

KS090633K-11	breeding line	2016-17	FALSE	0.72	0.01	-42.25	170.95	-1.39E-03	-5.09E-01	2.05E-03	1.48E-02	-4.16E-03	5.70E-06
KS090633K-7	breeding line	2016-17	FALSE	-8.39	0.01	173.11	627.95	-4.63E-05	3.75E+00	-1.38E-02	-5.19E-03	-2.22E-03	9.21E-06
KS090710K-1	breeding line	2016-17	FALSE	-1.04	0.00	41.73	35.29	-3.28E-03	-5.15E-01	-1.76E-03	-1.35E-02	-2.30E-02	-1.08E-04
KS12DH0013-37	breeding line	2016-17	FALSE	3.02	0.01	90.87	412.58	-1.12E-03	-1.10E+00	-4.04E-03	-9.24E-03	-1.67E-02	-7.25E-05
KS12DH0023-118	breeding line	2016-17	FALSE	7.55	-0.01	-65.12	265.43	-9.39E-04	1.23E+00	-4.53E-03	-1.23E-03	-8.46E-03	-3.55E-05
KS12DH0090-36	breeding line	2016-17	FALSE	3.39	0.00	57.66	217.78	-2.70E-03	-5.38E-01	-2.05E-03	-6.83E-03	-1.46E-02	-6.77E-05
KS12DH0090-83	breeding line	2016-17	FALSE	9.68	-0.01	-55.86	156.20	-4.46E-03	-1.93E+00	-7.22E-03	-2.40E-02	-1.09E-02	-4.51E-05
KS12DH0156-4	breeding line	2016-17	FALSE	2.18	-0.02	-130.22	484.75	-1.04E-03	-2.44E+00	-8.65E-03	-2.15E-02	-4.23E-03	-3.13E-05

KS12DH0214-65	breeding line	2016-17	FALSE	-4.40	0.01	107.08	169.66	7.97E-03	-1.25E+00	4.97E-03	-2.59E-03	2.74E-02	1.61E-04
KS12DH0214-95	breeding line	2016-17	FALSE	8.07	-0.01	105.36	227.14	3.20E-03	-6.97E-01	2.72E-03	-1.10E-03	7.96E-04	-1.27E-05
KS12DH0229-51	breeding line	2016-17	FALSE	5.19	0.00	-93.65	-90.29	-1.51E-03	-1.55E+00	5.37E-03	-1.41E-02	9.78E-03	-4.19E-05
KS12DH0229-99	breeding line	2016-17	FALSE	3.58	0.00	-79.13	-372.48	-8.56E-04	-2.35E+00	8.64E-03	-2.74E-02	3.32E-03	-2.18E-05
KS12DH0230-30	breeding line	2016-17	FALSE	0.26	0.02	68.42	121.45	3.30E-03	-2.00E+00	7.50E-03	-4.72E-03	2.10E-02	-1.07E-04
KS12DH0296-156	breeding line	2016-17	FALSE	-5.17	0.01	442.06	628.12	3.45E-03	-1.18E+00	4.52E-03	-1.05E-02	1.96E-02	-1.03E-04
KS12DH0296-159	breeding line	2016-17	FALSE	-6.97	0.00	0.46	36.92	-5.02E-04	-2.68E+00	9.70E-03	-7.73E-03	7.89E-03	-2.99E-05
KS12DH0296-43	breeding line	2016-17	FALSE	-11.36	0.00	132.79	365.38	5.85E-04	-1.06E+00	3.98E-03	-6.62E-03	4.86E-03	-1.98E-05

KS12DH0296-47	breeding line	2016-17	FALSE	-7.75	0.00	65.29	-153.33	1.50E-03	-7.61E-01	2.68E-03	1.73E-02	2.76E-02	-1.29E-04
KS12DH0296-48	breeding line	2016-17	FALSE	-7.03	0.00	59.37	-119.52	7.27E-04	8.04E-01	3.43E-03	4.69E-03	2.76E-02	1.32E-04
KS12DH0298-57	breeding line	2016-17	FALSE	10.29	-0.01	-40.16	407.67	-4.17E-03	-7.94E-01	3.41E-03	1.56E-02	4.24E-02	-2.18E-04
LCSPistol	cultivar	2016-17	NA	-1.61	0.00	175.22	-328.43	6.17E-04	1.62E+00	-6.15E-03	1.17E-02	2.81E-02	-1.41E-04
SYWolf	cultivar	2016-17	NA	1.83	0.00	-76.29	78.14	-2.32E-03	6.97E-04	8.13E-06	8.45E-03	5.40E-03	-2.61E-05
T158	cultivar	2016-17	FALSE	2.13	0.01	281.82	-572.84	1.60E-03	-7.24E-03	1.64E-04	2.19E-02	2.94E-02	-1.45E-04
WB4458	cultivar	2016-17	FALSE	1.47	-0.01	-37.77	200.61	-5.34E-03	1.27E+00	-4.84E-03	1.18E-02	-4.60E-03	-3.58E-05
WBCedar	cultivar	2016-17	NA	-6.32	-0.01	-94.69	289.60	-2.21E-03	-3.74E-02	3.25E-05	6.44E-03	2.29E-03	1.83E-05

KS120004M~8	breeding line	2017-18	FALSE	-1.21	0.00	13.25	29.15	7.40E-07	-1.65E-05	1.30E-03	2.26E-10	3.52E-11	2.93E-14
KS120029M~3	breeding line	2017-18	FALSE	0.67	0.00	-27.31	43.59	6.05E-08	-2.16E-07	6.36E-05	7.77E-11	4.43E-10	3.51E-12
KS120069M~2	breeding line	2017-18	FALSE	-3.73	0.00	36.25	33.60	3.06E-06	-5.92E-05	4.59E-04	5.67E-10	3.54E-10	4.07E-12
KS120081M~5	breeding line	2017-18	FALSE	-0.05	0.00	49.49	62.94	2.69E-03	1.64E-09	3.87E-11	7.64E-11	2.41E-02	3.41E-04
KS120126M~6	breeding line	2017-18	FALSE	-2.16	0.00	24.34	28.26	3.53E-07	8.28E-06	5.46E-04	2.66E-10	2.38E-11	6.37E-13
KS120148M~4	breeding line	2017-18	FALSE	-2.14	0.00	-8.59	2.46	9.91E-07	-2.08E-05	3.54E-05	3.04E-10	8.01E-11	1.31E-12
KS120148M~5	breeding line	2017-18	FALSE	4.78	0.00	-33.65	48.49	1.77E-06	-3.96E-05	3.14E-04	1.53E-10	9.07E-11	1.07E-12
KS120148M~7	breeding line	2017-18	FALSE	-2.14	0.00	-27.49	35.81	4.98E-07	-5.76E-06	2.13E-04	1.84E-10	8.63E-12	8.40E-14

KS120246M~3	breeding line	2017-18	FALSE	2.65	0.00	14.74	-2.21	5.86E-07	-1.01E-05	1.79E-03	1.39E-10	8.13E-10	7.30E-12
KS120252M~10	breeding line	2017-18	FALSE	8.24	0.00	17.25	22.03	9.95E-07	2.18E-05	9.98E-04	1.96E-10	9.90E-11	9.31E-13
KS120252M~14	breeding line	2017-18	FALSE	0.27	0.00	6.48	-4.16	4.60E-04	-2.26E-09	1.18E-11	9.70E-11	3.47E-01	1.72E-03
KS120269M~5	breeding line	2017-18	FALSE	6.29	0.00	7.79	10.91	9.37E-08	-1.53E-06	4.46E-04	4.81E-10	2.26E-10	3.77E-12
KS120297M~11	breeding line	2017-18	FALSE	3.46	0.00	8.97	-8.17	9.67E-07	1.97E-05	1.13E-03	1.25E-10	8.07E-10	7.30E-12
KS120300M~3	breeding line	2017-18	FALSE	11.15	0.00	-2.98	31.99	5.63E-07	-9.87E-06	1.11E-05	7.53E-11	9.44E-10	7.33E-12
KS120302M~1	breeding line	2017-18	FALSE	0.61	0.00	-0.38	8.30	8.60E-07	1.63E-05	6.81E-04	5.68E-11	1.12E-10	3.55E-13
KS120302M~7	breeding line	2017-18	FALSE	7.16	0.00	36.49	48.73	7.40E-07	-1.61E-05	2.01E-03	9.05E-10	2.16E-10	2.15E-12

KS120331M~17	breeding line	2017-18	FALSE	-1.77	0.00	33.07	77.88	1.56E-06	-2.53E-05	-1.97E-03	2.92E-10	2.89E-10	-1.84E-12
KS120332M~11	breeding line	2017-18	FALSE	5.39	0.00	-14.60	-21.13	7.82E-07	-1.64E-05	-4.69E-04	1.22E-11	2.53E-10	-3.41E-12
KS120332M~2	breeding line	2017-18	FALSE	0.70	0.00	35.27	32.94	3.11E-07	-1.19E-05	-1.57E-03	6.95E-10	3.81E-10	-2.76E-12
KS120332M~3	breeding line	2017-18	NA	-0.82	0.00	2.95	-14.23	9.08E-07	-1.57E-05	-3.57E-04	-1.64E-10	-7.75E-10	-6.75E-12
KS120380M~1	breeding line	2017-18	FALSE	-1.57	0.00	49.90	-11.78	-8.40E-07	1.74E-05	-5.71E-04	-3.91E-10	-1.55E-10	-9.80E-13
KS120414M~1	breeding line	2017-18	FALSE	0.07	0.00	22.46	37.22	2.67E-06	-5.08E-05	-4.41E-04	-9.78E-11	-7.82E-10	-6.39E-12
KS120414M~8	breeding line	2017-18	FALSE	-0.75	0.00	-40.90	-11.39	-7.32E-08	2.29E-06	-6.27E-04	-1.57E-10	-8.57E-10	-6.78E-12
KS120428M~1	breeding line	2017-18	TRUE	-5.44	0.00	29.40	90.39	-1.45E-07	-5.62E-06	-1.28E-03	-1.79E-10	-8.53E-10	-7.81E-12

KS120428M~2	breeding line	2017-18	TRUE	-2.77	0.00	-23.84	-21.79	1.85E-06	-3.65E-05	-7.75E-04	1.88E-10	-8.55E-10	-7.90E-12
KS120428M~4	breeding line	2017-18	TRUE	-3.45	0.00	-23.31	-29.08	8.86E-07	-1.71E-05	-6.18E-04	1.46E-10	-7.27E-11	-6.97E-14
KS120428M~5	breeding line	2017-18	TRUE	-4.27	0.00	13.54	-89.67	-1.45E-07	-6.33E-06	-1.02E-03	6.36E-10	-5.11E-10	-5.11E-12
KS120428M~6	breeding line	2017-18	TRUE	-4.70	0.00	31.12	-109.24	2.91E-06	-6.05E-05	-5.57E-04	3.27E-10	-7.89E-10	-7.67E-12
KS120428M~7	breeding line	2017-18	TRUE	-5.84	0.00	0.22	-4.40	-2.27E-07	-6.64E-07	-6.07E-04	3.59E-10	-2.37E-10	-1.59E-12
KS120435M~1	breeding line	2017-18	TRUE	-3.19	0.00	-24.73	-30.97	-4.47E-07	-9.98E-06	-8.05E-04	6.92E-10	-1.80E-10	-3.78E-13
KS120435M~3	breeding line	2017-18	NA	-2.92	0.00	14.79	-58.30	-8.47E-07	-1.15E-05	-4.23E-04	-7.55E-10	-1.87E-10	-1.09E-12
KS120435M~4	breeding line	2017-18	TRUE	1.65	0.00	29.99	-82.83	-1.49E-07	-4.64E-06	-6.83E-05	2.91E-10	-3.20E-10	-3.39E-12

KS120461M~5	breeding line	2017-18	FALSE	-1.34	0.00	-24.17	62.90	-1.02E-06	2.12E-05	6.41E-04	-3.79E-10	2.10E-10	-1.58E-12
KS120487M~1	breeding line	2017-18	TRUE	-5.29	0.00	33.94	57.46	2.48E-06	-4.83E-05	1.19E-03	-9.34E-11	-8.75E-10	-7.66E-12
KS120487M~10	breeding line	2017-18	TRUE	-3.26	0.00	-17.99	-20.01	-3.19E-07	4.10E-07	6.59E-04	-8.03E-11	5.34E-11	-7.44E-14
KS120487M~2	breeding line	2017-18	TRUE	-3.99	0.00	-49.70	-58.06	-2.32E-06	4.46E-05	1.53E-04	-2.33E-10	-9.41E-10	-7.38E-12
KS120487M~3	breeding line	2017-18	TRUE	-3.97	0.00	1.29	3.35	-5.15E-07	1.48E-05	-9.08E-05	-1.11E-09	3.72E-10	-4.35E-12
KS120487M~4	breeding line	2017-18	TRUE	-1.77	0.00	-49.57	-80.97	-1.59E-06	2.73E-05	2.00E-03	-2.33E-11	-6.28E-10	-6.27E-12
KS120487M~5	breeding line	2017-18	TRUE	-4.23	0.00	-7.50	9.13	-5.10E-07	-9.21E-06	-8.64E-04	-3.30E-10	-7.37E-10	-7.58E-12
KS120487M~7	breeding line	2017-18	TRUE	-4.98	0.00	-20.94	-8.44	-1.92E-06	3.14E-05	-5.52E-04	-3.71E-10	-3.66E-11	-1.15E-12

KS120487M~9	breeding line	2017-18	TRUE	2.56	0.00	-34.75	37.59	-1.66E-06	-3.23E-05	-8.34E-04	-1.80E-10	-1.76E-10	-2.76E-12
KS120493M~3	breeding line	2017-18	TRUE	-5.11	0.00	31.69	16.45	-2.62E-06	-5.14E-05	-2.89E-04	-1.02E-09	-7.11E-10	-6.23E-12
KS120493M~5	breeding line	2017-18	NA	0.25	0.00	13.42	20.96	3.26E-03	-2.51E-10	-1.24E-11	-1.02E-10	-7.10E-02	-4.60E-04
KS120494M~1	breeding line	2017-18	TRUE	-5.07	0.00	41.96	46.01	-1.09E-08	-6.88E-07	-4.52E-04	-9.69E-11	-9.33E-10	-8.57E-12
KS120494M~10	breeding line	2017-18	TRUE	-4.68	0.00	30.76	8.24	-1.15E-06	-2.67E-05	-1.53E-04	-5.36E-10	-7.64E-10	-7.96E-12
KS120494M~11	breeding line	2017-18	TRUE	-4.22	0.00	27.22	39.39	-9.15E-07	-1.35E-05	-1.44E-03	-8.00E-10	-2.98E-10	-3.08E-12
KS120494M~3	breeding line	2017-18	TRUE	-6.54	0.00	-10.14	20.48	-6.91E-07	-9.12E-06	-1.10E-03	-1.00E-10	-7.21E-10	-5.47E-12
KS120494M~5	breeding line	2017-18	TRUE	-4.39	0.00	33.08	2.01	-1.10E-06	-2.11E-05	-7.45E-04	-3.78E-10	-1.00E-09	-9.03E-12

KS120494M~6	breeding line	2017-18	TRUE	-2.57	0.00	-36.45	22.24	-3.23E-06	5.85E-05	-3.34E-04	2.07E-10	8.73E-10	7.92E-12
KS120494M~7	breeding line	2017-18	TRUE	-6.41	0.00	12.82	24.46	-1.50E-06	-3.09E-05	-4.89E-04	9.47E-10	1.32E-09	1.37E-11
KS120494M~9	breeding line	2017-18	TRUE	-5.07	0.00	56.27	89.72	1.41E-06	-2.46E-05	-6.59E-05	5.05E-10	8.79E-10	8.66E-12
KS120554M~5	breeding line	2017-18	FALSE	-0.31	0.00	4.41	11.39	-1.78E-06	-3.46E-05	-1.89E-04	5.30E-10	-3.63E-10	-3.88E-12
KS120554M~7	breeding line	2017-18	FALSE	-5.16	0.00	-29.66	51.60	-1.54E-06	-3.06E-05	-5.48E-04	4.41E-11	6.38E-10	6.54E-12
KS120557M~10	breeding line	2017-18	FALSE	0.25	0.00	-30.85	30.81	-2.40E-03	-1.01E-08	-6.98E-11	2.37E-10	-8.49E-01	-3.88E-03
KS120557M~2	breeding line	2017-18	FALSE	5.63	0.00	-34.76	62.28	-3.76E-07	-1.01E-06	-1.14E-03	2.24E-10	5.30E-11	6.51E-13
KS120557M~5	breeding line	2017-18	FALSE	2.38	0.00	-1.69	14.40	-2.06E-07	-1.16E-05	-1.70E-03	4.23E-10	2.51E-10	2.34E-12

KS120557M~6	breeding line	2017-18	FALSE	-0.94	0.00	35.25	63.14	3.16E-06	-6.16E-05	1.09E-03	3.05E-10	1.33E-10	5.14E-13
KS120558M~1	breeding line	2017-18	FALSE	-2.47	0.00	25.42	15.75	5.20E-07	1.08E-05	3.43E-04	3.30E-10	1.35E-09	1.31E-11
KS120559M~1	breeding line	2017-18	FALSE	-3.47	0.00	23.66	59.41	2.84E-06	-5.19E-05	2.02E-04	5.62E-11	2.43E-10	2.74E-12
KS120580M~6	breeding line	2017-18	FALSE	0.59	0.00	-1.43	-15.29	1.55E-06	3.48E-05	2.01E-03	9.14E-10	8.40E-10	7.68E-12
KS120580M~7	breeding line	2017-18	FALSE	-3.23	0.00	59.69	106.80	2.31E-06	-5.31E-05	1.61E-03	1.02E-09	2.64E-10	2.54E-12
KS120592M~1	breeding line	2017-18	FALSE	5.78	0.00	10.32	38.28	1.15E-07	-8.10E-07	1.59E-03	1.32E-09	3.89E-10	4.47E-12
KS120592M~4	breeding line	2017-18	FALSE	11.40	0.00	4.20	22.26	4.14E-07	3.94E-06	1.59E-03	5.62E-10	7.43E-10	6.52E-12
KS120612M~4	breeding line	2017-18	FALSE	7.13	0.00	11.30	42.95	5.87E-07	1.70E-05	1.89E-03	3.32E-11	4.48E-10	4.00E-12

KS120642M~11	breeding line	2017-18	FALSE	0.03	0.00	-25.21	-3.49	1.49E-07	-4.25E-06	4.21E-04	7.32E-10	5.16E-10	5.90E-12
KS120642M~12	breeding line	2017-18	FALSE	0.25	0.00	-13.61	18.90	-1.86E-06	3.63E-05	8.57E-04	9.54E-10	8.63E-10	8.35E-12
KS120643M~9	breeding line	2017-18	FALSE	1.43	0.00	27.35	38.94	2.59E-06	-5.22E-05	1.05E-03	3.35E-11	5.38E-10	4.76E-12
KS120646M~5	breeding line	2017-18	FALSE	15.79	0.00	-20.74	61.23	-1.18E-06	2.10E-05	4.07E-04	5.76E-10	1.49E-09	1.38E-11
KS120646M~6	breeding line	2017-18	FALSE	-3.33	0.00	-52.87	76.08	-3.27E-06	6.14E-05	8.57E-04	1.65E-10	7.77E-10	6.75E-12
KS120717M~11	breeding line	2017-18	TRUE	-6.16	0.00	-12.50	60.95	-1.34E-06	3.02E-05	3.77E-04	2.45E-11	5.51E-10	5.11E-12
KS120741M~1	breeding line	2017-18	TRUE	-2.61	0.00	-1.55	8.43	8.37E-07	-9.75E-06	6.07E-04	2.29E-10	4.65E-10	3.88E-12
KS120741M~3	breeding line	2017-18	TRUE	-4.30	0.00	-73.54	37.55	2.63E-06	-5.09E-05	1.06E-04	1.81E-10	7.61E-10	5.69E-12

KS120749M~3	breeding line	2017-18	FALSE	3.73	0.00	-20.80	-52.05	-1.46E-06	-2.80E-05	-8.64E-05	-1.03E-09	-6.18E-10	-3.77E-12
KS120794M~7	breeding line	2017-18	FALSE	0.45	0.00	-12.34	-23.30	-1.58E-03	3.35E-09	-1.25E-10	-6.23E-11	-2.45E-01	-1.22E-03
KS120802M~11	breeding line	2017-18	FALSE	10.11	0.00	3.99	5.16	-9.89E-07	-2.00E-05	-1.20E-03	-1.45E-09	-1.79E-09	-1.92E-11
KS120843M~3	breeding line	2017-18	FALSE	4.78	0.00	-30.15	-62.73	-3.08E-06	-5.86E-05	-2.52E-05	-9.21E-13	-1.19E-09	-9.78E-12
KS120905M~6	breeding line	2017-18	FALSE	9.01	0.00	-0.96	-27.36	-3.28E-06	-6.38E-05	-6.43E-04	-9.96E-10	-1.31E-09	-1.46E-11
KS120911M~2	breeding line	2017-18	FALSE	0.08	0.00	-45.37	-128.58	-9.10E-07	-1.45E-05	-1.80E-04	-9.12E-11	-5.33E-11	-4.20E-13
KS120914M~13	breeding line	2017-18	FALSE	0.70	0.00	11.34	6.66	-2.05E-06	-3.42E-05	-1.57E-04	-3.65E-10	-1.56E-10	-1.44E-12
18CP010011	cultivar	2018-19	NA	0.70	0.00	-17.50	-22.82	-2.11E-04	8.42E-09	-3.47E-11	-5.73E-12	-1.65E-01	-9.13E-04

18CP010302	cultivar	2018-19	NA	-0.90	0.00	2.23	-33.83	-2.56E-03	-5.99E-09	-1.11E-11	-4.22E-12	-3.00E-01	1.17E-03
18CP010312	cultivar	2018-19	NA	-1.29	0.00	0.37	-9.98	-2.45E-05	-1.66E-08	-7.62E-12	-3.20E-11	-1.40E-01	5.44E-04
18PE500000	cultivar	2018-19	NA	-0.06	0.00	35.17	19.02	-7.52E-04	-2.02E-08	-3.41E-12	-8.40E-11	-1.99E-01	9.00E-04
18PE500002	cultivar	2018-19	NA	-0.42	0.00	-0.54	-65.58	-2.06E-03	-5.73E-09	-4.01E-11	-2.93E-12	-2.08E-02	6.83E-05
BobDole	cultivar	2018-19	FALSE	0.39	0.00	-5.32	-3.81	-3.47E-04	-2.54E-09	-2.79E-12	-5.88E-11	-1.86E-01	1.06E-03
Jagger	cultivar	2018-19	FALSE	1.46	0.00	-10.17	17.15	-1.04E-04	-7.24E-09	-6.28E-11	-1.04E-10	-1.17E-01	7.14E-04
KS05HW14	breeding line	2018-19	FALSE	0.00	0.00	2.44	16.31	-5.64E-05	-2.06E-09	-8.29E-11	-4.65E-11	-2.02E-01	-8.61E-04
KS100028K-10	breeding line	2018-19	FALSE	-0.06	0.00	10.08	-25.84	-8.98E-04	-1.22E-09	-5.01E-11	-6.21E-10	-2.70E-01	-1.59E-03

KS100028K-11	breeding line	2018-19	FALSE	0.39	0.00	28.17	27.81	8.48E-04	1.11E-08	-2.66E-11	-8.10E-11	-3.03E-01	-1.45E-03
KS100060K-15	breeding line	2018-19	FALSE	-0.55	0.00	41.81	44.28	-8.28E-04	-1.71E-08	-5.42E-11	-1.20E-11	-1.01E-01	-3.26E-04
KS100060K-19	breeding line	2018-19	FALSE	-0.80	0.00	21.83	33.14	-1.63E-03	-1.59E-08	-4.09E-11	-3.39E-11	-9.27E-02	-4.10E-04
KS100196K-2	breeding line	2018-19	FALSE	2.42	0.00	-35.86	-57.94	-2.05E-03	-8.34E-09	-1.66E-10	-1.77E-10	-4.39E-01	-2.16E-03
KS100653K-7	breeding line	2018-19	FALSE	-0.42	0.00	-23.93	-33.48	-1.54E-03	-5.79E-09	-5.02E-11	-2.42E-11	-6.66E-02	-4.09E-04
KS120008M~4	breeding line	2018-19	FALSE	-0.06	0.00	-4.67	17.15	-1.92E-03	-4.96E-10	-1.60E-12	-5.05E-11	-2.47E-01	-1.23E-03
KS120081M~1	breeding line	2018-19	FALSE	0.42	0.00	-14.69	-9.49	-8.52E-04	-8.42E-09	-6.52E-11	-2.11E-11	-1.69E-02	-3.20E-04
KS120125M~1	breeding line	2018-19	FALSE	-0.05	0.00	1.96	-9.01	-3.34E-04	-7.90E-09	-3.33E-11	-5.59E-11	-2.08E-01	-9.63E-04

KS120125M~10	breeding line	2018-19	FALSE	-0.20	0.00	52.39	129.07	1.80E-03	1.71E-08	-6.38E-12	-6.02E-11	4.39E-02	-6.65E-05
KS120125M~5	breeding line	2018-19	FALSE	-0.42	0.00	43.81	81.10	2.13E-04	8.47E-09	9.94E-12	-5.66E-11	1.40E-01	-6.06E-04
KS120125M~9	breeding line	2018-19	FALSE	-0.17	0.00	13.69	38.47	-1.40E-04	1.34E-08	2.34E-11	-2.99E-11	2.26E-04	4.13E-05
KS120129M~4	breeding line	2018-19	FALSE	-0.05	0.00	8.88	-11.67	1.88E-06	-5.13E-09	2.35E-11	-4.76E-11	-2.83E-02	1.57E-04
KS120129M~5	breeding line	2018-19	FALSE	-0.20	0.00	-11.41	-57.81	7.59E-04	-1.38E-08	-8.10E-11	1.32E-11	-7.55E-02	3.67E-04
KS120129M~8	breeding line	2018-19	FALSE	-0.20	0.00	-32.56	-44.13	7.35E-04	-1.05E-08	6.03E-11	3.78E-11	-9.18E-02	3.55E-04
KS120149M~13	breeding line	2018-19	FALSE	0.11	0.00	-16.11	-6.83	-1.13E-04	-1.70E-09	-1.07E-10	-5.93E-11	3.03E-01	-1.43E-03
KS120149M~9	breeding line	2018-19	FALSE	-0.45	0.00	10.82	54.94	-4.01E-03	1.35E-08	2.90E-11	4.88E-11	2.49E-01	-1.20E-03

KS120215M~7	breeding line	2018-19	FALSE	-0.72	0.00	-45.28	-64.97	-4.00E-03	-8.49E-09	2.27E-11	-1.25E-10	-2.38E-01	-1.12E-03
KS120215M~8	breeding line	2018-19	FALSE	-0.11	0.00	-3.90	-6.47	2.50E-03	5.46E-09	9.50E-11	-4.60E-11	-1.03E-01	4.80E-04
KS120252M~7	breeding line	2018-19	FALSE	-0.20	0.00	2.11	6.49	2.10E-03	-6.80E-10	-4.49E-12	-7.04E-11	-4.95E-02	-3.97E-04
KS120269M~4	breeding line	2018-19	FALSE	-0.44	0.00	-8.09	-38.80	-1.51E-03	-9.88E-10	-1.94E-10	-6.05E-11	-5.12E-02	-1.72E-04
KS120282M~2	breeding line	2018-19	FALSE	-0.17	0.00	-8.90	6.49	4.06E-05	4.30E-09	5.72E-11	-4.85E-11	-4.49E-02	2.14E-04
KS120296M~1	breeding line	2018-19	FALSE	-0.06	0.00	-12.92	0.81	-3.95E-04	1.94E-09	5.57E-11	-7.93E-11	-4.22E-01	2.32E-03
KS120300M~2	breeding line	2018-19	FALSE	0.39	0.00	37.93	121.07	1.48E-03	-4.20E-10	6.18E-12	-3.35E-11	-2.79E-01	-1.16E-03
KS120300M~5	breeding line	2018-19	FALSE	0.07	0.00	8.41	42.18	-1.88E-03	-1.52E-09	-2.89E-11	-2.89E-11	-5.03E-02	1.95E-04

KS120332M~1	breeding line	2018-19	FALSE	0.00	0.00	-35.57	-49.95	-7.83E-04	-1.28E-10	-5.76E-11	-7.86E-11	-3.47E-02	-1.40E-04
KS120353M~1	breeding line	2018-19	FALSE	-0.34	0.00	-47.31	-68.12	-1.54E-03	-3.28E-09	-9.11E-11	-9.82E-11	-2.38E-01	-1.09E-03
KS120380M~3	breeding line	2018-19	FALSE	-0.13	0.00	-51.16	-148.05	-8.44E-04	-6.11E-09	-1.66E-11	-1.16E-11	-1.32E-01	-5.86E-04
KS120494M~8	breeding line	2018-19	TRUE	-0.93	0.00	16.06	18.46	-2.05E-03	-1.73E-08	-1.65E-11	-2.73E-11	-3.66E-02	-2.26E-04
KS120506M~7	breeding line	2018-19	FALSE	0.54	0.00	-43.40	-62.30	-1.92E-03	-1.25E-08	-4.41E-12	-1.25E-10	-4.44E-01	-2.06E-03
KS120510M~1	breeding line	2018-19	FALSE	-0.45	0.00	28.94	4.18	-2.60E-03	-1.08E-08	-3.33E-11	-3.32E-11	-7.06E-03	-3.54E-05
KS120510M~2	breeding line	2018-19	FALSE	-0.84	0.00	48.36	89.10	-1.41E-03	-1.46E-08	-4.13E-13	-1.40E-10	-3.97E-01	-1.92E-03
KS120511M~16	breeding line	2018-19	FALSE	-0.23	0.00	-1.11	22.48	-1.56E-03	-3.00E-09	-2.97E-11	-6.76E-11	-4.25E-02	-1.51E-04

KS120511M~9	breeding line	2018-19	FALSE	-0.11	0.00	-28.08	46.93	-4.41E-03	-5.31E-09	-6.40E-11	-9.56E-11	-1.56E-01	-6.46E-04
KS120513M~5	breeding line	2018-19	FALSE	-0.56	0.00	-3.19	22.82	-4.57E-04	6.04E-11	-1.23E-11	-5.68E-10	-3.90E-01	-2.03E-03
KS120522M~5	breeding line	2018-19	FALSE	-0.77	0.00	-25.06	44.13	-5.29E-03	1.13E-08	-1.83E-11	-1.03E-10	-1.83E-01	-8.48E-04
KS120529M~1	breeding line	2018-19	FALSE	-0.42	0.00	-25.10	22.46	-1.49E-03	1.68E-09	-3.75E-11	-1.89E-12	-1.97E-02	-4.73E-05
KS120529M~7	breeding line	2018-19	FALSE	-0.06	0.00	-12.75	44.13	-1.88E-03	3.61E-09	-8.67E-11	-1.00E-11	-2.18E-01	-9.15E-04
KS120552M~12	breeding line	2018-19	FALSE	-0.75	0.00	21.06	64.76	2.03E-04	4.21E-10	-4.99E-11	-2.61E-11	-2.05E-02	-2.28E-04
KS120552M~8	breeding line	2018-19	FALSE	-0.70	0.00	-21.59	25.48	-7.47E-04	6.04E-09	-6.16E-12	-6.40E-12	-1.36E-02	-9.63E-05
KS120559M~12	breeding line	2018-19	FALSE	0.00	0.00	2.28	25.97	-4.49E-04	3.55E-10	-1.13E-10	-3.56E-11	-1.91E-01	-8.80E-04

KS120559M~5	breeding line	2018-19	FALSE	-0.51	0.00	1.98	-46.44	-3.05E-03	-7.48E-09	1.55E-11	3.01E-13	2.09E-01	-1.01E-03
KS120581M~2	breeding line	2018-19	FALSE	0.01	0.00	19.80	22.48	-1.72E-03	-2.63E-09	1.49E-11	5.11E-11	2.56E-01	-1.23E-03
KS120582M~4	breeding line	2018-19	FALSE	-0.74	0.00	-0.60	-6.47	-1.99E-03	-2.12E-09	2.07E-11	1.54E-10	4.20E-01	-2.10E-03
KS120592M~6	breeding line	2018-19	FALSE	-0.56	0.00	-75.40	-100.09	-2.31E-03	-3.85E-09	4.24E-11	1.84E-11	-1.74E-01	7.70E-04
KS120592M~8	breeding line	2018-19	FALSE	-0.23	0.00	-14.87	-6.34	-3.79E-04	-3.75E-11	5.49E-11	5.76E-11	-1.76E-01	8.60E-04
KS120648M~5	breeding line	2018-19	FALSE	1.07	0.00	15.26	22.00	2.46E-03	4.82E-09	-3.11E-11	3.00E-11	3.27E-01	-1.52E-03
KS120729M~3	breeding line	2018-19	FALSE	-0.44	0.00	19.98	11.82	-1.86E-03	-6.56E-09	1.63E-11	-9.95E-11	-2.72E-01	1.41E-03
KS120802M~4	breeding line	2018-19	FALSE	-0.04	0.00	-5.25	-36.63	-2.65E-03	-2.63E-09	5.13E-11	-9.27E-11	-2.46E-01	1.27E-03

KS120905M~9	breeding line	2018-19	FALSE	2.34	0.00	-29.58	48.98	-6.75E-03	-4.89E-09	1.04E-10	4.01E-12	8.95E-02	-5.84E-04
KS13DH0001-6	breeding line	2018-19	FALSE	0.00	0.00	-15.05	36.27	-3.82E-04	3.84E-09	-1.10E-10	-5.98E-11	4.70E-02	-1.39E-04
KS13DH0002-19	breeding line	2018-19	FALSE	-0.11	0.00	43.03	78.44	-4.32E-04	-1.43E-08	-5.45E-12	-7.21E-10	3.98E-01	-2.24E-03
KS13DH0002-5	breeding line	2018-19	FALSE	-0.20	0.00	36.73	27.46	-2.61E-04	-1.85E-09	-1.72E-10	-5.89E-11	4.97E-01	-2.32E-03
KS13DH0008-23	breeding line	2018-19	FALSE	2.11	0.00	17.75	37.98	1.68E-03	-6.17E-09	1.29E-10	-1.28E-10	1.97E-01	1.04E-03
KS13DH0008-30	breeding line	2018-19	FALSE	0.09	0.00	15.64	30.61	8.70E-04	-5.18E-09	9.71E-11	-6.66E-11	5.20E-02	-1.23E-04
KS13DH0011-20	breeding line	2018-19	FALSE	-0.80	0.00	-4.38	3.83	-1.84E-03	-4.56E-09	-1.18E-10	-2.77E-11	-2.03E-01	-8.05E-04
KS13DH0012-51	breeding line	2018-19	FALSE	0.67	0.00	16.53	25.63	-2.76E-04	-1.02E-08	-6.37E-11	-1.14E-12	-5.39E-03	-6.18E-05

KS13DH0012-98	breeding line	2018-19	FALSE	-0.55	0.00	-49.25	-40.98	-5.69E-03	-2.63E-09	-5.31E-11	-4.02E-10	-4.10E-01	-2.25E-03
KS13DH0013-131	breeding line	2018-19	FALSE	-0.20	0.00	-6.03	-17.49	-1.36E-03	5.69E-09	-6.63E-11	-3.88E-11	-3.40E-01	-1.80E-03
KS13DH0016-53	breeding line	2018-19	FALSE	-0.11	0.00	21.99	25.50	9.67E-04	3.84E-09	-2.18E-12	5.76E-13	-1.35E-01	6.49E-04
KS13DH0016-6	breeding line	2018-19	FALSE	-0.20	0.00	-13.48	-1.54	2.63E-03	1.19E-09	-9.04E-11	2.24E-11	-2.92E-02	1.15E-04
KS13DH0018-29	breeding line	2018-19	FALSE	0.70	0.00	2.22	6.88	7.42E-04	-4.70E-09	-1.93E-11	7.18E-11	6.00E-02	-1.99E-04
KS13DH0018-49	breeding line	2018-19	FALSE	0.54	0.00	-14.75	20.30	2.12E-04	1.10E-08	-5.44E-11	1.43E-11	1.13E-01	-5.53E-04
KS13DH0021-W173	breeding line	2018-19	FALSE	-0.20	0.00	4.19	-20.15	-1.28E-04	2.06E-09	-7.02E-11	1.08E-10	5.85E-01	-2.77E-03
KS13DH0042-26	breeding line	2018-19	FALSE	0.62	0.00	-2.61	-12.64	-1.99E-03	2.16E-09	-4.17E-11	-1.16E-10	-2.94E-01	-1.41E-03

KS13DH0045-84	breeding line	2018-19	FALSE	-0.56	0.00	41.27	35.45	1.79E-03	3.73E-09	-8.67E-11	2.34E-10	4.80E-01	-2.33E-03
KS13DH0053-1	breeding line	2018-19	FALSE	-0.56	0.00	22.96	51.79	4.84E-04	-3.97E-10	-3.07E-11	-1.11E-10	-2.86E-01	-1.44E-03
Larry	cultivar	2018-19	FALSE	-0.06	0.00	11.48	12.18	1.91E-03	-1.85E-10	-3.15E-11	-2.24E-11	-8.27E-02	-3.90E-04
LCSMint	cultivar	2018-19	FALSE	2.05	0.00	-42.26	-39.16	-1.30E-03	-5.85E-09	-9.72E-11	-1.46E-11	-7.50E-02	-3.42E-04
U6893-1-1018-1H	breeding line	2018-19	NA	-0.45	0.00	-15.20	34.96	2.14E-10	-1.16E-03	-1.51E-08	-1.39E-10	-4.56E-02	-3.91E-04
Zenda	cultivar	2018-19	FALSE	0.25	0.00	1.39	0.81	-5.69E-04	-3.21E-09	-6.11E-11	-5.60E-13	-8.74E-02	-2.96E-04
AF03-1	cultivar	2019-20	NA	-1.52	0.00	-34.73	48.53	NA	-1.49E-01	-5.02E-04	-5.98E-10	-5.31E-02	-8.22E-05
AMEastwood	cultivar	2019-20	NA	-2.53	0.00	-1.63	-7.04	NA	-3.96E-01	-1.34E-03	-1.92E-10	-2.34E-02	-3.94E-05

KS100028K^11	breeding line	2019-20	NA	-4.22	0.00	32.84	29.47	NA	-5.62E-01	1.97E-03	-5.05E-10	-4.62E-02	1.45E-04
KS100028K^12	breeding line	2019-20	NA	-4.82	0.00	70.72	-27.69	NA	1.15E-01	-3.59E-04	-4.64E-10	-1.24E-01	3.32E-04
KS100510M^7	breeding line	2019-20	NA	-4.84	0.00	85.64	189.84	NA	1.31E-02	-1.88E-04	2.05E-10	-1.22E-01	3.58E-04
KS10DB-2	breeding line	2019-20	NA	9.78	0.00	116.60	234.97	NA	1.07E+00	-3.69E-03	1.97E-10	-5.59E-02	-1.81E-04
KS110069K-3	breeding line	2019-20	FALSE	6.75	0.00	-123.73	-94.38	NA	1.79E-01	-5.93E-04	-7.18E-10	-1.07E-02	5.49E-05
KS110116M-1	breeding line	2019-20	FALSE	-2.55	0.00	19.90	-105.35	NA	1.16E+00	-3.98E-03	-1.94E-10	-1.84E-02	-8.30E-05
KS110409M-1	breeding line	2019-20	FALSE	-1.52	0.00	-15.65	77.11	NA	-2.55E-01	8.67E-04	-6.89E-10	-1.60E-01	4.43E-04
KS110489M-1	breeding line	2019-20	FALSE	-3.16	0.00	22.67	58.06	NA	-6.35E-01	2.19E-03	-6.13E-11	-2.40E-02	-5.16E-05

KS110489M-6	breeding line	2019-20	FALSE	-2.88	0.00	26.73	39.86	NA	5.08E-01	-1.72E-03	4.33E-10	3.37E-02	-1.22E-04
KS110510K-6	breeding line	2019-20	FALSE	-3.18	0.00	-57.33	-67.39	NA	-7.72E-01	2.59E-03	-3.77E-10	-6.61E-02	2.03E-04
KS110515K-2	breeding line	2019-20	NA	-4.84	0.00	123.62	323.22	NA	-1.65E-02	4.54E-05	4.80E-11	1.41E-01	-3.68E-04
KS110532M-1	breeding line	2019-20	FALSE	6.27	0.00	48.47	172.38	NA	2.93E-02	-1.19E-04	-2.60E-10	-6.20E-02	1.49E-04
KS110532M-3	breeding line	2019-20	FALSE	1.62	0.00	42.75	116.82	NA	2.19E-01	-7.21E-04	-2.98E-10	1.80E-02	-5.78E-05
KS110729K-16	breeding line	2019-20	FALSE	-1.52	0.00	42.05	106.21	NA	-3.50E-01	1.18E-03	7.69E-11	-2.50E-02	6.83E-05
KS110826K-7	breeding line	2019-20	FALSE	-1.52	0.00	-50.33	-103.91	NA	-7.77E-01	2.57E-03	-1.39E-10	-3.37E-02	7.45E-05
KS110832M-2	breeding line	2019-20	FALSE	8.31	0.00	124.39	220.02	NA	6.23E-01	-1.98E-03	5.92E-10	6.44E-02	-2.09E-04

KS110865K-6	breeding line	2019-20	FALSE	0.16	0.00	-177.66	-227.76	NA	-1.02E+00	3.40E-03	4.37E-10	7.48E-02	1.96E-04
KS120008K-13	breeding line	2019-20	FALSE	-2.85	0.00	-64.22	6.21	NA	2.74E-01	-9.53E-04	-1.60E-11	-4.82E-03	-2.22E-05
KS120017K-15	breeding line	2019-20	FALSE	1.16	0.00	-48.80	-108.88	NA	9.25E-01	-3.17E-03	3.82E-10	5.32E-02	-1.43E-04
KS120017K-6	breeding line	2019-20	NA	-4.51	0.00	79.84	172.38	NA	-6.25E-01	2.09E-03	-2.22E-10	-3.10E-02	9.31E-05
KS120044K-5	breeding line	2019-20	FALSE	-1.50	0.00	-72.79	-46.74	NA	-4.32E-01	1.39E-03	-2.15E-10	-1.55E-02	-4.49E-05
KS120081K-1	breeding line	2019-20	FALSE	-4.80	0.00	-6.70	-11.07	NA	-9.55E-03	7.35E-05	6.58E-10	1.88E-01	-4.08E-04
KS120081K-7	breeding line	2019-20	FALSE	2.09	0.00	-36.55	-83.25	NA	7.83E-01	-2.63E-03	7.01E-12	-4.49E-02	-1.50E-04
KS120081M-2	breeding line	2019-20	FALSE	-4.87	0.00	83.11	134.27	NA	-6.62E-01	2.25E-03	5.48E-10	1.36E-01	-3.57E-04

KS120154K-5	breeding line	2019-20	FALSE	1.80	0.00	85.49	-112.65	NA	-1.36E-01	-4.01E-04	-3.30E-10	-5.23E-02	-1.47E-04
KS120159K-3	breeding line	2019-20	FALSE	0.14	0.00	13.47	-103.91	NA	-1.57E-01	-5.41E-04	-9.16E-11	-2.53E-02	-8.82E-05
KS120177K-23	breeding line	2019-20	FALSE	-2.28	0.00	15.55	-151.73	NA	-5.10E-01	-1.72E-03	-4.12E-10	-1.29E-01	-3.23E-04
KS120177K-28	breeding line	2019-20	FALSE	-2.85	0.00	-50.25	-124.44	NA	-6.64E-02	-2.85E-04	-2.21E-10	-9.20E-02	-2.56E-04
KS120205K-2	breeding line	2019-20	FALSE	-4.92	0.00	12.41	-8.01	NA	-5.80E-01	-1.92E-03	-2.24E-10	-1.83E-02	-5.02E-05
KS120215K-6	breeding line	2019-20	FALSE	-3.19	0.00	-72.66	-103.91	NA	-1.48E+00	-5.00E-03	-1.91E-10	-3.20E-02	-1.02E-04
KS120267K-5	breeding line	2019-20	FALSE	-1.20	0.00	-62.01	-111.84	NA	-7.56E-01	-2.45E-03	-3.73E-10	-5.41E-02	-1.33E-04
KS120267M-3	breeding line	2019-20	FALSE	-1.19	0.00	-57.09	-172.19	NA	-5.03E-01	-1.64E-03	-2.31E-10	-5.02E-03	-1.93E-05

KS120269K-3	breeding line	2019-20	FALSE	-4.85	0.00	57.78	48.53	NA	8.05E-01	-2.74E-03	1.73E-10	-4.30E-03	-1.36E-05
KS120310M-3	breeding line	2019-20	FALSE	-2.58	0.00	-87.55	-102.31	NA	-2.70E-03	1.10E-04	-5.56E-10	9.16E-02	-2.03E-04
KS120331K-9	breeding line	2019-20	FALSE	-3.24	0.00	57.59	134.27	NA	-3.89E-02	7.26E-05	-1.83E-10	1.92E-02	-4.92E-05
KS120351M-2	breeding line	2019-20	FALSE	-1.50	0.00	-41.02	10.42	NA	-3.03E-01	1.05E-03	-2.21E-10	-9.45E-02	2.53E-04
KS120375K-9	breeding line	2019-20	FALSE	-3.29	0.00	-129.93	-170.60	NA	-9.16E-01	3.05E-03	-4.48E-10	8.97E-03	-5.09E-05
KS120376M-4	breeding line	2019-20	FALSE	-4.49	0.00	114.97	153.33	NA	2.94E-03	-1.18E-04	2.17E-10	-5.17E-03	-2.99E-06
KS120426M-7	breeding line	2019-20	FALSE	0.16	0.00	-72.64	-113.43	NA	-1.81E+00	6.14E-03	-1.89E-10	5.03E-02	-1.28E-04
KS120494M-1	breeding line	2019-20	TRUE	-4.85	0.00	191.45	191.44	NA	2.27E+00	-7.63E-03	-9.20E-11	-7.51E-03	-2.90E-06

KS120506K-2	breeding line	2019-20	FALSE	-3.21	0.00	120.43	323.22	NA	8.45E-01	-2.82E-03	1.66E-10	-4.85E-03	-7.82E-06
KS120513M-3	breeding line	2019-20	FALSE	-4.84	0.00	15.63	113.62	NA	-2.04E+00	7.01E-03	-1.29E-10	1.03E-01	-2.10E-04
KS120522M-6	breeding line	2019-20	FALSE	-4.22	0.00	70.86	143.80	NA	-7.01E-01	2.43E-03	-3.16E-11	1.36E-03	-3.23E-05
KS120522M-7	breeding line	2019-20	FALSE	-4.55	0.00	58.28	67.58	NA	-4.79E-02	2.46E-04	6.33E-12	-3.43E-02	-5.68E-05
KS120529M-7	breeding line	2019-20	FALSE	1.80	0.00	-24.99	-27.69	NA	-5.63E-01	-1.89E-03	-2.93E-10	-9.44E-03	-3.40E-05
KS120559K-10	breeding line	2019-20	FALSE	-2.87	0.00	4.79	-26.09	NA	-4.73E-01	1.58E-03	-3.16E-10	-9.15E-02	-2.40E-04
KS120607K-4	breeding line	2019-20	FALSE	-2.87	0.00	-49.38	-54.67	NA	-3.99E-01	1.48E-03	-2.78E-10	-4.61E-02	-1.22E-04
KS120612K-5	breeding line	2019-20	FALSE	-1.23	0.00	23.72	69.18	NA	-9.21E-01	3.07E-03	-4.38E-10	-8.01E-02	-2.54E-04

KS120612K-7	breeding line	2019-20	FALSE	-1.58	0.00	40.93	152.33	NA	-9.52E-02	1.94E-04	4.09E-10	1.14E-01	-3.26E-04
KS120644K-4	breeding line	2019-20	FALSE	0.03	0.00	-60.01	-56.27	NA	9.89E-01	-3.43E-03	1.74E-10	-3.33E-02	-6.23E-05
KS120659K-15	breeding line	2019-20	FALSE	-4.53	0.00	-84.51	-35.62	NA	-1.45E+00	4.93E-03	1.57E-10	-5.53E-02	-1.41E-04
KS120685K-2	breeding line	2019-20	FALSE	-2.85	0.00	-31.70	-115.03	NA	-3.18E-01	1.01E-03	2.14E-10	-8.07E-02	-2.35E-04
KS120742M-1	breeding line	2019-20	FALSE	-2.85	0.00	-2.76	19.95	NA	1.07E-01	-3.68E-04	3.21E-10	-1.02E-02	-2.61E-05
KS120766M-6	breeding line	2019-20	FALSE	2.04	0.00	-142.01	-237.29	NA	-2.03E-01	8.13E-04	9.74E-12	-1.85E-02	-5.20E-05
KS120837K-4	breeding line	2019-20	FALSE	11.79	0.00	-44.17	-8.63	NA	-1.20E+00	4.04E-03	1.90E-10	-1.39E-02	-3.98E-05
KS120849K-9	breeding line	2019-20	FALSE	2.09	0.00	-23.75	-102.31	NA	6.56E-01	-2.13E-03	8.88E-11	-2.32E-02	-8.02E-05

KS120905M-4	breeding line	2019-20	FALSE	-4.63	0.00	10.40	77.11	NA	-1.01E-01	4.06E-04	-6.41E-11	-1.74E-01	4.54E-04
KS120905M-6	breeding line	2019-20	FALSE	3.48	0.00	-37.72	-37.22	NA	8.46E-01	-2.78E-03	-3.44E-10	-2.53E-02	-5.93E-05
KS120905M-7	breeding line	2019-20	FALSE	-1.65	0.00	-19.31	46.93	NA	1.41E-01	-4.80E-04	-3.05E-10	-1.60E-02	-5.85E-05
KS15DH0055-11	breeding line	2019-20	FALSE	2.09	0.00	11.34	-102.31	NA	6.06E-01	-1.93E-03	-3.40E-10	-1.25E-01	-3.52E-04
KS15DH0055-8	breeding line	2019-20	NA	2.81	0.00	-37.64	-75.32	NA	8.07E-01	-2.77E-03	-1.64E-10	-7.61E-03	-1.31E-05
KS15DH0140-8	breeding line	2019-20	FALSE	2.81	0.00	-37.64	-75.32	NA	8.07E-01	-2.77E-03	-1.64E-10	-7.61E-03	-1.31E-05
KS16DH0002-12	breeding line	2019-20	FALSE	4.76	0.00	49.22	78.71	NA	1.83E+00	-6.23E-03	-8.66E-12	-2.97E-02	-1.01E-04
KS16DH0002-14	breeding line	2019-20	FALSE	7.10	0.00	-129.02	-102.31	NA	-7.44E-01	-2.65E-03	-3.98E-10	-5.41E-02	-1.81E-04

												-		-
KS16DH0002-15	breeding line	2019-20	FALSE	-3.16	0.00	6.72	58.06	NA	-5.38E-01	1.80E-03	1.28E-10	5.49E-02	1.34E-04
										-	-	-	
KS16DH0002-9	breeding line	2019-20	FALSE	5.09	0.00	6.77	39.00	NA	7.18E-01	2.44E-03	2.63E-10	5.29E-02	1.38E-04
										-		-	
KS16DH0003-13	breeding line	2019-20	NA	8.44	0.00	261.17	391.51	NA	1.66E+00	5.45E-03	8.65E-11	1.52E-02	7.35E-06
												-	
KS16DH0004-30	breeding line	2019-20	FALSE	23.34	0.00	-3.23	-10.23	NA	-5.33E-01	1.84E-03	1.09E-11	1.45E-01	3.62E-04
										-		-	
KS16DH0005-23	breeding line	2019-20	FALSE	-4.82	0.00	-47.27	-46.74	NA	1.35E+00	4.46E-03	2.74E-11	5.09E-02	1.42E-04
							-			-			-
KS16DH0006-17	breeding line	2019-20	FALSE	-1.19	0.00	-50.02	171.73	NA	1.00E+00	3.36E-03	3.10E-10	2.23E-02	7.97E-05
							-				-		-
KS16DH0008-18	breeding line	2019-20	FALSE	6.78	0.00	-57.78	298.94	NA	-3.08E-01	1.06E-03	2.30E-10	8.57E-03	4.76E-05
													-
KS16DH0008-32	breeding line	2019-20	FALSE	3.38	0.00	86.24	162.86	NA	-4.23E-01	1.39E-03	1.39E-10	1.61E-02	4.55E-05

KS16DH0009-23	breeding line	2019-20	FALSE	5.10	0.00	79.50	85.04	NA	5.09E-01	-1.77E-03	6.63E-10	7.29E-02	-2.10E-04
KS16DH0010-17	breeding line	2019-20	FALSE	-0.54	0.00	35.54	10.42	NA	1.02E+00	-3.52E-03	2.24E-10	1.59E-02	-8.21E-06
KS16DH0010-28	breeding line	2019-20	FALSE	-1.17	0.00	-120.00	-332.56	NA	-5.11E-01	1.67E-03	-1.06E-10	-6.95E-02	1.73E-04
KS16DH0011-12	breeding line	2019-20	FALSE	-1.90	0.00	92.92	29.47	NA	1.01E+00	-3.48E-03	1.56E-10	7.40E-03	-3.87E-05
KS16DH0011-16	breeding line	2019-20	FALSE	0.16	0.00	19.50	48.53	NA	4.72E-01	-1.61E-03	-1.19E-10	-8.62E-02	2.19E-04
KS16DH0011-18	breeding line	2019-20	FALSE	7.08	0.00	7.64	-113.43	NA	-2.53E-01	1.01E-03	3.30E-10	9.52E-05	-1.36E-05
KS16DH0011-20	breeding line	2019-20	FALSE	11.79	0.00	-8.93	-75.32	NA	-7.05E-01	2.35E-03	-3.30E-11	-2.65E-02	5.51E-05
KS16DH0011-25	breeding line	2019-20	FALSE	-4.85	0.00	-75.77	-142.01	NA	-7.57E-01	2.51E-03	6.59E-11	-2.46E-02	9.00E-05

KS16DH0011-32	breeding line	2019-20	FALSE	-1.52	0.00	-51.10	-0.70	NA	-3.55E-01	1.16E-03	4.64E-10	-6.07E-02	1.63E-04
KS16DH0011-35	breeding line	2019-20	FALSE	1.07	0.00	86.03	18.35	NA	1.62E+00	-5.52E-03	1.65E-10	-4.49E-02	8.21E-05
KS16DH0011-41	breeding line	2019-20	FALSE	16.64	0.00	-104.39	-180.12	NA	-3.85E-01	1.29E-03	4.54E-11	-5.29E-02	1.23E-04
KS16DH0011-45	breeding line	2019-20	FALSE	-2.89	0.00	77.67	193.03	NA	3.85E-01	-1.19E-03	4.76E-10	-2.42E-02	4.01E-05
KS16DH0013-20	breeding line	2019-20	FALSE	0.16	0.00	35.52	19.95	NA	6.48E-01	-2.24E-03	3.95E-11	-3.02E-02	7.03E-05
KS16DH0013-23	breeding line	2019-20	FALSE	3.45	0.00	129.97	208.03	NA	8.55E-01	-2.86E-03	4.92E-10	-5.16E-02	1.43E-04
KS18EVACK-327	breeding line	2019-20	FALSE	11.76	0.00	54.83	-56.27	NA	-2.47E-01	9.06E-04	3.19E-10	-6.58E-02	-1.71E-04
KS18EVACK^118	breeding line	2019-20	FALSE	-4.82	0.00	-34.12	-218.23	NA	3.28E-01	-1.25E-03	2.53E-10	-2.39E-02	-5.96E-05

KS18EVACK^55	breeding line	2019-20	FALSE	-4.84	0.00	-25.65	27.88	NA	-1.32E-01	4.56E-04	3.02E-10	4.19E-03	-1.93E-05
KS18EVACM-12	breeding line	2019-20	NA	-0.87	0.00	39.34	212.09	NA	-2.44E-01	8.26E-04	-5.14E-10	-5.13E-02	1.31E-04
KS18EVACM-34	breeding line	2019-20	FALSE	-3.51	0.00	118.27	105.69	NA	2.29E+00	-7.77E-03	3.55E-11	3.29E-02	-9.18E-05
KS18EVACM-93	breeding line	2019-20	FALSE	3.73	0.00	-30.15	-92.78	NA	9.84E-01	-3.22E-03	-4.22E-11	-4.48E-03	1.44E-05
KS18EVACM^11	breeding line	2019-20	NA	-2.89	0.00	-2.38	86.64	NA	-4.56E-01	1.63E-03	-2.73E-10	1.20E-02	-1.12E-05
KS18RDK^249	breeding line	2019-20	FALSE	0.18	0.00	63.19	35.99	NA	-4.88E-01	1.62E-03	2.02E-10	9.00E-02	-2.50E-04
KS18RDK^277	breeding line	2019-20	FALSE	-4.84	0.00	-102.08	-29.29	NA	-1.15E+00	-3.86E-03	5.55E-11	6.53E-02	-1.46E-04
KS18RDK^315	breeding line	2019-20	FALSE	0.14	0.00	-165.08	-381.79	NA	7.87E-01	-2.57E-03	1.46E-10	4.02E-02	-8.95E-05

KS18RDM^42	breeding line	2019-20	FALSE	-1.50	0.00	32.13	105.69	NA	-1.52E-01	6.01E-04	3.42E-10	9.36E-02	-2.65E-04
LCSLink	cultivar	2019-20	NA	6.63	0.00	9.55	-19.76	NA	4.13E-02	-2.15E-05	1.39E-10	-1.39E-02	6.20E-05
SYBenefit	cultivar	2019-20	FALSE	-4.84	0.00	110.90	304.17	NA	2.76E-02	-2.40E-04	6.90E-11	4.27E-02	-9.88E-05
SYGrit	cultivar	2019-20	NA	-4.82	0.00	-75.81	-122.96	NA	-4.52E-01	1.60E-03	4.53E-11	-7.22E-02	1.89E-04
WB4303	cultivar	2019-20	NA	-3.84	0.00	-107.52	-208.70	NA	-7.38E-01	2.51E-03	1.48E-10	1.41E-01	-4.04E-04
WB4699	cultivar	2019-20	NA	11.53	0.00	4.11	-199.18	NA	1.57E-01	-5.41E-04	2.54E-10	-4.78E-02	1.56E-04
WB4792	cultivar	2019-20	NA	-0.22	0.00	-55.54	-149.94	NA	1.13E-01	-3.23E-04	2.60E-10	-1.64E-03	1.91E-05
Art	cultivar	All	FALSE	25.53	-0.01	-533.39	962.80	-4.22E-03	-2.81E+00	1.05E-02	2.63E-02	-5.49E-02	3.09E-04

Everest	cultivar	All	FALSE	-12.84	0.02	239.80	425.70	2.89E-03	2.19E+00	-8.37E-03	-4.68E-03	-2.33E-03	-1.73E-05

Table B.2 - Precipitation (inches) during the five field seasons in Riley county, KS, where Rocky Ford and Ashland Bottoms experimental units are located. Normal temperature is defined as a 30 year average from 1981 – 2010. Data was obtained from Kansas State University (http://climate.k-state.edu/precip/county/)

	Jan	Feb	Mar	Apr	May	Jun	Jul	Aug	Sep	Oct	Nov	Dec	Annual		Average	Cumulative	% diff
Normal	0.70	1.10	2.40	3.00	4.60	5.00	4.20	3.90	3.10	2.50	1.60	1.10	33	Historic	2.51	25.10	
2015	0.41	1.24	0.38	2.83	8.62	5.90	5.56	2.93	2.91	0.64	3.49	4.13	39	2015–16	2.75	27.50	9.56
2016	0.81	0.54	0.59	6.48	6.76	1.15	5.72	6.00	4.25	2.67	0.46	0.97	36	2016–17	2.69	26.86	7.01
2017	1.64	0.36	3.92	4.22	4.63	3.74	1.57	3.87	1.85	3.64	0.18	0.13	30	2017–18	1.66	**16.55**	**-34.06**
2018	0.57	0.70	0.75	1.15	4.21	3.37	3.46	5.44	5.16	5.48	0.96	3.22	35	2018–19	3.96	**39.61**	**57.81**
2019	0.84	1.14	2.24	2.05	12.32	6.20	3.80	9.52	2.96	2.97	0.59	1.13	46	2019–20	2.34	23.35	-6.97
2020	1.45	0.44	2.39	2.23	5.73	3.46	7.73	1.90	1.93	27.30							

Appendix C - Supplementary Material Chapter 3

This appendix contains supplementary figures and tables for Chapter 3, subchapter B.

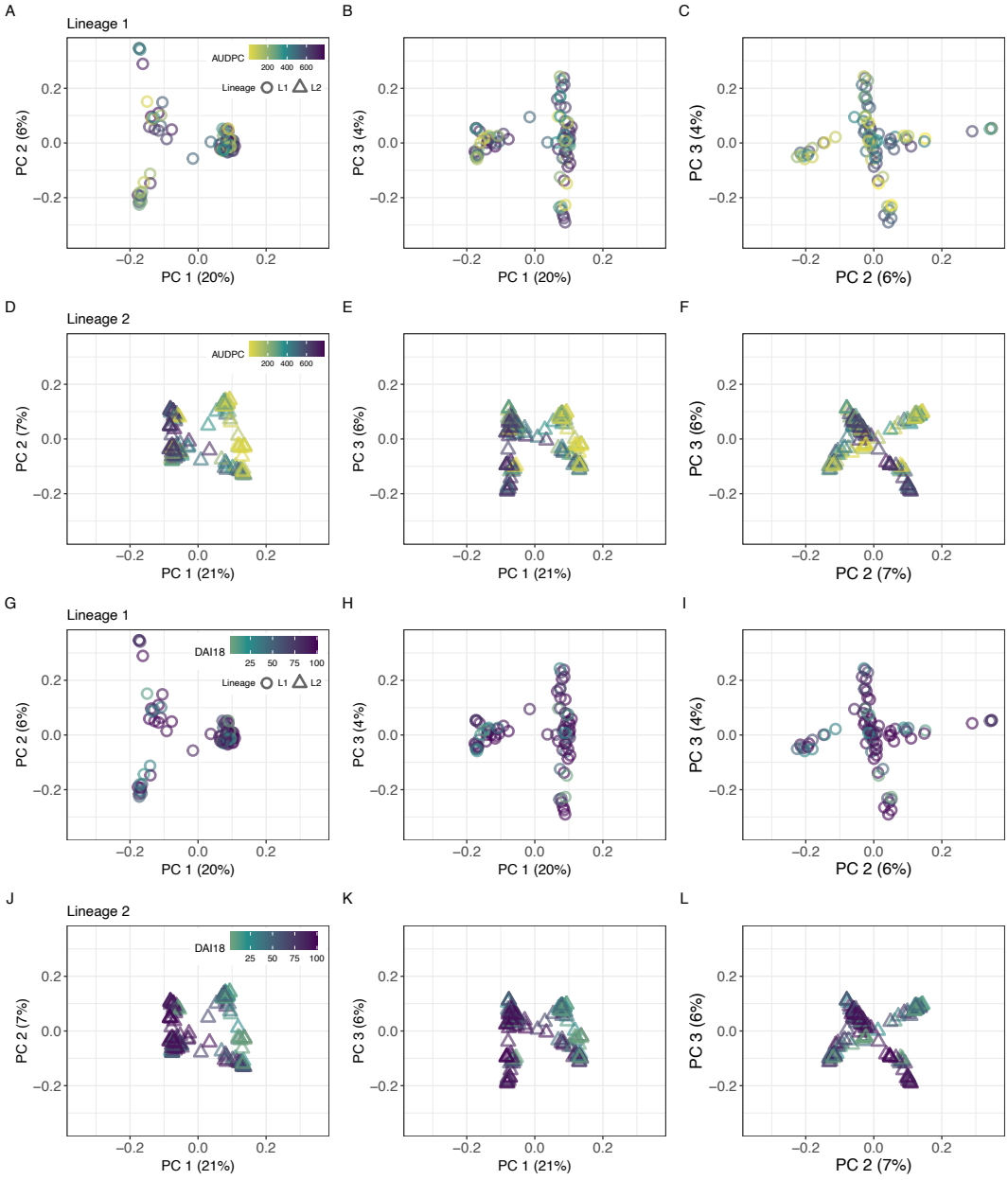

Figure C.1 - Principal component analysis (PCA) plot using GBS-SNP markers for lineage1 (A, B, C, G, H, I) and lineage 2 (D, E, F, J, K, L) showing the first three principal components (PC1, PC2, and PC3) and the percentage of variation explained by each component. Accessions are colored based on phenotypic response to wheat head blast (WHB) using the area under the disease progress curve (AUDPC) (A-F) and WHB severity (%) at 18 days after inoculation (DAI) (G-L). Empty circles represent L1 and empty triangles represent L2.

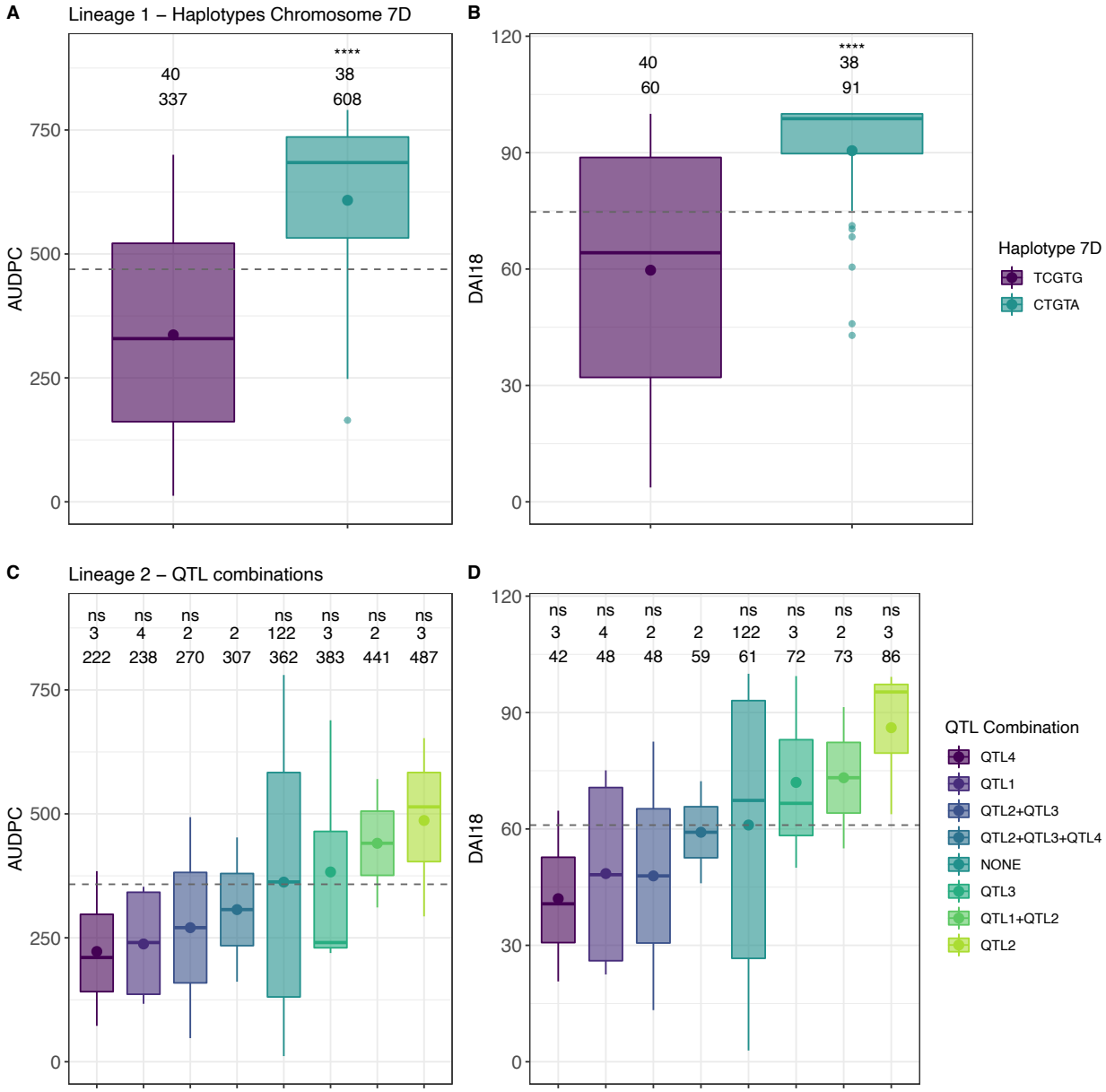

Figure C.2 - Boxplots of wheat head blast (WHB) phenotypic response for the different haplotypes or QTL combinations detected by GWAS for A-B) lineage 1 *Aegilops tauschii* accessions and C-D) lineage 2 *Ae. tauschii* accessions. The number of accessions in each group and the mean phenotypic values is shown at the top of each boxplot. A significant t-test was done using the most resistant group or the group combining more QTLs as the reference group. ns: non-significant.

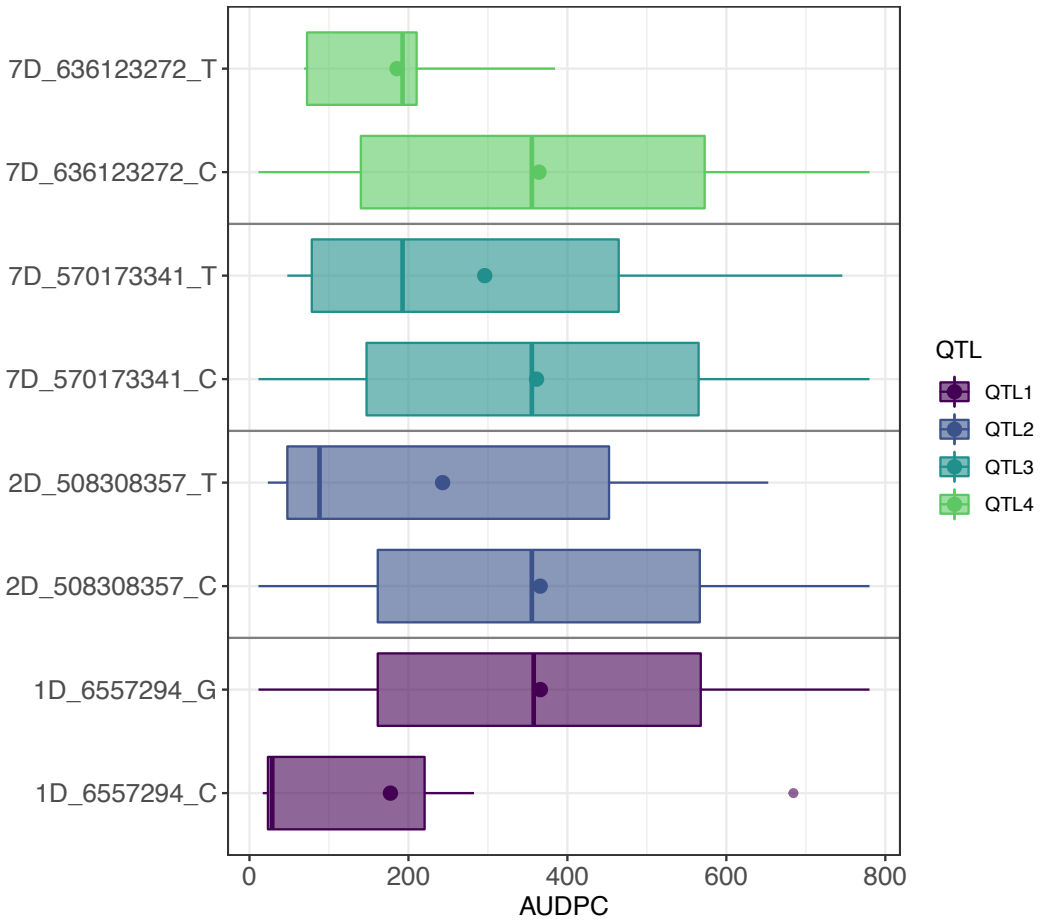

Figure C.3 - Allele substitution effect. Boxplots showing the allelic effect for the SNP markers for the four QTLs detected using GWAS for lineage 2. The y axis label indicates chromosome, physical position, and allele.

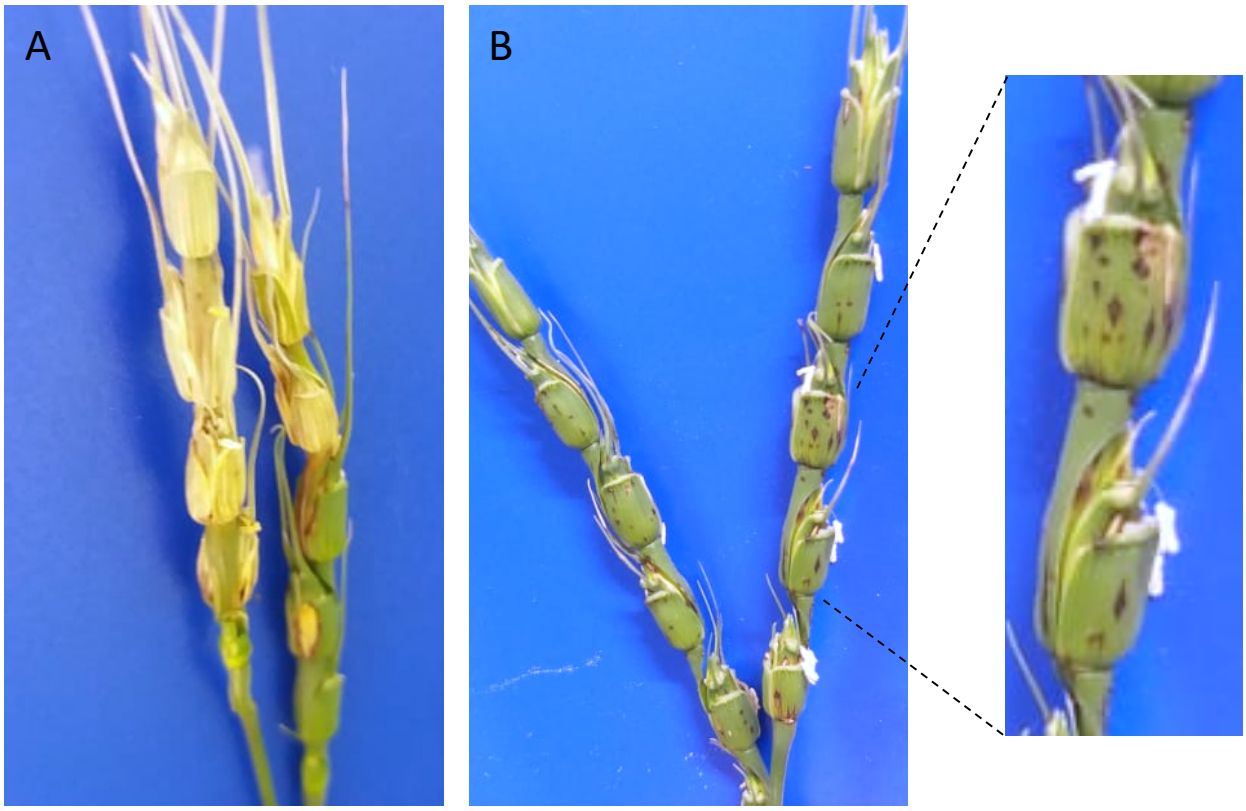

Figure C.4 - Wheat blast disease severity of *Aegilops tauschii* at 14 days after inoculation under controlled conditions using *Magnaporthe oryzae Triticum* isolate 008. A) Lineage 2 susceptible accession and B) Lineage 2 resistant accession displaying dark flecks resembling a hypersensitive response. Image modified from Cruppe et al., 2019.

Table C.1 - List of *Aegilops tauschii* accessions phenotypically evaluated in the study. The table includes the lineage, the adjusted means or best linear unbiased estimators (BLUEs) for five different time point evaluations or days after inoculation (dai), and the area under the disease progress curve value (AUDPC)

Taxa	Lineage	dai10	dai12	dai14	dai16	dai18	AUDPC
TA10069	L1	72.112155	90.309437	98.126912	99.462711	101.421242	749.331517
TA10071	L1	31.633617	43.800000	60.950000	68.400000	77.300000	455.233617
TA10080	L1	29.512155	50.209437	68.826912	83.462711	89.421242	523.931517
TA10082	L1	9.933617	18.350000	26.200000	47.500000	61.500000	255.533617
TA10100	L1	4.212155	6.409437	9.326912	11.862711	20.121242	79.531517
TA10105	L1	0.619332	1.071430	1.642855	2.642855	3.792855	15.126467
TA10114	L1	38.912155	57.009437	76.026912	87.962711	97.821242	578.731517
TA10120	L1	65.812155	78.309437	85.526912	88.162711	93.421242	663.231517
TA10123	L1	1.283617	1.750000	2.650000	3.600000	4.900000	22.183617
TA10127	L1	16.033617	24.400000	33.100000	51.000000	77.400000	310.433617
TA10135	L1	9.383617	14.850000	25.750000	41.500000	48.000000	221.583617
TA10136	L1	41.112155	70.134437	92.701912	96.912711	100.171242	660.781517
TA10143	L1	35.112155	63.509437	83.326912	95.662711	100.421242	620.531517
TA10165	L1	11.826445	24.866577	43.398342	47.519851	60.706952	304.102937
TA10169	L1	9.612155	14.409437	17.026912	21.362711	27.921242	143.131517
TA10172	L1	77.758617	88.900000	95.425000	97.500000	98.400000	739.808617
TA10175	L1	79.112155	95.309437	99.026912	90.762711	101.421242	750.731517
TA10177	L1	27.012155	64.809437	76.026912	81.262711	92.721242	563.931517

TA10179	L1	29.400000	46.800000	66.400000	82.800000	89.200000	518.600000
TA10182	L1	61.778825	85.176107	94.493582	96.829381	99.254572	714.031537
TA10183	L1	12.783617	23.650000	38.400000	54.300000	68.250000	313.733617
TA10196	L1	15.112155	22.809437	36.526912	47.362711	59.121242	287.631517
TA10202	L1	56.112155	76.009437	90.826912	100.662711	101.421242	692.531517
TA10210	L1	69.362155	77.259437	78.326912	85.662711	93.921242	645.781517
TA10213	L1	21.412155	35.309437	60.826912	69.662711	77.921242	430.931517
TA10292	L1	18.312155	34.709437	45.626912	53.362711	62.621242	348.331517
TA10293	L1	9.983617	13.725000	20.950000	28.100000	32.175000	167.708617
TA10307	L1	3.312155	6.209437	15.626912	10.762711	13.821242	82.331517
TA10312	L1	90.112155	98.509437	100.826912	100.662711	101.421242	791.531517
TA10319	L1	12.233617	27.050000	44.250000	56.350000	69.150000	336.683617
TA10323	L1	11.633617	15.350000	22.183335	26.716665	31.666665	171.800282
TA10918	L1	52.650282	66.750000	76.083335	82.483335	85.000000	588.283622
TA10922	L1	54.233617	72.700000	87.750000	91.250000	94.300000	651.933617
TA10932	L1	51.312155	78.209437	91.826912	98.462711	100.421242	688.731517
TA10957	L1	61.778825	88.676107	96.826912	98.996041	101.421242	732.198187
TA1592	L1	14.612155	32.259437	49.576912	65.662711	75.171242	384.781517
TA1625	L1	76.362155	84.759437	89.576912	91.912711	96.421242	705.281517
TA1630	L1	33.983617	54.800000	64.600000	75.900000	87.500000	512.083617
TA1634	L1	15.750282	41.300000	53.350000	67.516665	75.066665	415.150277
TA1655	L1	5.128062	8.700000	15.450000	19.400000	23.000000	115.228062

TA1676	L1	24.183617	32.700000	45.300000	60.250000	70.250000	370.933617
TA1694	L1	19.283617	29.000000	40.900000	51.200000	60.150000	321.633617
TA1698	L1	7.412155	13.309437	19.226912	27.162711	43.121242	169.931517
TA1707	L1	21.933617	24.316665	28.466665	37.250000	45.900000	247.900277
TA1717	L1	45.712155	70.509437	93.126912	96.762711	99.921242	666.431517
TA2379	L1	61.000282	91.500000	97.750000	98.900000	99.500000	736.800282
TA2381	L1	11.657227	20.479165	33.270835	50.111110	65.951390	285.330837
TA2382	L1	18.244727	24.800000	33.927780	43.511110	49.272220	271.994727
TA2384	L1	15.483617	20.322220	28.033335	41.988890	56.427780	252.600287
TA2392	L1	71.933617	85.500000	92.750000	97.800000	99.400000	723.433617
TA2397	L1	75.112155	87.676107	97.493582	99.996041	101.421242	746.864857
TA2398	L1	66.612155	85.509437	90.126912	93.162711	96.221242	700.431517
TA2399	L1	73.112155	90.809437	94.826912	99.162711	100.921242	743.631517
TA2403	L1	3.539172	7.027780	7.694445	11.750000	17.750000	74.233622
TA2405	L1	10.112155	71.009437	90.826912	95.662711	101.421242	626.531517
TA2410	L1	59.333617	72.150000	82.250000	94.300000	97.300000	654.033617
TA2417	L1	1.033617	1.650000	3.050000	5.750000	10.450000	32.383617
TA2426	L1	22.872507	51.000000	63.472220	75.722220	92.500000	495.761387
TA2432	L1	20.458617	33.400000	42.875000	61.275000	73.150000	368.708617
TA2433	L1	16.712155	35.709437	50.026912	65.862711	70.821242	390.731517
TA2437	L1	74.733617	86.875000	96.850000	98.250000	98.750000	737.433617
TA2440	L1	32.550282	47.500000	66.383335	90.222220	96.400000	537.161392

TA2445	L1	40.112155	76.009437	90.826912	100.662711	101.421242	676.531517
TA2462	L1	5.683617	9.650000	16.600000	26.000000	33.450000	143.633617
TA2486	L1	85.533617	92.250000	96.350000	98.500000	99.500000	759.233617
TA2489	L1	20.112155	56.009437	70.826912	80.662711	86.421242	521.531517
TA2502	L1	16.112155	31.009437	38.826912	60.662711	71.421242	348.531517
TA2507	L1	58.862155	93.009437	97.076912	96.912711	98.921242	731.781517
TA2508	L1	25.112155	36.009437	65.826912	80.662711	87.421242	477.531517
TA2510	L1	1.112155	3.009437	5.826912	10.662711	13.421242	53.531517
TA2511	L1	27.612155	76.009437	88.326912	99.662711	101.421242	657.031517
TA2514	L1	45.112155	80.509437	93.126912	98.662711	100.921242	690.631517
TA2519	L1	90.612155	100.342767	100.826912	100.662711	101.421242	795.698177
TA2520	L1	55.633617	69.675000	79.600000	89.350000	93.000000	625.883617
TA2566	L1	64.712155	86.409437	90.226912	90.862711	91.621242	691.331517
TA2573	L1	51.250282	70.125000	81.475000	89.100000	93.666665	626.316947
TA2577	L1	26.850282	46.133335	75.000000	88.666665	93.500000	539.950282
TA2581	L1	78.783617	86.250000	94.900000	96.650000	99.000000	733.383617
TA2586	L1	7.083617	11.483335	21.533335	30.350000	39.400000	173.216957
TA2587	L1	0.033617	0.650000	1.550000	2.050000	3.650000	12.183617
TA10081	L2	9.266383	26.250000	67.500000	83.750000	92.000000	456.266383
TA10085	L2	22.972263	55.147060	76.294120	83.823530	93.529410	547.031093
TA10086	L2	21.986474	51.178063	62.735588	83.837289	89.891258	507.379612
TA10087	L2	30.066383	53.100000	76.525000	86.250000	94.800000	556.616383

TA10089	L2	19.156114	31.597703	55.458798	70.765859	86.793048	421.593882
TA10090	L2	27.923974	69.240563	88.423088	91.837289	92.328758	619.254612
TA10091	L2	7.215644	16.712783	25.173088	41.115069	65.912088	239.129612
TA10092	L2	70.710828	88.263890	95.680555	99.111110	99.722220	736.544158
TA10093	L2	47.298974	77.553063	91.048088	96.837289	97.641258	675.817112
TA10094	L2	27.266383	48.035715	60.464285	64.678570	67.892855	441.516378
TA10095	L2	9.348974	20.590563	25.373088	33.837289	40.078758	209.029612
TA10098	L2	5.555273	17.294445	24.266665	33.827780	43.011110	199.344163
TA10101	L2	6.883617	13.300000	22.950000	35.200000	48.550000	198.333617
TA10124	L2	1.821938	3.361110	5.202020	7.691920	13.265155	47.597193
TA10130	L2	4.048974	4.990563	6.673088	11.837289	20.078758	71.129612
TA10132	L2	25.148974	90.390563	94.173088	95.737289	97.378758	683.129612
TA10142	L2	2.196034	7.755273	18.996618	36.690229	46.814048	175.894322
TA10417	L2	23.916383	40.218180	48.678790	53.757575	62.675755	371.901228
TA10837	L2	33.670228	34.846155	36.461540	37.141025	38.717950	289.285618
TA10838	L2	10.311838	32.318180	50.818180	58.545455	63.954545	357.630013
TA10839	L2	41.944953	81.207145	94.192855	98.307145	99.364285	688.723528
TA10872	L2	21.048974	35.490563	50.173088	63.337289	64.078758	383.129612
TA10919	L2	35.548974	68.490563	84.173088	88.920619	96.495428	615.212942
TA10921	L2	53.604534	76.490563	94.839758	98.503959	98.578758	691.851852
TA10933	L2	5.349718	5.866665	6.600000	12.033335	13.266665	67.616383
TA10934	L2	3.548974	12.133423	30.958798	39.337289	53.435898	221.843892

TA10935	L2	43.271194	54.657233	69.561978	74.059509	83.023198	522.851832
TA10937	L2	58.112155	83.509437	89.201912	89.412711	91.421242	673.781517
TA10939	L2	51.490154	69.461153	84.173088	92.278469	93.578758	636.894332
TA10940	L2	60.599713	72.916665	84.458330	91.041665	95.291665	652.724698
TA10941	L2	9.215644	7.323893	95.839758	99.337289	98.578758	512.796282
TA10942	L2	1.817122	5.009437	6.160242	6.996041	9.421242	47.569804
TA10944	L2	29.783048	47.705555	57.777780	67.361110	76.333335	451.805273
TA10946	L2	47.298974	68.490563	83.573088	87.187289	92.328758	618.129612
TA10948	L2	3.087434	17.298253	27.942318	48.183439	57.886448	247.821902
TA10952	L2	50.433048	72.805555	89.888890	93.472220	97.111110	659.877488
TA11021	L2	56.460828	82.388890	88.972220	95.819445	98.333335	689.155273
TA1581	L2	1.094303	1.772725	3.110390	4.129870	5.090910	24.211183
TA1582	L2	26.798974	70.240563	79.173088	79.337289	79.828758	564.129612
TA1583	L2	14.798974	53.990563	79.673088	91.837289	94.328758	560.129612
TA1584	L2	47.634028	81.058825	94.970590	97.676470	99.117645	694.163443
TA1585	L2	40.548974	68.990563	84.173088	99.337289	98.578758	644.129612
TA1586	L2	42.412218	72.937500	84.020835	86.250000	88.541665	617.370553
TA1600	L2	-0.182878	2.009437	1.993582	2.746041	4.671242	17.986484
TA1605	L2	20.866383	40.683335	55.525000	64.658335	75.500000	418.099723
TA1612	L2	46.916383	63.375000	71.100000	76.475000	83.825000	552.641383
TA1613	L2	1.599718	5.500000	8.708335	12.041665	12.916665	67.016383
TA1615	L2	2.125078	4.043480	9.978260	16.195650	25.586955	88.146813

TA1616	L2	33.483792	42.509437	72.493582	73.996041	83.087912	494.569824
TA1618	L2	20.298203	30.781820	45.609090	54.818180	65.618180	348.334563
TA1619	L2	0.554263	4.450755	6.181820	6.443180	6.651515	41.357288
TA1624	L2	17.089298	19.697915	25.812500	27.500000	29.531250	192.641378
TA1626	L2	19.183048	24.666665	35.166665	46.333335	51.000000	282.516378
TA1635	L2	1.016383	3.200000	15.450000	38.550000	46.000000	161.416383
TA1641	L2	8.048974	28.990563	49.173088	59.337289	68.578758	351.629612
TA1642	L2	10.561838	14.704545	20.636365	31.250000	37.704545	181.448203
TA1644	L2	1.107293	2.159090	3.886365	8.272725	16.772725	46.516378
TA1645	L2	9.383048	13.838890	18.733335	27.072220	37.777780	166.449718
TA1649	L2	17.766383	30.958335	44.875000	53.000000	63.958335	339.391388
TA1651	L2	3.571938	5.245725	8.452990	12.846155	16.788460	73.450138
TA1653	L2	4.431324	17.637623	50.643678	60.984349	66.166998	329.129622
TA1656	L2	1.968763	3.857145	6.226190	15.047620	16.452380	68.683053
TA1660	L2	27.599718	60.750000	88.750000	93.750000	96.250000	610.349718
TA1662	L2	28.099718	40.694445	66.638890	68.694445	72.277780	452.433058
TA1664	L2	1.785613	7.346155	9.615385	12.869230	14.361540	75.808693
TA1665	L2	4.382304	26.657233	38.589758	46.920619	63.162088	291.879612
TA1666	L2	53.953883	69.250000	82.675000	87.062500	91.050000	622.978883
TA1668	L2	17.202748	31.877275	57.250000	60.954545	77.431820	394.798208
TA1669	L2	-0.516208	2.009437	2.826912	5.662711	11.421242	31.903154
TA1670	L2	16.301972	25.645797	46.008732	55.571801	67.148512	337.903144

TA1671	L2	34.380018	87.318180	93.204545	95.863635	97.272725	684.425463
TA1673	L2	20.549718	54.650000	69.333335	89.316665	94.083335	541.233053
TA1674	L2	8.948203	26.750000	43.613635	56.681820	75.136365	338.175478
TA1675	L2	0.497153	1.865385	3.038460	4.115385	4.961540	23.497153
TA1677	L2	2.412218	13.375000	15.458335	19.395835	33.770835	132.641393
TA1678	L2	17.333048	26.208335	43.175000	50.050000	55.008335	311.208053
TA1679	L2	4.048974	96.990563	99.173088	99.337289	98.578758	693.629612
TA1680	L2	82.641383	88.541665	94.583335	98.750000	99.583335	745.974718
TA1682	L2	57.048974	73.990563	86.173088	91.837289	96.078758	657.129612
TA1690	L2	15.399498	25.931820	35.922080	40.951295	49.581170	270.591058
TA1691	L2	11.311838	13.090910	23.954545	41.977275	49.977275	219.334573
TA1693	L2	0.718763	1.738095	2.464285	3.416665	7.190480	23.147333
TA1695	L2	4.076728	8.250000	12.017240	15.560345	17.103450	92.835348
TA1696	L2	44.482198	59.739320	71.598290	85.863245	91.354705	570.238613
TA1703	L2	0.083792	2.209437	4.526912	7.162711	10.021242	37.903154
TA1713	L2	12.882304	28.723893	46.573088	61.670619	79.578758	366.396262
TA1715	L2	5.516383	9.750000	27.625000	38.791665	45.333335	203.183048
TA1718	L2	51.481663	70.229165	79.319445	88.979165	93.104165	621.641378
TA2369	L2	33.166383	60.600000	76.250000	89.250000	94.900000	580.266383
TA2375	L2	63.966383	86.500000	94.250000	99.250000	100.000000	723.966383
TA2376	L2	58.334684	84.347703	89.030228	93.122999	89.650188	680.986732
TA2377	L2	8.283792	15.509437	20.826912	36.462711	45.021242	198.903154

TA2378	L2	0.430668	1.014285	2.200000	2.971430	3.885715	16.687813
TA2446	L2	32.364868	60.768940	78.931820	88.852275	94.954545	584.425483
TA2449	L2	9.710828	13.152775	17.458335	22.263890	27.166665	142.627493
TA2450	L2	21.950462	35.609437	42.693582	51.129381	62.554572	343.369834
TA2451	L2	11.405273	16.111115	20.361115	32.027775	40.361115	188.766398
TA2452	L2	3.333048	5.708335	10.266665	12.841665	17.225000	78.191378
TA2453	L2	4.766383	7.175000	12.525000	20.000000	31.825000	115.991383
TA2454	L2	2.763264	3.633423	6.887378	12.408719	15.221618	63.843922
TA2455	L2	6.653223	9.126315	12.594735	15.536840	17.289475	98.458478
TA2456	L2	18.766383	39.295455	51.409090	58.159090	64.386365	380.880018
TA2457	L2	11.433048	18.625000	34.000000	42.750000	49.291665	251.474713
TA2459	L2	31.215644	52.101673	70.839758	86.781729	87.689868	538.351832
TA2460	L2	0.891383	1.312500	2.375000	7.312500	10.937500	33.828883
TA2461	L2	1.882304	67.323893	75.839758	82.670619	86.912088	540.462932
TA2463	L2	6.053883	10.406250	14.631250	19.093750	22.543750	116.860133
TA2464	L2	6.089108	8.345455	11.030300	17.033335	22.593940	101.501228
TA2465	L2	16.183792	35.509437	74.426912	83.762711	85.421242	489.003154
TA2466	L2	12.945332	23.163287	35.211532	43.278091	50.498162	266.749314
TA2467	L2	1.747153	3.048075	6.423075	9.192310	11.596155	50.670228
TA2469	L2	7.800000	17.800000	24.900000	35.500000	51.100000	215.400000
TA2470	L2	3.649713	8.366665	19.566670	22.633330	25.700000	130.483043
TA2471	L2	1.266383	1.857145	2.142860	2.785715	4.535715	19.373538

TA2473	L2	1.482304	0.457233	2.706418	4.203959	5.512088	21.729612
TA2474	L2	-0.216208	2.309437	2.726912	2.862711	3.921242	19.503154
TA2475	L2	0.492573	1.392855	2.500000	3.607145	4.178570	19.671143
TA2476	L2	9.474718	14.916665	24.958335	47.291665	69.666665	253.474713
TA2477	L2	2.560828	8.372220	21.950000	30.161110	37.794445	161.321933
TA2478	L2	31.439458	58.423075	72.615385	82.076925	86.576925	544.247153
TA2479	L2	21.116383	45.000000	62.550000	77.600000	91.500000	482.916383
TA2480	L2	12.490408	18.051945	26.344155	40.116885	51.850650	233.367028
TA2481	L2	0.238603	0.833335	1.333330	1.944445	2.888890	11.349713
TA2483	L2	27.262418	46.730160	56.023810	67.420635	72.103175	439.714803
TA2484	L2	82.641383	98.750000	100.000000	100.000000	100.000000	780.141383
TA2490	L2	54.639884	79.445113	93.718538	97.064559	96.669668	691.765972
TA2491	L2	32.498974	61.490563	85.173088	91.987289	94.978758	604.779612
TA2496	L2	2.856664	27.836713	76.711548	82.644979	84.347988	461.591132
TA2497	L2	10.716383	14.741665	40.541665	47.366665	65.208335	281.224708
TA2498	L2	4.849718	35.833335	44.000000	50.833330	57.083335	323.266383
TA2499	L2	1.658048	3.241665	5.300000	9.275000	14.866665	52.158043
TA2524	L2	62.048974	77.776273	88.315948	90.265859	90.007328	664.772462
TA2525	L2	62.548974	84.523893	93.706418	95.403959	95.578758	705.396272
TA2527	L2	27.716383	38.277780	60.944445	74.111110	83.577780	457.960833
TA2528	L2	6.385613	15.161540	37.730770	56.184615	71.653845	296.193308
TA2529	L2	7.977544	8.204853	13.601658	16.980149	21.078758	106.629622

TA2530	L2	37.113783	44.928570	61.363635	77.181820	83.051945	487.113778
TA2561	L2	5.016383	19.133335	31.422220	36.688890	52.933335	232.438608
TA2563	L2	44.288104	70.294913	82.173088	89.989459	91.317888	620.520912
TA2564	L2	51.694953	71.750000	84.857145	91.857145	97.500000	646.123533
TA2565	L2	7.548974	11.546123	16.506418	21.337289	23.800978	130.129612
TA2568	L2	22.236474	58.740563	77.985588	86.712289	93.828758	562.942112
TA2578	L2	6.856664	25.836713	48.403858	77.106519	93.963378	403.514222
TA2584	L2	55.308048	68.283335	76.500000	84.083335	92.000000	605.041388
TA2585	L2	23.141383	40.958335	57.083330	92.708335	94.791670	499.433053

Table C.2 - Wheat germplasm released by the Wheat Genetic Resource Center (WGRC) at Kansas State University (KSU) derived from *Aegilops tauschii* accession displaying a resistant response to wheat head blast that could be phenotypically tested for their response to wheat head blast.

Wheat Line	*Aegilops tauschii* donor	Lineage	WHB AUDPC	Category*	Reference
KS85WGRC01	TA1644	L2	46.5	R	Gill et al., 1986
KS89WGRC03	TA1642	L2	181.4	I	Gill et al., 1991
KS89WGRC04	TA1695	L2	92.8	MR	Gill et al., 1991
KS89WGRC06	TA2452 and TA1642	L2	78.2	MR	Gill et al., 1991
KS90WGRC10	TA2460	L2	33.8	R	Cox et al., 1992
KS92WGRC16	TA2470	L2	130.5	MR	Cox et al., 1997
KS93WGRC26	TA2473	L2	23	R	Gill et al., 2006
KS96WGRC39	TA2460	L2	33.8	R	Brown-Guedira et al., 1999
KS96WGRC40	TA2460	L2	33.8	R	Cox et al., 1999
KS00WGRC44	TA1715	L2	203.2	I	Brown-Guedira et al., 2004

* R: resistant, MR: moderately resistant, I: intermediate

Appendix D - Supplementary Material Chapter 4

This appendix contains supplementary figures and tables for Chapter 4.

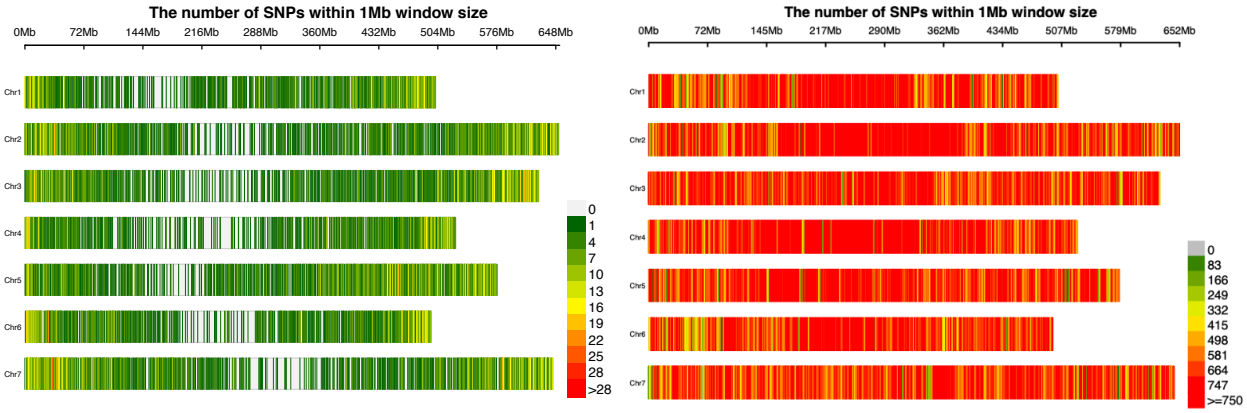

Figure D.1 - Distribution and density of SNP markers along the seven chromosomes of *Aegilops tauschii.* Left panel shows 13,069 GBS-SNP markers and right panel shows 3 million WGS-SNP markers randomly selected out of the 27.2 million SNP markers detected

Figure D.2 - Detail of the purple color on the coleoptile associated with *Aegilops tauschii* spp *strangulata* (or lineage 2) resistant accessions.